Universidade de Aveiro Departamento de Eletrónica, Telecomunicações e Informática
2019
Programa Doutoral em Informática das Universidades do Minho, de Aveiro e do Porto

Ana Patrícia Oliveira Ferreira da Rocha

Sistema para Análise Automatizada de Movimento durante a Marcha Usando uma Câmara RGB-D

System for Automated Motion Analysis during Gait Using an RGB-D Camera

Universidade de Aveiro Departamento de Eletrónica, Telecomunicações e Informática
2019
Programa Doutoral em Informática das Universidades do Minho, de Aveiro e do Porto

Ana Patrícia Oliveira Ferreira da Rocha

Sistema para Análise Automatizada de Movimento durante a Marcha Usando uma Câmara RGB-D

System for Automated Motion Analysis During Gait Using an RGB-D Camera

Tese apresentada às Universidades do Minho, Aveiro e Porto para cumprimento dos requisitos necessários à obtenção do grau de Doutor no âmbito do programa de doutoramento conjunto MAP-i, realizada sob a orientação científica do Doutor José Maria Amaral Fernandes, Professor Auxiliar do Departamento de Eletrónica, Telecomunicações e Informática da Universidade de Aveiro, e do Doutor João Paulo Trigueiros da Silva Cunha, Professor Associado com Agregação do Departamento de Engenharia Eletrotécnica e de Computadores da Faculdade de Engenharia da Universidade de Porto.

Apoio financeiro da Fundação para a Ciência e Tecnologia (FCT), Fundo Social Europeu (FSE) e Fundo Europeu de Desenvolvimento Regional (FEDER) no contexto da bolsa com identificação SFRH/BD/110438/2015 e dos projetos PTDC/EEI-ELC/2760/2012, PTDC/NEU-SCC/0767/2012, UID/CEC/00127/2013, CMUPERI/FIA/0031/2013, Incentivo/EEI/UI0127/2014 e NORTE-01-0145-FEDER-000016.

o júri / the jury

presidente / president	**Doutora Silvina Maria Vagos Santana** Professora Catedrática da Universidade de Aveiro
vogais / examiners committee	**Doutor António Joaquim da Silva Teixeira** Professor Associado com Agregação da Universidade de Aveiro
	Doutor Gabriel de Sousa Torcato David Professor Associado da Faculdade de Engenharia da Universidade do Porto
	Doutor Paulo José Monteiro Peixoto Professor Auxiliar da Faculdade de Ciências e Tecnologia da Universidade de Coimbra
	Doutor Paulo Luís Serras Lobato Correia Professor Auxiliar do Instituto Superior Técnico da Universidade de Lisboa
	Doutor José Maria Amaral Fernandes Professor Auxiliar da Universidade de Aveiro (orientador)

acknowledgments

I would like to express my deepest gratitude to everyone who contributed directly or indirectly to this PhD thesis and supported me in the course of this journey. Although it is impossible to thank every single person, I would like to acknowledge those who contributed more decisively to the conclusion of this research work:

- my PhD supervisors Professor José Maria Fernandes and Professor João Paulo Cunha for their guidance, availability, advices and unconditional support given throughout my PhD studies, which were essential to improve the quality of this thesis;

- Hugo Choupina of INESC-TEC Porto (presently at INOVA+) for contributions in *KiT* and *KiMA* applications and collaboration in the papers of this thesis, as well as for the important help in the acquisitions at São João Hospital and LABIOMEP (Porto Biomechanics Laboratory) and for the support since the beginning of the PhD;

- Maria do Carmo Vilas-Boas of INESC-TEC Porto for the collaboration in the papers of this thesis, support in the acquisitions at LABIOMEP and in many other situations, and for the encouragement;

- Dr. Rui Vaz and Dr. Maria José Rosas, physicians of the Movement Disorders and Functional Surgery Unit of São João Hospital (Porto, Portugal), for the collaboration and for providing all the necessary conditions for carrying out the data acquisitions with the Parkinson's disease (PD) patients;

- the nurses and staff of the Neurosurgery and Neurology Services of São João Hospital, mainly nurses Filipe Cunha and Susana Marques de Sousa, for their availability and help in the acquisitions with PD patients;

- the PD patients and all the volunteers who generously agreed to participate in the acquisitions at São João Hospital and LABIOMEP, which were indispensable for this research work;

- Dr. Ana Isabel Martins of IEETA and Dr. Andreia Sousa of Neuroinova for helping in the acquisitions performed with the PD patients at São João Hospital, and Dr. Ana Isabel Martins for the companionship in the trips to Porto;

- Professor João Paulo Vilas-Boas and the staff of LABIOMEP (University of Porto), mainly Pedro Fonseca, for the support during the acquisitions performed at this laboratory;

- Eduardo Pereira for the initial software that evolved into the *KiT* application;

- all colleagues, teachers and staff of IEETA and MAP-i, especially Professor Ilídio Oliveira, Dr. Susana Brás, Dr. Raquel Sebastião, Dr. Diogo Pratas, João Carvalho and Seyed Morteza Hosseini for the scientific discussions, conversations and advices;

- all colleagues from the BRAIN group of INESC-TEC Porto (Engineering Faculty of University of Porto) for always making me feel welcome;

- University of Aveiro, DETI and IEETA, as well as University of Porto, FEUP and INESC-TEC Porto, for providing the necessary conditions to perform this work, including financial support in various occasions;

- Portuguese Foundation for Science and Technology (FCT) for funding this work with the SFRH/BD/110438/2015 scholarship;

- my friends and family, especially my parents, for the patience and advices, genuine and unconditional support, and for always believing in me.

palavras-chave

Análise de movimento humano em 3-D, análise automatizada de marcha, câmara RGB-D, aprendizagem máquina, reconhecimento de atividades, identificação humana

resumo

Atualmente ainda é comum na prática clínica avaliar a marcha (ou o modo de andar) de uma certa pessoa através da observação visual e utilização de uma escala de classificação, o que é uma abordagem subjetiva. No entanto, existem sensores incluindo câmaras RGB-D, como a Microsoft Kinect, que podem ser usados para obter informação quantitativa que permite realizar a análise da marcha de um modo mais objetivo. Os resultados quantitativos da análise da marcha podem ser muito úteis, por exemplo, para apoiar a avaliação clínica de pessoas com doenças que podem afetar a sua marcha, como a doença de Parkinson.

Assim, a principal motivação desta tese foi fornecer apoio à avaliação da marcha, permitindo realizar a análise quantitativa da marcha de forma automatizada. Este objetivo foi atingido usando dados em 3-D, fornecidos por uma única câmara RGB-D, para automaticamente selecionar os dados correspondentes a andar e, em seguida, detetar os ciclos de marcha executados pelo sujeito durante a marcha. Para cada ciclo de marcha identificado, obtemos vários parâmetros de marcha, que são usados em conjunto com medidas antropométricas para identificar automaticamente o sujeito que está a ser avaliado.

A seleção automatizada de dados de marcha usa técnicas de aprendizagem máquina para reconhecer três atividades diferentes (andar, estar parado em pé e marchar), bem como duas posições diferentes do sujeito em relação à câmara (de frente para a câmara e de costas para ela). Para a deteção dos ciclos da marcha, desenvolvemos um algoritmo que estima os instantes correspondentes a determinados eventos da marcha. A identificação do sujeito com base na sua marcha é realizada usando uma solução que também foi desenvolvida com base em aprendizagem máquina.

As soluções desenvolvidas foram integradas num sistema de análise automatizada de marcha, que demonstrámos ser uma alternativa viável a sistemas padrão de referência para obter vários parâmetros de marcha espácio-temporais e alguns parâmetros angulares. Além disso, o sistema é adequado para uso em ambientes clínicos, bem como em cenários ambulatórios, pois depende de apenas de uma câmara RGB-D que não usa marcadores e é menos dispendiosa, mais portátil, menos intrusiva e mais fácil de configurar, quando comparada com os sistemas padrão de referência (múltiplas câmaras e vários marcadores colocados no corpo do sujeito).

keywords

3-D human motion analysis, automated gait analysis, RGB-D camera, machine learning, activity recognition, human identification

abstract

Nowadays it is still common in clinical practice to assess the gait (or way of walking) of a given subject through the visual observation and use of a rating scale, which is a subjective approach. However, sensors including RGB-D cameras, such as the Microsoft Kinect, can be used to obtain quantitative information that allows performing gait analysis in a more objective way. The quantitative gait analysis results can be very useful for example to support the clinical assessment of patients with diseases that can affect their gait, such as Parkinson's disease.

The main motivation of this thesis was thus to provide support to gait assessment, by allowing to carry out quantitative gait analysis in an automated way. This objective was achieved by using 3-D data, provided by a single RGB-D camera, to automatically select the data corresponding to walking and then detect the gait cycles performed by the subject while walking. For each detected gait cycle, we obtain several gait parameters, which are used together with anthropometric measures to automatically identify the subject being assessed.

The automated gait data selection relies on machine learning techniques to recognize three different activities (walking, standing, and marching), as well as two different positions of the subject in relation to the camera (facing the camera and facing away from it). For gait cycle detection, we developed an algorithm that estimates the instants corresponding to given gait events. The subject identification based on gait is enabled by a solution that was also developed by relying on machine learning.

The developed solutions were integrated into a system for automated gait analysis, which we found to be a viable alternative to gold standard systems for obtaining several spatiotemporal and some kinematic gait parameters. Furthermore, the system is suitable for use in clinical environments, as well as ambulatory scenarios, since it relies on a single markerless RGB-D camera that is less expensive, more portable, less intrusive and easier to set up, when compared with the gold standard systems (multiple cameras and several markers attached to the subject's body).

Contents

Contents i

List of Figures v

List of Tables ix

List of Acronyms xvii

1 Introduction 1

1.1 Motivation 2

1.2 Objectives 2

1.3 Main Contributions 3

1.4 Publications 6

1.5 Thesis Outline 8

2 Human Motion Analysis 11

2.1 Motion Analysis 11

2.1.1 Gait Analysis 14

2.2 Sensors for Gait Analysis 17

2.2.1 Vision-Based Sensors 19

2.3 Summary 24

3 Preliminary Studies with Parkinson's Disease Patients 27

3.1 Parkinson's Disease 27

3.1.1 Symptoms 28

3.1.2 Diagnosis and Follow-up 29

3.1.3 Treatment 31

3.2 Parkinson's Disease Assessment Support Using an RGB-D Camera 32

3.3 Materials and Methods 33

3.3.1 Subjects 33

3.3.2 Experimental Setup and Protocol 33

3.3.3 Data Acquisition and Processing 37

3.3.4 Statistical Analysis 41

3.4 Results 42

3.4.1 Distinction between Healthy Subjects and Parkinson's Disease Patients 42

3.4.2 Estimation of UPDRS Scores 45

3.5 Discussion 47
3.5.1 Distinction between Healthy Subjects and Parkinson's Disease Patients 47
3.5.2 Estimation of UPDRS Scores 47
3.5.3 Other Outcomes 48
3.6 Summary 48

4 *KiT* and *KiMA*: RGB-D Camera Data Acquisition and Visualization 51
4.1 *KinecTracker* (*KiT*) Application 51
4.2 *Kinect Motion Analyser* (*KiMA*) Application 57
4.3 Summary 59

5 Automated Gait Cycle Detection Using an RGB-D Camera 61
5.1 Related Work 61
5.1.1 Activity Recognition 61
5.1.2 Gait Cycle Detection 62
5.2 Materials and Methods 64
5.2.1 Subjects 64
5.2.2 Experimental Setup 65
5.2.3 Experimental Protocol 67
5.2.4 Data Acquisition and Pre-Processing 68
5.2.5 Activity Recognition 71
5.2.6 Gait Cycle Detection 76
5.3 Results 83
5.3.1 Activity Recognition 83
5.3.2 Gait Cycle Detection 85
5.4 Discussion 89
5.4.1 Activity Recognition 89
5.4.2 Gait Cycle Detection 90
5.4.3 Comparison with the State of the Art 92
5.5 Summary 96

6 Validation of an RGB-D Camera for Gait Analysis 97
6.1 Related Work 98
6.2 Materials and Methods 100
6.2.1 Subjects 101
6.2.2 Experimental Setup and Protocol 101
6.2.3 Data Acquisition and Pre-Processing 101

6.2.4 Gait Parameter Computation ... 102
6.2.5 Kinect Validation ... 105
6.3 Results ... 106
6.3.1 Kinect Version Comparison ... 108
6.3.2 Walking Activity Comparison ... 111
6.3.3 Kinect Configuration Comparison ... 114
6.4 Discussion ... 117
6.4.1 Kinect Version Comparison ... 117
6.4.2 Walking Activity Comparison ... 118
6.4.3 Kinect Configuration Comparison ... 119
6.4.4 Comparison with the State of the Art ... 120
6.5 Summary ... 124

7 Human Identification Based on Gait Using an RGB-D Camera ... 125
7.1 Related Work ... 126
7.2 Materials and Methods ... 128
7.2.1 Subjects ... 128
7.2.2 Experimental Setup and Protocol ... 129
7.2.3 Datasets ... 129
7.2.4 Subject Identification ... 131
7.3 Results ... 132
7.3.1 Identification of Healthy Subjects ... 133
7.3.2 Identification of Parkinson's Disease Patients ... 135
7.4 Discussion ... 140
7.4.1 Identification of Healthy Subjects ... 140
7.4.2 Identification of Parkinson's Disease Patients ... 141
7.4.3 Comparison with the State of the Art ... 143
7.5 Summary ... 145

8 Gait Assessment Support System ... 147
8.1 System Integration ... 148
8.1.1 Online Gait Analysis ... 149
8.1.2 Offline Gait Analysis ... 154
8.2 Summary ... 155

9 Conclusion and Future Work ... 157
9.1 Conclusion ... 157

9.2 Future Work 159

References 163

Appendix A *KiT* and *KiMA* File Format 177

A.1 File Format for Kinect Data 177

A.2 File Format for Label and Event Information 181

Appendix B Study on Interference between Motion Capture Systems 183

Appendix C Additional Information Regarding Gait Cycle Detection 187

C.1 Selection of Walking Towards and Away from the Kinect 187

C.2 Identification of the Actual Gait Events from Qualisys Data 187

Appendix D Window Size Selection for Gait Cycle Detection 191

D.1 Results for Both Kinect Versions and Walking Activities 192

D.2 Results for Different Kv2 Configurations (WF Trials) 204

Appendix E Kinect Physical Configuration Selection 213

Appendix F Butterworth Filter Optimization for Gait Parameter Computation 215

F.1 Results for Both Kinect Versions and Walking Activities 216

F.2 Results for Different Kv2 Configurations (WF Trials) 224

Appendix G Additional Kinect Validation Results 231

G.1 Kinect Version Comparison 232

G.2 Walking Activity Comparison 235

G.3 Kinect Configuration Comparison 238

G.4 Results for Kinect v2 when varying the Number of Gait Cycles 241

Appendix H Additional Results for Subject Identification 247

List of Figures

Figure 1.1. Automated gait analysis using a single RGB-D camera, including data acquisition, activity recognition, gait parameter computation and subject identification. 4

Figure 2.1. Right gait cycle performed by a subject while walking, including the associated gait events and phases (adapted from the figures included in [134]). 15

Figure 2.2. Spatial gait parameters for a right gait cycle or stride (adapted from the figure included in [22]). 17

Figure 2.3. First (a) and second (b) generations of the Microsoft Kinect camera and associated coordinate system (adapted from the figure included in [175] and obtained from [176], respectively). 22

Figure 2.4. Body joints tracked by Kinect v1 and v2. 24

Figure 3.1. Location of experiments EXP1 (a), EXP2 (b), and EXP3 (c), and used setup including a Kinect v1 and/or a Kinect v2 mounted on a tripod and connected to laptop. 35

Figure 3.2. Experimental setup used in experiment EXP1 (a), EXP2 (b) and EXP3 (c), including the height and tilt angle of the Kinect(s), the walking trajectory, and the relevant distances. 36

Figure 3.3. Coordinate systems of a non-tilted and tilted Kinect, and the effect that the tilting has on the distance between the Kinect and a given object in the z-axis. 38

Figure 3.4. Angle at the elbow computed over Kv2 data versus the elapsed time for a given gait cycle performed by a heathy subject and PD patient in both Stim-on and Stim-off states. 44

Figure 4.1. Preview, acquisition, review and management of the multimodal data provided by the Kinect camera, using *KiT* and *KiMA* software applications. 51

Figure 4.2. Use case diagram associated with the *KiT* application. 52

Figure 4.3. *KiT*'s main window GUI (Kv2), including the display of depth, body index and body data. 53

Figure 4.4. Preferences window of *KiT* for Kinect v1 (a) and v2 (b). 54

Figure 4.5. Use case diagram associated with the *KiMA* application. 58

Figure 4.6. *KiMA*'s main window GUI, including the display of depth and body data, as well as labels and events. 59

Figure 5.1. Experimental setup including two RGB-D cameras (Kv1 and Kv2) mounted on a tripod, and a Qualisys system with twelve infrared cameras (figure adapted from the image of the Qualisys setup provided by LABIOMEP). 66

Figure 5.2. Physical configuration (height and tilt angle) of the RGB-D cameras (Kinect v1 and v2), which were mounted on a tripod and connected to a portable computer each. 66

Figure 5.3. Retro-reflective markers placed at the subject's body (image provided by LABIOMEP). 67

Figure 5.4. Solution for gait cycle detection, including activity recognition and gait event detection. MAF stands for moving average filter. 72

Figure 5.5. Different phases of a right gait cycle, as well as the gait events that define them. 77

Figure 5.6. Filtered left and right foot vertical velocity (a), distance between ankles and between knees (b) and left and right ankle velocity (c), versus the elapsed time, computed over Qualisys data acquired from a given subject while walking towards the Kv2. 78

Figure 5.7. Filtered left and right foot vertical velocity (a), xz-plane distance between left ankle and spine base and between right ankle and spine base (b), and left and right shank angle and absolute difference between left and right shank angle (c), versus the elapsed time, computed over Qualisys data acquired from the same subject and trial as Figure 5.6. 80

Figure 5.8. Mean value for the overall accuracy achieved by the models built with the different machine learning algorithms versus the size of the window used of the moving average filter used over the Kinect 3-D joint data. 83

Figure 5.9. Distance between ankles (a), velocity of left and right ankles (b) and angle of left and right shanks and corresponding absolute difference (c), computed over unfiltered and filtered Kv2 data, versus the elapsed time, for the same subject and WF trial of Figure 5.6. 88

Figure 6.1. Mean value for Pearson's correlation coefficient (r) and concordance correlation coefficient (r_c) when considering all gait parameters and both walking activities, versus the number of gait cycles used to compute the parameters' value for each subject. 112

Figure 7.1. Mean (a) and standard deviation (b) values for the class accuracy and class F_1 score (DS4 and random forest) versus the number of gait cycles per subject used for training/testing, when using all gait cycles available for identification. 135

Figure 7.2. Confusion matrix for identification of PD patients over time (DS7) considering all gait cycles available per subject (outlier removal). 140

Figure 8.1. System for supporting the assessment of a given subject's gait. 148

Figure 8.2. Preferences window of the *KiT* application (Kv2) after the integration of gait analysis. 149

Figure 8.3. *KiT*'s main window GUI (Kv2) after the integration of automated online gait analysis, where it is possible to indicate the number of minimum gait cycles required for analysis. 150

Figure 8.4. *KiT*'s main window GUI (Kv2) after the integration of automated online gait analysis, where the number of detected gait cycles since the beginning of the acquisition is displayed. 150

Figure 8.5. Results of gait analysis shown in the *KiT* application, including the subject's information and the mean value of the gait parameters for left, right and both gait cycles. 151

List of Tables

Table 2.1. Sensors used for gait analysis, including their main advantages and disadvantages. 18

Table 2.2. Main differences between first and second versions of the Kinect (Kinect v1 and v2) [24, 178-181, 183]. 23

Table 3.1. Demographics of the subjects that participated in each experiment. 33

Table 3.2. UPDRS motor and gait scores assigned to the PD patients when the DBS stimulator is switched on (Stim-on) and off (Stim-off), for each experiment. 34

Table 3.3. Datasets obtained in each experiment, including the number of days and subjects, DBS state for PD patients, and number of data acquisitions per subject and of gait trials per acquisition. 37

Table 3.4. Number of gait cycles included in each dataset. 39

Table 3.5. Kruskal-Wallis test *p*-value for the gait parameters, computed for dataset DS1 (unfiltered and filtered data), presenting a statistically significant difference (p-value ≤ 0.05) between healthy subjects and PD patients in Stim-on and Stim-off states. 42

Table 3.6. Kruskal-Wallis test *p*-value for the gait parameters, computed for dataset DS2 (Kv1 and Kv2), when comparing healthy subjects and PD patients in Stim-on and Stim-off states. 44

Table 3.7. Pearson's correlation coefficient (r) results for the gait parameters for which $|r| \geq 0.7$, when considering the parameter values versus the UPDRS gait scores. 45

Table 5.1. Characterization of the subjects that participated in the experiment. 65

Table 5.2. Tasks performed by the subjects. 68

Table 5.3. Number of frames for the selected Kv1 and Kv2 data, for each and all activities, when considering all subjects and each subject (mean and standard deviation). 69

Table 5.4. Number of actual heel strikes and gait cycles performed by all subjects, for all analysed WF and WB trials of task T1, when using Kv1 and Kv2. The mean and standard deviation values per subject and per trial are also included. 70

Table 5.5. Measures computed over the 3-D body joint data and corresponding equations. 71

Table 5.6. Overall accuracy and overall F_1 score achieved by the models built with different machine learning algorithms, for Kv1 and Kv2. 83

Table 5.7. Mean and standard deviation values for the models' training time (five runs) and prediction time per frame, as well as the associated prediction time for 1,800 frames (≈1 min of data). 84

Table 5.8. Accuracy and F_1 score values achieved by the final MLP model over a dataset corresponding to five "never seen" subjects, when using the Kv1 and Kv2. 84

Table 5.9. Size of the windows used for gait cycle detection, for both Kinect versions and both walking activities. The achieved precision and sensitivity results, as well as the number of gait cycles detected per WF/WB trial (mean and standard deviation), are also included. 85

Table 5.10. True errors achieved by the gait cycle detection algorithm, for Kv1 and Kv2 and for WF and WB. 86

Table 5.11. Absolute errors achieved by the gait cycle detection algorithm, for Kv1 and Kv2 and for WF and WB. 87

Table 5.12. Comparison between our algorithm and the methods proposed in other contributions, regarding the true error for estimating heel strike and toe off instants. 93

Table 5.13. Comparison between our algorithm, and the methods proposed in other contributions, regarding the true error for estimating stride, step, stance, swing and double support duration. 94

Table 5.14. Comparison between our algorithm, and the methods proposed in other contributions, regarding the absolute error for estimating stride, step, stance, swing and double support duration. 95

Table 6.1. Height and tilt angle associated with each explored physical configuration of the Kinect (KC1, KC2 and KC2), for both Kv1 and Kv2. 101

Table 6.2. Spatiotemporal gait parameters computed over 3-D joint data, including a description and the equation used for its computation. 103

Table 6.3. Kinematic gait parameters computed over 3-D joint data, including a description and the equation used for its computation. 104

Table 6.4. Computation of the 3-D position of joints from Qualisys data. 104

Table 6.5. Butterworth filter's order and cut-off frequency values for each gait parameter, when using Kv1 and Kv2. 107

Table 6.6. Mean and standard deviation values for the practical depth range of both Kinect versions (Kv1 and Kv2), when considering the WF activity and configuration KC1. 108

Table 6.7. Number of actual gait cycles for each Kinect version (Kv1 and Kv2), when considering the WF activity and configuration KC1. 109

Table 6.8. Validation results for each gait parameter and Kinect version (Kv1 and Kv2), when considering the WF activity and configuration KC1. 110

Table 6.9. Mean and standard deviation values for the practical depth range of Kv2 for both walking activities (WF and WB), when using configuration KC1. 111

Table 6.10. Number of actual gait cycles for Kv2 in the case of both walking activities (WF and WB), when using configuration KC1. 111

Table 6.11. Validation results for each gait parameter and walking activity (WF and WB), when considering Kv2 and configuration KC1. 113

Table 6.12. Mean and standard deviation values for the practical depth range of Kv2, when considering the WF activity, for configurations KC1, KC2 and KC3. 114

Table 6.13. Number of actual gait cycles for each Kinect configuration (KC1, KC2, and KC3), when using the Kinect v2 and WF data. 115

Table 6.14. Window sizes used for detecting gait cycles using Kinect v2 (Kv2) data acquired while the subject walked towards the camera (WF), for each considered configuration (KC1, KC2 and KC3). 115

Table 6.15. Validation results for each gait parameter and Kinect configuration (KC1, KC2 and KC3), when using the Kinect v2 (Kv2) and data corresponding to walking towards the camera (WF)... 116

Table 6.16. Comparison between our gait analysis solution (Kv2, WF, KC1) and methods proposed in the literature, regarding the validity of the Kinect for computing spatiotemporal gait parameters. 121

Table 6.17. Comparison between our gait analysis solution (Kv2, WF, KC1) and methods proposed in the literature, regarding the validity of the Kinect for computing kinematic gait parameters. .. 122

Table 7.1. Characterization of the subjects considered for studying subject identification. 129

Table 7.2. Datasets used for studying subject identification based on gait. 130

Table 7.3. Results for identification of healthy subjects (DS4) considering a single gait cycle. ... 133

Table 7.4. Results for identification of healthy subjects (DS4) considering all gait cycles available per subject. 134

Table 7.5. Results for identification of healthy subjects (DS4) considering all gait cycles available per subject, when varying the number of gait cycles used for model training/testing. 134

Table 7.6. Results for identification of PD patients (DS5) considering a single gait cycle. 135

Table 7.7. Results for identification of PD patients (DS5) considering all gait cycles available per subject. 136

Table 7.8. Results for identification of PD patients (DS5) considering all gait cycles available per subject, when varying the number of gait cycles used for model training/testing. 136

Table 7.9. Results for identification of both healthy subject and PD patients (DS6) considering all gait cycles available per subject. 137

Table 7.10. Results for identification of both healthy subject and PD patients (DS6) considering all gait cycles available per subject, for different feature subsets. 137

Table 7.11. Results for identification of PD patients over time (DS7) considering all gait cycles available per subject. 138

Table 7.12. Results for identification of PD patients over time (DS7) considering all gait cycles available per subject, with outlier removal. 139

Table 7.13. Results for identification of PD patients over time (DS7) considering all gait cycles available per subject (outlier removal), for different feature subsets. 139

Table 7.14. Subject identification results reported in different contributions using the Kinect camera, when considering gait and healthy subjects. 144

Table B.1. Mean and standard deviation values for the noise measure computed over Kv1 and Kv2 data acquired from subjects while standing still, with only Kv1/Kv2 switched on, both Kv1 and Kv2 switched on (Kv1+Kv2) and both Kinects and Qualisys system switched on (Kv1+Kv2+Q). 184

Table D.1. Results for heel strike instant estimation when using Kv1 and WF data (KC1, 10 trials), considering different value pairs for the window sizes *NF1* and *ND1*..... 192

Table D.2. Results for heel strike side identification when using Kv1 and WF data (KC1, 10 trials), considering different value pairs for the window sizes *NF2* and *ND2*..... 193

Table D.3. Results for toe off instant estimation when using Kv1 and WF data (KC1, 10 trials), considering different values for the window size *NF3*..... 194

Table D.4. Results for heel strike instant estimation when using Kv1 and WB data (KC1, 10 trials), considering different value pairs for the window sizes *NF1* and *ND1*..... 195

Table D.5. Results for heel strike side identification when using Kv1 and WB data (KC1, 10 trials), considering different value pairs for the window sizes *NF2* and *ND2*..... 196

Table D.6. Results for toe off instant estimation when using Kv1 and WB data (KC1, 10 trials), considering different values for the window size *NF3*..... 197

Table D.7. Results for heel strike instant estimation when using Kv2 and WF data (KC1, 10 trials), considering different value pairs for the window sizes *NF1* and *ND1*..... 198

Table D.8. Results for heel strike side identification when using Kv2 and WF data (KC1, 10 trials), considering different value pairs for the window sizes *NF2* and *ND2*..... 199

Table D.9. Results for toe off instant estimation when using Kv2 and WF data (KC1, 10 trials), considering different values for the window size *NF3*..... 200

Table D.10. Results for heel strike instant estimation when using Kv2 and WB data (KC1, 10 trials), considering different value pairs for the window sizes *NF1* and *ND1*..... 201

Table D.11. Results for heel strike side identification when using Kv2 and WB data (KC1, 10 trials), considering different value pairs for the window sizes *NF2* and *ND2*..... 202

Table D.12. Results for toe off instant estimation when using Kv2 and WB data (KC1, 10 trials), considering different values for the window size *NF3*..... 203

Table D.13. Results for heel strike instant estimation when using configuration KC1 (Kv2, WF, 5 trials), considering different value pairs for the window sizes *NF1* and *ND1*. 204

Table D.14. Results for heel strike side identification when using configuration KC1 (Kv2, WF, 5 trials), considering different value pairs for the window sizes *NF2* and *ND2*. 205

Table D.15. Results for toe off instant estimation when using configuration KC1 (Kv2, WF, 5 trials), considering different values for the window size *NF3*..... 206

Table D.16. Results for heel strike instant estimation when using configuration KC2 (Kv2, WF, 5 trials), considering different value pairs for the window sizes *NF1* and *ND1*. 207

Table D.17. Results for heel strike side identification when using configuration KC2 (Kv2, WF, 5 trials), considering different value pairs for the window sizes *NF2* and *ND2*. 208

Table D.18. Results for toe off instant estimation when using configuration KC2 (Kv2, WF, 5 trials), considering different values for the window size *NF3*..... 209

Table D.19. Results for heel strike instant estimation when using configuration KC3 (Kv2, WF, 5 trials), considering different value pairs for the window sizes *NF1* and *ND1*. 210

Table D.20. Results for heel strike side identification when using configuration KC3 (Kv2, WF, 5 trials), considering different value pairs for the window sizes *NF2* and *ND2*. 211

Table D.21. Results for toe off instant estimation when using configuration KC3 (Kv2, WF, 5 trials), considering different values for the window size *NF3*..... 212

Table E.1. Practical depth range for different Kinect tilt angles, for each Kinect version (Kv1 and Kv2) considered height. 213

Table F.1. Mean estimation error for spatiotemporal gait parameters (Kv1, WF, KC1, 10 trials), when considering different value pairs for the Butterworth filter parameters (order and cut-off frequency). 216

Table F.2. Mean estimation error for kinematic gait parameters (Kv1, WF, KC1, 10 trials), when considering different value pairs for the Butterworth filter parameters (order and cut-off frequency). 217

Table F.3. Mean estimation error for spatiotemporal gait parameters (Kv1, WB, KC1, 10 trials), when considering different value pairs for the Butterworth filter parameters (order and cut-off frequency). 218

Table F.4. Mean estimation error for kinematic gait parameters (Kv1, WB, KC1, 10 trials), when considering different value pairs for the Butterworth filter parameters (order and cut-off frequency). 219

Table F.5. Mean estimation error for spatiotemporal gait parameters (Kv2, WF, KC1, 10 trials), when considering different value pairs for the Butterworth filter parameters (order and cut-off frequency). 220

Table F.6. Mean estimation error for kinematic gait parameters (Kv2, WF, KC1, 10 trials), when considering different value pairs for the Butterworth filter parameters (order and cut-off frequency). 221

Table F.7. Mean estimation error for spatiotemporal gait parameters (Kv2, WB, KC1, 10 trials), when considering different value pairs for the Butterworth filter parameters (order and cut-off frequency). 222

Table F.8. Mean estimation error for kinematic gait parameters (Kv2, WB, KC1, 10 trials), when considering different value pairs for the Butterworth filter parameters (order and cut-off frequency). 223

Table F.9. Mean estimation error for spatiotemporal gait parameters (Kv2, WF, KC1, 5 trials), when considering different value pairs for the Butterworth filter parameters (order and cut-off frequency). 224

Table F.10. Mean estimation error for kinematic gait parameters (Kv2, WF, KC1, 5 trials), when considering different value pairs for the Butterworth filter parameters (order and cut-off frequency). 225

Table F.11. Mean estimation error for spatiotemporal gait parameters (Kv2, WF, KC2, 5 trials), when considering different value pairs for the Butterworth filter parameters (order and cut-off frequency). 226

Table F.12. Mean estimation error for kinematic gait parameters (Kv2, WF, KC2, 5 trials), when considering different value pairs for the Butterworth filter parameters (order and cut-off frequency). 227

Table F.13. Mean estimation error for spatiotemporal gait parameters (Kv2, WF, KC3, 5 trials), when considering different value pairs for the Butterworth filter parameters (order and cut-off frequency). 228

Table F.14. Mean estimation error for kinematic gait parameters (Kv2, WF, KC3, 5 trials), when considering different value pairs for the Butterworth filter parameters (order and cut-off frequency). 229

Table G.1. Mean and standard deviation values for each gait parameter obtained when using the Kinect and Qualisys, in the case of both Kinect versions (Kv1 and Kv2), considering the WF activity and configuration KC1. 232

Table G.2. Bland Altman's mean difference (Mean diff) and 95% limits of agreement (LoA) for each gait parameter, in the case of both Kinect versions (Kv1 and Kv2), considering the WF activity and configuration KC1. 233

Table G.3. Pearson's correlation coefficient (r) and concordance correlation coefficient (r_c), and associated 95% confidence interval (CI), for each gait parameter, in the case of both Kinect versions (Kv1 and Kv2), considering the WF activity and configuration KC1. 234

Table G.4. Mean and standard deviation values for each gait parameter obtained when using the Kv2 and Qualisys, in the case of both walking activities (WF and WB), considering the configuration KC1. 235

Table G.5. Bland Altman's mean difference (Mean diff) and 95% limits of agreement (LoA) for each gait parameter, in the case of both walking activities (WF and WB), considering the Kv2 and configuration KC1. 236

Table G.6. Pearson's correlation coefficient (r) and concordance correlation coefficient (r_c), and associated 95% confidence interval (CI), for each gait parameter, in the case of both walking activities (WF and WB), considering the Kv2 and configuration KC1. 237

Table G.7. Mean and standard deviation values for each gait parameter obtained when using the Kv2 and Qualisys, in the case of the three configurations (KC1, KC2 and KC3), considering the WF activity. 238

Table G.8. Bland Altman's mean difference (Mean diff) and 95% limits of agreement (LoA) for each gait parameter, in the case of the three configurations (KC1, KC2 and KC3), considering the Kv2 and WF activity. 239

Table G.9. Pearson's correlation coefficient (r) and concordance correlation coefficient (r_c), and associated 95% confidence interval (CI), for each gait parameter, in the case of the three configurations (KC1, KC2 and KC3), considering the Kv2 and WF activity. 240

Table G.10. Bland Altman's mean difference values obtained for Kv2 and WF (KC1), when varying the number of gait cycles used to compute the gait parameters. 241

Table G.11. Pearson's correlation coefficient (r) values obtained for Kv2 and WF (KC1), when varying the number of gait cycles used to compute the gait parameters. 242

Table G.12. Concordance correlation coefficient (r_c) values obtained for Kv2 and WF (KC1), when varying the number of gait cycles used to compute the gait parameters. 243

Table G.13. Bland Altman's mean difference values obtained for Kv2 and WB (KC1), when varying the number of gait cycles used to compute the gait parameters. 244

Table G.14. Pearson's correlation coefficient (r) values obtained for Kv2 and WB (KC1), when varying the number of gait cycles used to compute the gait parameters. 245

Table G.15. Concordance correlation coefficient (r_c) values obtained for Kv2 and WB (KC1), when varying the number of gait cycles used to compute the gait parameters. 246

Table H.1. Number of gait cycles detected for the healthy subjects, when using the Kv2 and considering walking towards the sensor. 247

Table H.2. Number of gait cycles detected for the PD patients, when using the Kv2 and considering walking towards the sensor. 248

List of Acronyms

2-D	Two-dimensional or two dimensions
3-D	Three-dimensional or three dimensions
BMI	Body Mass Index
CI	Confidence Interval
DBS	Deep Brain Stimulation
DTW	Dynamic time warping
GUI	Graphical User Interface
IR	Infrared
KiT	KinecTracker
KiMA	Kinect Motion Analyser
k-NN	k-Nearest Neighbours
Kv1	Kinect v1 (first version of the Microsoft Kinect sensor)
Kv2	Kinect v2 (second version of the Microsoft Kinect sensor)
LED	Light emitting diode
LoA	Limits of Agreement
MLP	Multilayer Perceptron
MLPE	Multilayer Perceptron Ensemble
OLS	Ordinary least squares
PD	Parkinson's Disease
RGB-D	Red, Green, Blue, and Depth
SD	Standard Deviation
SDK	Software Development Kit
Stim-on	Stimulator (for deep brain stimulation) switched on
Stim-off	Stimulator (for deep brain stimulation) switched off
SVM	Support Vector Machines
TTR-FAP	Transthyretin Familial Amyloid Polyneuropathy
UPDRS	Unified Parkinson's Disease Rating Scale

1 Introduction

The technology available nowadays enables capturing, gathering and processing of information about the real world, including the human being. For example, human motion can be quantified using sensors that are becoming increasingly common in our daily lives, such as wearable sensors (e.g., accelerometer, gyroscope) and vision-based sensors (e.g., RGB, infrared and RGB-D cameras). The quantitative motion information provided by these sensors can be used for various applications, including activity recognition [1-4], human identification [5-9] and posture, balance, and/or motor function assessment [10-17], which are useful in different areas, such as sports, healthcare, security, human-interface interaction and entertainment [18-21].

Walking is a motor activity that can be affected by an injury or disease (e.g., neurological disease) [22]. Therefore, the analysis of human gait or way of walking is very important in the areas of sports and healthcare, since it can help in the prevention, diagnosis and monitoring/rehabilitation of injuries or diseases that affect the gait [13, 14, 23]. Nowadays, it is still common to use traditional rating scales for gait assessment in clinical practice, in which experts observe the patient's gait and decide on its quality by assigning a score [23], which is a rather subjective method. However, this subjectivity can be overcome by using sensors to carry out gait analysis in a more objective way.

RGB-D cameras provide both colour (RGB) images and depth information, which can be used to track the full-body movements of subjects in 3-D (three dimensions) without relying on any markers. The emergence of low-cost RGB-D cameras, such as the Microsoft Kinect, has led to a renewed interest regarding markerless motion analysis in the area of computer vision [24, 25]. A single RGB-D camera enables 3-D (three-dimensional) motion analysis, without requiring the control of the ambient lighting (indoors) or the colour of the background or subject's clothing, which is not possible or is more complex when using a single RGB camera and no markers.

Furthermore, RGB-D cameras are less expensive and more portable when compared to multi-camera marker-based systems. They are also less intrusive and their setup is less time-consuming than systems that rely on markers/sensors attached to the subject's body. In the specific case of gait, they allow to obtain more complete information than floor sensors (e.g., force plates, pressure-sensitive mats/walkways).

1.1 Motivation

In the context of an on-going collaboration with the Movement Disorders Unit of São João Hospital, Porto, Portugal (Rui Vaz, M.D. and Maria José Rosas, M.D.), and considering our previous work on sensor-based human monitoring and/or motion quantification and analysis [26-37], the following challenge was presented: using technology to support the clinical motor assessment of subjects with diseases affecting their movement, such as Parkinson's disease (PD).

To address this challenge, it was firstly necessary to select a sensor that provides quantitative information that can be used to obtain human motion information. A single RGB-D camera enables full-body 3-D motion capture. Furthermore, it meets several of the requirements that are important in clinical scenarios, including low-cost, portability, minimal intrusiveness and quick setup. Therefore, the RGB-D camera was our choice for motion quantification.

It was also necessary to define the motor function to be assessed. From the motor tasks that are usually evaluated in PD, gait is a task that involves the whole body and does not require any intervention by the physicians (which could lead to occlusions) or the use of any object (e.g., chair). For this reason, we considered the assessment of a simple gait task: walking back and forth in front of the camera.

In preliminary studies we carried out with PD patients, it became clear the need to avoid manual intervention as much as possible in the whole process of gait analysis. For a fully automated gait analysis, it is important to perform the following tasks automatically: selection of the sensor data corresponding to walking; detection of gait cycles carried out during the walking activity; extraction of relevant gait information for each gait cycle; identification of the subject being assessed.

Although several studies relied on an RGB-D camera for activity recognition [4, 38-54], gait cycle detection [55-65] and human identification [66-75], there is no contribution that integrated the different solutions to enable gait analysis in an automated way, to the best of our knowledge. Thus, the main motivation of this thesis was to study and propose a solution for automated motion analysis during gait, which can be used to support the assessment of a given subject's gait.

1.2 Objectives

The main objective of this thesis was to provide a tool for supporting the assessment of a subject's gait, by enabling quantitative human gait analysis. This tool should be suitable for use in different scenarios, including clinical scenarios, i.e., it should portable, easy to set up and use, minimally intrusive for the subjects being assessed, and not be very expensive. Regarding the process of

gait analysis, it should not require expertise knowledge and should be performed in the shortest time possible, by avoiding manual intervention in the different steps involved in the process.

To achieve the defined objective, we investigated if the 3-D body joint data provided by a single RGB-D camera, namely a Kinect, can be used to carry out automated online gait analysis. This investigation was carried out by defining the following goals:

- Explore the use of machine learning techniques and measures extracted from the 3-D data for online activity recognition, to enable the automated identification of data corresponding to the walking activity;
- Explore if a few measures extracted from the 3-D data can be used for estimating the instants corresponding to gait events, for enabling the online detection of gait cycles and associated phases in an automated way;
- Ascertain if our gait analysis solution based on a single Kinect can be used as an alternative to a gold standard system (multi-camera marker-based system) for gait assessment;
- Explore the use of machine learning techniques, together with gait analysis results and/or other measures (e.g., anthropometric measures), for human identification, with the aim of enabling the automatic association between a gait assessment session and the identity of the corresponding subject.

1.3 Main Contributions

This thesis' work contributed with different solutions (Figure 1.1) for enabling quantitative human gait analysis in an automated way. The developed solutions were integrated into a system for automated gait analysis, which was shown to be a viable alternative to a gold standard system (multi-camera marker-based system) for obtaining several spatiotemporal and some kinematic gait parameters. These parameters can be used to support the gait assessment of subjects, including patients with diseases or injuries that affect their gait.

The system is suitable for use in clinical settings, as well as ambulatory scenarios, since it relies on a single markerless RGB-D camera that is less expensive, more portable, less intrusive and easier to set up than the gold standard systems (multiple cameras and several markers attached to the subject's body).

Furthermore, our system allows saving time in the whole process of gait analysis when compared with solutions requiring manual intervention. We enable fully automated gait analysis (except

for starting the data acquisition) by using the 3-D data provided by the RGB-D camera to automatically select the data corresponding to walking and detect the gait cycles performed during the walking activity [76]. Furthermore, the gait parameters computed for each detected gait cycle are used to identify the associated subject [77].

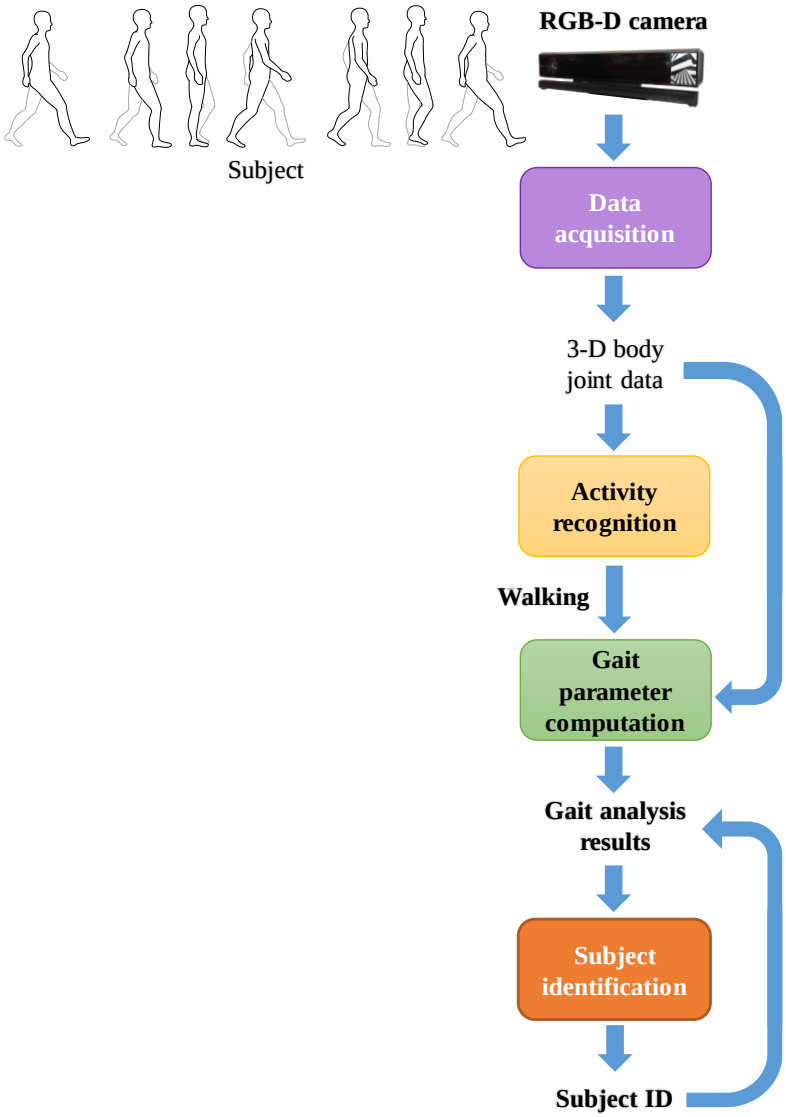

Figure 1.1. Automated gait analysis using a single RGB-D camera, including data acquisition, activity recognition, gait parameter computation and subject identification.

The data provided by the RGB-D camera, namely a Kinect (v1 or v2), are acquired from a given subject using the solution we developed for online visualization and acquisition of Kinect data [78]. For automated gait data selection, the walking activity is automatically recognized by relying on a predictive model that distinguishes between standing, walking and marching (while facing the

Kinect or facing away from it) [76]. This model was obtained using machine learning techniques, and depends only on measures extracted from the 3-D body joint data.

For the identified gait data, several gait parameters are computed for each gait cycle performed by the subject. The gait cycles are automatically detected by using an algorithm we developed for estimating the instants corresponding to relevant gait events [76]. Both solutions for activity recognition and gait cycle detection were developed having online gait analysis in mind. In contrast with an offline solution, online gait analysis allows defining of a minimum number of required gait cycles and automatically stopping the acquisition of data when the defined number of gait cycles has already been detected.

The computed gait parameters provide information regarding the gait of the subject. In our system, these parameters are also used together with three anthropometric measures (length of the main body segments) to automatically identify the corresponding subject. This identification is carried out using a predictive model also obtained relying on machine learning techniques. When considering healthy subjects, our proposed solution was able to identify the subjects using a single gait cycle with a higher overall accuracy comparing with similar contributions, while using a lower number of features [77].

Another contribution that resulted from this thesis' work was a study on the validity of the gait analysis results provided by our system, when compared with those obtained with a gold standard system. In this study, we found that the agreement between systems was overall better for spatiotemporal than kinematic gait parameters. Furthermore, the agreement was overall better when using: the second version of the Kinect (Kv2) instead of the first sensor version; data acquired while the subject is walking towards the Kinect (WF) rather than away from it (for Kv2); a physical configuration of the Kinect corresponding to a height of 1 m comparing with the heights of 0.6 m or 1.34 m (for Kv2 and WF). When compared with similar contributions, our system outperformed the other proposed methods when considering all gait parameters.

Some of the solutions described above were used to carry out preliminary studies on the use of the Kinect for supporting the clinical gait assessment of patients with diseases that can affect the ability to walk, namely PD [79-84] and Transthyretin Familial Amyloid Polyneuropathy (TTR-FAP) disease [85]. The results of these studies show that gait information extracted from Kinect data can potentially be used to evaluate the severity of gait impairments and thus detect relevant changes in patients' gait. Further studies with more data from a greater number of patients are needed to confirm the obtained results.

The solutions for acquiring and reviewing Kinect data [78] have also been used in the clinical routine of the epilepsy monitoring unit of Klinikum Großhadern (Ludwig Maximilians University of

Munich, Germany) to continuously acquire data from epileptic patients [86, 87]. The data corresponding to seizures were used in a study where we found that some parameters, which were obtained using another solution developed by our group, can possibly be used to distinguish between different types of seizures [86].

This work was supported by European Union funds through the Human Capital Operational Programme (POCH) and by national funds through the Portuguese Foundation for Science and Technology (FCT), in the context of the PhD scholarship SFRH/BD/110438/2015.

1.4 Publications

The results of this thesis' research work have been reported in relevant journals, book chapters and conferences. The published contributions are listed below.

International Journals

A. P. Rocha, H. M. P. Choupina, M. d. C. Vilas-Boas, J. M. Fernandes, and J. P. S. Cunha, "System for automatic gait analysis based on a single RGB-D camera," *PLoS One*, vol. 13, p. e0201728 (24 pages), Aug. 2018. DOI: 10.1371/journal.pone.0201728 [ISI Impact Factor 2017: 2.766, Quartile 2017: Q1, Rank 2017: 15/64]

J. P. S. Cunha, H. M. P. Choupina, **A. P. Rocha**, J. M. Fernandes, F. Achilles, A. M. Loesch, et al., "NeuroKinect: A novel low-cost 3Dvideo-EEG system for epileptic seizure motion quantification," *PLoS One*, vol. 11, p. e0145669 (17 pages), Jan. 2016. DOI: 10.1371/journal.pone.0145669 [ISI Impact Factor 2017: 2.766, Quartile 2017: Q1, Rank 2017: 15/64]

Book chapters

H. M. P. Choupina, **A. P. Rocha**, J. M. Fernandes, C. Vollmar, S. Noachtar, and J. P. S. Cunha, "NeuroKinect 3.0: Multi-Bed 3Dvideo-EEG System for Epilepsy Clinical Motion Monitoring," in *Building Continents of Knowledge in Oceans of Data: The Future of Co-Created eHealth*, D. K. Adrien Ugon, Gunnar O. Klein, Anne Moen, Ed., ed: IOS Press, 2018, pp. 46-50. DOI: 10.3233/978-1-61499-852-5-46

International Conferences

A. P. Rocha, J. M. Fernandes, H. M. P. Choupina, M. d. C. Vilas-Boas, and J. P. S. Cunha, "Subject Identification Based on Gait Using a RGB-D Camera," in *Conference on Soft Computing and Pattern Recognition*, Porto, Portugal, 2018 (to be published in Advances in Intelligent Systems and Computing, Springer).

M. d. C. Vilas-Boas, **A. P. Rocha**, H. M. P. Choupina, J. M. Fernandes, T. Coelho, and J. P. S. Cunha, "The first Transthyretin Familial Amyloid Polyneuropathy gait quantification study - preliminary results," in *Annual International Conference of the IEEE Engineering in Medicine and Biology Society (EMBC)*, Seogwipo, Jeju Island, South Korea, 2017, pp. 1368-1371. DOI: 10.1109/EMBC.2017.8037087

J. P. S. Cunha, **A. P. Rocha**, H. M. P. Choupina, J. M. Fernandes, M. J. Rosas, R. Vaz, et al., "A novel portable, low-cost Kinect-based system for motion analysis in neurological diseases," in *Annual International Conference of the IEEE Engineering in Medicine and Biology Society (EMBC)*, Orlando, Florida, USA, 2016, pp. 2339-2342. DOI: 10.1109/EMBC.2016.7591199

A. P. Rocha, H. Choupina, J. M. Fernandes, M. J. Rosas, R. Vaz, and J. P. S. Cunha, "Kinect v2 based system for Parkinson's disease assessment," in *Annual International Conference of the IEEE Engineering in Medicine and Biology Society (EMBC)*, Milan, Italy, 2015, pp. 1279-1282. DOI: 10.1109/EMBC.2015.7318601

M. J. Rosas, J. P. S. Cunha, **A. P. Rocha**, H. Choupina, J. M. Fernandes, and R. Vaz, "Movement quantification for evaluation of gait in Parkinson's disease using a RGB-D camera system," *Movement Disorders*, vol. 30, pp. S470-471, 2015. DOI: 10.1002/mds.26295 [ISI Impact Factor 2017: 8.324, Quartile 2017: Q1, Rank 2017: 11/197]

A. P. Rocha, H. Choupina, J. M. Fernandes, M. J. Rosas, R. Vaz, and J. P. S. Cunha, "Parkinson's disease assessment based on gait analysis using an innovative RGB-D camera system," in *Annual International Conference of the IEEE Engineering in Medicine and Biology Society (EMBC)*, Chicago, IL, USA, 2014, pp. 3126-3129. DOI: 10.1109/EMBC.2014.6944285

National Journals

A. P. Rocha, H. Choupina, J. M. Fernandes, M. J. Rosas, R. Vaz, and J. P. S. Cunha, "Quantificação de movimento para apoio ao diagnóstico da doença de Parkinson utilizando um sistema de baixo custo baseado em RGB-D," *Sinapse*, vol. 15, p. 64, May 2015.

J. P. S. Cunha, **A. P. Rocha**, H. Choupina, J. M. Fernandes, M. J. Rosas, and R. Vaz, "Sistema de quantificação 3D de movimento portátil e de baixo custo para estimativa do sub-score de marcha em doentes parkisónicos," *Sinapse*, vol. 14, p. 67, May 2014.

National Conferences and Meetings

A. P. Rocha, J. M. Fernandes, J. P. Cunha, H. M. Choupina, M. J. Rosas, and R. Vaz, "A portable, low-cost Kinect-based system for motion analysis in neurological diseases," in *Encontro Ciência*, Lisbon, Portugal, 2017.

A. P. Rocha, J. M. Fernandes, J. P. Cunha, H. M. Choupina, M. J. Rosas, and R. Vaz, "A portable, low-cost Kinect-based system for motion analysis in neurological diseases," in *Research Day*, Aveiro, Portugal, Jun. 2017.

A. P. Rocha, H. Choupina, J. M. Fernandes, M. J. Rosas, R. Vaz, and J. P. S. Cunha, "Estimativa do sub-score UPDRS de marcha em doentes parkinsónicos usando um sistema de quantificação 3D de movimento portátil e de baixo custo," in *Congresso Nacional da Sociedade Portuguesa de Neurocirurgia*, Lisbon, Portugal, 2014, p. 20.

1.5 Thesis Outline

This thesis is divided into eight chapters, excluding this one:

- **Chapter 2** introduces the main applications of quantitative human motion analysis, including gait analysis. This chapter also describes the main sensors used for motion/gait analysis, with a greater focus on vision-based sensors, as well as the main steps and methods involved in the analysis. The sensors used for gait analysis are then described in more detail, along with a discussion of their main advantages and disadvantages, with a greater focus on vision-based sensors and particularly the Kinect (RGB-D camera).
- **Chapter 3** presents preliminary studies on the use of an RGB-D camera (Kinect) for supporting the clinical gait assessment of PD patients [79-84]. This chapter gives an overview of PD, including the associated symptoms and available treatments, as well as the methods used for clinical assessment. Then, the different studies carried out with PD patients and/or healthy subjects are described and the obtained results are presented and discussed.

- **Chapter 4** describes the software applications *KinectTracker* (*KiT*) and *Kinect Motion Analyzer* (*KiMA*) [78], which enable the online visualization and acquisition of the multimodal data provided by the Kinect camera (Kv1 or Kv2), as well as the review and selection of the acquired data for motion analysis, respectively.
- **Chapter 5** presents our solution for automated online gait cycle detection using a single RGB-D camera [76], which involves activity recognition for detecting the walking activity and the estimation of gait event instants needed for computing gait parameters. This chapter also includes the results of the validation of both activity recognition and gait event detection solutions, when using data acquired from healthy subjects.
- **Chapter 6** includes the evaluation of the validity of our automated gait analysis system based on the Kinect camera against a gold standard system. The chapter presents the results obtained when comparing: the two versions of the Kinect; two different walking activities; three different physical configurations of the Kinect.
- **Chapter 7** describes the solution for subject identification relying on machine learning techniques, as well as the results provided by our gait analysis system and [76, 77]. This chapter also presents the results of the validation of the proposed solution, when considering different groups of subjects (healthy subjects and/or PD patients).
- **Chapter 8** presents the final system for automated gait analysis, which resulted from the integration of the developed solutions for data acquisition, activity recognition, gait parameter computation and subject identification. The chapter gives an overview of the system, as well as a more detailed description of the integration of the different solutions for automated online gait analysis.
- **Chapter 9** summarizes the main conclusions of this thesis, and discusses possible directions for future work.

2 Human Motion Analysis

This chapter gives an overview of human motion analysis, including examples of its applications in different areas, as well as the different steps and methods involved in quantitative motion analysis relying on sensors, with a greater focus on vision-based sensors. The specific case of gait analysis is then presented, including the description of the main events that occur during gait, and the gait parameters that are traditionally computed. The sensors used for gait analysis are described in detail, with a greater focus on vision-based sensors and particularly the Microsoft Kinect camera. The main advantages and disadvantages of each type of sensor or sensor-based system are also presented and discussed.

2.1 Motion Analysis

Human motion analysis is the analysis of the human body's movements. The first studies on human motion relied on naked-eye observations [88, 89], which is a rather subjective approach. Nowadays, the available technology allows obtaining quantitative motion-related information from the real world, including people, bringing more objectivity to motion analysis. Quantitative motion analysis based on sensors has been an active research topic in the past years due to its different possible applications in various areas, including biomechanics, sports, healthcare, security, entertainment and human-computer interaction [18-21, 90-92].

Biomechanics is the study of the mechanical aspects of biological systems, including the human body and its movements [93, 94]. Quantitative motion analysis is thus very important in biomechanics, since it contributes to a better understanding of the mechanics of the human body [92, 95]. In sports, motion analysis involving professional athletes and sports activities in general has a great importance for personalized training, as well as injury detection or prevention [18, 20, 96].

In healthcare, motion analysis is especially important in the context of diseases or injuries that affect the movements of the patient. It can help in the diagnosis and/or assessment of patients with diseases that are characterized by abnormal and/or involuntary movements, the detection of movement-related injuries, and/or the physical rehabilitation of patients with movement impairments [26-30, 32, 58, 97-103]. Motion analysis can help detect relevant health-related events, such as falls in the elderly [55, 104-111].

In the security field, motion analysis can be useful for smart surveillance [18-21, 91] to automatically track subjects in a scene and/or detect abnormal behaviours, for example. It can also be

used for biometric identification for controlling the access to physical spaces, by using motion-related characteristics obtained from a given subject while performing a specific action or activity, such as walking [6-9, 18, 20].

Motion capture and analysis is also important in the areas of human-computer interaction and entertainment, which include the gaming and film industries [1, 18-20, 112-115]. Regarding human-computer interaction, gesture/action recognition can enable the interaction between people with computer applications through defined gestures/actions [20, 90, 91, 116, 117]. In the case of computer or video games, Microsoft has used a motion sensing device (Kinect camera) together with their Xbox video game console to allow interaction between players and video games using gestures, without requiring the players to hold any device [24]. In both the film and gaming industries, motion capture has also been used for digital character animation [112-115].

Quantitative human motion analysis relies on sensors, which measure physical quantities that can be used to detect and quantify human motion. The sensors most commonly used for motion analysis include wearable sensors, vision-based sensors, and floor sensors [13, 18-21, 23, 90, 91, 110, 118], which are described in more detail below.

Motion analysis based on wearable sensors usually involves the computation of measures over the data provided by sensor(s) attached to one or more parts of the body. Floor sensors (e.g., force plates or platforms, and pressure-sensitive mats or walkways) allow obtaining measures related with balance or gait when a subject stands or walks over them (they are installed or placed on the floor), based on ground reaction force or pressure data. Vision-based sensors provide colour (RGB), infrared (IR) or both RGB and IR/depth images (depth information is obtained relying on IR light). Systems based on vision-based sensors can be either marker-based or markerless (do not use markers), and rely either on a single or multiple cameras.

In the case of markerless camera-based systems, the first step of motion analysis is human detection, i.e., the segmentation of the regions corresponding to people from the rest of the image [18]. For human detection, it is firstly necessary to segment the image regions corresponding to moving objects in the scene. In the case of RGB images, motion segmentation relies mostly on temporal or spatial information of the images. One of the most popular methods for motion segmentation is background subtraction, where moving objects are detected by differencing between the current image and a reference background image (sensitive to changes in the background). Other approaches that are more adaptive to a dynamic environment include statistical methods, temporal differencing and optical flow [18].

When using depth data (i.e., distance between the camera and the object in the scene for each image pixel [91, 119]), motion segmentation is simpler when compared with RGB images, since the

objects in the scene can be easily segmented based on the depth information [91]. Since the depth information is obtained using IR light, segmentation is not affected by changes in the background, such as variations in lighting conditions.

If there are other moving objects in the scene besides people, the next step of motion analysis is object classification, i.e., the recognition of which segmented regions correspond to people [18]. This recognition is usually performed using machine learning techniques based on shape or motion information, for example. If the moving regions are known to be people, the human recognition step is not necessary.

For each region corresponding to a person, it is then necessary to track it over time [18]. Tracking usually involves matching objects in consecutive frames through features such as points, lines or blobs. Depending on the considered criteria, subject tracking can be divided into different groups: tracking of different body parts or whole body; single-, multi-, or omni-directional view; 2-D (two-dimensional) or 3-D (three-dimensional); indoors or outdoors; tracking of a single or multiple persons; moving or stationary camera.

The tracking methods include tracking based on models, regions, active contouring or features [18]. In model-based tracking, the geometric structure of the human body is represented as a stick figure (combination of line segments connected by joints), 2-D contour (2-D ribbons or blobs) or volumetric model (3-D volumes, such as elliptical cylinders, cones, and spheres). Region-based tracking consists of tracking a connected region (e.g., combination of blobs representing different body parts) associated with each moving person over time, using a cross-correlation measure. Active-contour-based tracking tries to obtain a representation of the outline of the object relying on active contour models or snakes, and then dynamically update it over time. Feature-based tracking uses low-level features, such as points or lines, on the object for tracking.

In the specific case of the Kinect (RGB-D camera), besides colour and/or IR images and depth information, it also provides silhouette information and the 3-D position of several body joints. Kinect's tracking algorithm for joint position estimation (or pose estimation) is based on the research presented in [119]. Firstly, per-pixel body part recognition is performed over each silhouette (region corresponding to a person), using depth image features and machine learning techniques. Then, hypotheses of joint positions are estimated by finding local centroids of the body part probability mass using mean shift mode detection [24, 119]. Finally, a skeleton model (or stick figure) is fitted to the hypothesized joint positions, taking into account temporal and kinematic constraints [24].

For marker-based vison-based systems, motion analysis consists of detecting and tracking the position of markers attached to the subject's body [120, 121]. There are two main types of markers: active and passive [92, 120, 121]. Active markers are light-emitting diodes (LED), which emit

light in the visible or infrared light spectrum, presenting a high contrast with the background. Each LED is activated at a time, enabling the automatic identification and tracking of each marker. Passive markers are retro-reflective markers, which reflect infrared light and thus present a high contrast with the background in infrared images. To deal with the presence of several markers at the same time in each image it is necessary to use labelling algorithms for identifying and tracking each marker [120]. For both types of markers, the high contrast between markers and background facilitates their segmentation using thresholding [120, 122].

When the position of body joints is tracked, it is possible to extract measures that characterize the subject's movements. Some examples of these measures are the velocity and acceleration of joints, the distance between adjacent or non-adjacent joints, and the angle at certain joints.

Gait Analysis

Human gait analysis is a special branch of human motion analysis, which involves the study of human walking [22, 95]. Gait analysis is also useful in different areas, including biomechanics, sports, healthcare and security [5-9, 13, 23, 92, 121]. In biomechanics, it helps to better understand the mechanics of the human body during the walking activity [92]. In sports, it can be used for improving the performance of athletes, and injury prevention [13]. In healthcare, it can help to detect and/or assess gait impairments resulting from injuries or diseases, and evaluate the improvement or decline of gait function during treatment and/or rehabilitation [13, 23, 121]. In the security industry, gait information can be used for verifying the identity of a given subject [5-9], with the aim of smart surveillance or access control, for example.

In clinical practice, it is still common to use traditional rating scales for gait assessment, in which experts observe the patient's gait by asking them to walk and then decide on the gait quality by assigning a score [23]. This assessment method can be rather subjective. However, with the advent of sensors and their widespread use in our daily lives, systems based on sensors can be used to detect, track and quantify human motion during gait, allowing a more objective gait analysis.

Quantitative human gait analysis usually relies on wearable sensors [13, 23, 123-125], vision-based sensors [23, 55-57, 65, 126-131] and/or floor sensors [23, 127-133]. These sensors are described in more detail below, along with a discussion of their main advantages and disadvantages.

Gait analysis has some overlap with motion analysis, including the detection and tracking of people over time in the case of vision-based sensors and/or the computation of measures that characterize motion. In the case of gait analysis, it also traditionally involves the computation of parameters for each gait cycle performed by the subject while walking. Therefore, when computing traditional gait parameters, it is firstly necessary to identify gait cycles.

A gait cycle or stride corresponds to the time interval between two successive occurrences of a repetitive gait event [22], such as the foot contact or heel strike, i.e., the instant when the foot makes contact with the ground. When considering this gait event, a left/right gait cycle is the time interval between two consecutive left/right heel strikes. A right gait cycle and associated heel strikes are illustrated in Figure 2.1. Each gait cycle includes two steps, where a step is the time interval between two consecutive heel strikes of opposite sides.

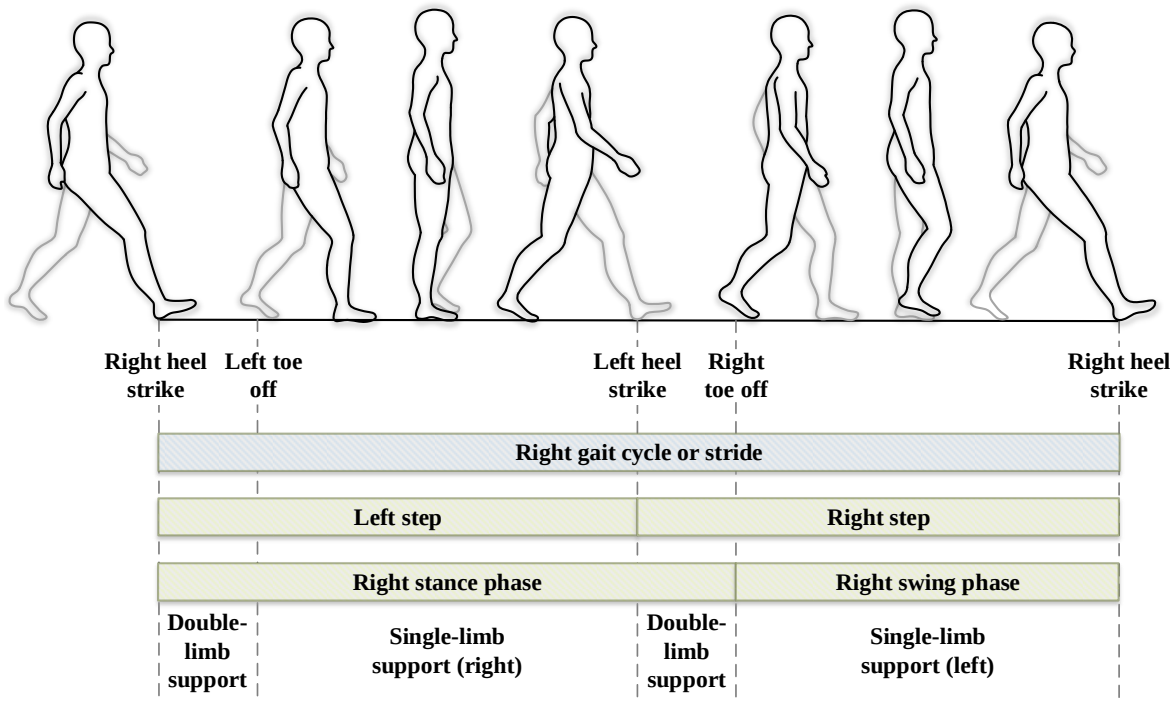

Figure 2.1. Right gait cycle performed by a subject while walking, including the associated gait events and phases (adapted from the figures included in [134]).

Other gait event that occurs during a gait cycle is the toe off, i.e., the instant at which the foot leaves the ground. The toe off events that occur during a right gait cycle are also shown in Figure 2.1. Considering the heel strike and toe off events, a gait cycle can be divided in two main phases: stance and swing. The stance phase is the time interval between a heel strike and the following toe off associated with the same foot. The swing phase is the time interval between a toe off and the following heel strike associated with the same foot.

A gait cycle can also be divided according to whether only one or both feet are in contact with the floor: single-limb and double-limb support phases, respectively. The single-support phase corresponds to the time intervals between each toe off and the following heel strike of the opposite feet. The double-support phase correspond to the time intervals between each heel strike and the

following toe off associated with the opposite feet. The different phases of a right gait cycle are also represented in Figure 2.1.

The gait parameters traditionally computed include the following [22, 57, 60, 61, 64, 65]:

- Spatiotemporal
  - Spatial
    - **Stride length** – distance between two consecutive placements of the same foot (see Figure 2.2 for a right stride)
    - **Step length** – distance between two consecutive placements of opposite feet (see Figure 2.2 for left and right steps)
    - **Stride/Step width** (or walking base) – side-to-side distance between the line of the two feet, usually considering the midpoint of the back of the heel (see Figure 2.2)
  - Temporal
    - **Stride duration or time** – duration of a gait cycle or stride
    - **Step duration or time** – duration of a step
    - **Stance duration or time** – duration of the stance phase of a gait cycle
    - **Swing duration or time** – duration of the swing phase of a gait cycle
    - **Single-support duration or time** – duration of the single-limb support phase of a gait cycle
    - **Double-support duration or time** – duration of the double-limb support phase of a gait cycle
  - **Gait speed –** distance covered by the whole body in a given time interval (for a gait cycle, it is computed as the stride length divided by the stride duration)
  - **Cadence –** number of steps taken in a given time (for a gait cycle, it is computed as 1 divided by the stride duration)
  - **Foot swing velocity** – maximum velocity of the left/right foot during the swing phase of a left/right gait cycle
- Kinematic
  - **Peak hip flexion** – maximum value for the left/right hip angle in the sagittal plane during hip flexion for a left/right gait cycle
  - **Peak hip extension** – minimum value for the left/right hip angle in the sagittal plane during hip extension for a left/right gait cycle
  - **Total hip range of motion** – difference between the maximum and minimum values for the left/right hip angle in the sagittal plane for a left/right gait cycle
  - **Peak knee flexion** – maximum value for the left/right knee angle in the sagittal plane during knee flexion for a left/right gait cycle

- **Peak knee extension** – minimum value for the left/right knee angle in the sagittal plane during knee extension for a left/right gait cycle
- **Total knee range of motion** – difference between the maximum and minimum values for the left/right knee angle in the sagittal plane for a left/right gait cycle
- **Total ankle range of motion** – difference between the maximum and minimum values for the left/right ankle angle in the sagittal plane for a left/right gait cycle

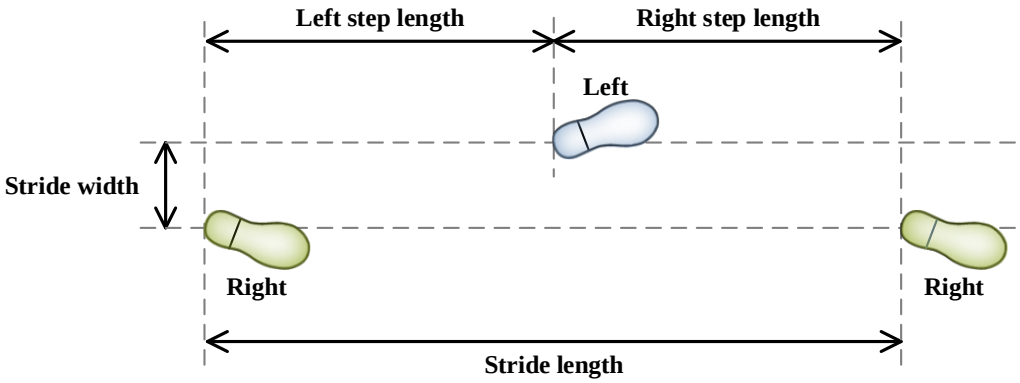

Figure 2.2. Spatial gait parameters for a right gait cycle or stride (adapted from the figure included in [22]).

2.2 Sensors for Gait Analysis

The sensors most commonly used for gait analysis can be divided into the following three main groups [23]:

- Wearable sensors (e.g., accelerometer, gyroscope, force sensor [2, 13, 23]);
- Vision-based sensors (e.g., RGB, infrared and RGB-D cameras [91, 120, 122]);
- Floor sensors (e.g., force plates/platforms, pressure-sensitive mats/walkway [23]).

The main advantages and disadvantages of these sensors are included in Table 2.1.

Wearable sensors are meant to be worn, by attaching them the body or placing them inside a pocket or the shoes, for example. These sensors include accelerometers, gyroscopes, force sensors, flexible goniometers and electromyography sensors, which measure acceleration, angular velocity, ground reaction forces, angles and muscle activity information, respectively [13]. These measurements can be used to compute spatiotemporal and/or kinematic gait parameters.

Table 2.1. Sensors used for gait analysis, including their main advantages and disadvantages.

Sensors		Advantages	Disadvantages
Wearable sensors		– Low-cost – Portable	– Limited number of traditional gait parameters when using one sensor type – Intrusive and can restrict movements – Time-consuming setup (for a large number of sensors) – Need to be frequently charged
Vision-based sensors	**Marker-based multi-camera system**	– Gold standard for motion capture – 3-D motion tracking – Less sensitive to self-occlusions than single-camera systems – Not sensitive to changes in the environment (e.g., lighting conditions) when using infrared cameras – Can be used to obtain all traditional gait parameters	– Expensive – Not portable – Time-consuming setup (marker placement and calibration) – Intrusive and can restrict movements – Requires tight-fitting clothing
	RGB camera	– Low-cost (comparing with marker-based multi-camera systems) – Portable and fast to set up (single camera) – Minimally intrusive (markerless) – Can be used to obtain all traditional gait parameters	– 2-D motion tracking only (single camera); 3-D tracking possible but requires multiple cameras – Sensitive to self-occlusions (single camera) – May require the control of the environment (e.g., lighting conditions, background colour) and subject's clothing
	RGB-D camera	– Low-cost (comparing with marker-based multi-camera systems) – Portable and fast to set up (single camera) – Minimally intrusive – 3-D motion tracking with a single camera – Not sensitive to changes in the environment (e.g., lighting conditions) – Calibration not required (single camera) – Can be used to obtain all traditional gait parameters	– Sensitive to self-occlusions (single camera)
Floor sensors	**Force plates**	– Minimally intrusive	– Expensive – Not portable (when installed on the floor) – Limited to spatiotemporal gait parameters
	Pressure-sensitive mats/walkway	– Portable – Minimally intrusive	– Expensive – Limited to spatiotemporal gait parameters

From the sensors included in Table 2.1, only the wearable sensors are carried by the subject, allowing long-term continuous monitoring at any time and place [23]. They are also generally less expensive and more portable than non-wearable sensors. On the other hand, wearable sensors rely on a battery with limited capacity, which needs to be regularly charged (sometimes every day). Moreover, they can be uncomfortable to wear and restrict the natural movements, and their setup is time-consuming when using a large number of sensors. Another disadvantage is that only a limited number of traditional gait parameters can be obtained when using only one type of wearable sensor.

For regular or sporadic gait assessments, floor sensors or vision-based sensors are an alternative to wearable sensors. Floor sensors include force plates or platforms (e.g., Kistler [135], Bertec [136], AMTI [137]) and pressure-sensitive mats/walkways (e.g., GAITRite [138], Tekscan [139]), which have embedded force or pressure sensors and are installed or placed on the floor [23]. Force plates/platforms measure the ground reaction forces generated when a body stands or moves along them, and can be used to analyse balance and gait [23, 135-137]. A pressure-sensitive mat or walkway measures pressure, and can be used to study gait and foot pressure distribution [23].

Floor sensors are not as intrusive as systems using sensors or markers placed on the subject's body. Pressure-sensitive mats or walkways, as well as some force plates, are portable. However, both types of systems only allow obtaining spatiotemporal gait parameters. Furthermore, commercial force plates are expensive (prices vary between US$ 10,000 and US$ 20,000 [140]). Although there is a commercial low-cost portable force platform, the Nintendo Wii balance board (less than US$ 100), it was shown to have several limitations when compared with more expensive alternatives [140]. Pressure-sensitive mats/walkways are also expensive, with prices ranging from €4,000 to €54,000 depending on the number of sensors and specifications [23].

When compared with floor sensors, vision-based sensors can be used to track the position of joints from the whole body, allowing the computation of all traditional gait parameters described above. This type of sensors are described in more detail below.

Vision-Based Sensors

Vision-based sensors are image sensors included in cameras, which are able to detect and convert light within a spectral range (e.g., visible or IR light) into electronic signals [141]. These cameras include RGB, IR and RGB-D cameras [91, 120, 122]. RGB cameras have a sensor that is sensitive to visible light, providing images in the RGB (red, green, and blue) colour model. These cameras are the most commonly used in our daily life (e.g., digital and smartphone cameras). Nevertheless, IR and RGB-D cameras have also been widely used for motion/gait analysis [22, 23, 90, 91, 120, 121]. IR cameras have a sensor that is sensitive to infrared light, providing infrared image

sequences. RGB-D cameras include both type of sensors, being able to provide RGB images, as well as IR images and/or depth information [24, 91].

Vision sensor-based systems can be divided according to the type and number of used cameras. They can also be divided according to the use or not of markers attached to the subject's body: marker-based or markerless. It is also possible to divide them based on the number of dimensions in which they track movements: 2-D or 3-D.

Regarding marker-based systems, there are two main types of markers: active and passive [120]. Active markers include light-emitting diode (LED) markers, which are usually connected with wiring to a control unit also placed on the subject's body. Passive markers include retroreflective markers, i.e., markers that reflect IR light. There are several commercially available motion capture systems that rely on active LED markers, such as the systems by Northern Digital Inc. [142] and Codamotion [143]. Passive retroreflective markers are used in the systems by Vicon [144], OptiTrack [145] and Qualisys [146].

Marker-based systems usually rely on multiple cameras [142-146], allowing to minimize self-occlusions and obtain highly accurate 3-D marker trajectories [92, 147, 148]. For these reasons, these systems are often considered as the gold standard systems for motion capture, having been extensively used for validating other systems in the context of motion/gait analysis [12, 16, 55, 57, 60-65, 98, 100, 131, 149-156].

However, the use of marker-based multi-camera systems is mainly limited to laboratories [60, 92, 148, 150], since they are quite expensive (prices vary between US$ 5,000 and US$ 250,000 depending on the number of cameras [115]) and are not portable. Another disadvantage of these systems is that their setup is rather complex and time-consuming, since it requires not only the careful placement of markers at specific parts of the subject's body, but also calibration [21, 22]. Moreover, the markers and/or wiring can be uncomfortable for the subject to wear and can even interfere with or restrict the natural movements [92].

Single-camera systems are less expensive and more portable than multi-camera systems. They also have the advantage of not requiring calibration or synchronization between several cameras. Markerless systems have the advantage over marker-based systems of being less intrusive for the subjects and having a less time-consuming setup, since there is no need to place markers on several parts of the body.

Despite of the advantages referred above, markerless systems relying on a single RGB camera have the disadvantage of only enabling 2-D motion analysis. Motion analysis in 3-D using RGB cameras is possible, but only if two or more cameras are used simultaneously. Another disadvantage

of RGB camera-based systems is that they can be sensitive to changes in the environment, requiring a careful control of certain aspects (e.g., ambient lighting, background and/or clothing colour [122]) or the use of motion analysis methods that are robust to those changes [18]. These limitations can be overcome by using a camera that relies on IR rather than visible light.

RGB-D cameras provide colour images in a similar way to RGB cameras, as well as depth data and/or infrared images similarly to IR cameras. Systems based on RGB-D cameras commonly rely on the depth data obtained using an IR sensor for detecting subjects and tracking the position of their body joints, in a markerless way. Furthermore, a single RGB-D camera can be used for 3-D motion analysis, which is not possible when using a single RGB camera.

Therefore, a system relying on a single RGB-D camera has most of the advantages of markerless single-camera and marker-based multi-camera systems: motion capture in 3-D, low-cost, portable, fast to set up, minimally intrusive, and not sensitive to changes in the environment. However, it is sensitive to self-occlusions as other single-camera systems, and its joint position estimation can be less accurate comparing with marker-based multi-camera systems [17].

Although nowadays there are several available commercial RGB-D cameras, such as Intel's RealSense depth cameras [157], VicoVR [158], Orbbec cameras [159] and Stereolabs' ZED camera [160], the Microsoft Kinect was one of the first available low-cost RGB-D cameras. The Kinect was initially released as an add-on for Microsoft's Xbox 360 gaming console, becoming the fast-selling consumer electronics device in a period of 60 days [161]. Since its release, the Kinect has been widely used for research in the area of computer vision [12, 14-17, 38, 39, 42, 55-73, 75, 98-100, 103, 106, 107, 109, 149-152, 162-167].

Microsoft Kinect

The Microsoft Kinect was initially released in 2010 (US$ 150 [168]) as an accessory for the Xbox 360 gaming console to allow users to play games based on gestures without holding any controller (camera shown in Figure 2.3 (a)) [169]. In 2011, Microsoft released a beta version of a software development kit (SDK) [170], which enabled the development of Kinect-based applications running on Windows computers for use in various fields other than gaming, such as healthcare, robotics, retail, and education.

In 2012, the "Kinect for Windows" was released at a suggested price of US$ 249 together with the version 1.0 of the SDK, which allowed the development of commercial applications [171]. The last version (1.8) of the SDK for the first generation of the Kinect was released in 2013 [172]. The second generation of the Kinect was released in 2013 for Xbox One (camera shown in Figure

2.3 (b)) [173]. The "Kinect for Windows v2" was made available in 2014, together with the version 2.0 of the SDK, at a price of US$ 200 [174].

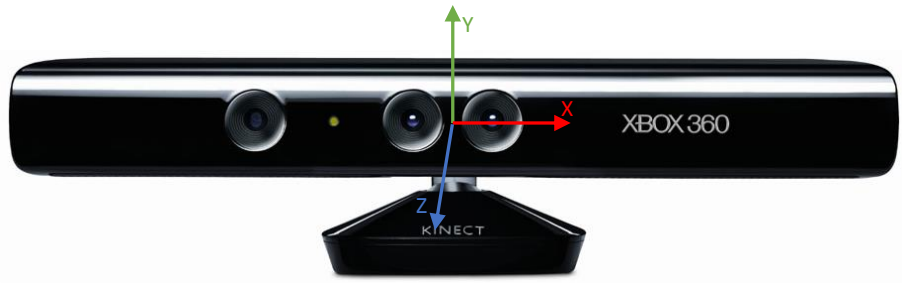

(a)

(b)

Figure 2.3. First (a) and second (b) generations of the Microsoft Kinect camera and associated coordinate system (adapted from the figure included in [175] and obtained from [176], respectively). The origin of the coordinate system is located at the centre of the first Kinect version [177] and at the centre of the IR sensor of the second Kinect version [176].

The Kinect camera includes a colour (RGB) camera, a depth sensor (composed of an IR projector or emitter and an IR camera) and a tilt motor (first camera version only) [24, 178, 179]. The depth sensor is used to provide depth information, which allows the extraction of the silhouette of the subjects in the scene, as well as the estimation of the 3-D position of their body joints relying on the proprietary algorithm running on the camera (described above) [119].

The main differences between the first and second versions of the Kinect (Kv1 and Kv2) are indicated in Table 2.2 [24, 178-181]. The provided data types are similar, with the difference that only the Kv2 allows the acquisition of both colour and IR images simultaneously [182]. The resolution of the data types is different when comparing the two Kinect versions (see Table 2.2), with the Kv2 providing colour data with better resolution (1920×1080 or Full HD) and depth data with slightly lower resolution than the Kv1. The maximum frame rate is of 30 Hz for both versions.

Table 2.2. Main differences between first and second versions of the Kinect (Kinect v1 and v2) [24, 178-181, 183].

	Kinect v1	Kinect v2
Data types	Colour, depth and body joint data	Colour, infrared, depth and body joint data
Data resolution (frame rate)	640×480 (30 Hz) or 1280×1024 (10 Hz) for colour, and 640×480 for depth data (30 Hz)	1920×1080 for colour (30 Hz), and 512×424 for infrared and depth data (30 Hz)
Body data	20 joints per subject (tracks up to six people, with full-body joint tracking for two subjects)	25 joints per subject (full-body joint tracking for up to six subjects)
Depth sensing approach	Structured light	Time-of-flight
Depth range	0.8–4 m (default mode); 0.4–3 m (near mode)	0.5–8 m
Field of view	57.5 degrees horizontally and 43 degrees vertically	70 degrees horizontally and 60 degrees vertically
Tilt motor	Yes (±27 degrees horizontally)	No
USB standard	2.0	3.0

One of the most important differences between the two Kinects is the improvement of the subject/joint tracking in the second version over the first one [182]. The Kv1 uses the structured light approach, which obtains the depth information by projecting a known light pattern onto the scene and analysing the distortion of the reflected pattern [1, 91, 180, 181]. On the other hand, the Kv2 relies on the time-of-flight approach, where the depth information is obtained by measuring the time that the light emitted by the IR projector takes to travel to an object in the scene and back to the camera, for each image pixel. The latter approach allows the Kv2 to provide better depth measurements, and consequently more precise 3-D joint position estimations [181].

The Kv1 tracks up to two subjects simultaneously (full body) and 20 joints per subject, while the Kv2 is able to track a greater number of subjects and joints (maximum of 6 subjects, and 25 joints). The additional body joints include the spine shoulder, thumbs and hand tips. The joints tracked by each Kinect version are illustrated in Figure 2.4. In this thesis, we use the Kv2 nomenclature to refer to the joints. For each joint, the provided position is the estimated position in relation to the coordinate system associated the Kinect, which is illustrated in Figure 2.3. The Kv2 also provides the hand state (opened, closed, “lasso”). Moreover, the Kv1 has two different tracking modes (near and default modes), while the Kv2 has a single mode.

Another difference between Kinect versions is their depth range (considering the default mode for Kv1): the maximum distance for Kv2 is twice as much as for Kv1 (8 m versus 4 m), and the minimum distance is smaller for Kv2 comparing with Kv1 (0.5 m versus 0.8 m). This leads to a considerably larger range for Kv2 (7.5 m) when compared with Kv1 (3.2 m). Moreover, Kv2 has a

wider field of view than Kv1. For this reason, the second version does not include a tilt motor, unlike the first version, which has a motor that can be used to adjust the camera's tilt angle horizontally.

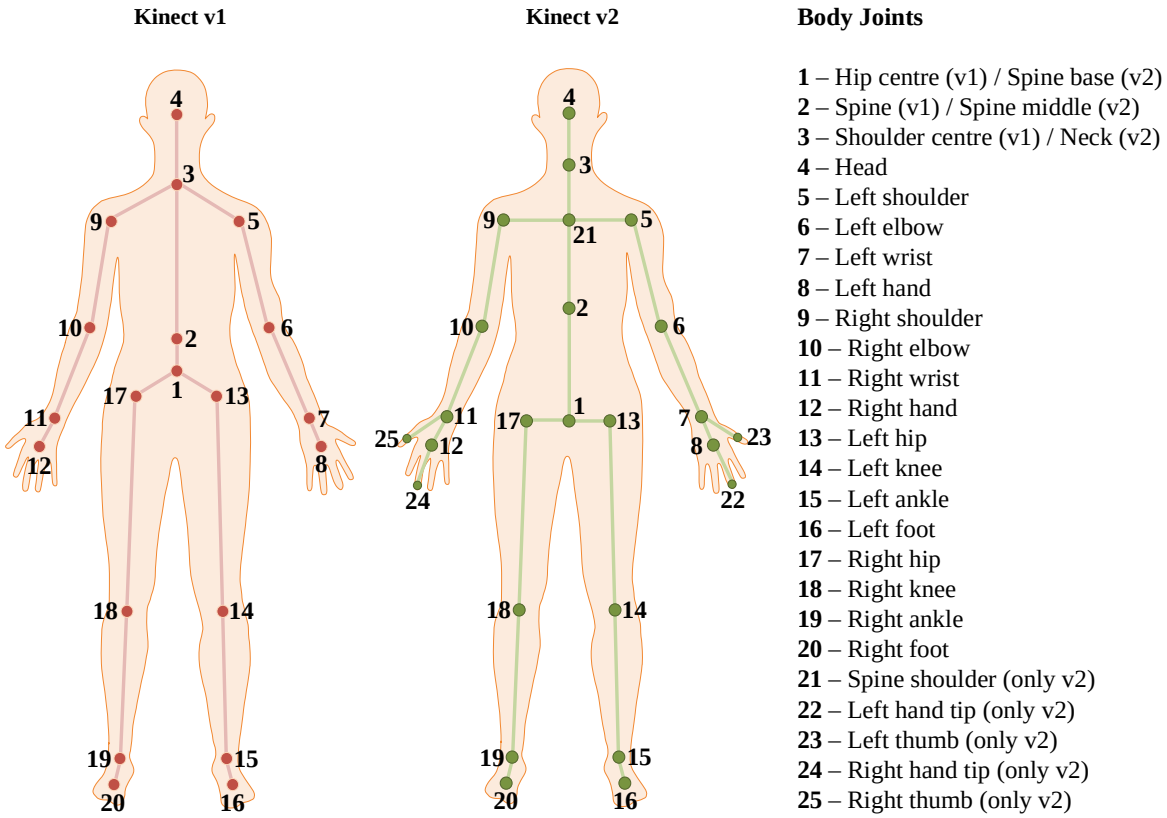

Figure 2.4. Body joints tracked by Kinect v1 and v2.
The Kinect v2 nomenclature is used in this thesis.

2.3 Summary

Quantitative analysis of human motion, including gait, has many applications in different areas, such as sports, healthcare, security and entertainment. The review of the main applications, which include activity recognition, motor function assessment and human identification, has allowed the identification of possible research directions for the thesis work.

The sensors used for gait analysis include wearable sensors (e.g., accelerometer, gyroscope), vision-based sensors (e.g., RGB, infrared and RGB-D cameras) and floor sensors (e.g., force plates, pressure-sensitive walkways). In this chapter, we discussed the main advantages and disadvantages of each sensor type. This discussion contributed to the choice of a markerless RGB-D camera, namely the Microsoft Kinect, for enabling quantitative gait analysis.

Motion analysis based on markerless vision-based sensors involves human detection, recognition and tracking. In the case of gait, the analysis also usually includes the identification of gait cycles and associated phases, as well as the computation of several parameters for each gait cycle. This chapter described the gait parameters that are traditionally computed during gait analysis, which have been considered for our objective of supporting gait assessment.

3 Preliminary Studies with Parkinson's Disease Patients

Parkinson's disease (PD) is a neurodegenerative disease that can lead to several motor symptoms, including hand tremor, slowness of movement and gait impairments [184, 185]. These symptoms have a negative impact on the patient's quality of life, but can be controlled using medication and/or surgical therapy (e.g., deep brain stimulation – DBS). In clinical practice, it is still common to assess the motor function of a PD patient using a rating scale [185, 186], such as the Unified PD Rating Scale (UDPRS), which can be rather subjective. This subjectivity can be overcome by using technology available today to obtain information that is more objective.

In the context of a collaboration with the Movement Disorders Unit of São João Hospital, Porto, Portugal (Rui Vaz, M.D. and Maria José Rosas, M.D.), preliminary studies were carried out with PD patients treated with DBS, with the main aim of answering the following question:

- Can a single RGB-D camera be used to support the clinical assessment of gait in PD?

The studies relied on 3-D data acquired from PD patients and/or healthy subjects, while they performed a simple gait task in a hospital environment. To verify if the information extracted from the 3-D data can be used to evaluate the severity of gait impairments in PD patients treated with DBS, we explored if that information allows distinguishing between healthy subjects and PD patients in different DBS states. The obtained results are presented in [81-84].

Since the physicians typically use the UPDRS for assessing PD patients, we also explored the possibility of using the quantitative gait information for estimating UPDRS gait and motor subscores. The results obtained with initial data acquisitions are presented in [79, 80].

The carried out studies additionally allowed verifying the suitability of our system based on an RGB-D camera for clinical environments. Moreover, they enabled the identification of desirable improvements regarding not only the software, but also the used setup and protocol.

3.1 Parkinson's Disease

Parkinson's disease is a progressive neurological disorder, which was firstly formally described by James Parkinson in 1817 [184, 185, 187]. This disease is associated with the loss of brain cells in the substantia nigra (a brain structure) that produce dopamine (a neurotransmitter), which can

lead to a large number of symptoms. The primary cause of PD is still unknown. However, in a similar way to other neurodegenerative diseases, the main known risk factor is age [184]. Genetic and environmental risk factors have also been associated with the disease.

Parkinson's disease is currently the second most common neurodegenerative disorder after Alzheimer's disease [188, 189]. In 2000, it was estimated that PD had a prevalence of 1.8% in European populations aged 65 or older, with an increase from 0.6% for ages between 65 and 69 to 2.6% for subjects aged between 85 and 89 years [190]. In 2005, it was estimated that there were over four million individuals worldwide with PD aged 50 or older, considering the five and ten most populous nations in Western Europe and the world, respectively [191]. This number is expected to double by 2030 [191], due to ageing of western populations [184]. Individuals under 50 years of age can also suffer from PD. Parkinson's disease in subjects with ages between 21 and 39 is called early or young onset PD, and it can correspond to 5–10% of PD patients [192].

3.1.1 Symptoms

Parkinson's disease symptoms can be divided into motor and non-motor symptoms [184, 185, 193]. Motor symptoms include the following:

- Bradykinesia (slowness or poverty of movement);
- Muscular rigidity (increased resistance when stretching a muscle passively);
- Rest tremor (tremor of head, upper and/or lower extremities when at rest);
- Postural instability or balance impairment (loss of postural reflexes);
- Festinating or shuffling gait (small shuffling steps);
- Freezing of gait (sudden and transient inability to move, usually when initiating or during walking or turning);
- Flexed posture (flexed neck and trunk posture, and flexed elbows and knees);
- Masked face (immobile and rigid facial expression);
- Slow, quiet speech.

Rest tremor, bradykinesia, rigidity and postural instability are generally considered the four cardinal symptoms of PD. Bradykinesia includes difficulties with planning, initiating and executing movement, and with performing sequential and/or simultaneous motor tasks, such as walking (usually with reduced arm swing). Postural instability, together with freezing of gait, is the most common cause of falls.

Gait impairments are one of the most important factors that contribute to a reduced quality of life in PD patients [194]. The assessment of gait should take into account several aspects, including the following:

- Raising from chair (difficulty standing up and the need to use arms of the chair to stand up);
- First step (difficulties taking the first step);
- Posture while walking (more stooped than expected for age);
- Speed (slower movement than expected for age – related to bradykinesia);
- Stride length (shorter steps);
- Turning (taking many steps to turn);
- Steadiness (impaired balance – related to postural instability).

3.1.2 Diagnosis and Follow-up

The first step of the clinical process associated with PD is diagnosis. After a patient has been diagnosed with PD, is then important to monitor the disease's progression and/or the outcome of the clinical therapeutic, to help the physician decide on the need or not to prescribe a new treatment and/or adjust the current treatment. Both diagnosis and follow-up assessment are typically carried out in a clinical environment by one or more physicians (e.g., neurologist, movement disorder specialist) [195].

Diagnosis

There is no definitive test for the diagnosis of PD [185]. Therefore, PD diagnosis is generally based on clinical criteria. The most widely accepted PD diagnostic criteria are the United Kingdom PD Society Brain Bank clinical criteria of probable PD, which are grouped in three main steps [185, 196]. The first step is the diagnosis of Parkinsonian syndrome, which involves the observation of the presence/absence of bradykinesia and at least muscular rigidity, 4–6 Hz rest tremor or postural instability. The second step is the exclusion of criteria for PD, including negative response to large doses of levodopa (medication), and a set of different symptoms, which can suggest an alternative diagnosis. The third step includes supportive prospective positive criteria for PD, such as asymmetric onset, excellent response to levodopa and clinical course of 10 years or more.

Other PD diagnostic criteria exist, such as those introduced by the National Institute of Neurological Disorders and Stroke [185], where symptoms or features are divided into two groups: char-

acteristic of PD (rest tremor, bradykinesia, rigidity and asymmetric onset) and suggestive of alternative diagnoses (e.g., freezing of gait in the first three years). The criteria are divided into three groups: definite, probable and possible.

Diagnosis may be difficult, especially early in the course of the disease, since some of the most characteristic PD symptoms may occur as a result of normal aging or other medical conditions [185].

Follow-up

Parkinson's disease clinical assessment during follow-up usually relies on a rating scale [185]. Several rating scales have been developed for the evaluation of motor impairment and/or disability of PD patients [186]. The scales considered as the most valid and reliable are the Columbia University Rating Scale (impairment only), Northwestern University Disability Scale (disability only) and Unified PD Rating Scale (both impairment and disability). Other scales include the Schwab and England Activities of Daily Living Scale (disability) and the Hoehn and Yahr Scale (severity of PD).

The Unified PD Rating Scale (UPDRS) was developed due to the problem of variability of existing scales and their frequent modifications, which made it difficult to compare the studied patient population and the obtained results [197]. This scale is a compromise and combination of various previous scales. Probably for this reason, it is broadly accepted for PD evaluation and has been used in many trials [186].

The UPDRS consists of the following six sections, where most items are rated from zero (normal) to four (severely affected) according to interview and/or clinical observation [198]:

I. Mentation, Behaviour and Mood – evaluation of intellectual impairment, thought disorder, depression and motivation/initiative.

II. Activities of Daily Living – self-evaluation of thirteen activities of daily living, including speech, handwriting, falling and walking.

III. Motor Examination – evaluation of motor function through fourteen items based on the Columbia University Rating Scale, including speech, facial expression, tremor at rest, rigidity, finger taps, leg agility, rising from chair, posture, gait, postural stability, body bradykinesia and hypokinesia.

IV. Complications of Therapy – evaluation of therapy complications (dyskinesias, clinical fluctuations and other complications), which are rated as "yes" or "no".

V. Modified Hoehn and Yahr Staging – modified version of the Hoehn and Yahr Scale, which divides the overall disease severity into eight stages (stage 0 corresponding to no signs of disease and stage 5 to wheelchair bound or bedridden unless assisted).

VI. Schwab and England Activities of Daily Living Scale – measure of a person's ability to perform daily activities in terms of speed and independence (0%–100%, with high percentages indicating a high level of independence, and low percentages indicating dependence).

3.1.3 Treatment

Presently, PD has no cure, but available treatment can provide a considerable improvement of life quality and functional capacity [184]. The main treatment approaches are medication and surgical therapy.

Medication

The main objective of the medication approach is to manage the motor symptoms, contributing to an improvement of the patient's quality of life and functional capacity [184, 199]. Levodopa in combination with a peripheral dopa decarboxylase inhibitor (e.g., carbidopa) is considered the most effective medication available for treating PD motor symptoms [184, 199]. Motor symptoms usually initially improve by 20–70%, with some symptoms steadily improving between the first week or two and the following three months. This medication can be maintained over the first five years of the disease for most patients.

Levodopa treatment has several possible side effects, including motor effects such as dyskinesias and motor fluctuations [184, 200]. Dyskinesia is the involuntary, erratic movement of the face, arms, legs and/or trunk, which tends to be more severe when increasing the dose of levodopa [189, 200]. Motor fluctuations are related to the "on-off" phenomenon, i.e., the change between "on" and "off" states [201]. The "on" state refers to periods during which the PD patient responds to levodopa, and symptoms are generally well controlled. On the other hand, the "off" state corresponds to periods of poor patient response to levodopa during which previous symptoms are again experienced.

Surgery

The surgical therapy approach consists mainly in implanting stimulating electrodes in the brain [202-204]. These electrodes are connected to an impulse generator, typically placed in the chest

under the skin. The generator is used to produce high frequency pulses to perform deep brain stimulation (DBS), through the stimulating electrodes. DBS can provide benefits for people with a variety of neurologic conditions, such as essential tremor and PD [202]. In the case of PD, DBS is used in patients whose motor symptoms have become difficult to manage with medication [204]. The best candidates are non-demented advanced PD patients with tremor, dyskinesia, significant motor fluctuations with considerable "off" time and good response to levodopa in the "on" state [202-204].

Deep brain stimulation is likely to improve some PD motor symptoms (e.g. tremor, bradykinesia and rigidity), as well as drug-induced dyskinesia and "off" states [202, 204]. On the other hand, it may worsen speech and cognition, and also involves inherent surgical risks [203]. In addition, as for the other treatments described above, DBS does not stop progression of the disease [204]. Furthermore, in order to achieve optimal results, it requires the adjustment of the stimulation settings (e.g., impulse duration, frequency and voltage) according to the response of each patient. An optimized electrode placement in the brain target is also necessary for achieving the best possible results. The benefit from surgery is usually maintained for at least four years [202].

3.2 Parkinson's Disease Assessment Support Using an RGB-D Camera

In the context of our collaboration with the Movement Disorders Unit of São João Hospital, preliminary studies were carried out to investigate if the quantitative data provided by a single RGB-D camera can be used to support the clinical gait assessment of PD patients treated with DBS.

In these studies we explored if the information extracted from 3-D body joint data can be used to distinguish between healthy subjects and PD patients in two different DBS states, with the aim evaluating the severity of gait impairments in PD. Given that the physicians commonly use a rating scale such as the UPDRS for PD assessment, we also verified if the gait and/or motor subscore of UPDRS can be estimated using the same gait information.

The studies were performed with three datasets acquired in different experiments involving PD patients treated with DBS and/or healthy subjects, where they performed a simple gait task in a hospital environment. The distinction between patients and healthy subjects was studied using initial acquisitions [81], as well as a larger dataset [82-84]. The estimation of UPDRS scores was also explored using initial acquisitions [79, 80], as well as a larger dataset.

All experiments were conducted at São João Hospital (Porto, Portugal) and were approved by the hospital's Ethics Committee.

3.3 Materials and Methods

3.3.1 Subjects

The demographics of the subjects that participated in each one of the three experiments (EXP1, EXP2 and EXP3) are presented in Table 3.1. The UPDRS scores assigned by one or two physicians to each PD patient before or after each data acquisition are presented in Table 3.2. In this table, the gait/motor score is indicated for each data acquisition session and each considered DBS state (stimulator switched on or off – Stim-on or Stim-off). For EXP3, one or more sessions were performed always in the Stim-on state. For some of those sessions, the scores are not indicated, since they were not available due to various reasons (e.g., the appointment with the physician did not take place in that day, or the scores were not included in the physician's notes).

3.3.2 Experimental Setup and Protocol

Experiment EXP1 took place at a room in São João hospital (Porto, Portugal), which is shown in Figure 3.1 (a). The location of EXP2 was changed to a corridor in the same hospital (see Figure 3.1 (b)), due to the availability of more space, which allowed to increase the distance walked in each trial. Due to logistical limitations, the experiment EXP3 took place in another corridor in the hospital, which can be seen in Figure 3.1 (c).

Table 3.1. Demographics of the subjects that participated in each experiment. SD, Min, Max and BMI stand for standard deviation, minimum, maximum and body mass index.

		EXP1		EXP2		EXP3
		PD patients	**Healthy subjects**	**PD patients**	**Healthy subjects**	**PD patients**
Gender (male/female)		2/1	2/1	9/2	4/4	8/3
Age (years)	**Mean ± SD**	54 ± 5	49 ± 4	61 ± 9	56 ± 13	59 ± 5
	[Min, Max]	[47, 59]	[46, 54]	[43, 77]	[40, 74]	[50, 68]
Height (m)	**Mean ± SD**	1.68 ± 0.09	1.65 ± 0.06	1.67 ± 0.07	1.68 ± 0.13	1.68 ± 0.08
	[Min, Max]	[1.59, 1.80]	[1.58, 1.72]	[1.50, 1.80]	[1.45, 1.86]	[1.57, 1.85]
Weight (kg)	**Mean ± SD**	82.7 ± 5.2	83.3 ± 26.4	81.6 ± 11.5	79.0 ± 12.7	70.3 ± 9.7
	[Min, Max]	[78.0, 90.0]	[54.0, 118.0]	[59.0, 96.0]	[65.0, 99.0]	[60, 93]
BMI (kg/m^2)	**Mean ± SD**	29.7 ± 3.7	30.4 ± 9.3	29.3 ± 4.5	28.0 ± 4.6	24.8 ± 2.8
	[Min, Max]	[24.7, 33.5]	[21.6, 43.3]	[22.2, 37.8]	[22.5, 38.0]	[21.5, 30.7]

Table 3.2. UPDRS motor and gait scores assigned to the PD patients when the DBS stimulator is switched on (Stim-on) and off (Stim-off), for each experiment.

Experiment	PD patient	Data acquisition session	UPDRS score			
			Motor[a]		Gait[b]	
			Stim-on	Stim-off	Stim-on	Stim-off
EXP1	1	#1	13	31	1	1
	2		7	26	1	1
	3		11	42	0	2
EXP2	1	#1	19	36	0	2
	2		12	50	0	2
	3		37	63	3	3
	4		9	22	1	2
	5		21	26	0	0
	6		9	27	0	1
	7		40	46	2	2
	8		16	24	2	2
	9		18	—	1	—
	10		26	—	2	—
	11		14	46	1	2
EXP3	1	#1	1	—	0	—
		#2	5		0	
		#3	3		0	
	2	#1	9		1	
		#2	11		0	
		#3	16		1	
	3	#1	9		0	
		#2	9		0	
		#3	—		—	
		#4	—		—	
	4	#1	12		0	
		#2	30		0	
	5	#1	14		1	
		#2	17		1	
		#3	20		2	
	6	#1	—		—	
		#2	—		—	
		#3	7		0	
	7	#1	13		1	
		#2	9		0	
		#3	—		—	
	8	#1	—		—	
		#2	—		—	
	9	#1	12		0	
		#2	—		—	
	10	#1	3		0	
		#2	—		—	
	11	#1	—		—	

[a] Part III of UPDRS, with the score value ranging from 0 to 108 [198, 205].

[b] Item 29 of UPDRS, with the score value ranging from 0 (normal) to 4 (cannot walk) [198].

(a) (b) (c)

Figure 3.1. Location of experiments EXP1 (a), EXP2 (b), and EXP3 (c), and used setup including a Kinect v1 and/or a Kinect v2 mounted on a tripod and connected to laptop.

In Figure 3.1, we can also see the setup used in each experiment. The setup of EXP1included a Kinect v1 mounted on a tripod and connected to a laptop. The setup of both EXP2 and EXP3 included two Kinects, a Kinect v1 (Kv1) and a Kinect v2 (Kv2), connected to a laptop each. In EXP2, each Kinect was mounted on a tripod, while a single tripod was used in EXP3 for both Kinects (Kv1 placed on top of the Kv2).

An illustration of each experiment's setup is presented in Figure 3.2, including the relevant distances, as well as the Kinects' height (i.e., the distance between its base and the floor) and tilt angle (i.e., the angle between the z-axis associated with the camera and the horizontal plane perpendicular to the gravity force). The approximate practical depth range for each Kinect (i.e., the distance range in relation to camera for which all body joints are tracked) is represented by the diagonal stripe pattern. This range depends on the associated height and tilt angle.

In EXP1, the height and tilt angle of the Kv1 were chosen with the aim of maximizing the practical depth range of the sensor, while also taking into account the room dimension. In EXP2, the Kv1 and Kv2 were placed facing each other, with a distance of approximately 8 m between them. In EXP3, the used height of 1 m corresponds to an intermediate value in relation to the heights used for Kv1 and Kv2 in EXP2. The tilt angle for each Kinect was adjusted to maximize the practical depth range for the chosen height.

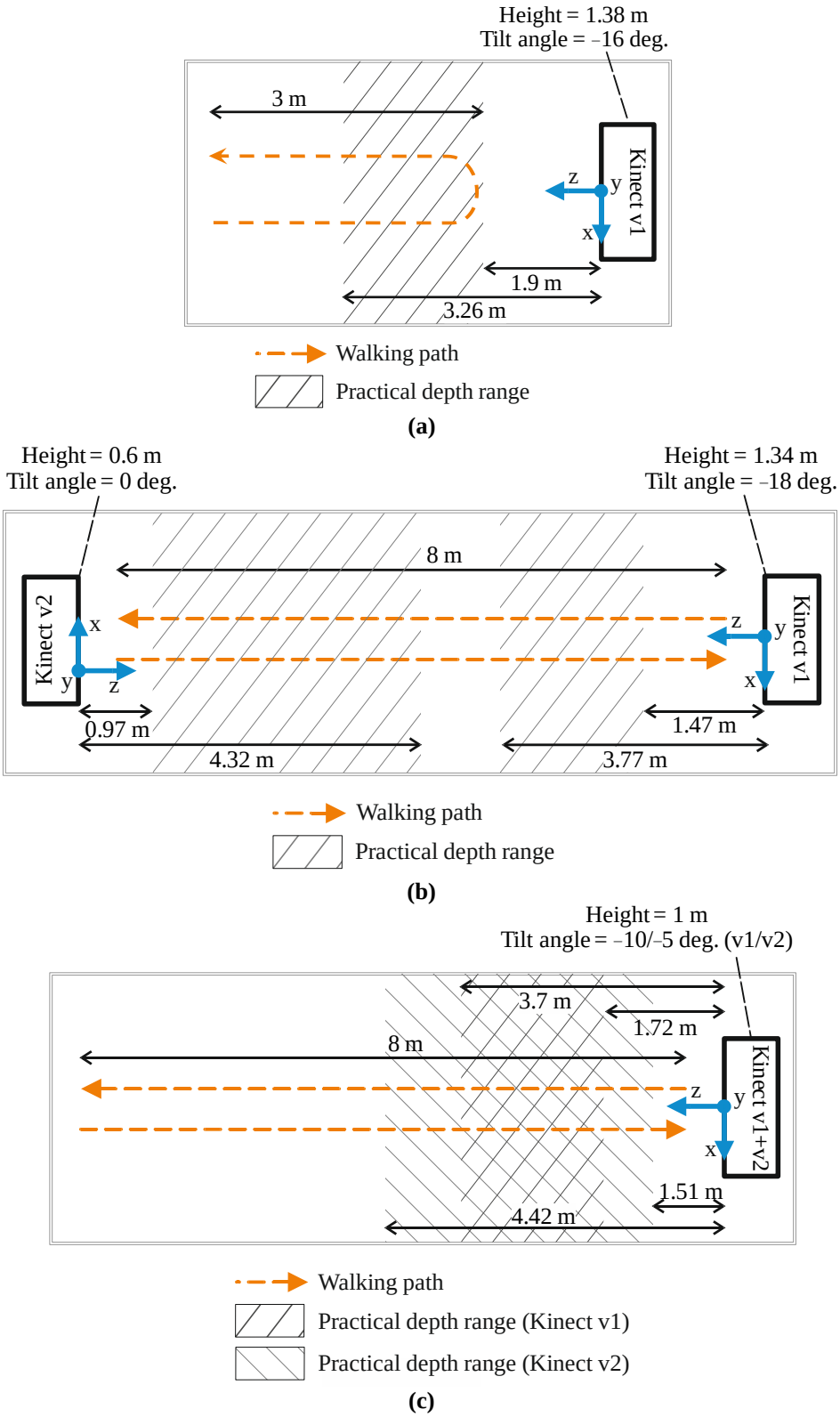

Figure 3.2. Experimental setup used in experiment EXP1 (a), EXP2 (b) and EXP3 (c), including the height and tilt angle of the Kinect(s), the walking trajectory, and the relevant distances.

For all experiments, the protocol included a simple gait task: walking towards and then away from the Kinect, at a self-selected comfortable pace. The arrowed dashed line in Figure 3.2 represents the walking path for each experiment. The total covered distance was of 6 m for EXP1, and 16 m for EXP2 and EXP3.

In EXP1, the task was performed once by the healthy subjects, and twice by the PD patients (first in the Stim-on state, and then about 15–18 min later in the Stim-off state). In EXP2, each subject carried out the gait task 2 to 15 times (8 ± 5 trials), depending on the gait difficulties. For the PD patients, the task was performed in both Stim-on and Stim-off states, with a time interval between acquisitions in the different states ranging from 8 min to 1h40 (39 ± 38 min).

EXP3 included one or more data acquisitions with each patient, in different days, but always in the Stim-on state. An acquisition was carried out with each patient on the day of discharge from hospital, after undergoing DBS surgery. Whenever possible, we also performed an acquisition in each follow-up appointment, during the six months after surgery. The number of gait trials per acquisition varied between 1 and 12 (8 ± 2 trials), depending on the gait difficulties of each patient.

3.3.3 Data Acquisition and Processing

The datasets obtained in each experiment are presented Table 3.3, including the corresponding number of days, number of subjects, DBS state for PD patients, number of data acquisitions per subject and number of gait trials per acquisition (mean and standard deviation for DS2 and DS3). For each acquisition, the Kinect data were acquired at an approximate frame rate of 30 Hz, using our *KiT* application [78].

Table 3.3. Datasets obtained in each experiment, including the number of days and subjects, DBS state for PD patients, and number of data acquisitions per subject and of gait trials per acquisition.

Datasets	Number of days	Number of subjects			DBS state for patients	Number of data acquisitions per subject	Number of gait trials per acquisition
		PD patients	Healthy	All			
DS1	1	3	3	6	Stim-on and Stim-off	1 for healthy subjects, and 2 on the same day for patients (one in each DBS state)	1
DS2	3 (period of 9 months)	11	8	19			8 ± 5
DS3	19 (period of 12 months)	11	—	—	Stim-on	1 to 4 (3 ± 1), on different days	8 ± 2

The first step of data processing consisted of converting the 3-D position of each joint (x, y, z) into a coordinate system corresponding to a non-tilted camera (tilt angle of 0 degrees), for each body joint data frame. This coordinate conversion facilitates the comparison between the 3-D joint positions acquired using different camera tilt angles, and was performed for all studies presented in this thesis.

Tilting the Kinect by rotating it around its x-axis leads to the effect illustrated in Figure 3.3. Assuming that the camera is placed in such a way that its z-axis is parallel to the horizontal plane (tilt angle of 0 degrees) where a vertical object is standing, two points A and B on this object will have the same value for the z-coordinate ($z_A = z_B$ in the figure). However, if the Kinect is tilted around its x-axis, so that its z-axis rotates by an angle α relative to its horizontal position, then the coordinates of points A and B will have different values in the rotated coordinate system $x'y'z'$ ($z'_A < z'_B$ in the figure). In a similar way the y'-coordinates will be different from the y-coordinates.

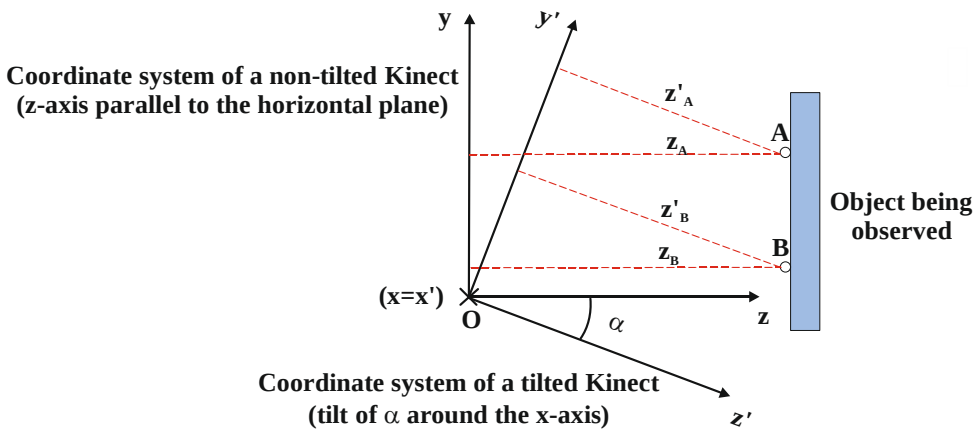

Figure 3.3. Coordinate systems of a non-tilted and tilted Kinect, and the effect that the tilting has on the distance between the Kinect and a given object in the z-axis.

To convert a position (x, y, z) into the coordinate system corresponding to a non-tilted camera, the coordinates of the converted position (x', y', z') were computed using the following equations:

$$x' = x \tag{3.1}$$

$$y' = -\sin(\alpha) \times z + \cos(\alpha) \times y \tag{3.2}$$

$$z' = \cos(\alpha) \times z + \sin(\alpha) \times y \tag{3.3}$$

The next step of data processing consisted of identifying the gait cycles performed by the subjects during the gait trials. For the first studies, the gait cycles of DS1 and DS2 were manually selected, by identifying the instants corresponding to heel strikes relying on the acquired colour and/or depth data. In the case of DS2, the instants corresponding to heel strikes were saved in our *KiMA* application [78]. Only the data corresponding to walking towards the camera were considered, since we visually verified that the data acquired while walking away from the camera were much noisier.

For the last study presented below, the gait cycles of DS2 and DS3 were automatically detected using the solution described later in this thesis. We again considered only the data corresponding to walking towards the camera, since we confirmed in a validation study also presented in this thesis that the data corresponding to walking away from the sensor leads to higher detection errors.

The number of identified gait cycles for each dataset (manually for DS1 and DS2 and automatically for DS3) is presented in Table 3.4. In the second day of EXP2, Kv2 data were not acquired since the camera was unavailable due to technical problems. In the third day of EXP2, it was not possible to acquire data from two patients in the Stim-off state. In addition, the battery of the DBS stimulator was low for another patient, so the acquisition carried out in the Stim-on state was not considered in the studies presented below. It was also not possible to acquire Kv2 data from another patient, due to difficulties of the camera in tracking the subject.

Table 3.4. Number of gait cycles included in each dataset.
The version of the used Kinect(s) and the associated number of subjects are also indicated.

Dataset	Kinect	Number of subjects	Number of gait cycles			
			PD patients		Healthy subjects	All subjects
			Stim-on	Stim-off		
DS1	**Kv1**	3 healthy + 3 PD patients	5	6	6	17
DS2[a]	**Kv1**	8 healthy + 11 PD patients	109	122	58	289
	Kv2[b]	5 healthy + 8 PD patients	157	143	118	418
DS3	**Kv1**	11 PD patients	282	—	—	—
	Kv2		667			

[a] For both Kv1 and Kv2, data were not acquired from two patients while in the Stim-off state. Additionally, the battery of the DBS stimulator was low for another patient.

[b] Kv2 data were not acquired from one of the patients.

For each data frame of a left/right gait cycle, the following 34/43 measures (Kv1/Kv2) were computed:

- Velocity of the head, neck, spine base and spine middle, the right/left shoulder, elbow, wrist and hand, and the left/right foot, ankle, knee and hip, using (3.4);
- Velocity of the left/right hand tip and thumb, and the spine shoulder (Kv2 only), using (3.4);
- Acceleration of the head, neck, spine base and spine middle, the right/left shoulder, elbow, wrist and hand, and the left/right foot, ankle, knee and hip, using (3.5);
- Acceleration of the left/right hand tip and thumb, and the spine shoulder (Kv2 only), using (3.5);
- Distance between the feet, ankles, knees, hands, wrists and elbows, using (3.6);
- Distance between the hand tips and thumbs (Kv2 only), using (3.6);
- Angle at the left/right knee (defined by hip, knee and ankle joints), right/left elbow (defined by shoulder, elbow and wrist joints), neck (defined by head, neck and spine middle/shoulder joints) and spine middle (defined by neck/spine shoulder, spine middle and spine base joints), using (3.7).
- Angle at the spine shoulder (defined by neck, spine shoulder and spine middle joints) (Kv2 only), using (3.7).

$$\text{velocity} = \sqrt{v_x^2 + v_y^2 + v_z^2} \approx \sqrt{\frac{\Delta x^2 + \Delta y^2 + \Delta z^2}{\Delta t^2}} \tag{3.4}$$

$$\text{acceleration} = \sqrt{a_x^2 + a_y^2 + a_z^2} \approx \sqrt{\frac{\Delta v_x{}^2 + \Delta v_y{}^2 + \Delta v_z{}^2}{\Delta t^2}} \tag{3.5}$$

$$\text{distance} = \left\| \overrightarrow{P_1 P_2} \right\| \tag{3.6}$$

$$\text{angle} = \arccos\left(\frac{\overrightarrow{P_2 P_1} \cdot \overrightarrow{P_2 P_3}}{\left\| \overrightarrow{P_2 P_1} \right\| \times \left\| \overrightarrow{P_2 P_3} \right\|} \right) \tag{3.7}$$

In (3.4), v_x is the x-axis component of the velocity vector for a given joint, and Δx is the difference between the x-coordinate of the joint position for two consecutive frames. In (3.5), a_x is the x-axis component of the acceleration vector for a given joint. Similar notations are used for the y- and z-axis. In (3.4) and (3.5), Δt is the time elapsed between two consecutive frames. In (3.6), P_1 and P_2 refer to the 3-D position of two different joints. In (3.7), P_1, P_2 and P_3 correspond to the 3-D

position of three different joints. In (3.6) and (3.7), $\overrightarrow{P_iP_j}$ is the 3-D vector defined by the positions P_i and P_j.

For each gait cycle, the mean, median, variance and normalized variance (variance divided by the mean) were computed over each measure. Four traditional gait parameters were also computed: stride duration and length, gait speed and cadence.

For some of the studies presented below, only a subset of the indicated parameters were considered. Moreover, in the last study on UPDRS estimation, only the following 22 traditional gait parameters were considered:

- Stride, step, stance, swing, single support and double support duration;
- Stride and step length;
- Step width;
- Gait speed and gait speed variability;
- Foot and arm swing velocity;
- Angle at neck, spine shoulder and spine middle;
- Elbow angle minimum and maximum;
- Knee angle minimum and maximum;
- Hip and ankle angle range.

The computation of these parameters are described in more detail in the study on Kinect validation presented later in this thesis.

3.3.4 Statistical Analysis

We explored the possibility of using the quantified gait parameters to distinguish between healthy subjects, PD patients in the Stim-on state and PD patients in the Stim-off state, by performing for each parameter the Kruskal-Wallis test over the values obtained for the three groups.

The Kruskal-Wallis test is a non-parametric method (i.e., does not assume a normal distribution) for determining whether three or more independent groups have the same distribution [206, 207]. The null hypothesis is that the samples come from identical populations. One of the outputs of the hypothesis test is the *p*-value. The *p*-value is the probability of obtaining results at least as extreme as the result in the sample data, assuming that the null hypothesis is true [208]. Smaller *p*-values correspond to smaller probabilities of making a mistake by rejecting the null hypothesis. Therefore, if the *p*-value is small, one can reject the idea that the difference is due to random sampling and conclude instead that the populations have different distributions (null hypothesis is rejected).

To verify the possibility of estimating UPDRS sub-scores relying on the gait parameters, we computed for each parameter the Pearson's correlation coefficient (*r*) between the parameter values and the associated motor/gait sub-scores assigned by the physicians.

The Kruskal-Wallis test and computation of the Pearson's correlation coefficient were carried out in the R environment [209], using the "stats" package [210].

3.4 Results

3.4.1 Distinction between Healthy Subjects and Parkinson's Disease Patients

To verify if the computed gait parameters can be used to distinguish between the three considered groups (healthy subjects, PD patients in the Stim-on state, and PD patients in the Stim-off state), we firstly considered the initial acquisitions corresponding to dataset DS1. The Kruskal-Wallis test results (*p*-value) for the gait parameters that presented a statistically significant difference (*p*-value ≤ 0.05) between the three groups are included in Table 3.5. To investigate if filtering the 3-D joint data improves the distinction, the results were obtained for two different situations: unfiltered and filtered data.

Table 3.5. Kruskal-Wallis test *p*-value for the gait parameters, computed for dataset DS1 (unfiltered and filtered data), presenting a statistically significant difference (*p*-value ≤ 0.05) between healthy subjects and PD patients in Stim-on and Stim-off states.

<table>
<tr><th colspan="3" rowspan="2">Parameter</th><th colspan="2">p-value[a]</th></tr>
<tr><th>Unfiltered data</th><th>Filtered data</th></tr>
<tr><td>Mean</td><td>Acceleration</td><td>Neck</td><td rowspan="2">N.S.</td><td rowspan="2">≤ 0.05</td></tr>
<tr><td rowspan="6">Variance</td><td rowspan="4">Velocity</td><td>Head</td></tr>
<tr><td>Neck</td><td>≤ 0.05</td><td>≤ 0.01</td></tr>
<tr><td>Shoulder</td><td>N.S.</td><td rowspan="3">≤ 0.05</td></tr>
<tr><td>Acceleration</td><td>Neck</td><td rowspan="3">≤ 0.05</td></tr>
<tr><td>Distance</td><td>Elbows</td></tr>
<tr><td>Angle</td><td>Elbow</td><td>N.S.</td></tr>
<tr><td rowspan="5">Normalized variance</td><td rowspan="3">Velocity</td><td>Neck</td><td>≤ 0.01</td><td>≤ 0.01</td></tr>
<tr><td>Shoulder</td><td>N.S.</td><td rowspan="2">≤ 0.05</td></tr>
<tr><td>Elbow</td><td>N.S.</td></tr>
<tr><td>Acceleration</td><td>Neck</td><td rowspan="4">≤ 0.05</td><td>≤ 0.01</td></tr>
<tr><td>Distance</td><td>Elbows</td><td rowspan="3">≤ 0.05</td></tr>
<tr><td colspan="3">Stride duration</td></tr>
<tr><td colspan="3">Cadence</td></tr>
</table>

[a] N.S. stands for non-significant (*p*-value > 0.05).

For filtered data, the parameters were computed over measures extracted from 3-D data that were processed using a low-pass Butterworth filter. The values of the filter's parameters (order and cut-off frequency) were chosen by exploring the values of 5 and 10 Hz for the cut-off frequency, taking into account the values typically used in other studies (6 to 10 Hz [16, 100, 211]). For 5 Hz, we explored the filter order values from 1 to 5 (integer values). The best overall result, when taking into account the Kruskal-Wallis test *p*-values, was achieved for order 1. We then explored the orders 1 and 2 for the cut-off frequency of 10 Hz, which led to worse results than those obtained for 5 Hz. Therefore, we used a first order low-pass Butterworth filter with cut-off frequency of 5 Hz.

With the same aim of distinguishing between three groups, a similar statistical analysis was performed using dataset DS2, which corresponds to a larger number of subjects and a greater amount of data per subject comparing with DS1. To verify if one of the two Kinect versions is more appropriate for the defined objective, we considered only the acquisition sessions for which we obtained data from both Kv1 and Kv2. Furthermore, only the mean and variance were computed for each measure (72 and 90 parameters for Kv1 and Kv2, respectively).

The obtained Kruskal-Wallis *p*-values are presented in Table 3.6, where we can see that there is a statistically significant difference between the three groups (p-value ≤ 0.05) for all parameters when using Kv2, and for all parameters except three (variance of wrist, hand and foot acceleration) when using Kv1.

The gait parameters were obtained from 3-D joint data processed using a third order low-pass Butterworth filter with a cut-off frequency of 5 Hz. Taking into account the previous results regarding filtering, we explored different filter order values (integer value from 1 to 5), for a cut-off frequency of 5 Hz, when considering the Kv2 data. The best overall result considering the Kruskal-Wallis test *p*-values was achieved for the third order. We then confirmed that the best cut-off frequency is 5 Hz, when varying the cut-off frequency between 4 and 7 Hz (integer values).

An example of the angle at the elbow versus the elapsed time is shown in Figure 3.4 for a gait cycle performed by a healthy subject and a PD patient in both Stim-on and Stim-off states. For this example, the mean and variance for the considered measure is higher for the healthy subject when compared with the PD patient. This difference was expected since patients with PD tend to have reduced arm movement amplitude. When comparing the two different DBS states for the PD patient, the mean value for Stim-on was slightly higher than for Stim-off, which was also expected because the stimulation treatment usually leads to an improvement of the patient's motor symptoms.

Table 3.6. Kruskal-Wallis test *p*-value for the gait parameters, computed for dataset DS2 (Kv1 and Kv2), when comparing healthy subjects and PD patients in Stim-on and Stim-off states.

Parameter			*p*-value[a]	
			Kv1	Kv2
Mean	Acceleration	Elbow	≤ 0.01	≤ 0.001
		Wrist		
		Foot		
	Angle	Neck	≤ 0.001	≤ 0.05
		Spine middle	≤ 0.01	≤ 0.01
		Knee	≤ 0.001	≤ 0.05
Variance	Velocity	Wrist	≤ 0.01	≤ 0.001
		Ankle	≤ 0.05	
		Foot		
	Acceleration	Spine middle	≤ 0.01	≤ 0.001
		Spine base		
		Shoulder		
		Elbow	≤ 0.05	
		Wrist	N.S.	
		Hand		
		Hip	≤ 0.05	
		Ankle		
		Foot	N.S.	
	Angle	Neck	≤ 0.05	≤ 0.001
		Spine middle	≤ 0.001	≤ 0.001
		Elbow	≤ 0.01	≤ 0.001
		Knee	≤ 0.05	≤ 0.05
Stride duration			≤ 0.01	≤ 0.001
Cadence				
All other parameters			≤ 0.001	≤ 0.001

[a] N.S. stands for non-significant (*p*-value > 0.05)

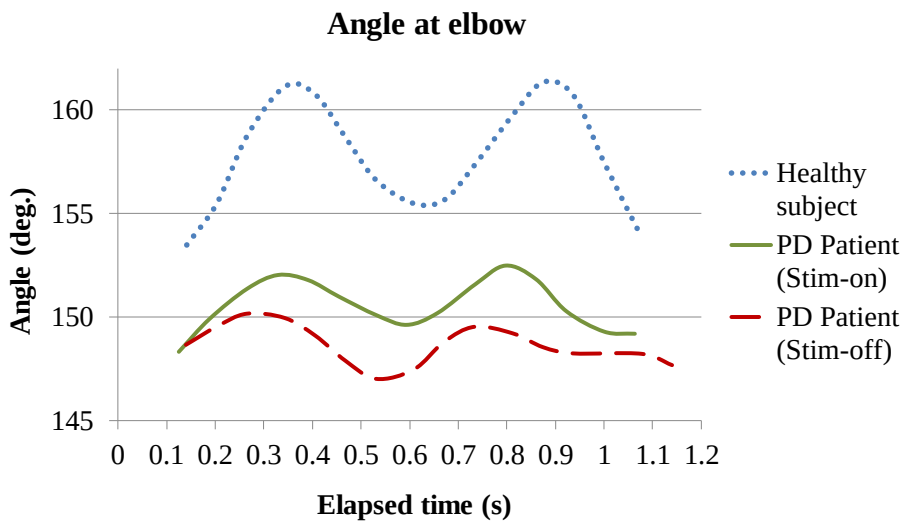

Figure 3.4. Angle at the elbow computed over Kv2 data versus the elapsed time for a given gait cycle performed by a heathy subject and PD patient in both Stim-on and Stim-off states.

3.4.2 Estimation of UPDRS Scores

With the objective of using gait parameters for estimating the UPDRS gait sub-score, the Pearson's correlation coefficient (*r*) between the parameter values and the corresponding gait scores was obtained for each gait parameter, when considering DS1 (PD patients only). The velocity, acceleration and angle parameters were computed for both left and right joints (in the case of symmetrical joints) from unfiltered data, and the traditional gait parameters were not taken into account.

Table 3.7 presents the results obtained for the parameters for which $|r| \geq 0.7$ (results for both left and right sides are included in the case of symmetrical joints).

Table 3.7. Pearson's correlation coefficient (*r*) results for the gait parameters for which $|r| \geq 0.7$, when considering the parameter values versus the UPDRS gait scores.
For symmetrical joints, the result is indicated for both the left and right sides. The values $|r| \geq 0.7$ are indicated in bold.

Parameter			*r*
Mean	**Velocity**	**Left/Right hand**	−0.64 / **−0.73**
	Acceleration	**Left/Right wrist**	−0.66 / **−0.71**
		Left/Right hand	**−0.83** / −0.53
	Distance	**Ankles**	**−0.85**
Median	**Velocity**	**Left/Right ankle**	−0.26 / **−0.85**
	Distance	**Ankles**	**−0.74**
	Acceleration	**Left/Right hand**	**−0.76** / −0.60
Variance	**Velocity**	**Left/Right ankle**	**−0.77** / 0.46
	Acceleration	**Left/Right knee**	**−0.72** / 0.02
	Angle	**Left/Right elbow**	−0.13 / **−0.72**
Normalized variance	**Velocity**	**Left/Right ankle**	−0.63 / **0.83**

Although the results suggest that some of the parameters may be used for UDPRS gait score estimation, it was necessary to confirm them with a larger dataset. Therefore, a similar analysis was performed using the data from both DS2 and DS3, which correspond to a greater number of patients and a greater amount of data per patient. Only Kv2 data were considered, since a greater number of gait cycles was obtained using Kv2 when compared with Kv1 (see Table 3.4). Moreover, we only took into account the acquisitions sessions for which the UPDRS scores were available. The explored parameters included the 22 traditional gait parameters referred above. Both gait and motor sub-scores were investigated.

The *r* results ranged between –0.61 and 0.49 for the gait score, and between −0.48 and 0.47 for the motor score. When considering the mean parameter value for each data acquisition, the results

improved in the case of the motor score, but were similar for the gait score: best *r* value of −0.64 for the gait speed variability (motor) and −0.62 for the foot swing velocity and hip angle range (gait).

We further investigated if better results can be achieved when considering all parameters together, by using machine learning techniques to obtain a predictive model for estimating the considered UPDRS scores. For the gait sub-score, a classification task was considered, since there are only four possible values (0, 1, 2 and 3; 4 was excluded because it corresponds to the inability to walk). Several machine learning algorithms were explored: k-nearest neighbours (k-NN), decision tree, random forest, support vector machines (SVM), multilayer perceptron, and multilayer perceptron ensemble. The algorithms and considered evaluation metrics are the same as those used in other studies presented in this thesis (described in more detail in Chapter 5).

Regarding the motor sub-score, regression was considered for estimating this score, since the value range is much larger (integer numbers from 0 to 108) and not all the values are represented in the used dataset. Besides the algorithms referred above, we explored other algorithms used for regression tasks, which are available in the "rminer" package [212]: multiple regression; multivariate adaptive regression splines; M5 rule-based model; relevance vector machine. To evaluate the model's performance, we considered the mean error, mean absolute error, root mean squared error and Pearson's correlation coefficient (*r*).

For each algorithm, the associated model was validated by using a "leave-one-acquisition-out" cross validation approach. In this approach, all data acquisitions except one are used for training the model, which is then tested using the gait cycles of the left out acquisition. This process is repeated for each acquisition. Besides estimating a score based on a single gait cycle, we also studied the possibility of estimating a single score for the acquisition when several gait cycles are available (mean value rounded to units, when considering the scores predicted for all gait cycles).

The best result for the gait score when predicting the score relying on a single gait cycle was obtained by the k-NN model: overall accuracy of 69% and F_1 score of 63 ± 19%. When taking into account all available gait cycles per acquisition, the best result was also achieved by the k-NN model: overall accuracy of 67% and F_1 score of 64 ± 13%. For the motor score, the best trade-off between the considered metrics was achieved for the multiple regression model (all available gait cycles): mean error of 0.33, mean absolute error of 10, root mean squared error of 12 and *r* of 0.57.

3.5 Discussion

3.5.1 Distinction between Healthy Subjects and Parkinson's Disease Patients

The results of the initial study on the distinction between healthy subjects and PD patients in Stim-on and Stim-off states show that some of the computed gait parameters may be used for distinguishing between the three groups (Table 3.5). The obtained results also indicate that filtering the data used to compute the parameters contributes to a better distinction between the groups (results overall better for filtered data than for unfiltered data). This was expected since the Kinect data can be rather noisy, and filtering the data removes some of that noise.

The results obtained when considering a larger number of subjects, as well as a greater amount of data per subject provided by both versions of the Kinect (Kv1 and Kv2), confirm that the extracted gait information can possibly be used to distinguish between the three considered groups. If the value of one or a set of parameters can be used to predict the group to which a subject belongs, then it may also enable the evaluation of the gait impairment severity of a given PD patient treated with DBS.

Overall, Kv2 is more appropriate than Kv1 for supporting PD patient assessment, since the percentage of parameters for which p-value ≤ 0.001 (Kruskal-Wallis test) is higher for Kv2 (96% versus 71%). Moreover, Kv2 has a larger practical depth range (see Figure 3.2), which allows to acquire a higher number of gait cycles for the same number of trials (mean of 29 and 11 gait cycles per subject using Kv2 and Kv1, respectively, in our study).

3.5.2 Estimation of UPDRS Scores

When considering UPDRS score estimation, the results of the initial study indicate that some of the gait parameters may be used for estimating the gait sub-score, with the best Pearson's correlation coefficient ($r = -0.85$) being achieved for the mean of ankle distance and median of right ankle velocity. It is interesting to note that most obtained r values are negative, indicating that lower parameter values correspond to higher gait sub-scores. This relationship was expected, since the motor symptoms of PD patients include slowness of movement, with reduced range of motion and smaller steps during gait.

To confirm the achieved results, we explored the possibility of estimating the UPDRS gait score by relying on traditional parameters, which were computed over a greater amount of data acquired from a larger number of patients. When considering each parameter separately, the correlation

between the computed values and the associated UPDRS gait scores assigned by physicians varies from poor to moderate ($|r| < 0.75$). Similar results were achieved for the motor score. When considering all parameters together, by using machine learning techniques to obtain a predictive model for score estimation, the obtained results suggest that the considered parameters cannot be used to estimate gait/motor scores.

The obtained moderate results can be due to different reasons. Firstly, the dataset used in the studies included only two data acquisitions with an associated gait sub-score value of 3, both belonging to the same subject. Furthermore, the UPDRS items of the motor section are rated with a relatively low level of granularity (discrete scores ranging from 0 to 4), and the assigned scores can be affected by subjectivity since they depend on the physician's experience and opinion.

3.5.3 Other Outcomes

The initial carried out studies further led to the identification of some aspects regarding software, setup and protocol that needed improvement, which were then taken into account for the following studies. Regarding the software, the improvements included changes related with the saved data (e.g., file format, relevant information on the camera and data) and the user interface (e.g., management of acquisition sessions, indication and visualization of events/instants of interest). As for the setup and protocol, the improvements mainly included changes for increasing the amount of data acquired from the subject in each acquisition session.

We also identified the necessity of developing a solution to detect gait cycles in an automated way, since we verified that their manual selection is rather time-consuming, especially when a large amount of data needs to be analysed. For 54 data acquisitions (both Kv1 and Kv2) from the first two experiments, it was necessary at least 121 min or 2 h to manually select 724 gait cycles, assuming that it takes 10 s to identify and save one gait cycle (identification of heel strikes instants only). Although in a real practical situation gait analysis is performed for a single data acquisition at a time, the manual indication of several heel strikes is still tedious and is more prone to human error than automatic identification.

3.6 Summary

Our studies with Parkinson's disease (PD) patients showed that there is potential in using an RGB-D camera, namely the Kinect, for supporting clinical gait assessment in PD. The obtained results suggest that gait parameters, extracted from 3-D data provided by the Kinect, can be used to distinguish between healthy subjects and PD patients with the DBS stimulator switched on and off.

Therefore, the quantitative gait information can possibly be used to evaluate the severity of gait impairments in PD patients treated with deep brain stimulation (DBS). However, more data from a greater number of subjects is necessary to confirm the results.

We were also able to verify that our system for gait analysis based on an RGB-D camera is suitable for a clinical environment, since it has been successfully used to acquire data from both healthy subjects and PD patients at different locations of a hospital. The initial studies also enabled the identification of important aspects related to the software, setup and protocol that needed improvement. Furthermore, it became clear the need for automated gait cycle detection to save time in the whole gait analysis process, since the manually identification of gait cycles was very time-consuming and tedious.

4 *KiT* and *KiMA*: RGB-D Camera Data Acquisition and Visualization

The main objective of this thesis was to develop an inexpensive, portable and minimally intrusive solution for automated gait analysis to support the gait assessment of a given subject. To carry out human gait analysis, we relied on the quantitative motion information provided by a single low-cost, markerless vision-based sensor, namely the Microsoft Kinect (RGB-D camera). In our solution, the online visualization and acquisition of the multimodal data provided by the Kinect is enabled by the *KiT* (*KinecTracker*) software application.

Another application – *KiMA* (*Kinect Motion Analyser*) – was developed to enable offline visualization of the data acquired using *KiT*, as well as selection of relevant data or instants, which is useful for research in the context of motion/gait analysis (see Figure 4.1). Both *KiT* and *KiMA* have a version for each generation of the Kinect (Kv1 and Kv2). These applications were presented in the context of motion analysis in neurological diseases in [78].

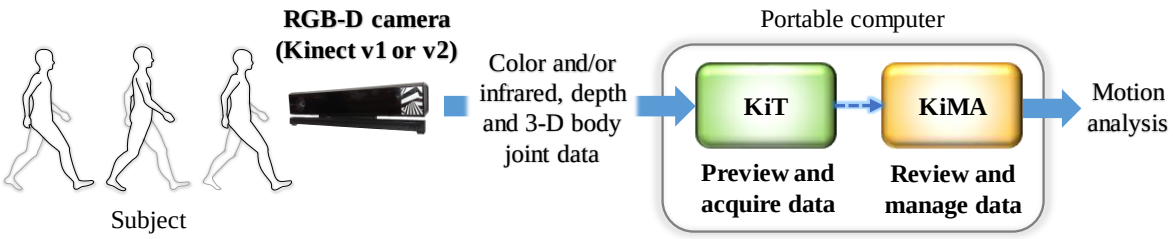

Figure 4.1. Preview, acquisition, review and management of the multimodal data provided by the Kinect camera, using *KiT* and *KiMA* software applications.

4.1 *KinecTracker* (*KiT*) Application

The main requirements that were defined for the *KiT* application are the following:

1.1. Online visualization of data provided by a Kinect sensor, including the possibility of viewing two or more data types simultaneously;

1.2. Acquisition of one or more data types provided by the Kinect, in a synchronous way;

1.3. Possibility of saving a "label" associated with a given instant, during an acquisition;

1.4. Management of different acquisition sessions;

1.5. Possibility of discarding the oldest data of the current acquisition, according to the available disk space or a given time duration indicated by the user;

1.6. Selection of the sensor tilt angle (Kv1 only).

Most of these requirements correspond the use cases illustrated in Figure 4.2. In a scenario where the data acquisition takes place at a clinical environment, the clinician (e.g., physician, nurse) is responsible for choosing the appropriate preferences, managing the acquisition sessions and carrying out the data acquisitions. The data are provided by a single Kinect camera, which is connected to the computer where *KiT* is running through a USB cable. The subject being assessed is involved in the data acquisitions by being in the field of view of the camera. In other scenarios, such as ambulatory monitoring, the patient itself, a relative or a caregiver performs the role of the clinician.

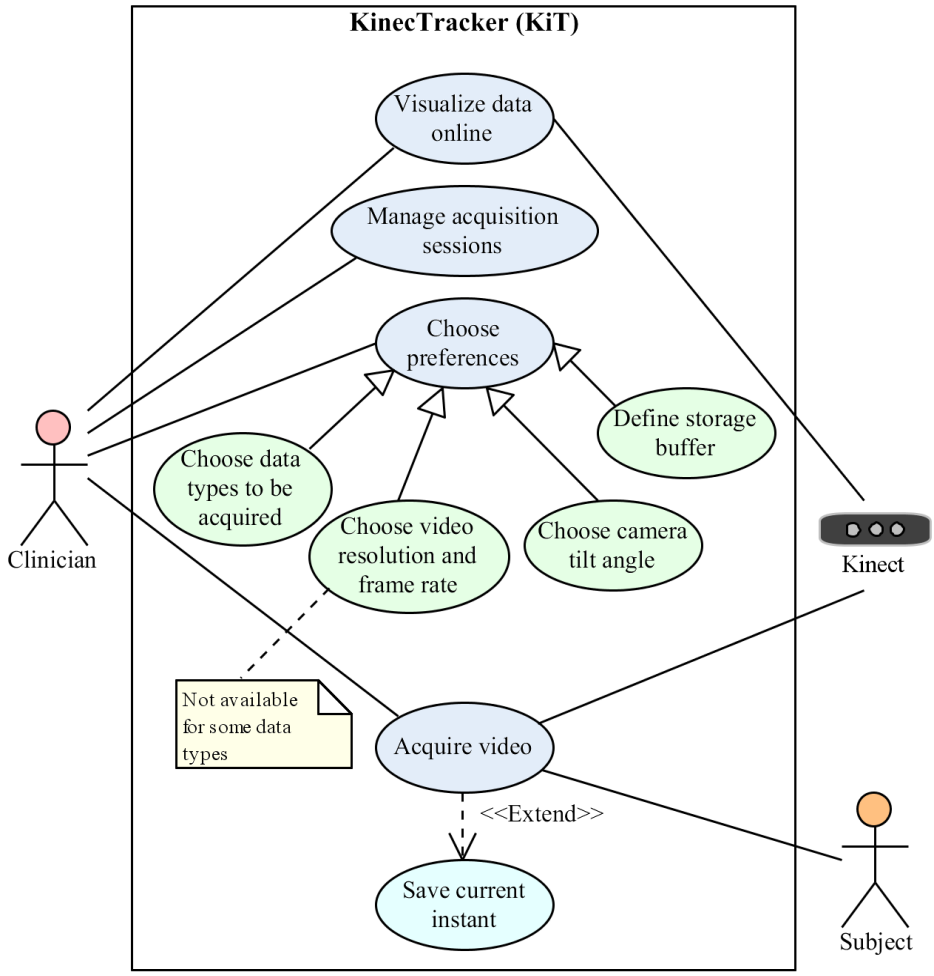

Figure 4.2. Use case diagram associated with the *KiT* application.

The graphical user interface (GUI) of the main window of *KiT* for Kv2 is shown in Figure 4.3 (*KiT* for Kv1 is similar). There are two visualization areas corresponding to the primary and

secondary data sources. For each visualization area, it is possible to choose one of the available data types. For colour, IR, depth and body index data, it is also possible to have the body joint data drawn over the image (colour + body, depth + body, etc.). Therefore, *KiT* allows viewing up to three data types simultaneously (requirement 1.1).

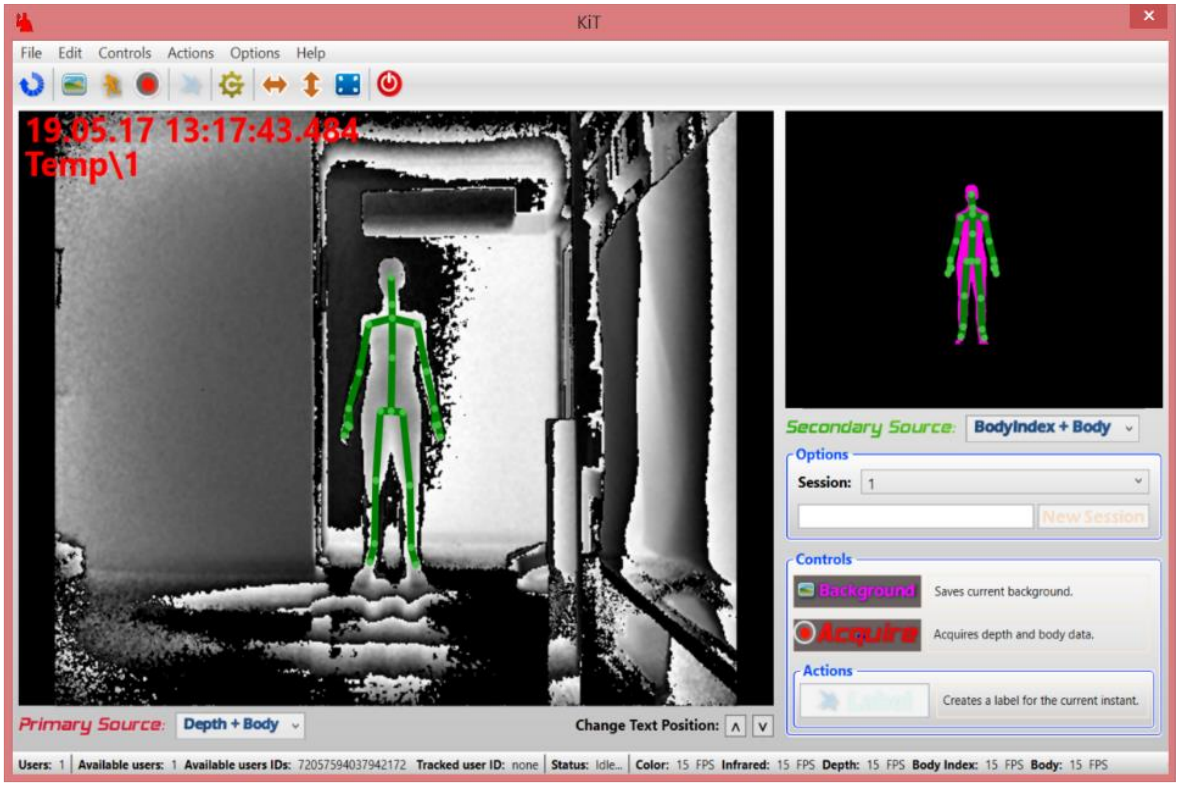

Figure 4.3. *KiT*'s main window GUI (Kv2), including the display of depth, body index and body data.

Some preferences regarding data acquisition or the Kinect itself can be indicated in the "Preferences" window, shown in Figure 4.4 for Kv1 and Kv2, which is opened when choosing the Preferences option in the Edit menu. The available options depend on the used Kinect version. For both versions, it is possible to choose the folder where the different sessions/acquisitions will be stored and define a storage buffer. The latter is defined by indicating the percentage of the disk space that can be used, or the acquisition duration in minutes/hours/days, until the oldest data starts being erased (requirement 1.5). This functionality is useful when the total duration of an acquisition is unknown (e.g., continuous monitoring of epileptic patients, where the relevant movements correspond to unpredictable sporadic seizures).

In Preferences, it is also possible to choose any combination of data types to be saved (requirement 1.2). In the case of the Kv1, choosing not to save the body joint data (skeleton) corresponds to disabling joint tracking. Moreover, the user can select the resolution and frame rate of the colour

and depth data, choose to track only the upper body joints and define the camera tilt angle (last option corresponds to requirement 1.6). For the Kv2, the IR image brightness can be adjusted (for online preview only).

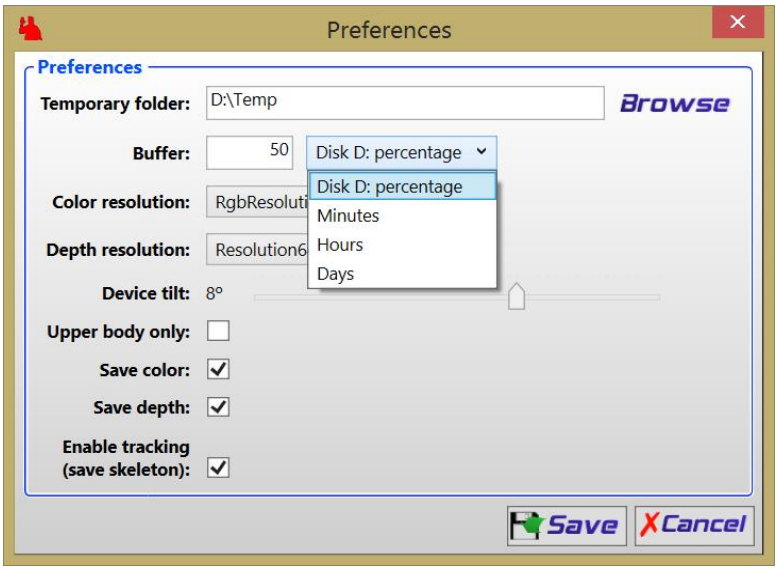

(a)

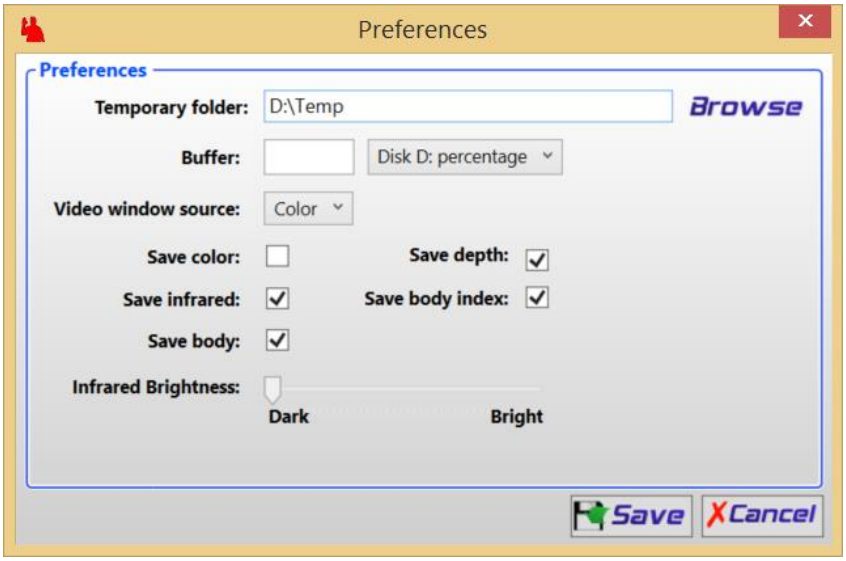

(b)

Figure 4.4. Preferences window of *KiT* for Kinect v1 (a) and v2 (b).

In the Options panel of the main window (below the Secondary Source drop down menu), the user can manage different acquisition sessions (requirement 1.4), facilitating the organization of the acquisitions according to the different subjects or days. The current session can be indicated by creating a new session or by selecting an existing session. These options are also presented to the user when *KiT* is opened.

In the Controls panel of the main window (below the Options panel), there are three options related to the acquisition of data. The first one ("Background" button) allows the acquisition of a single frame, which can be useful if we wish to carry out motion analysis by using a background subtraction technique over the colour data. The "Acquire" button starts a data acquisition (requirement 1.2). During the acquisition, the name button's name changes to "Stop" and can be used to stop the current acquisition.

The third option in the ("Label" button) is included in the Actions panel within the Controls panel, and is only available during an acquisition. When selected, it creates a label for the current instant (requirement 1.3), which consists of saving the timestamp and frame number associated with that instant. The user can indicate a name and an optional description through a dialog window. This option can be useful to indicate the beginning of a relevant movement (e.g., epileptic seizure), so it can be easily found when reviewing the acquisition in *KiMA*.

Some additional features are available in the menu and/or tool bar: reset image display; flip image horizontally and vertically; show colour/IR data in full screen; open the last acquisition in *KiMA*; and quit application. Furthermore, the status bar presents information regarding subject tracking, application status, and current frame rate for each data type.

KiT was implemented based on an existing application developed for Kv1, by performing the following main improvements:

- Elimination of unnecessary data frame processing for visualization/acquisition (i.e., only the data types chosen for visualization and/or acquisition are processed);
- Possibility of visualizing IR/depth and body data simultaneously (only body over colour was displayed in the original application);
- Possibility of indicating the data types to be acquired, which in the case of the body joint data also corresponds to enabling/disabling subject tracking (Kv1 only);
- Management of acquisition sessions through the application's GUI;
- Acquisition of data in a synchronized way (using an event provided by the Kinect SDK);
- Acquisition of body joint data corresponding to one of the detected subjects as default (previously, body joint data were only acquired if a specific subject detected by Kinect was chosen by the user, which led to data loss if the subject left the camera's depth range, since the ID attributed to the subject by the Kinect changes when this happens);

- Use of a queue for storing the frames while they are not written to file (this prevents data frames loss in computers with less processing power and facilitates the creation of different files every minute);
- Increase of flexibility in the definition of the storage buffer, by adding the possibility of indicating any size (within the valid values) and choosing from different types (percentage of used disk, minutes, hours or days);
- Modification of file format to facilitate parsing during video review and motion analysis, and addition of a header with relevant information (e.g., resolution, tilt angle, application version);
- Addition of an option for saving a label, which replaced the option for saving an event corresponding to the last 3 minutes of data;
- Possibility of changing the position of the overlay text (date, time, session folder path) vertically, and flipping the images both vertically and horizontally;
- Option for opening the last acquisition (if any) in *KiMA*.

Regarding the Kinect data, the SDK (v1.8 [213] and v2.0 [214] for Kv1 and Kv2, respectively, in C#) provides the data frames as they become available. In *KiT*, for each frame and data type, the data itself and associated information (e.g., image size in the case of image frames) are extracted and then stored together with the associated timestamp (date and time when it became available).

For the colour, IR, depth and body index, the data corresponds to image pixel information. For the body, the data includes the 3-D position of the tracked joints (i.e., body), as well as the associated mapped colour and depth points. The latter information is used for displaying the body joints over the colour and depth images, respectively. The mapping is performed by relying on the "CoordinateMapper" class provided by the Kinect SDK [176].

If a given data type is to be displayed, the corresponding stored data are firstly processed and then the corresponding image/body is drawn in the GUI. When the user starts an acquisition, a thread is started for each data type and the data of each new data frame are inserted in a FIFO (first-in-first-out) queue (one queue per data type). The thread then gets the frames from the queue and saves the associated data to file. The same thread is responsible for creating a new file each minute.

The format of the files used to store each data type is presented in Appendix A.1. The header of each file includes the tilt angle and height of the Kinect. These values are computed based on the clipping floor plane detected by the Kinect itself [213-215]. For each body joint data frame, the

Kinect provides a floor-clipping-plane vector (A,B,C,D), where A, B, C and D are the coefficients of an estimated floor-plane equation $Ax+By+Cz+D=0$. (A,B,C) is the unit vector corresponding to the normal of the floor plane. D is the distance from the floor plane to the origin of the coordinate system associated with the Kinect, i.e., the height of the camera from the floor (in meters). When the floor is not visible or detectable, the floor clipping plane is a zero vector. The tilt angle in radians is obtained using (4.1).

$$\text{tilt angle} = \text{atan}\left(\frac{C}{B}\right) \tag{4.1}$$

The file extension used for the different data types are: ".kvid", ".kir", ".kdpt", ".kbi", and ".kpos", for colour, IR, depth, body index, and 3-D body joint data, respectively. For each acquisition and data type, a new file is created every minute. The name of the file is the timestamp of the first frame followed by the "#" symbol and the number of the acquisition (it is possible to carry out several acquisitions per session). When using the Kv2, a file with information regarding coordinate mapping is also saved (extension ".kmap"), which can be used for offline mapping between depth and camera spaces (more details can be found in [176]).

4.2 *Kinect Motion Analyser* (*KiMA*) Application

To allow the review of the data acquired with *KiT*, as well as the indication of relevant movements for motion analysis, we developed a different application: *Kinect Motion Analyser* or *KiMA*. The main requirements defined for *KiMA* are the following:

2.1. Offline visualization of a data acquisition carried out in the *KiT* application, as a video, including the possibility of viewing two or more data types simultaneously;

2.2. Selection of the session and acquisition to be reviewed (based on the same session organization used in *KiT*);

2.3. Creation, edition and deletion of "labels" and "events" associated with a given instant and time interval, respectively;

2.4. Exportation of events.

These requirements corresponds to the use cases represented the diagram shown in Figure 4.5. These use cases are carried out by the clinician in the clinical scenario, but can also be carried out by another person in other scenarios (e.g., ambulatory monitoring, research).

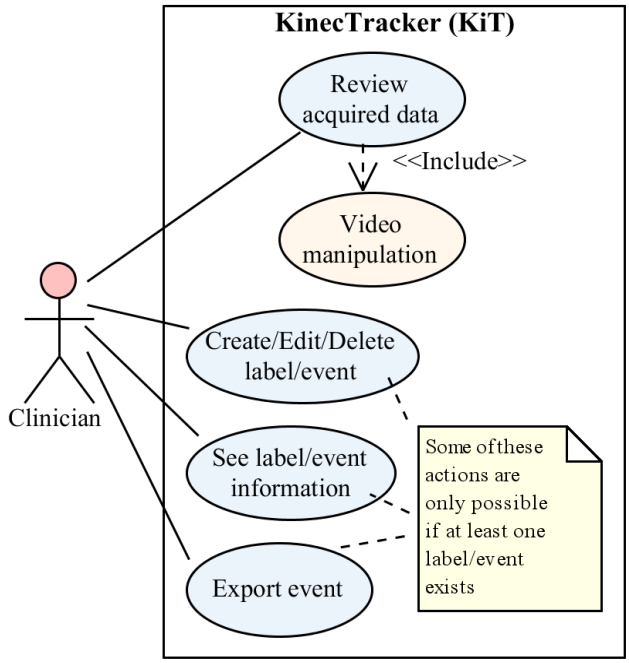

Figure 4.5. Use case diagram associated with the *KiMA* application.

The GUI of *KIMA*'s main window is shown in Figure 4.6. The data acquired using *KiT* can be reviewed as a video in *KiMA* (requirement 2.1), by using the typical video manipulation controls (e.g., play, pause, stop, fast forward, rewind). It is also possible to define the speed of the video, and jump to the previous or next frame (when paused). The data are presented to the user in a similar way to *KiT* (i.e., up to three data types can be viewed at the same time).

To review an acquisition, it is firstly necessary to choose the folder where the session is stored (Options panel). Then, it is possible to select one of the sessions available for the indicated folder. Finally, the user can chose one of the acquisition performed in the selected session (requirement 2.2). When an acquisition is chosen, the first frame of the video is shown. Only the data types available for that acquisition can be selected as primary and secondary sources. The video manipulation (play, stop, etc.) involves obtaining the data from the files that corresponds to the current frame number, ensuring the synchronization between the different data types.

KiMA also facilitates the creation, edition and deletion of tags (labels and events), which enable the identification of relevant movements that occur during an acquisition (requirement 2.3). A label has an associated frame number and timestamp, as well as a name and an optional description. An event is similar to a label, with the difference that it has a beginning and an ending instant.

The information associated with tags created by the user is saved to an XML file, which can the be used in other application to carry out motion analysis taking into account the created tags. The used format is shown in the example included in Appendix A.2.

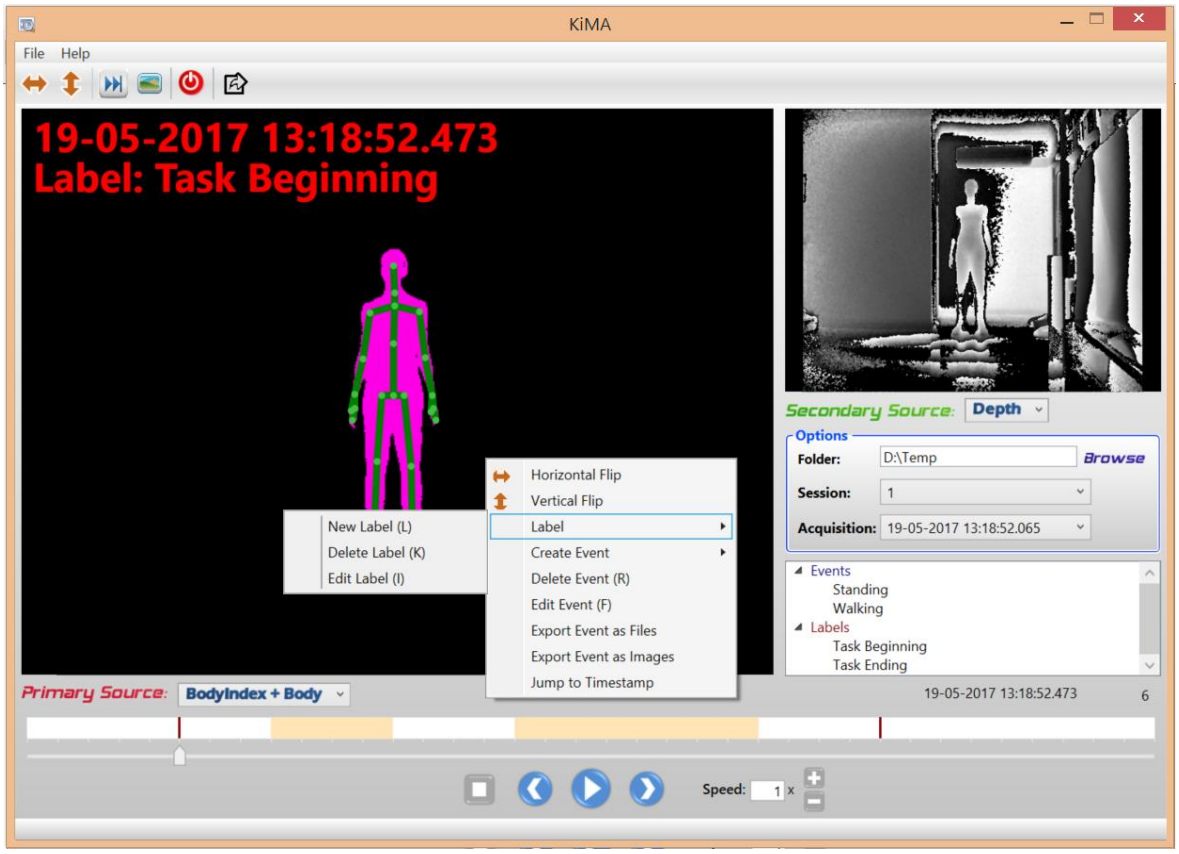

Figure 4.6. *KiMA*'s main window GUI, including the display of depth and body data, as well as labels and events.

Tags can be created/deleted/edited by using the context menu shown in Figure 4.6, or the shortcuts indicted in the same menu. The tags are visually represented in the white bar above the video manipulation controls, and listed in the tree view below the Options panel (see Figure 4.6). The events can be exported as images or files (requirement 2.4), allowing to save only the data corresponding to relevant movements and discard uneventful data. This feature is especially useful for long term monitoring (several hours or days corresponding to several gigabytes of data), in which movements of interest only occur sporadically.

4.3 Summary

With the main aim of developing a solution for automated gait analysis, we relied on an RGB-D camera to obtain quantitative information regarding the movements of a given subject. The selected camera was the Microsoft Kinect, which provides both colour (RGB) and/or IR images and depth information. Furthermore, it also provides the 3-D position of several body joints, which is essential for our gait analysis solution. Therefore, we developed the *KiT* (*KinecTracker*) software

application for enabling the online visualization and acquisition of the multimodal data provided by the Kinect (v1 or v2). The data acquired with *KiT* can be reviewed in our *KiMA* (*Kinect Motion Analyser*) application, which also allows the indication and/or exportation of instants or events of interest for further analysis.

KiT has been used in the last few years for acquiring data in different scenarios: gait analysis in healthy subjects, Parkinson's disease (PD) patients and Transthyretin Familial Amyloid Polyneuropathy (TTR-FAP) patients; and seizure analysis in epileptic patients. *KiMA* was used to manually identify gait events in studies using the data acquired from PD patients and/or healthy subjects [79-84] and TTR-FAP patients [85]. It was also used in studies with epilepsy patients to select data corresponding to relatively short and unpredictable seizure events in data acquisitions lasting several hours or days [86, 87].

5 Automated Gait Cycle Detection Using an RGB-D Camera

Our preliminary studies with Parkinson's disease patients showed the need for automating the detection of gait cycles. A solution for detecting gait cycles in an automated way eliminates the step of manual identification, consequently leading to time savings in the gait analysis process. Therefore, the main objective of this chapter is to answer the following research question:

- Can the 3-D data provided by a single RGB-D camera be used to automatically detect the different gait cycles performed by a given subject while walking?

To answer this question, we designed and developed a solution for automated gait cycle detection using a Kinect (RGB-D camera), and validated it with data acquired from healthy subjects. In contrast with other contributions, our aim was to enable fully automatic gait analysis by automatically selecting the data corresponding to walking, prior to gait cycle detection, relying on activity recognition. Therefore, it was also necessary to answer another question:

- Can machine learning techniques, together with 3-D data provided by a single RGB-D camera, enable activity recognition?

This chapter reflects the work presented in [76], with the following additional contributions: identification of different gait cycle phases by including the detection of one more type of gait event (toe off), and validation of the solution for the first version of the Kinect (besides the second version).

5.1 Related Work

5.1.1 Activity Recognition

In the past years, RGB-D cameras have been used in several studies on human activity recognition [4, 38-54, 216]. Most of these studies focus on the recognition of very specific daily life activities (e.g., talking on the phone, drinking water, working on computer, cooking) [38, 39, 42, 43, 48, 50] or gestures and/or gaming actions (e.g., wave, punch, kick, clap, jogging) [40, 44-46].

There are several publicly available RGB-D action/activity datasets [1, 4, 47, 217]. From single-view datasets, one of the first available was the MSR-Action3D dataset [46]. This dataset includes depth and body joint data (15 Hz) for 20 actions carried out 2 or 3 times by 10 subjects,

where the actions were chosen in the context of game console interaction (does not include walking). The MSRDailyActivity3D contains colour, depth and joint data (Kv1, colour and depth not synchronized) collected from 10 subjects during 16 daily life activities, including walking [52].

The RGBD-HuDaAct dataset also comprises daily life activities (12 activities; walking considered as a random activity) performed by 30 subjects [50]. However, it only has colour and depth data (Kv1, 30 Hz). The Cornell Activity Datasets (CAD-60 and CAD-120) also include several activities (60 and 120 examples, respectively). The CAD-60 includes colour, depth and body joint data (Kv1, 15 joints only) acquired from 4 subjects during 12 activities (walking not considered) in 5 different environments [38]. The CAD-120 is similar to CAD-60, with the difference that it includes more examples and more activities (10 high-level activities and 10 sub-activities, also not including walking) [48].

Other datasets that contain body joint data, and consider the walking activity, include the following: UTKinect (10 activities, 10 subjects, 2 repetitions, Kv1) [53]; IAS-Lab Action (15 activities, 12 subjects, 3 repetitions, Kv1) [49]; UPCV (10 activities, 20 subjects, 2 sessions, Kv1, joint data only) [51]; G3D (20 gaming actions, 10 subjects, 3 repetitions, Kv1) [45]; KARD (10 gestures and 8 activities, 10 subjects, 3 repetitions, Kv1, 15 joints only) [41].

Most studies relied on datasets with a relatively large number of activities (>10 activities), including the datasets described above. There are some studies that explored a smaller set of activities: Zhang et al. considered only five activities (standing, fall from sitting, fall from standing, sit on chair and sit on floor) [42] and Le et al. four postures/activities (standing, sitting, bending and lying) [54]. However, none of these two studies included the walking activity. Ballin et al. explored six activities, including standing, hand waving, sitting down, getting up, pointing and walking [216] (performed by six subjects only).

5.1.2 Gait Cycle Detection

In the context of gait analysis, different methods for gait cycle detection using the Kinect were proposed [55-65]. Cancela et al. implemented a finite-state machine that detects different gait cycles phases, based on the left and right foot position provided by the Kinect v1 (Kv1) [58]. For data corresponding to seventeen healthy subjects, the detection error (i.e., percentage of steps not detected) ranged between 6% and 75%, for different walking paths and rhythms, as well as different sensor heights.

A state machine was also used by Gabel et al. for identifying gait cycles [56]. However, they used the output of a predictive model, which detects whether the foot is in contact with the ground

or not, as the input of the state machine. The model was built using the Multiple Additive Regression Trees algorithm, and features computed over Kv1 data acquired from twenty-three healthy subjects. The proposed solution achieved an estimation error of 8 ± 62 ms and 2 ± 46 ms for the duration of the left and right strides, respectively (actual duration obtained from pressure sensor data). The mean absolute error was of 45 and 32 ms, respectively.

With the aim of measuring stride-to-stride gait variability for fall risk assessment, Stone et al. proposed a solution for computing gait parameters using Kv1 [55]. This solution includes the detection of left and right heel strikes, by finding the local minima and maxima of the time series of a correlation coefficient. The latter was computed over normalized ground plane projections of 3-D point cloud representing the subject's silhouette. For data collected from three subjects, the proposed solution was able to compute the stride duration with an error of 7 ± 62 ms (ground truth obtained from Vicon data).

Clark et al. and Mentiplay et al. proposed the identification of toe off/heel strike instants by finding the local minima of the foot/ankle velocity (in the anterior–posterior plane) immediately preceding/after the foot/ankle velocity first exceeding/dropping below a threshold of 0.1 m/s [57, 64]. The performance of the proposed method was evaluated for twenty-one subjects and thirty subjects when using the Kv1 and Kv2 (against a Vicon system), respectively. Clark et al. reported a mean estimation error of −200 ms for stride duration and −170 ms for step duration. Mentiplay et al. reported a mean error of 0.03 to 0.04 s for step duration and 0.00 to 0.01 s for stance duration.

Instead of relying on the position of the feet/ankles, Auvinet et al. proposed the detection of heel strikes by finding the local maxima of the distance between knees, along the longitudinal walking axis [59]. For the Kv1 sensor, the z-axis coordinate of the knees' position was obtained from depth data using k-means clustering. An estimation error of 17 ± 24 ms was achieved, when considering data acquired from eleven healthy subjects during treadmill walking (actual instants obtained from Vicon data). The estimation error for stride duration was of 0 ± 12 ms.

Xu et al. also used Kv1 data acquired during treadmill walking for evaluating the method they proposed for gait event detection, when compared with a gold standard system (Optotrak Certus system) [60]. In this method, heel strike and toe off instants are estimated by finding the local maxima of the anterior-posterior distance between the ankle of the front foot and the hip centre joint, and the distance between the ankle of the rear foot and hip centre, respectively. For data collected from twenty healthy subjects, the obtained estimation errors were of 5 ± 27 ms and 3 ± 22 ms (left and right heel strikes) and of −44 ± 62 ms and −38 ± 57 ms (left and right toe offs). For the stride duration, the error varied between 0 ± 19 ms and 2 ± 33 ms, depending on the walking speed of the subject.

Pfister et al. defined the duration of a gait cycle as the time elapsed between two consecutives peaks of the hip/knee angle during flexion for the same limb [65]. For Kv1 data acquired from twenty heathy subjects while walking in a treadmill at three different controlled speeds, the error for estimation the stride duration varied between 118 ± 12 ms and 159 ± 24 ms (Vicon used as the gold standard system), with the mean error decreasing with an increase in speed.

Eltoukhy et al. also explored the use of the Kv2 for gait event detection [63]. They firstly obtained the position of 26 joints relying on the provided depth data, as well as anthropometric models. Then, heel strikes and toe offs were detected by finding the local maxima and minima, respectively, of the anteroposterior distance between the ankle and mid-posterior superior iliac spine. When comparing the Kv2 with a Vicon system, the true estimation error varied between 0.00 ± 0.01s and 0.00 ± 0.02 s for stride duration, and between –0.03 ± 0.01 s and –0.02 ± 0.01 s for step duration. The absolute error ranged from 0.01 ± 0.01 s to 0.01 ± 0.02 s, and from 0.02 ± 0.01 s to 0.03 ± 0.01 s, respectively.

The Kv2 was also used in the studies by Geerse et al. [61] and Müller et al. [62]. However, in contrast with the contributions described above, these studies considered the use of multiple Kinect cameras at the same time. Geerse et al. relied on four Kv2 sensors (Optotrak system as gold standard) and detected heel strikes and toe offs by finding the local maxima and minima, respectively, of the anterior-posterior distance between the ankle and the spine base. They achieved a mean estimation error 0.01 s for both stride and step duration, when considering a comfortable walking speed. Müller et al. considered a setup of six two-sided Kinects and identified heel strikes by finding the intersection between the left and right ankle trajectories in the walking direction. They were able to achieve a true error of 0.00 ± 0.03 s when estimating the step duration (Vicon system as gold standard).

5.2 Materials and Methods

5.2.1 Subjects

An experiment was conducted at LABIOMEP, the Porto Biomechanics Laboratory (Porto, Portugal), with the participation of twenty healthy subjects: ten male and ten female. The demographics of the participants are presented in Table 5.1.

The participants were recruited from the community of the University of Porto (Porto, Portugal). The only exclusion criterion for subject selection was the existence of any disease or injury that affected their gait (no limits were imposed regarding the age, height and weight). The experiment

was approved by the Ethics Committee of Santo António Hospital (Porto, Portugal) and all subjects signed an informed consent form.

Table 5.1. Characterization of the subjects that participated in the experiment. SD, Min, Max and BMI stand for standard deviation, minimum, maximum and body mass index.

		All subjects (20)	Male (10)	Female (10)
Age (years)	**Mean ± SD**	31 ± 8	31 ± 9	31 ± 8
	[Min, Max]	[23, 52]	[24, 50]	[23, 52]
Height (m)	**Mean ± SD**	1.71 ± 0.11	1.79 ± 0.08	1.63 ± 0.08
	[Min, Max]	[1.50, 1.94]	[1.68, 1.94]	[1.50, 1.73]
Weight (kg)	**Mean ± SD**	67.9 ± 15.3	78.9 ± 13.0	56.9 ± 7.3
	[Min, Max]	[48.0, 105.0]	[63.0, 105.0]	[48.0, 72.0]
BMI (kg/m^2)	**Mean ± SD**	23.0 ± 3.3	24.6 ± 3.0	21.4 ± 2.7
	[Min, Max]	[16.7, 31.0]	[20.1, 31.0]	[16.7, 24.9]

5.2.2 Experimental Setup

The experimental setup, which is depicted in Figure 5.1, comprised three different systems, including two RGB-D cameras, namely a Kinect v1 (Kv1) and a Kinect v2 (Kv2), and a gold standard Qualisys system [218]. There is no interference between the three used systems, according to our study presented in Appendix B.

The Kv2 was mounted on a tripod at a height of 1 m. The Kv1 was placed on top of Kv2, as can be seen from Figure 5.2. Each Kinect was connected to a portable computer. The tilt angle was of −10 degrees for Kv1 and −5 degrees for Kv2. For the used physical configuration, the practical depth range was of 1.8–2.1 m for Kv1 and 2.7 m for Kv2.

The Qualisys system included twelve Oqus cameras and sixty-one retro-reflective markers, which were placed on different body landmarks as illustrated in Figure 5.3. The subjects were asked to wear tight-fitting clothing to allow a proper placement of the markers.

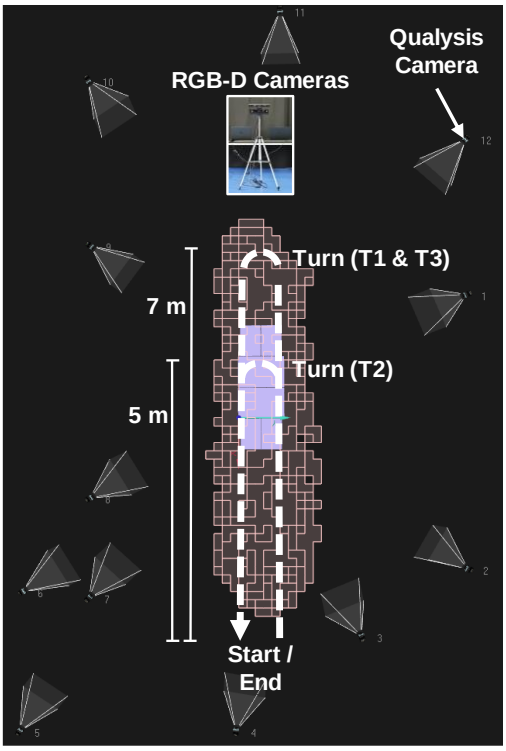

Figure 5.1. Experimental setup including two RGB-D cameras (Kv1 and Kv2) mounted on a tripod, and a Qualisys system with twelve infrared cameras (figure adapted from the image of the Qualisys setup provided by LABIOMEP).

The calibrated volume for Qualisys is illustrated by the salmon-coloured blocks. The walking path carried out by the subjects, for each task included in the protocol (T1, T2 and T3), is represented by the dashed arrowed lines. The relevant distances are also indicated.

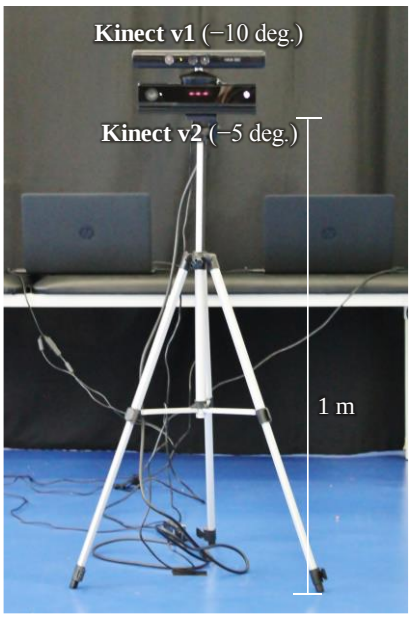

Figure 5.2. Physical configuration (height and tilt angle) of the RGB-D cameras (Kinect v1 and v2), which were mounted on a tripod and connected to a portable computer each.

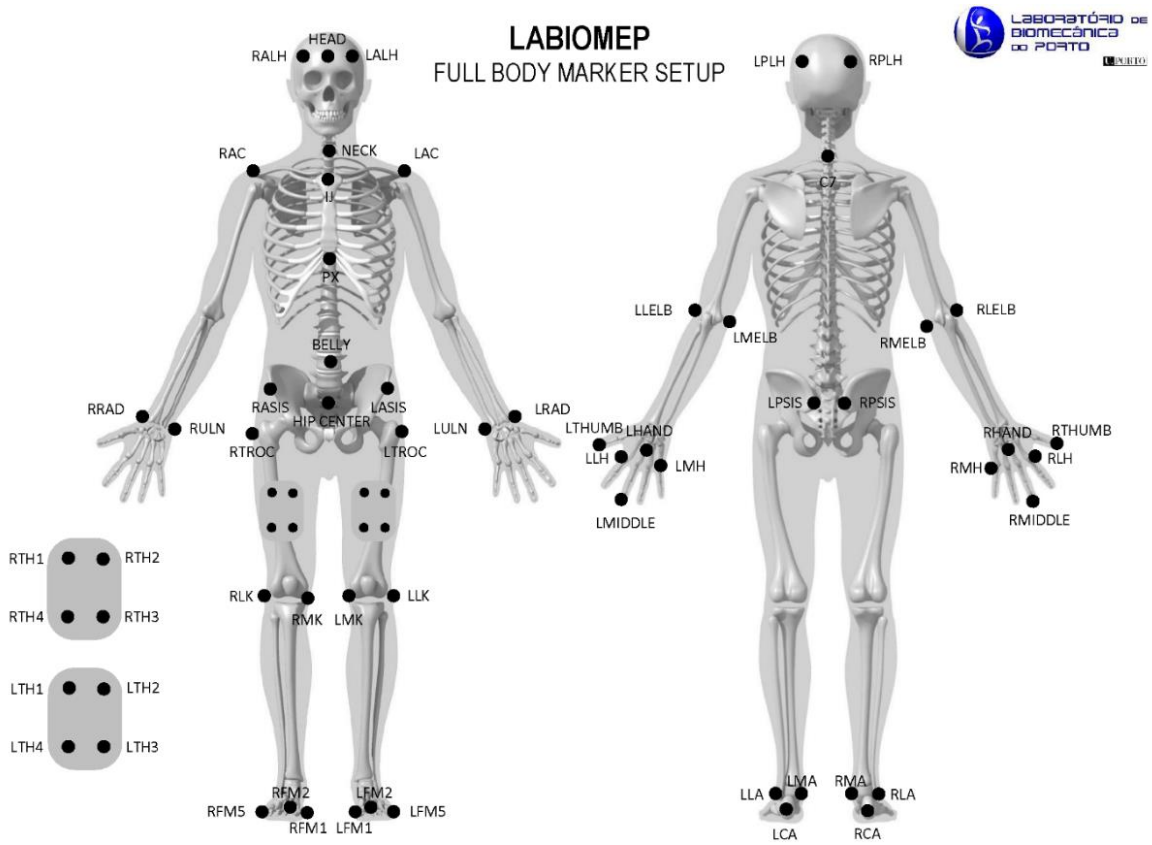

Figure 5.3. Retro-reflective markers placed at the subject's body (image provided by LABIOMEP).

5.2.3 Experimental Protocol

The experimental protocol included three different tasks (T1, T2 and T3), which are described in detail in Table 5.2. Both T1 and T2 consist of walking towards and away from the Kinect sensor, only differing in the distance covered (7 m for T1 and 5 m for T2) and the distance from the sensor at which the subjects turns around (outside and inside the Kinect's practical depth range, respectively). Task T3 is similar to T1, but it also includes the activities of standing still and marching in place (see Table 5.2). The latter activities were included in the protocol, since in a real situation the subject may not always perform only the defined gait task.

Each subject carried out the number of trials per task indicated in Table 5.2. For all tasks, walking was performed at a self-selected comfortable pace. For synchronization purposes, the experimental protocol also included the action of dropping an extra marker on the floor, within the Kinects' field of view, before the beginning of each trial.

Table 5.2. Tasks performed by the subjects.

Task name	Description	Number of trials
T1	Walk towards the Kinects for 7 m; turn around at 1.2 m from the sensors (outside their practical depth range); walk away from the sensors for another 7 m.	10
T2	Walk towards the Kinects for 5 m; turn around at 3.2 m from the sensors (within their practical depth range); walk away from the sensors for another 5 m.	5
T3	Walk towards the Kinects for 5 m; stop at 3.2 m from the sensors and stand still for 5 seconds; march in place (i.e., move the left and right feet up and down alternately, three times each); walk towards the sensors for 2 m; turn around at 1.2 m from the sensors; walk away from the sensors, repeating the same activities as for walking towards the sensors.	5

5.2.4 Data Acquisition and Pre-Processing

Data provided by the Kinects were acquired at approximately 30 Hz, using our *KiT* software application [78]. Data provided by the Qualisys system were acquired at 200 Hz. The Kinect data included colour/IR (Kv1/Kv2), depth and 3-D body joint data. Each frame of the latter includes the 3-D position of the tracked joints (Figure 2.4), as well as the tracking state of each joint (tracked, inferred or not tracked) and information regarding whether the subject's body is outside the field of view or not (i.e., clipped edges' information). The Qualisys data included the 3-D position of the markers, which was measured with an accuracy of at least 0.6 mm.

For activity recognition, we manually selected the time intervals corresponding to the different activities (walking, standing and marching), using our *KiMA* software application. Only the frames for which the subject was within the Kinect's field of view were taken into account. We also distinguished between two different postures: facing the Kinect (front) or facing away from it (back). The following six activities were considered:

- Walking towards the sensor (WF);
- Walking away from the sensor (WB);
- Standing still, while facing the sensor (SF);
- Standing still, while facing away from the sensor (SB);
- Marching (military style) in place, while facing the sensor (MF);
- Marching (military style) in place, while facing away from the sensor (MB).

We differentiated between facing the Kinect and facing away it, because the Kinect itself does not distinguish between these two positions of the subject in relation to the sensor. The Kinect

assumes that the subject is always facing the sensor, which means that when the subject is facing away from it, the left and right joints are interchanged. Therefore, the ability to distinguish between the two postures is important for gait analysis, when the acquired data includes both walking towards and away from the sensor.

The number of selected frames is presented in Table 5.3, for each Kinect version, as well as for each and all activities. The table includes the total number for all subjects, as well as the mean and standard deviation values per subject.

Table 5.3. Number of frames for the selected Kv1 and Kv2 data, for each and all activities, when considering all subjects and each subject (mean and standard deviation).

Activity	Number of frames			
	All subjects		Per subject	
	Kv1	Kv2	Kv1	Kv2
WF	15,459	22,439	773 ± 76	1,122 ± 96
WB	17,547	23,899	877 ± 82	1,195 ± 104
SF	12,555	12,558	628 ± 60	628 ± 60
SB	12,197	12,198	610 ± 66	610 ± 67
MF	13,285	13,280	664 ± 43	664 ± 44
MB	13,459	13,443	673 ± 42	672 ± 42
All	84,502	97,817	4,225 ± 258	4,891 ± 314

For implementing and evaluating the algorithm for gait cycle detection, we used only the data corresponding to the walking activity performed during task T1 (more trials and more gait cycles per trial). For each gait trial, the time intervals during which the subject walked towards and away from the Kinects (WF and WB, respectively) were automatically selected based on the acquired Kinect data (3-D position of the spine middle joint, tracking state of all joints and clipped edges' information), using the method described in detail in Appendix C.1.

The total number of actual heel strikes and gait cycles is indicated in Table 5.4. The mean and standard deviation values per subject and per trial are also included. These results are indicated for both Kinects (v1 and v2), both walking activities (WF and WB), and for left, right and both heel strikes/gait cycles.

To evaluate the performance of our algorithm, it was necessary to synchronize the data provided by the three used systems. Similar to other studies [60, 61, 63], synchronization was enabled by including in the protocol a specific action or movement before each gait trial. In our case, the following action was performed: dropping an extra marker on the floor. The instant the marker hits

the floor was used as a common time reference. That instant was identified by visualizing the acquired colour/IR images in the case of Kv1/Kv2, and by finding the first local minima with value less than 20 cm for the y-coordinate of the extra marker's position in the case of the Qualisys.

Table 5.4. Number of actual heel strikes and gait cycles performed by all subjects, for all analysed WF and WB trials of task T1, when using Kv1 and Kv2. The mean and standard deviation values per subject and per trial are also included.
The values are indicated for the left, right and both heel strikes/gait cycles.

Kinect version			Kv1		Kv2	
Walking activity			WF	WB	WF	WB
All subjects and trials	Heel strike	Left	247	293	463	387
		Right	289	273	407	384
		Both	536	566	870	771
	Gait cycle	Left	50	95	265	189
		Right	91	80	209	186
		Both	141	175	474	375
Per subject	Heel strike	Left	12.4 ± 3.4	14.7 ± 2.7	23.1 ± 3.5	19.4 ± 2.0
		Right	14.4 ± 3.2	13.7 ± 3.9	20.4 ± 2.1	19.2 ± 3.2
		Both	26.8 ± 4.2	28.3 ± 4.1	43.5 ± 4.2	38.5 ± 4.8
	Gait cycle	Left	2.5 ± 3.4	4.8 ± 2.6	13.3 ± 3.4	9.4 ± 1.9
		Right	4.5 ± 3.1	3.8 ± 3.9	10.4 ± 2.1	9.3 ± 3.1
		Both	7.0 ± 4.1	8.5 ± 4.0	23.7 ± 4.1	18.8 ± 4.6
Per trial	Heel strike	Left	1.2 ± 0.5	1.5 ± 0.6	2.3 ± 0.6	2.0 ± 0.5
		Right	1.5 ± 0.5	1.4 ± 0.6	2.1 ± 0.5	1.9 ± 0.5
		Both	2.7 ± 0.6	2.9 ± 0.7	4.4 ± 0.9	3.9 ± 0.9
	Gait cycle	Left	0.2 ± 0.5	0.5 ± 0.6	1.3 ± 0.6	1.0 ± 0.5
		Right	0.5 ± 0.5	0.4 ± 0.6	1.1 ± 0.5	0.9 ± 0.5
		Both	0.7 ± 0.6	0.9 ± 0.7	2.4 ± 0.9	1.9 ± 0.9

For each trial, the synchronization was validated based on the joint data. For this validation, the Kinect data were resampled to a fixed frame rate of 200 Hz, so that the frame rate is the same for all systems. Then, we computed the Pearson's correlation coefficient (r) between the signals for the Kinect and Qualisys corresponding to the sum of the three coordinates of the left and right ankle position (r_{la} and r_{ra}, respectively). To ensure that only trials with good synchronization between systems were considered, the trials for which r_{la} or r_{ra} was lower than 0.9 were not taken into account.

The resampling of the Kinect data was performed only for confirming the synchronization between systems. Similar to the study presented in [63], we used the original data for each system to evaluate the performance of the gait cycle detection algorithm, to avoid introducing noise to the Kinect data when up-sampling it or losing resolution for the Qualisys data when down-sampling it.

5.2.5 Activity Recognition

Our solution detects the time intervals corresponding to the walking activity by recognizing the following six activities or classes: walking towards and away from the camera (WF and WB); standing while facing the Kinect and facing away from it (SF and SB); marching while facing the Kinect and facing away from it (MF and MB). The activity recognition is carried out using a predictive model and several features extracted from filtered 3-D body joint data. The different steps involved detecting the walking activity are illustrated in Figure 5.4 by the second to fourth blocks.

Feature Extraction

The extracted features include the thirty and thirty-eight measures presented in Table 5.5, which were computed for each Kv1 and Kv2 data frame, respectively. The 3-D data were previously processed using a moving average filter with a window size of *NF* frames: for each axis, the filtered value of sample *i* is the mean value of all samples within the window (centred on sample *i*).

Table 5.5. Measures computed over the 3-D body joint data and corresponding equations.

Measure	Joints[a]	Equation
Velocity	Head, neck, spine middle, spine base and spine shoulder	(3.4)
	Shoulder, elbow, wrist, hand, hip, knee, ankle, foot, hand tip and thumb[b]	
Z-axis velocity	Head, neck, spine middle, spine base and spine shoulder	(5.1)
Distance between symmetrical joints	Left and right feet, ankles, knees, hands, wrists, elbows, hand tips and thumbs	(3.6)
Angle	Neck, spine shoulder and spine middle	(3.7)
	Knee and elbow[b]	
YZ-plane angle	Neck, spine shoulder and spine middle	(5.2)
	Knee and elbow[b]	

[a] the spine shoulder, hand tips and thumbs are only tracked by the Kv2.

[b] corresponds to the mean between left and right joint measures, where the measure for each side is computed using the indicated equation.

$$v_z \approx \frac{\Delta z}{\Delta t} \tag{5.1}$$

$$\text{angle}_{yz} = \arctan\left(\frac{y_1 z_2 - z_1 y_2}{y_1 y_2 + z_1 z_2}\right),\ \overrightarrow{P_2P_1} = (x_1, y_1, z_1) \text{ and } \overrightarrow{P_2P_3} = (x_2, y_2, z_2) \tag{5.2}$$

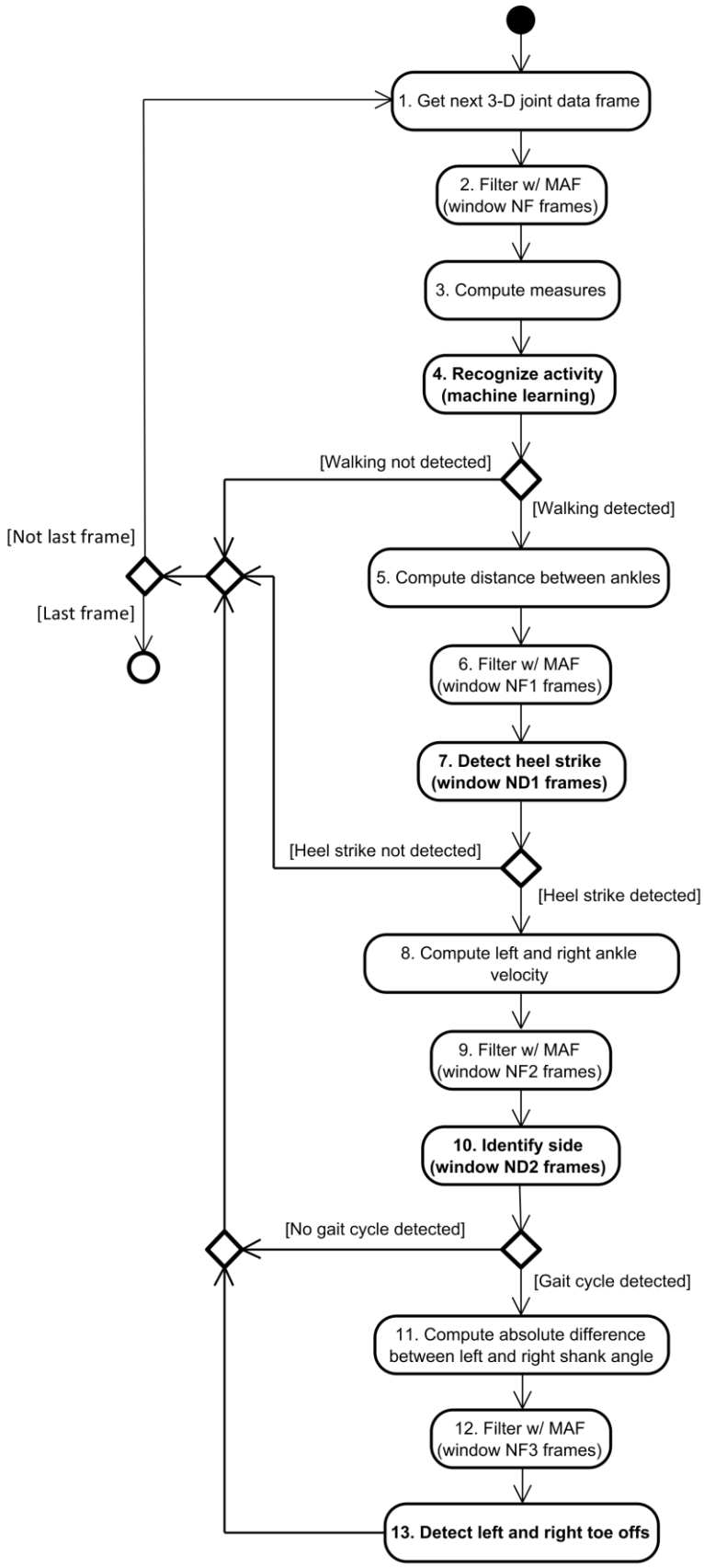

Figure 5.4. Solution for gait cycle detection, including activity recognition and gait event detection. MAF stands for moving average filter.

The measures include the velocity of each tracked joint. The velocity of the trunk joints (head, neck, and spine middle, base and shoulder) may help distinguish between walking and the other two activities (standing and marching). The velocity of the remaining joints may help distinguish between standing and the other two activities (walking and marching). We also considered the z-axis velocity (i.e., the z-axis component of the velocity vector) of the trunk joints, since it should help distinguishing between walking towards and away from the sensor.

We also computed the distance between symmetrical joints (e.g., left and right hands), since it varies for the walking and marching activities, while it is expected to not vary significantly for standing. Other extracted measure is the angle at given joints of the trunk, which should provide information regarding posture. For the body limbs (arms and legs), we computed the angle at the elbows and knees, since these should have the largest variation during walking. We also considered the YZ-plane angle (considers only the y- and z-component of the joints' position), since its value indicates the direction of the angle in relation to the XY-plane, and can be useful for detecting if the subject is facing the sensor or facing away from it.

Machine Learning Algorithms

To obtain the best predictive model for activity recognition, the following machine learning algorithms were explored:

- k-nearest neighbours (k-NN);
- Decision tree;
- Random forest;
- Support vector machines (SVM);
- Multilayer perceptron (MLP);
- Multilayer perceptron ensemble (MLPE).

These are some of the main supervised machine learning classification algorithms [22, 219], which are often used for activity recognition [2]. They correspond to different types of learning techniques: instance-based or lazy learning (k-NN), decision tree learning, support vector machines, artificial neural networks (MLP) and classifier ensemble (random forest and MLPE).

In our study, we used a weighted version of the k-NN algorithm [220, 221]. The number of considered nearest neighbours (k) was 7, the distance between two instances was computed using the Euclidean distance, and the weight of the k nearest neighbours was obtained using the "optimal" kernel function [222].

For the decision tree, we used an implementation [223, 224] of the recursive partitioning method for building classification and regression trees (CART) [225]. The Gini index was used to compute the impurity of a node. The class frequency in the training set was considered as the class prior probability. In the used implementation, a split is not attempted if the node does not have a minimum of 20 instances, or if the split does not lead to an improvement by a factor of 0.01 (complexity parameter) [223, 224].

For the random forest algorithm, we used an implementation [226] of Breiman's random forest [227]. The number of grown trees was 500, and the size of the feature subset selected for each node was $\lfloor \sqrt{n} \rfloor$, where n is the number of features in the training set.

For the SVM algorithm, we used the C-SVM formulation, with a cost parameter value of 1. For the kernel function, we used the Gaussian radial basis function $K(\mathbf{x},\mathbf{x}') = \exp\left(-\sigma \|\mathbf{x}-\mathbf{x}'\|^2\right)$, where $\mathbf{x}$ and $\mathbf{x}'$ are two instances. In the used implementation of SVM [228, 229], the value of parameter σ is the median of the 0.1 and 0.9 quantile of the $\|\mathbf{x}-\mathbf{x}'\|^2$ statistics for a sample of the training set [230]. The optimization problem is solved by relying on the sequential minimal optimization (SMO) algorithm [231]. For multi-class problems, the one-against-one approach is used.

For the MLP algorithm, we used the implementation described in [232]. The activation function of the hidden neurons is the logistic function. For multi-class problems, the output layer has a linear neuron per class. The search for the best set of weights between nodes is carried out by the BFGS (Broyden–Fletcher–Goldfarb–Shanno) algorithm, which minimizes a fitting criterion (maximum likelihood, in the case of classification) [212, 232]. It is stopped when the error slope approaches zero or after a maximum number of iterations (we considered 100 iterations). The number of hidden neurons was set to 10.

Since the training of a MLP model is not optimal, to avoid the dependence of the final solution on the choice of starting weights (chosen at random), a given number of different MLP models are built [212] (we considered three models). Then, the one with the lowest value of the fitting criterion is selected. In the case of the MLPE, all built MLPs are used, and the output is the mean between the individual predictions.

Model Evaluation

For each algorithm, the performance of the corresponding model for activity recognition was evaluated using a stratified 10-fold cross-validation approach [233]. The used dataset corresponds to fifteen subjects, which were randomly chosen from the twenty subjects that participated in the study.

This dataset includes 35,190/35,010 frames or instances and 30/38 different measures (Kv1/Kv2). It is a balanced dataset, which was obtained from the original dataset by randomly selecting 391/389 instances per subject and activity (random under-sampling without replacement). The number of instances per subject and activity corresponds to the minimum number of instances, when taking into account all subject-activity combinations in the original dataset.

A final model was built using the algorithm that led to the model with best trade-off between the metrics described below. The performance of this model was then assessed using a dataset corresponding to the five subjects whose data were not used for model training ("never seen" subjects), which includes 20,407/23,412 instances.

The considered performance evaluation metrics included accuracy and F_1 score. The class and overall accuracy were computed using (5.3) and (5.4), respectively. The class and overall F_1 score were computed using (5.5) and (5.6), respectively. The value of both accuracy and F_1 score ranges between 0% and 100% inclusive, where a higher value is better.

$$\text{Class accuracy}(\%) = \frac{\text{TP} + \text{TN}}{\text{TP} + \text{TN} + \text{FP} + \text{FN}} \times 100 \tag{5.3}$$

$$\text{Overall accuracy}(\%) = \frac{\text{no. of correctly classified instances}}{\text{no. of total instances}} \times 100 \tag{5.4}$$

$$\text{Class } \text{F}_1 \text{ score} = 2 \times \frac{\text{class precision} \times \text{class sensitivity}}{\text{class precision} + \text{class sensitivity}} \tag{5.5}$$

$$\text{Overall } \text{F}_1 \text{ score} = \sum_{i=1}^{C} \text{F}_1(c_i).\text{prev}(c_i) \tag{5.6}$$

$$\text{Class sensitivity}(\%) = \frac{\text{TP}}{\text{TP} + \text{FN}} \times 100 \tag{5.7}$$

$$\text{Class precision}(\%) = \frac{\text{TP}}{\text{TP} + \text{FP}} \times 100 \tag{5.8}$$

In (5.3), (5.7) and (5.8), TP, TN, FP and FN correspond to:

- True positives (TP): the number of instances correctly classified as belonging to the considered class;
- True negatives (TN): the number of instances correctly classified as belonging to a class other than the one considered;

- False positives (FP): the number of instances incorrectly classified as belonging to the considered class;
- False negatives (FN): the number of instances incorrectly classified as belonging to a class other than the one considered.

In (5.6), C is the number of classes, $\mathrm{F}_1(c_i)$ is the F_1 score for class c_i, and $\mathrm{prev}(c_i)$ is the prevalence of class c_i given by N_{c_i}/N, where N and N_{c_i} are the number of total instances and instances of class c_i, respectively, in the test set.

As our objective is to develop an online solution for gait cycle detection, the model should be able to predict the activity in the shortest possible amount of time, besides achieving a high accuracy and F_1 score. A low training time is also desirable. Therefore, we additionally considered the training time, as well as the prediction time for a single data frame and 1 min of data (≈1,800 frames).

All predictive models were built and validated in the R environment [209], relying on the *rminer* package [212].

5.2.6 Gait Cycle Detection

For the detection of gait cycles and associated phases, we developed an algorithm that automatically identifies the instants corresponding to gait events. To evaluate this algorithm, we took into account the data corresponding to task T1, as described above. The algorithm implementation and evaluation were performed in Matlab (version R2015a) [234].

Figure 5.5 illustrates the different phases of a right gait cycle, which are defined by different gait events. The events include three consecutive heel strikes: an initial right heel strike $\mathrm{HS_R}(k)$, a left heel strike $\mathrm{HS_L}(k+1)$ and a final right heel strike $\mathrm{HS_R}(k+2)$. They also include two consecutive toe offs: a left toe off $\mathrm{TO_L}(k)$ and a right toe off $\mathrm{TO_R}(k+1)$, which occur between $\mathrm{HS_R}(k)$ and $\mathrm{HS_L}(k+1)$ and between $\mathrm{HS_L}(k+1)$ and $\mathrm{HS_R}(k+2)$, respectively. In the expressions used to indicate the gait events, k is the number of the detected heel strike/toe off. For a left gait cycle, the gait events and gait cycle phases are similar, but the left and right sides are interchanged.

To find the best method for detecting heel strikes and toe offs using Kinect data, we firstly obtained the actual instants corresponding to those gait events. This identification was carried out based the feet vertical velocity extracted from the Qualisys data (ground truth), taking into account the findings of O'Connor et al. [128] (detailed description of our used method can be found in Appendix C.2).

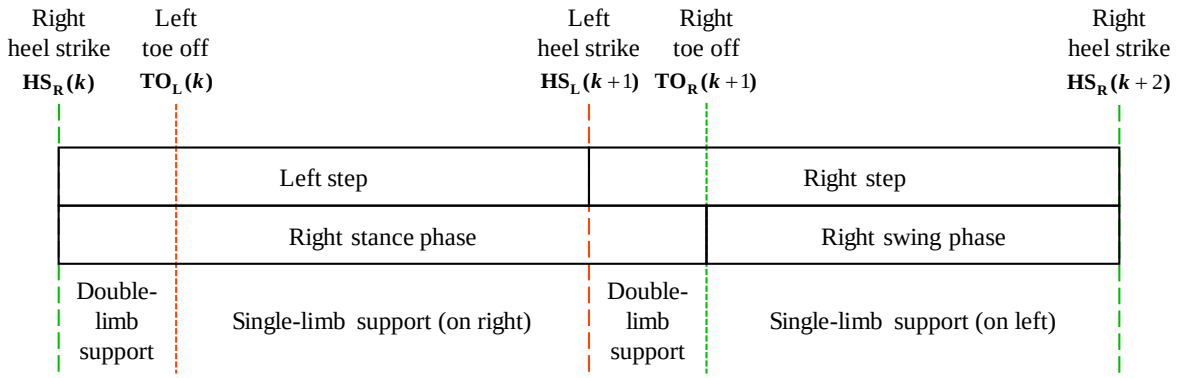

Figure 5.5. Different phases of a right gait cycle, as well as the gait events that define them.

The feet vertical velocity signal computed over Kinect data is rather noisy (even after filtering), making it more difficult to detect the gait events based on this measure when using the Kinect. Therefore, we explored other measures that could be used for gait event detection. The explored measures involved the feet, ankles, knees and spine base joints. In the case of Qualisys, the position of these joints correspond to the position of the following markers: LFM2 (left foot), RFM2 (right foot), LLA and LMA (left ankle), RLA and RMA (right ankle), LLK and LMK (left knee), RLK and RMK (right knee) and HIP CENTER (spine base). For the left/right ankle and knee, the position is the mean of the coordinate values for the 3-D position of the two indicated markers.

Heel Strike Estimation

As referred above, we identified the actual heel strikes relying on the feet vertical velocity computed over Qualisys data. Figure 5.6 (a) shows an example of the left and right foot vertical velocity (Qualisys) versus the elapsed time, for a given subject and WF trial. The corresponding actual left and right heel strikes are also indicated.

For the Kinect, we investigated other measures less affected by noise that can also be used for heel strike detection. We considered detecting heel strikes by finding the local maxima of the distance between knees, in a similar way to the method proposed by Auvinet et al. [59]. However, we verified that in most cases the actual heel strike instants are closer to the instants corresponding to the local maxima of the distance between ankles, when compared with the knee distance. An example of both knee distance and ankle distance (Qualisys) versus the elapsed time is shown in Figure 5.6 (b). The actual heel strike instants are also indicated.

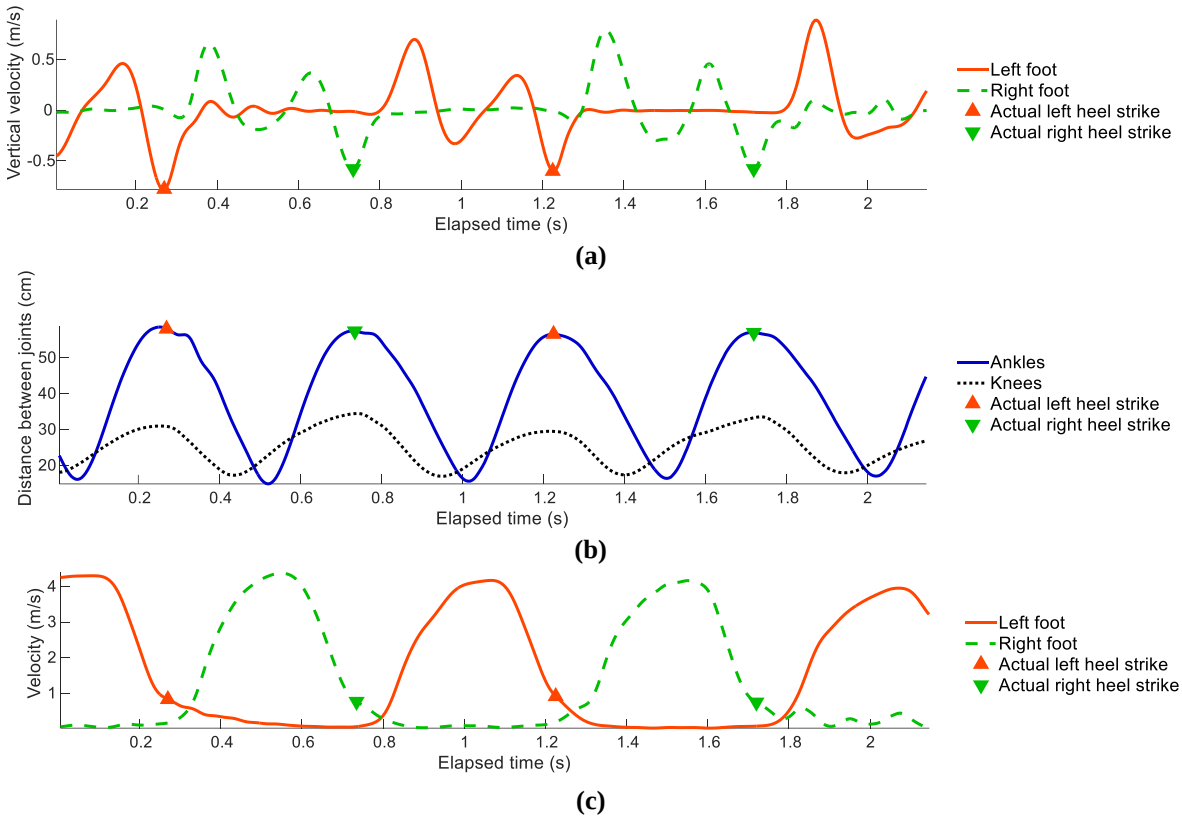

Figure 5.6. Filtered left and right foot vertical velocity (a), distance between ankles and between knees (b) and left and right ankle velocity (c), versus the elapsed time, computed over Qualisys data acquired from a given subject while walking towards the Kv2.
The actual left and right heel strikes are also indicated in each plot.

Taking the above observation into account, our solution estimates heel strike instants by finding the local maxima of the ankle distance. A sample *i* is identified as a heel strike if the associated ankle distance is maximum, when considering a window with size of *ND1* samples (centred on sample *i*). Prior to this processing, a moving average filter with a window size of *NF1* samples is applied to the ankle distance signal. Even after filtering, there can still be some noise, especially at the beginning/end of the trial. Therefore, to avoid false positives due to noise, we considered a local maximum as a heel strike only if the ankle distance increased for all frames of the first half of the window and decreased for all frames of the second half of the window. The main operations involved in heel strike detection are represented in Figure 5.4 by the fifth to seventh blocks.

To identify the side (left or right) associated with each detected heel strike, we investigated the use of the velocity of the left and right feet. Figure 5.6 (c) shows the left and right foot velocity (Qualisys) versus the elapsed time, as well as the actual heel strike instants, for the same subject and trial as Figure 5.6 (a) and (b). As can been seen in Figure 5.6 (c), for each instant corresponding to a

left/right heel strike, the velocity of the left/right ankle is decreasing, while the velocity of the right/left ankle is increasing, as expected.

Therefore, our algorithm identifies the side of a given heel strike by using the following decision rule:

$$\Delta v_{\text{left}} - \Delta v_{\text{right}} \begin{cases} < 0 & \rightarrow \text{left heel strike} \\ = 0 & \rightarrow \text{undefined} \\ > 0 & \rightarrow \text{right heel strike} \end{cases}$$

In this expression, $\Delta v_{side} = v_{side}(i+N) - v_{side}(i-N)$, where *side* is left or right, $v_{side}(k)$ is the ankle velocity for sample *k*, *i* is the sample corresponding to the detected heel strike, and $N = (ND2-1)/2$, where *ND2* is the size of the processing window. We considered the ankle joint instead of the foot joint, since we verified that the associated data are less noisy. The ankle velocity data are previously processed using a moving average filter with a window size of *NF2* samples. The main operations related to side detection are illustrated in Figure 5.4 by the eighth to tenth blocks.

To find the best values for *NF1* and *ND1*, we explored the odd integer values ranging from 1 to 9 inclusive and from 3 to 9 inclusive, respectively. From all window size pairs, we selected the one that we considered to have the best trade-off between precision, sensitivity and mean absolute error for estimating heel strike instants and stride/step duration. For the chosen *NF1* and *ND1* values, we then performed a similar selection for the window sizes *NF2* and *ND2* used for side identification. In this case, we chose the pair of values that led to the highest mean value for precision and sensitivity, where the precision/sensitivity value is the mean between the left and right sides. If more than one value pair led to the best result, then the lowest sizes were selected.

Toe Off Estimation

The actual toe off events were also estimated using the vertical velocity of the feet, as already explained above. Figure 5.7 (a) shows the left and right foot vertical velocity (Qualisys) versus the elapsed time, for the same subject and WF trial as Figure 5.6. The corresponding actual left and right toe offs are also shown in this figure.

In a similar way to heel strikes, toe offs are difficult to detect based on feet vertical velocity when using Kinect data, due to noise. Other studies used measures such as the knee angle, ankle height, or foot velocity [57, 64, 165]. However, the proposed methods relied on thresholds, which makes them not very generalizable. Another measure that was used in other contributions, which does not require the use of thresholds, is the anterior-posterior distance between the left/right ankle

and spine base joints [60, 61, 63]. As can be seen in Figure 5.7 (b), the local maxima of the distance between those joints (in the xz-plane) occur before the actual toe offs.

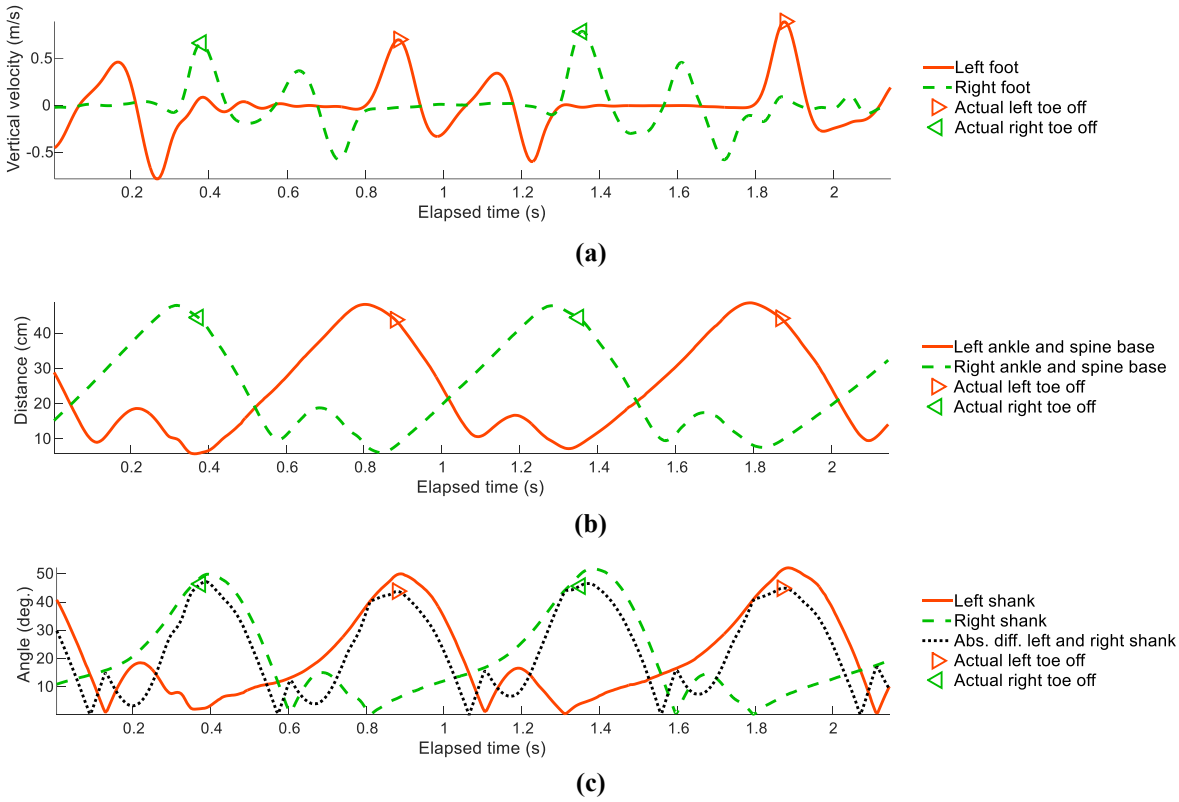

Figure 5.7. Filtered left and right foot vertical velocity (a), xz-plane distance between left ankle and spine base and between right ankle and spine base (b), and left and right shank angle and absolute difference between left and right shank angle (c), versus the elapsed time, computed over Qualisys data acquired from the same subject and trial as Figure 5.6.
The actual left and right toe offs are also indicated in each plot.

We also explored the shank angle (i.e., the angle defined by the knee, ankle and the point with knee y-coordinate and ankle x- and z-coordinates). As we can see from Figure 5.7 (c), the local maxima for the shank angle are closer to the toe off instants, when compared with the distance between the ankle and spine base. Moreover, we verified that lower estimation errors are achieved overall for the absolute difference between the left and right shank angle comparing with the left/right shank angle.

Therefore, for each detected gait cycle, our algorithm finds the instants corresponding to the left/right toe off by finding the maximum of the shank angle absolute difference, when considering the frames between the instants corresponding to the right/left heel strike and the following instant

when the ankle distance is minimum. If the estimated instant corresponds to the first or last frame of that interval, it is considered that the toe off was not successfully detected (false negative).

The shank angle data are previously processed using a moving average filter with a window size of *NF3* samples. To find the best value for *NF3*, we explored the odd integer values ranging between 1 and 11 inclusive, and selected the one that we considered to have the best trade-off between the estimation errors for stance, swing, single-limb support and double-limb support duration. The main operations involved in toe off detection are illustrated in Figure 5.4 by the eleventh to thirteenth blocks.

Evaluation of the Gait Cycle Detection Algorithm

The performance of the gait cycle detection algorithm was evaluated by obtaining the true and absolute estimation errors for each heel strike and toe off instant, using (5.9) and (5.10), respectively. The estimated and actual values are the values obtained from the Kinect and Qualisys data, respectively.

$$\text{true error} = \text{estimated value} - \text{actual value} \tag{5.9}$$

$$\text{absolute error} = \left|\text{estimated value} - \text{actual value}\right| \tag{5.10}$$

For each gait cycle, similar errors were obtained for six temporal gait parameters: duration of the gait cycle (or stride) and step, as well as of the stance, swing, single-limb support and double-limb support phases. These parameters were computed using (5.11) to (5.16), respectively. In these equations, $\mathrm{HS}_{\mathrm{L/R}}$ and $\mathrm{TO}_{\mathrm{L/R}}$ stand for left or right heel strike and toe off respectively, and k is the number of the detected heel strike or toe off. The left/right stance, swing, single support and double support are the corresponding phases of a left/right gait cycle.

$$k\text{th left/right stride duration} = \mathrm{HS}_{\mathrm{L/R}}(k+2) - \mathrm{HS}_{\mathrm{L/R}}(k) \tag{5.11}$$

$$k\text{th left/right step duration} = \mathrm{HS}_{\mathrm{L/R}}(k+2) - \mathrm{HS}_{\mathrm{R/L}}(k+1) \tag{5.12}$$

$$k\text{th left/right stance duration} = \mathrm{TO}_{\mathrm{L/R}}(k+1) - \mathrm{HS}_{\mathrm{L/R}}(k) \tag{5.13}$$

$$k\text{th left/right swing duration} = \mathrm{HS}_{\mathrm{L/R}}(k+2) - \mathrm{TO}_{\mathrm{L/R}}(k+1) \tag{5.14}$$

$$k\text{th left/right single support duration} = \left(\mathrm{HS}_{\mathrm{R/L}}(k+1) - \mathrm{TO}_{\mathrm{R/L}}(k)\right) + \left(\mathrm{HS}_{\mathrm{L/R}}(k+2) - \mathrm{TO}_{\mathrm{L/R}}(k+1)\right) \tag{5.15}$$

$$k\text{th left/right double support duration} = \left(\mathrm{TO}_{\mathrm{R/L}}(k) - \mathrm{HS}_{\mathrm{L/R}}(k)\right) + \left(\mathrm{TO}_{\mathrm{L/R}}(k+1) - \mathrm{HS}_{\mathrm{R/L}}(k+1)\right) \tag{5.16}$$

We also considered the sensitivity (5.7) and precision (5.8) regarding the detection of heel strikes and the identification of the heel strike side.

For the heel strike detection, TP, FN and FP correspond to:

- True positives (TP): the number of estimated heel strike instants that fall in time interval $]t_i - 0.25, t_i + 0.25[$ s, where t_i is the instant of the actual heel strike i;
- False negatives (FN): the number of actual heel strikes for which no heel strike is detected in time interval $]t_i - 0.25, t_i + 0.25[$ s;
- False positives (FP): the number of estimated heel strike instants that are not within any time interval $]t_i - 0.25, t_i + 0.25[$ s.

If more than one heel strike is detected within a given time interval $]t_i - 0.25, t_i + 0.25[$ s, only the first one is considered as a true positive (the remaining are false positives). The value of 0.25 s used above corresponds to half of 0.5 s, which is the mean for the step duration for our healthy dataset (see Appendix G).

For heel strike side identification, when considering the left/right side as the positive class, TP, FP and FN correspond to:

- True positives (TP): the number of actual left/right heel strikes correctly identified as left/right;
- False positives (FP): the number of actual right/left heel strikes incorrectly identified as left/right;
- False negatives (FN): the number of actual left/right heel strikes incorrectly identified as right/left.

The sensitivity was also computed for toe off detection, where TP and FN correspond to:

- True positives (TP): the number of actual toe offs that were successfully detected;
- False negatives (FN): the number of actual toe offs that were not successfully detected.

5.3 Results

5.3.1 Activity Recognition

The overall accuracy and overall F_1 score achieved by the models built using different machine learning algorithms are presented in Table 5.6, for both Kinect versions. The 3-D joint data were filtered using a window size (*NF*) of 17 frames. This was the chosen size because it led to the highest mean value for the overall accuracy of all explored algorithms (see Figure 5.8), when considering window sizes from 1 to 25 frames (odd integer numbers) and both Kinect versions.

Table 5.6. Overall accuracy and overall F_1 score achieved by the models built with different machine learning algorithms, for Kv1 and Kv2.

Algorithm	Kv1		Kv2	
	Overall accuracy (%)	Overall F_1 score (%)	Overall accuracy (%)	Overall F_1 score (%)
k-NN	98.5		98.6	
Decision tree	93.8		95.1	
Random forest	98.4		98.6	
SVM	98.2		98.3	
MLP	98.2		98.3	
MLPE	98.4		98.4	

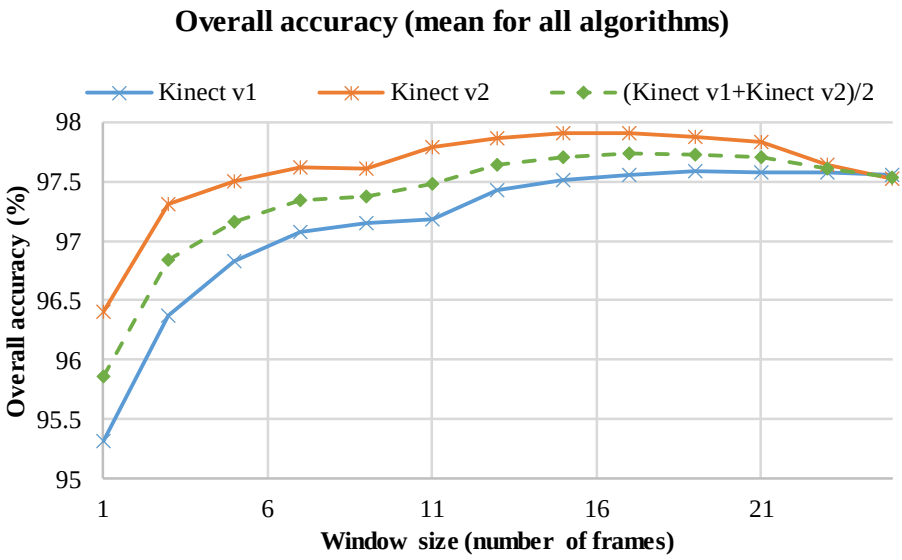

Figure 5.8. Mean value for the overall accuracy achieved by the models built with the different machine learning algorithms versus the size of the window used of the moving average filter used over the Kinect 3-D joint data.

The mean and standard deviation values for the models' training time, when considering the training set and five runs, is presented in Table 5.7. This table also includes the mean and standard deviation values for the prediction time per frame, which were computed over the prediction time for all frames in the test set. The prediction time for 1,800 frames (≈ 1 min of data), when considering the mean prediction time per frame, is also indicated in the table. These results were obtained for Kv2 (higher number of features than Kv1) on a computer with an i7-4600U CPU (dual-core, 2.1 GHz) and 8 GB RAM.

Table 5.7. Mean and standard deviation values for the models' training time (five runs) and prediction time per frame, as well as the associated prediction time for 1,800 frames (≈1 min of data).

Algorithm	Training time (min)	Prediction time	
		1 frame (ms)	1,800 frames (min)
k-NN	0.0 ± 0.0	349 ± 165	10.5
Decision tree	0.1 ± 0.0	3 ± 7	0.1
Random forest	3.3 ± 0.4	67 ± 44	2.0
SVM	0.5 ± 0.0	10 ± 10	0.3
MLP	1.7 ± 0.1	5 ± 8	0.2
MLPE	1.5 ± 0.1	12 ± 9	0.4

From the explored algorithms, we selected the MLP algorithm, since the associated model presented the best trade-off between all considered metrics (overall accuracy/F_1 score, training and prediction time). Table 5.8 shows the accuracy and F_1 score achieved by the final MLP model, when performing activity recognition over the dataset of five "never seen" subjects.

Table 5.8. Accuracy and F_1 score values achieved by the final MLP model over a dataset corresponding to five "never seen" subjects, when using the Kv1 and Kv2.
The accuracy and F_1 score for each activity were obtained using (5.3) and (5.5), respectively. The overall values were computed using (5.4) and (5.6), respectively.

Activity	Accuracy (%)		F_1 score (%)	
	Kv1	Kv2	Kv1	Kv2
WF	98.5	99.3	95.8	98.4
WB	98.6	98.7	96.6	97.4
SF	98.5	99.6	95.0	98.4
SB	98.8	99.3	96.0	97.3
MF	99.0	99.5	97.0	98.2
MB	99.2	99.0	97.3	96.5
Overall	96.3	97.7	96.3	97.7

5.3.2 Gait Cycle Detection

The gait cycle detection algorithm uses different window sizes for ankle distance filtering (*NF1*), heel strike detection (*ND1*), ankle velocity filtering (*NF2*), heel strike side identification (*ND2*) and shank angle filtering (*NF3*). The used window sizes are included in Table 5.9, for both Kinect versions and both walking activities. The table also presents the precision and sensitivity achieved for heel strike detection and side identification and/or toe off detection, as well as the mean and standard deviation values for number of gait cycles detected for each WF/WB gait trial.

Table 5.9. Size of the windows used for gait cycle detection, for both Kinect versions and both walking activities. The achieved precision and sensitivity results, as well as the number of gait cycles detected per WF/WB trial (mean and standard deviation), are also included.

Sensor			**Kv1**		**Kv2**	
Walking activity			**WF**	**WB**	**WF**	**WB**
Window size (number of frames)	**Ankle distance filtering (*NF1*)**		5	7	5	5
	Heel strike detection (*ND1*)		7	7	9	5
	Ankle velocity filtering (*NF2*)		7	7	9	9
	Heel strike side identification (*ND2*)		3	9	3	5
	Shank angle filtering (*NF3*)		9	7	9	7
Precision (%)	**Heel strike detection**		99.6	97.7	99.8	98.6
	Side identification	**Left**	100.0	99.3	100.0	99.7
		Right	99.3	100.0	100.0	100.0
Sensitivity (%)	**Heel strike detection**		92.4	91.7	96.4	97.7
	Side identification	**Left**	99.6	100.0	100.0	100.0
		Right	100.0	100.0	100.0	99.7
	Toe off detection		94.6	98.1	99.7	100.0
Number of detected gait cycles per trial		**Left**	0.2 ± 0.4	0.4 ± 0.5	1.3 ± 0.5	1.0 ± 0.3
		Right	0.4 ± 0.5	0.4 ± 0.5	1.1 ± 0.3	1.0 ± 0.5
		Both	0.6 ± 0.6	0.8 ± 0.5	2.4 ± 0.6	2.0 ± 0.6

Table 5.10 and Table 5.11 present the obtained true and absolute errors, respectively, achieved by our algorithm for estimating heel strike and toe off instants, as well as the stride, step, stance, swing, single support and double support duration. These results are indicated as the mean and standard deviation values considering all gait events/cycles from all subjects and trials.

Table 5.10. True errors achieved by the gait cycle detection algorithm, for Kv1 and Kv2 and for WF and WB.

The results are presented as mean and standard deviation values when considering all detected gait events/cycles, for the estimation of heel strike and toe off instants, as well as the stride, step, stance, swing, single support and double support duration.

		True error (ms)			
Kinect		**Kv1**		**Kv2**	
Walking activity		**WF**	**WB**	**WF**	**WB**
Heel strike instant	**Left**	8.9 ± 19.0	20.4 ± 22.5	14.2 ± 24.7	12.6 ± 24.1
	Right	8.6 ± 19.3	20.6 ± 21.2	12.4 ± 18.6	11.7 ± 20.8
	Both	8.7 ± 19.2	20.5 ± 21.9	13.4 ± 22.0	12.2 ± 22.5
Toe off instant	**Left**	17.5 ± 32.1	19.6 ± 27.9	13.4 ± 23.5	16.6 ± 98.7
	Right	23.5 ± 26.0	20.2 ± 24.4	11.7 ± 21.2	12.4 ± 115.0
	Both	20.4 ± 29.3	19.9 ± 26.0	12.5 ± 22.3	24.9 ± 24.4
Stride duration	**Left**	0.5 ± 25.2	−4.2 ± 28.0	8.9 ± 27.5	0.9 ± 23.7
	Right	4.1 ± 25.4	−6.0 ± 25.3	−0.5 ± 17.3	−0.9 ± 23.3
	Both	2.5 ± 25.4	−5.6 ± 26.7	4.8 ± 24.0	−0.1 ± 23.6
Step duration	**Left**	0.6 ± 24.1	−1.4 ± 24.4	4.4 ± 26.3	2.0 ± 25.2
	Right	0.8 ± 22.5	−2.2 ± 24.1	2.9 ± 20.0	−1.2 ± 24.3
	Both	0.7 ± 23.3	−1.8 ± 24.2	3.6 ± 23.2	0.4 ± 24.8
Stance duration	**Left**	−9.0 ± 44.3	−3.0 ± 32.3	4.1 ± 22.9	11.7 ± 28.0
	Right	19.7 ± 26.1	−5.3 ± 31.6	0.6 ± 20.8	11.2 ± 26.6
	Both	11.4 ± 34.7	−4.2 ± 31.9	2.5 ± 22.0	11.8 ± 27.3
Swing duration	**Left**	8.3 ± 43.4	−3.2 ± 26.7	5.1 ± 29.8	−10.1 ± 29.2
	Right	−16.0 ± 22.5	−1.1 ± 29.7	−1.2 ± 22.7	−12.0 ± 26.0
	Both	−8.9 ± 31.9	−2.1 ± 28.2	2.2 ± 27.0	−11.5 ± 27.7
Single support duration	**Left**	12.6 ± 54.8	−3.7 ± 43.0	7.3 ± 38.5	−26.1 ± 39.1
	Right	−21.6 ± 45.4	−2.1 ± 50.7	−3.9 ± 33.8	−26.6 ± 43.0
	Both	−12.8 ± 41.9	−1.6 ± 40.7	2.5 ± 35.7	−29.9 ± 37.4
Double support duration	**Left**	−13.9 ± 55.7	−2.4 ± 47.6	1.7 ± 34.5	27.9 ± 39.8
	Right	24.6 ± 50.8	−5.2 ± 51.5	2.9 ± 31.9	26.2 ± 42.8
	Both	13.8 ± 54.8	−3.8 ± 49.3	2.3 ± 33.4	27.6 ± 41.1

Table 5.11. Absolute errors achieved by the gait cycle detection algorithm, for Kv1 and Kv2 and for WF and WB.
The results are presented as mean and standard deviation values when considering all detected gait events/cycles, for the estimation of heel strike and toe off instants, as well as the stride, step, stance, swing, single support and double support duration.

		Absolute error (ms)			
Kinect		**Kv1**		**Kv2**	
Walking activity		**WF**	**WB**	**WF**	**WB**
Heel strike instant	**Left**	17.6 ± 11.4	25.4 ± 16.8	21.4 ± 18.7	21.4 ± 16.7
	Right	17.0 ± 12.5	23.7 ± 17.7	17.9 ± 13.4	19.0 ± 14.5
	Both	17.3 ± 12.0	24.6 ± 17.2	19.8 ± 16.5	20.2 ± 15.7
Toe off instant	**Left**	27.4 ± 24.1	28.0 ± 19.4	19.8 ± 16.8	37.6 ± 92.7
	Right	28.1 ± 20.9	26.7 ± 17.0	19.0 ± 16.8	38.9 ± 108.9
	Both	27.7 ± 22.5	27.3 ± 18.1	19.4 ± 16.8	28.7 ± 19.8
Stride duration	**Left**	20.6 ± 14.2	21.6 ± 18.1	20.6 ± 20.3	18.2 ± 15.2
	Right	19.6 ± 16.6	20.0 ± 16.4	13.4 ± 10.9	17.1 ± 15.8
	Both	19.8 ± 15.9	21.0 ± 17.4	17.5 ± 17.2	17.7 ± 15.5
Step duration	**Left**	18.0 ± 16.0	19.2 ± 15.0	19.9 ± 17.7	19.6 ± 15.9
	Right	18.1 ± 13.3	19.1 ± 14.7	15.8 ± 12.5	18.4 ± 15.8
	Both	18.0 ± 14.7	19.2 ± 14.8	17.7 ± 15.3	19.1 ± 15.8
Stance duration	**Left**	29.2 ± 34.1	25.4 ± 19.9	21.3 ± 16.7	24.6 ± 17.7
	Right	25.8 ± 20.0	24.2 ± 20.8	18.9 ± 15.2	22.7 ± 17.7
	Both	26.8 ± 24.8	24.8 ± 20.3	20.0 ± 16.0	23.9 ± 17.8
Swing duration	**Left**	29.9 ± 32.1	20.8 ± 16.8	18.3 ± 14.3	25.1 ± 18.0
	Right	22.7 ± 15.7	24.0 ± 17.2	15.9 ± 13.3	23.3 ± 16.5
	Both	24.8 ± 21.8	22.5 ± 17.0	17.2 ± 13.9	24.4 ± 17.4
Single support duration	**Left**	43.4 ± 34.8	32.4 ± 28.1	21.5 ± 21.2	39.5 ± 25.4
	Right	41.2 ± 28.5	40.9 ± 29.6	17.8 ± 14.1	43.0 ± 26.5
	Both	34.4 ± 27.2	32.7 ± 24.3	19.8 ± 18.5	39.5 ± 27.1
Double support duration	**Left**	44.1 ± 35.8	35.0 ± 32.0	28.9 ± 26.5	40.4 ± 26.9
	Right	44.7 ± 34.2	39.9 ± 32.6	27.4 ± 20.0	41.9 ± 27.4
	Both	44.5 ± 34.5	37.3 ± 32.3	27.1 ± 23.4	41.4 ± 27.0

Figure 5.9 (a) shows the ankle distance computed from both unfiltered and filtered Kinect v2 data, versus the elapsed time, for the same subject and trial of Figure 5.6. It also shows the heel strike instants estimated by our algorithm, as well as the actual heel strikes instants. The identification of the side (left or right) associated with the detected heel strikes is indicated in Figure 5.9 (b). This figure is similar to Figure 5.9 (a), with the difference that it presents the left and right ankle velocity, which were used for side identification.

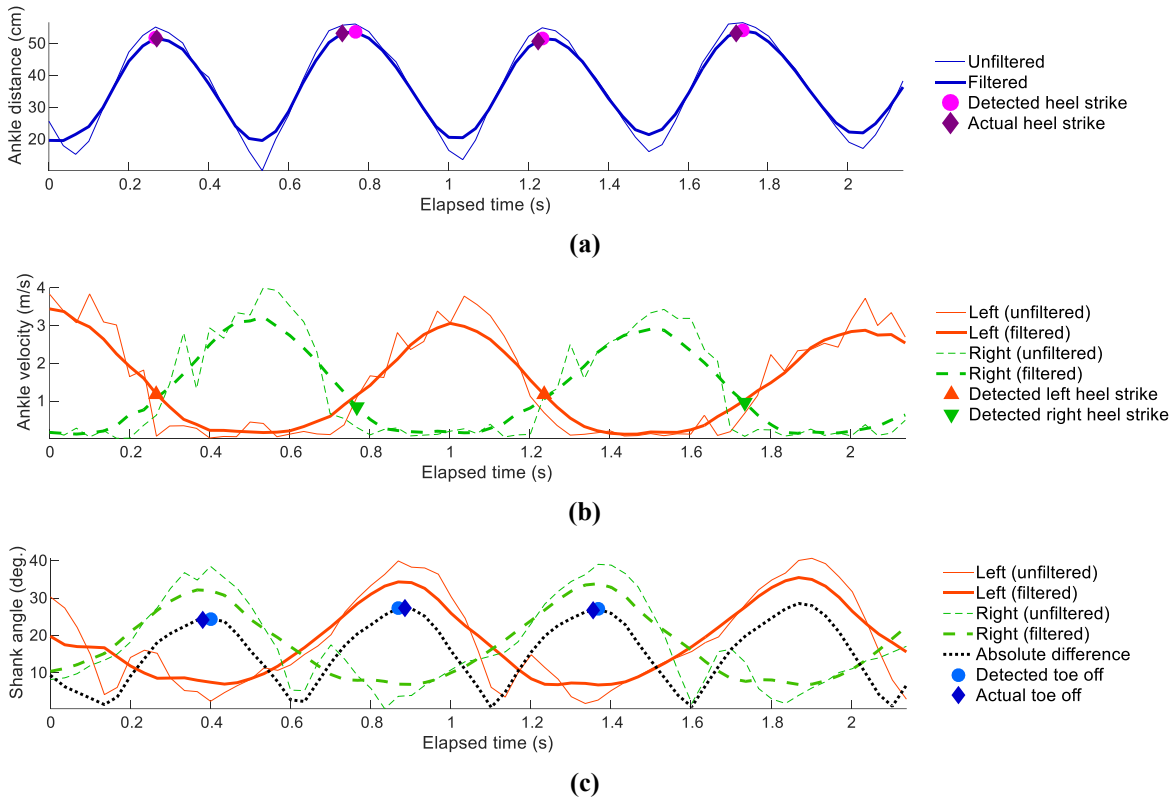

Figure 5.9. Distance between ankles (a), velocity of left and right ankles (b) and angle of left and right shanks and corresponding absolute difference (c), computed over unfiltered and filtered Kv2 data, versus the elapsed time, for the same subject and WF trial of Figure 5.6.

The heel strike instants estimated by our algorithm and the corresponding actual instants are indicated in (a). The left and right heel strikes detected by our algorithm are indicated in (b). The toe off instants estimated by our algorithm and the corresponding actual instants are indicated in (c).

Figure 5.9 (c) presents the left and right shank angle (unfiltered and filtered) versus the elapsed time, for the same situation as (a) and (b). The same figure shows the absolute difference between the two angles, which was used for toe off detection, as well as the toe off instants estimated by our algorithm and the associated actual toe off instants. The last toe off for the trial is not indicated in the figure, since our algorithm only attempts to detect a toe off when two consecutive heel strikes have been detected.

5.4 Discussion

5.4.1 Activity Recognition

Our study on activity recognition showed that machine learning techniques can be used to recognize three activities (walking, standing and marching) and two positions of the subject in relation to the camera (facing it and facing away from it), relying on measures extracted from 3-D joint data provided by a single RGB-D camera. From the different explored algorithms, the MLP led to the predictive model that presented the best trade-off between the considered metrics (overall accuracy, overall F_1 score, training and prediction time). The final built model was able to recognize the considered activities with an overall accuracy of 96% for Kv1 and 98% for Kv2.

Regarding the impact that filtering the 3-D joint data has on the model's performance, a higher mean value for the overall accuracy of all considered algorithms was achieved when filtering the data (Figure 5.8) comparing with no data filtering (window size of 1 frame). This trend was observed for both Kinect versions, with the best result being achieved for a window size between 17 and 25 frames for Kv1 (97.6% instead of 95.3% for non-filtered data), and between 13 and 19 frames for Kv2 (97.9% instead of 96.4% for non-filtered data). When taking into account both Kinects, the best result was obtained for a size of 15 to 21 frames. Between the two intermediate sizes (17 and 21 frames), we chose the smallest one, i.e., 17 frames, to filter the data for activity recognition.

When comparing the models built with the different explored algorithms, all achieved a high overall accuracy and overall F_1 score (≥ 93.8% for Kv1 and ≥ 95.1% for Kv2 – see Table 5.6). Nevertheless, the decision tree model had the poorest performance. All other models achieved similar results (98.2–98.5% for Kv1 and 98.3–98.6% for Kv2).

Although the k-NN model does not require any training (mean training time of 0 min), the associated mean prediction time for a single data frame (349 ms) was much higher than for the other models (Table 5.7). The random forest not only had the highest training time (3 min), but also had a high prediction time (67 ms per frame) comparing with the remaining models. The time required to predict the activity for 1 minute of data for the last two models was of 11 and 2 min, respectively, which makes them not suitable for online activity recognition.

From the remaining algorithms, the SVM has the lowest training time (0.5 min), while the MLP had the lowest prediction time (5 ms per frame). Since a low prediction time is desirable for online activity recognition, and the training time for the MLP model is still reasonable (1.7 min), we considered that this model presents the best trade-off between the considered metrics, being the most adequate for online activity recognition.

When using the final MLP model to predict activities for a dataset corresponding to five "never seen" subjects, the obtained overall accuracy and F_1 score values (96% for Kv1 and 98% Kv2) are similar to those obtained when comparing the different algorithms. When considering the different activities, accuracy and F_1 score were always higher than 98.5% and 95.0%, respectively (Table 5.8).

5.4.2 Gait Cycle Detection

To verify if Kv1 and Kv2 can be used interchangeably for gait cycle detection, the developed algorithm was validated for both Kinect versions. The obtained results show that Kv2 is more appropriate than Kv1 for detecting gait cycles, since it presented a higher sensitivity for detecting gait events, enabled the detection of a higher number of gait cycles per gait trial, and achieved overall lower estimation errors for gait event detection and temporal gait parameter estimation. These results were expected since, according to Microsoft, the Kv2 has a larger depth range and improvements regarding joint tracking when compared with Kv1 [182].

We also investigated if all data acquired during each gait task can be used for gait analysis, by validating our algorithm for both WF and WB activities. For Kv2, results were overall better for WF than WB, with the biggest error differences being verified for the estimation of single and double support duration. This difference between using WF and WB was also to be expected. The Kinect assumes the subject is always facing the camera, since it was originally intended for gaming, and thus it is expected that the data acquired when the subject faces away from the camera are noisier than when the subject faces it.

The detection of gait cycles involves the detection of gait events, such as heel strikes and toe offs. In the case of heel strikes, we found that filtering the used measures led to a better precision and sensitivity overall than when the data were not filtered (Tables D.1, D.4, D.7 and D.10, Appendix D.1). However, larger window sizes (*NF1*) led to larger estimation errors in most cases.

When detecting the instants corresponding to heel strikes, we verified that larger window sizes (*ND1*) led to a higher precision. However, they also led to a lower sensitivity, which means that less actual heel strikes and consequently less actual gait cycles are detected. Nevertheless, a higher precision is more important than a higher sensitivity, since the detection of heel strikes that do not correspond to actual heel strikes (i.e., false positives) leads to the incorrect identification of gait cycles and consequently to the incorrect computation of gait parameters. Therefore, the choice of the window size pair for each Kinect version and walking activity took into account the best trade-off between precision, sensitivity and mean absolute estimation errors.

For identifying the heel strike side, precision and sensitivity did not vary considerably when using different window sizes (*NF2* and *ND2*), except in the case of *NF2* = 1 frame and *ND2* = 3 frames, for which the results were much lower comparing with the other explored window size pairs (Tables D.2, D.5, D.8 and D.11, Appendix D.1). The window size pair chosen for each Kinect version and walking activity took into account the highest mean value for precision and sensitivity (lowest sizes selected when there is more than one value pair led to the best result).

Regarding toe off detection, it is important to note that the lowest error for estimating the toe off instants did not always lead to the lowest error for estimating the duration of gait cycle phases (Tables D.3, D.6, D.9 and D.12, Appendix D.1). This happens because the computation of these parameters also depends on the heel strike instants, which are also detected by our algorithm with a given error. The *NF3* value that presented the best trade-off between the sensitivity and the mean absolute estimation errors was of 9 frames for WF and 7 frames for WB (both Kinects).

For the chosen window sizes (Table 5.9), the precision for heel strike detection is high in all cases (≥ 97.7%), with higher values for WF trials (≈100%). The sensitivity is also relatively high in all cases (≥ 91.7%), with higher values for Kv2 (≥ 96.4%). A high sensitivity for heel strike detection is desirable, since it means that a greater number of actual gait cycles are detected for the same amount of data. This is useful when we wish to perform gait analysis based on a minimum number of gait cycles, because it allows saving time during the process of data acquisition and analysis. However, a higher precision is more important, since false positives lead to the incorrect identification of gait cycles and consequently an incorrect computation of gait parameters.

The precision and sensitivity for identifying the heel strike side were also high in all cases (≥ 99.3%). Regarding toe off detection, our algorithm achieved a high sensitivity. However, it was lower for Kv1 and WF (94.6%) when compared with the other cases (≥ 98.1%). This difference is probably due to the fact that the Kv1 data were noisier at the beginning of the WF trials of some subjects, when compared with the other cases.

The number of detected gait cycles per trial was quite different for Kv1 and Kv2, especially when considering WF trials: mean of 0.6 gait cycles and 2.4 gait cycles, respectively (Table 5.9). Although the sensitivity for heel strike detection was higher for Kv2 when compared with Kv1, the main reason for the observed difference is that the practical depth range for Kv2 (2.7 m) is larger than for Kv1 (1.8 m), leading to a larger number of actual gait cycles per gait trial (Table 5.4). Therefore, using the Kv2 instead of Kv1 has the advantage of requiring a smaller number of gait task repetitions to obtain a given number of gait cycles, consequently saving time in the whole gait analysis process.

Regarding the estimation of gait event instants, the mean true error for heel strikes ranged between 8 and 21 ms (Table 5.10). Although the best result was achieved for Kv1 (WF), this sensor also led to the worst error (WB). On the other hand, the Kv2 had similar errors for both walking activities (mean value of 13 ms for WF and 12 ms for WB). Therefore, the Kv2 has a better balance when considering both WF and WB.

The mean error when estimating toe offs instants varied between 12 and 25 ms. The results are similar in the case of Kv1. However, the result was better for WF than WB when using the Kv2. The standard deviation for the true error was much higher for Kv2 and WB, which may be because the shank angle signals were noisier for the WB trials of some subjects when using the Kv2, comparing with the other cases. Nonetheless, the estimation of the duration of gait phases, which depends on the toe off instants, was not greatly affected (standard deviation values are similar for all cases).

The absolute errors we obtained ranged between 17 ms and 29 ms. When considering both types of gait events, the best results were achieved for Kv2 and WF: 20 ms for heel strikes and 19 ms for toe offs. Regarding these absolute estimation errors, it is important to note that there is a maximum intrinsic error of 17 ms (half of the time interval between two consecutive frames) associated with the Kinect, assuming a constant frame rate of 30 Hz.

When estimating the duration of a gait cycle and its different phases, the errors varied depending on the Kinect version and walking activity. The mean absolute error for the stride, step, stance and swing duration ranged between 17 and 27 ms (both sides). The error was higher for the single support and double support duration (19–45 ms), which was expected since these durations are computed based on four gait events, while the stride, step, stance and swing duration are computed based on only two gait events.

Overall, the Kv2 and WF data led to lowest absolute errors. For this case, the percentage of the mean error in relation to the mean duration of the temporal parameter was of 2% for stride duration, 3% for step, stance and single support duration, 5% for swing duration and 10% for double support duration. The values used for the mean parameter duration are those presented in Table G.1 (Appendix G.1) for Qualisys in the case of Kv2.

5.4.3 Comparison with the State of the Art

In contrast with other studies, we evaluated the performance of our algorithm for both Kv1 and Kv2, as well as for the two different activities of walking towards (WF) and walking away (WB) from the Kinect. Since the obtained results were overall better for Kv2 and WF, our results presented below are for this combination.

The true errors we obtained when estimating heel strike and toe offs are presented in Table 5.12, together with the results reported in other studies. For heel strikes, our mean true error is lower than the value obtained by Auvinet et al. [59], but is higher when compared to Xu et al [60]. However, it is important to note that the other studies considered treadmill walking, while our results were obtained for overground walking. The last situation is more challenging, since the distance between the subject and Kinect varies within each gait trial, while it remains constant when walking on a treadmill.

Table 5.12. Comparison between our algorithm and the methods proposed in other contributions, regarding the true error for estimating heel strike and toe off instants.

Method		True error (ms)		
		Our[a]	**Auvinet et al., 2015 [59]**	**Xu et al., 2015 [60][b]**
Heel strike instant	**Left**	14.2 ± 24.7	—	5.0 ± 26.7
	Right	12.4 ± 18.6		3.0 ± 21.7
	Both	13.4 ± 22.0	17 ± 24	—
Toe off instant	**Left**	13.4 ± 23.5	—	−43.5 ± 61.7
	Right	11.7 ± 21.2		−37.5 ± 56.7
	Both	12.5 ± 22.3		—

[a] Results for Kv2 and WF.

[b] values converted from number of frames (the frame rate was of 60 Hz, so an error of 1 frame corresponds to an error of 17 ms).

For toe offs, our solution was able to estimate the corresponding instants with a mean true error between 11 and 14 ms. This is considerably lower than the mean errors reported by Xu et al. (−44 ms and −38 ms), corresponding to a difference of 26 to 30 ms when considering the absolute value of the mean true error. The difference when considering the standard deviation is even larger. These results indicate that the measure we relied on for toe off detection (shank angle absolute difference) is more appropriate for this purpose than the one used by Xu et al. (distance between the ankle and hip centre). The solution proposed by Auvinet et al. does not include toe off detection.

Although other contributions proposed a method for detecting gait events, the associated estimation error was not reported. Nevertheless, the error for estimating the stride, step, stance, swing and/or double support duration was presented. The true and absolute estimation errors for these parameters achieved by our algorithm, as well as other proposed methods, are presented in Table 5.13 and Table 5.14, respectively. For the contributions that explored different walking speeds, the indicated results are for the speed(s) closer to the mean gait speed for our study (approximately 1.2 m/s).

For the studies that reported the errors in seconds with only two decimals places, the values of 0.00 s are indicated as]–5, 5[ms.

A direct comparison between our results and the results achieved in the other studies is not possible, due to the use of a different experimental setup and/or protocol (e.g., first version of the Kinect [55-57, 59, 60, 65], multiple Kinects [61, 62], treadmill walking [59, 60, 63, 65]). Nevertheless, it is interesting to see how our results stand in relation with those reported in other contributions.

Table 5.13. Comparison between our algorithm, and the methods proposed in other contributions, regarding the true error for estimating stride, step, stance, swing and double support duration.

		True error (ms)										
Method		**Our[a]**	**Stone et al., 2011 [55][b]**	**Gabel et al., 2012 [56]**	**Clark et al., 2013 [57]**	**Pfister et el., 2014 [65][c]**	**Auvinet et al., 2015 [59]**	**Xu et al., 2015 [60][d]**	**Mentiplay et al., 2015 [64][e]**	**Geerse et al., 2015 [61]**	**Eltoukhy et al., 2017 [63][f]**	**Müller et al., 2017 [62][f]**
Stride duration	**Left**	8.9 ± 27.5	—	8 ± 62	—	157 ± 31	—	—	—	—	—	—
	Right	−0.5 ± 17.3		2 ± 46		153 ± 28						
	Both	4.8 ± 24.0	7.47 ± 62.2	—	−200 ± 66	—	0 ± 12	1 ± 25 / 0 ± 19		10	]–5, 5[± 10	
Step duration	**Left**	4.4 ± 26.3	—	—	—	—	—	—	—	—	—	−10 ± 15
	Right	2.9 ± 20.0										]–5, 5[± 15
	Both	3.6 ± 23.2			−170 ± 71			0 ± 26 / 0 ± 19	]–5, 5[/ −10	10	−20 ± 10	]–5, 5[± [0, 5[
Stance duration	**Left**	4.1 ± 22.9	—	−8 ± 110	—	—	—	—	—	—	—	—
	Right	0.6 ± 20.8		−20 ± 90								
	Both	2.5 ± 22.0		—				−48 ± 55 / −36 ± 58	30 / 40			
Swing duration	**Left**	5.1 ± 29.8	—	6 ± 115	—	—	—	—	—	—	—	—
	Right	−1.2 ± 22.7		27 ± 104								
	Both	2.2 ± 27.0		—				46 ± 57 / 35 ± 57				
Double support duration	**Both**	2.3 ± 33.4	—	—	—	—	—	−45 ± 54 / 34 ± 57	—	—	—	—

[a] Results for Kv2 and WF.

[b] Results for the second (#2) Kinect.

[c] Results for the hip time and a controlled speed of 1.30 m/s.

[d] Results for the controlled speeds of 1.07 m/s and 1.30 m/s.

[e] Results for days 1 and 2 (comfortable pace).

[f] Results for a controlled speed of 1.30 m/s.

[g] Results for the mean of the parameter value for left/right/both gait cycles per subject.

Table 5.14. Comparison between our algorithm, and the methods proposed in other contributions, regarding the absolute error for estimating stride, step, stance, swing and double support duration.

Method		Absolute error (ms)		
		Our	Gabel et al., 2012 [56]	Eltoukhy et al., 2017 [63][a]
Stride duration	Left	20.6 ± 20.3	45	—
	Right	13.4 ± 10.9	32	
	Both	17.5 ± 17.2	—	10 ± 10
Step duration	Left	19.9 ± 17.7	—	—
	Right	15.8 ± 12.5		
	Both	17.7 ± 15.3		20 ± 10
Stance duration	Left	21.3 ± 16.7	70	—
	Right	18.9 ± 15.2	67	
	Both	20.0 ± 16.0	—	
Swing duration	Left	18.3 ± 14.3	71	—
	Right	15.9 ± 13.3	70	

[a] Results for a controlled speed of 1.30 m/s.

When considering the parameters included in the tables, we were able to achieve lower true and absolute estimation errors overall. Our solution outperformed the other studies regarding the estimation of parameters that involve both types of gait events, i.e., the stance, swing and double support duration. For stance and swing duration, not only the mean true error is overall lower when compared with the study by Gabel et al. [56], but the associated standard deviation is also considerably lower (21 to 30 ms versus 90 to 115 ms). The mean absolute error is also much lower (16 to 21 ms versus 67 to 71 ms). Our mean true error (2 to 3 ms, both sides) is also much lower when compared with the studies by Xu et al. [60] (−48 or 46 ms) and Mentiplay et al. [64] (30 to 40 ms for the stance). For double support duration, our mean true error is also much lower when compared with the study by Xu et al. (2 ms versus −45 ms).

As for stride and step duration, our true error results (5 ± 24 ms and 4 ± 23 ms) are considerably better than those obtained by Clark et al. [57] (−200 ± 66 ms and −170 ± 71 ms) and by Pfister et al. [65] (153 ± 28 ms and 157 ± 31 ms for the stride). When compared with the studies by Gabel et al. and Stone et al. [55], although the mean error for stride duration is similar, our standard deviation considerably lower (less than half). Some of the other studies presented slightly lower mean true errors than ours for stride and step duration. However, the maximum difference was of 5 ms. Furthermore, in those studies the data were collected during treadmill walking [59, 60], which is a more controlled situation than over ground walking, as explained above.

5.5 Summary

We enabled automated gait analysis of a given subject using a single RGB-D camera (Kinect), by avoiding any manual intervention in the whole analysis process (besides starting the data acquisition) [76]. Firstly, the sensor data corresponding to walking is automatically selected. Then, gait events that occur during this activity are automatically detected. Finally, gait parameters are computed taking into account the detected gait events. This automated data selection and event detection allows time savings when compared with the manual identification of data/events.

The automated selection of gait data relies on a predictive model that recognizes three different activities (walking, standing and marching), as well as two different positions of the subject in relation to the camera (facing it and facing away from it), with a high overall accuracy (96% and 98% for the first and second Kinect versions, respectively). When walking is detected, the gait cycles and associated phases are identified using an algorithm that estimates the instants corresponding to two different types of gait events (heel strikes and toe offs). This algorithm outperformed other methods proposed in the literature regarding the estimation of toe off instants and consequently the estimation of the duration of gait cycle phases.

The developed solutions for activity recognition and gait cycle detection enable online gait analysis, which allows defining the minimum number of gait cycles required for analysis and automatically stopping the acquisition only when the defined number of gait cycles has been detected. An online solution can also allow additional time savings when compared with offline solution.

For each gait cycle (or stride), several spatiotemporal and kinematic gait parameters (e.g., stride duration and length, gait speed, elbow angle minimum and maximum) are computed over the 3-D body joint data, taking into account the detected gait events. The validity of these gait parameters is evaluated in the next chapter.

6 Validation of an RGB-D Camera for Gait Analysis

The body joint positions estimated from the depth data provided by a single markerless RGB-D camera can be less accurate than those obtained with a multi-camera marker-based system (gold standard for motion capture). For this reason, it is important to verify if the information provided by a given RGB-D camera is reliable for the aim of assessing gait, by evaluating its validity against a gold standard system.

The main objective of this chapter is thus answering the following question:

- Can a single RGB-D camera be used as an alternative to gold standard systems for supporting gait assessment?

To the best of our knowledge, there is no study that validates both versions of the Kinect simultaneously, or explores the impact of the Kinect configuration (height and tilt angle) on its validity, in the context of gait analysis (overground walking, frontal-plane view). In addition, most studies that consider a frontal-plane view do not validate the Kinect for walking towards and away from the sensor separately.

According to Microsoft, the second version of the Kinect has improvements over the first version, including improved body tracking [180]. Therefore, it is important to answer the following question:

- Can the first and second versions of the Kinect be used interchangeably for gait analysis?

In our studies, the gait task performed by the subjects includes walking towards and away from the Kinect. The use of the data acquired during both walking activities would allow to minimize the required number of task repetitions and consequently the duration of each data acquisition. However, the Kinect's joint tracking algorithm assumes that the subject is always facing the camera. For this reason, it is also important to answer another question:

- Can both the data acquired while the subject walks towards and away from the sensor be used for gait analysis?

After some modifications regarding the physical configuration of the Kinect in the preliminary studies, due to changes in the location of the associated experiments, the following question also emerged:

- Is there a given Kinect configuration that is more appropriate for gait analysis?

To answer the different questions, we studied the agreement between the Kinect and a gold standard system (marker-based multi-camera Qualisys system) for several gait parameters, when considering both Kinect versions, both walking activities and three different Kinect configurations.

6.1 Related Work

Several studies were carried out on the validity of the Kinect for estimating joint locations [17, 152], as well as for assessing gait [14, 56, 57, 60-65], postural control and/or standing balance [15, 163, 164, 166, 167], upper and/or lower body movements [16, 98, 100, 149, 150] and clinically relevant activities [12, 151]. In the specific case of gait, initial studies evaluated the validity of the first version of Kinect (Kv1) [56, 57, 60, 65], while the most recent studies validated its second version (Kv2) [61-64].

The approach used in the studies is not uniform due to the use of different setups (e.g., single or multiple Kinects, front- or side- view) and/or protocols (e.g., overground or treadmill walking, self-selected or controlled walking speed). The gait parameters explored in each study also varied. Nevertheless, most studies verified that the Kinect is a valid option for obtaining most spatiotemporal parameters, but is not appropriate for measuring most kinematic parameters.

Clark et al. studied the validity of Kv1 for obtaining spatiotemporal gait parameters (step duration and length, stride duration and length, gait speed and foot swing velocity) [57]. The validity results were obtained over data collected from twenty-one healthy adults, considering overground walking at a self-selected pace and a frontal-plane view (i.e., Kinect with an angle of 0 degrees in relation to the walking path). They verified that gait speed, step length and stride length have excellent agreement between the Kinect and a gold standard system (Vicon). For the remaining parameters, relative agreement was excellent for foot swing velocity and step duration, while it was only modest for stride duration. Absolute agreement was modest for foot swing velocity and poor for stride and step duration. The achieved mean error was of −200 ms and −170 ms for stride and step duration, −4.2 mm and 11.5 mm for stride and step length, −0.01 m/s for gait speed and 0.43 ms/s for foot swing velocity.

The Kv1 was also used by Gabel et al. to obtain temporal gait parameters, including the left and right stride, stance and swing duration [56]. They obtained a mean true error between −20 and

27 ms, standard deviation for the true error between 46 and 115 ms, and a mean absolute error between 32 and 71 ms, when considering the values obtained with in-shoe pressure sensors as the ground truth. These results were achieved for data collected from eleven subjects, with the Kinect placed at 45 degrees to the middle of the walking path line and at a height of 30–60 cm.

Other studies with Kv1 considered treadmill walking at various controlled speeds [60, 65]. Xu et al. explored both spatiotemporal parameters (step, stride, stance, swing and double support duration and step width) and kinematic parameters (knee flexion angle and hip flexion and extension angle), for three different gait speeds (0.85 m/s, 1.07 m/s and 1.30 m/s) [60]. The agreement between the Kinect and a gold standard system (Optotrak) was assessed using data acquired from twenty healthy subjects, with the Kinect positioned in front of the subject (frontal view). For the spatiotemporal parameters, the stride and step duration and the step width achieved the best results overall, while the stance, swing and double support duration had the worst agreement results. The kinematic parameters presented relatively high mean errors (varying between −39 and 7 degrees). Statistically significant differences between at least two of the gait speeds were detected for the stance, swing and double support duration, as well as for the hip flexion and extension angle.

Pfister et al. also validated the Kv1 for obtaining temporal and kinematic parameters (stride duration and flexion and extension angle for left and right hip and knee), during treadmill walking at three different speeds (≈1.3, 2.0 and 2.5 m/s) [65]. Data were acquired from twenty healthy subjects, using a Kv1 placed at 43 cm from the floor and at 45 degrees relative to the treadmill, as well as a Vicon system as the gold standard. For the kinematic parameters, results were overall better for the knee than the hip. The best relative agreement between systems was achieved for the intermediate speed, while the lowest mean error was obtained for the lowest speed. For stride duration, the best relative agreement was achieved when using the knee angle, considering all three speeds. The mean error were better for the highest speed (118–121 ms).

More recently, several validation studies were carried out for Kv2 [61-64]. Mentiplay et al. acquired data from thirty young, injury-free subjects, while they performed overground walking at comfortable and fast paced speeds, using the Kv2 with a frontal-plane view and a Vicon system [64]. They then computed several spatiotemporal parameters (e.g., step and stance duration, step length and width, gait speed and gait speed variability, and foot swing velocity) and kinematic parameters (knee flexion and adduction angle, and ankle and hip flexion angle range). They verified that the relative agreement between systems was excellent for most spatiotemporal parameters, but it varied between modest and poor for the kinematic parameters.

Another study using the Kv2 considering a frontal view was performed by Eltoukhy et al., but for treadmill walking at two different controlled speeds (1.3 and 1.6 m/s) [63]. They evaluated

the validity of Kv2 against a Vicon system, for computing spatiotemporal parameters (e.g., stride and step duration, step length and width, and foot swing velocity) and kinematic parameters (total hip, knee and ankle range of motion). They verified that the difference between systems is statistically significant for the step duration, length and width, foot swing velocity, total hip and ankle range of motion (both speeds). The mean error varied between −0.03 s and 0.00 s for stride and step duration, 0.04 m and 0.10 m for step length and width, and −2.27 and 20.63 degrees for the kinematic parameters. Similar to the studies previously described, the agreement was overall better for spatiotemporal than kinematic parameters.

Some studies on the validity of Kv2 for gait analysis relied on multiple Kinect cameras simultaneously. In a study carried out by Geerse et al., four Kv2 cameras were placed at a height of 0.75 m with a 70 degrees angle relative to the walkway direction, on the same side of the walkway [61]. The data provided by the Kinects and a gold standard Optotrak system were collected from twenty-one healthy subjects, while they walked at two speeds (comfortable and maximum walking speed). The agreement between systems was evaluated for seven spatiotemporal gait parameters: gait speed, cadence, step and stride length, step width, step and stride duration. All parameters presented a high agreement, with the exception of the step width. When comparing the two explored gait speeds, the cadence led to the highest difference considering the mean estimation error.

Müller et al. studied two different setups using multiple Kv2: three one-sided cameras and six two-sided cameras [62]. All cameras were placed at 35 degrees angle relative to the walking direction. A Vicon system was used as the gold standard system. For both setups, the step duration, stride and step length and step width were computed over data acquired from ten healthy subjects, while they performed overground walking at a comfortable pace. The validity of the multi-Kinect system was evaluated considering all left and right gait cycles separately, the mean value for left and right gait cycles per subject, and the mean value for all gait cycles per subject. The agreement between systems was overall better for the mean of all gait cycles, and for the two-sided setup when compared with the one-sided setup.

6.2 Materials and Methods

The dataset used to validate both Kinect versions for gait assessment is similar to the dataset used to evaluate our gait cycle detection solution. More details on the subjects, experimental setup and protocol, as well as data acquisition and pre-processing, can be found in Section 5.2. For comparing between different Kinect configurations, additional data were acquired with two new different configurations. The three considered configurations correspond to a Kinect height of 0.6 m, 1 m and 1.34 m.

6.2.1 Subjects

The subjects are the same twenty healthy subjects that participated in the experiment carried out for the study on gait cycle detection.

6.2.2 Experimental Setup and Protocol

The experimental setup included the two Kinect versions (Kv1 and Kv2) and a Qualisys system (twelve cameras and sixty-one retro-reflective markers). As referred above, three different physical configurations of the Kinect (KC1, KC2 and KC3) were considered. The height and tilt angle associated with each configuration are indicated in Table 6.1. The height for KC2 is the recommended minimum height for the Kinect [235, 236] and for KC3 is the tripod's maximum height. The height for KC1 corresponds to an intermediate height between KC2 and KC3. The method used to choose the tilt angle for each height and Kinect version is described in Appendix E.

Table 6.1. Height and tilt angle associated with each explored physical configuration of the Kinect (KC1, KC2 and KC2), for both Kv1 and Kv2.

Kinect configuration	Height (m)	Tilt angle (degrees)	
		Kv1	Kv2
KC1	1	−10	−5
KC2	0.6	0	5
KC3	1.34	−18	−15

The protocol included ten trials (KC1) or five trials (KC2 and KC3) per subject of the following gait task: walking towards and then away from the Kinects for a total of 14 m, at a self-selected comfortable pace.

6.2.3 Data Acquisition and Pre-Processing

The Kinect data (colour/IR, depth and 3-D body joint data) were acquired at 30 Hz, while the Qualisys data (3-D position of markers) were acquired at 200 Hz. The time intervals corresponding to walking towards and away from the Kinects (WF and WB) were automatically selected (see Appendix C.1). The data provided by the different systems were synchronized using the method described in Section 5.2.

6.2.4 Gait Parameter Computation

For each subject and WF/WB trial, the performed gait cycles were automatically detected using Kinect data by relying on our gait cycle detection algorithm (same window sizes as those used in the study presented in the previous chapter). The corresponding actual gait cycles were automatically identified using Qualisys data relying on the method described in Appendix C.2.

For each gait cycle, we computed the 13 spatiotemporal gait parameters (i.e., parameters involving time and/or distance) included in Table 6.2, and the 8/9 (Kv1/Kv2) kinematic gait parameters (i.e., parameters involving angles) included in Table 6.3. For each parameter, we then obtained the mean value per subject, when taking into account N gait cycles (chosen randomly if the number of gait cycles for a subject is higher than N).

For Qualisys, the 3-D position of each body joint used for gait parameter computation was calculated from the 3-D position of the relevant markers, as indicated in Table 6.4. The 3-D joint data were then processed using a zero-lag low-pass fourth order Butterworth filter with a cut-off frequency of 15 Hz. The filter parameter values were chosen by taking into account the frequency content of the signals.

For Kinect, the velocity, distance and angle signals were processed using a zero-lag low-pass Butterworth filter. For each gait parameter, we explored the filter order values of 2, 4 and 6, and cut-off frequency values between 1 and 9 Hz inclusive (integer values). We then chose the value for the filter parameters that minimized the mean absolute error between Kinect and Qualisys.

For each gait parameter, we excluded the gait cycles with outliers for the associated measure obtained from Qualisys data. For velocity and distance measures, we considered as outliers the frames with value above 5 m/s and 2 m, respectively. For all measure types, we also considered as outliers the frames for which the value is more than 40 scaled median absolute deviations away from the median for the following signal: sum of absolute difference of the joint position between consecutive frames in each axis.

All signal processing and analysis, including outlier detection, filter optimization, gait cycle detection and gait parameter computation, were performed in Matlab (version R2015a) [234].

Table 6.2. Spatiotemporal gait parameters computed over 3-D joint data, including a description and the equation used for its computation.

Spatiotemporal gait parameter	Definition	Equation
Stride duration	Duration of the gait cycle or stride.	(5.11)
Step duration	Duration of the left/right step, when considering a left/right gait cycle.	(5.12)
Stance duration	Duration of the stance phase.	(5.13)
Swing duration	Duration of the swing phase.	(5.14)
Single support duration	Duration of the single-limb support phase.	(5.15)
Double support duration	Duration of the double-limb support phase.	(5.16)
Stride length	Distance (in the xz-plane) between the position of the left/right ankle at the beginning and end of the left/right gait cycle.	The distance is computed using (3.6), where P_1 and P_2 correspond to the position of the ankle (in the xz-plane) at the two considered instants.
Step length	Distance (in the xz-plane) between the position of the left/right ankle at the instant during the swing phase when the ankle distance is minimum, and at the instant corresponding to the end of the left/right gait cycle.	
Step width	Minimum of the ankle distance (in the xz-plane) during the swing phase.	The ankle distance is computed for each frame using (3.6), where P_1 and P_2 correspond to the position of the left and right ankle (in the xz-plane), respectively.
Gait speed	Mean of the trunk velocity (mean of velocity of the head, neck, spine shoulder, spine middle, and spine base joints).	The velocity of each joint is computed for each frame using (3.4).
Gait speed variability	Standard deviation of the trunk velocity (mean of velocity of the head, neck, spine shoulder, spine middle, and spine base joints).	
Foot swing velocity	Maximum of the left/right ankle joint velocity during the swing phase, when considering a left/right gait cycle.	
Arm swing velocity	Maximum of the left/right hand velocity (mean of velocity of the left/right wrist and hand joints) during the stance phase, when considering a left/right gait cycle.	

Table 6.3. Kinematic gait parameters computed over 3-D joint data, including a description and the equation used for its computation.

Kinematic gait parameter	Definition	Equation
Neck angle	Mean of the angle at neck (defined by the head, neck and spine base joints).	The angle was computed for each frame using (3.7).
Spine shoulder angle[a]	Mean of the angle at spine shoulder (defined by the head, spine shoulder and spine base joints).	
Spine middle angle	Mean of the angle at spine middle (defined by the head, spine middle and spine base joints).	
Elbow angle minimum	Minimum of angle at the left/right elbow during the stance phase, when considering a left/right gait cycle. The angle at the elbow is defined by the corresponding shoulder, elbow, and wrist joints.	
Elbow angle maximum	Maximum of angle at the left/right elbow during the stance phase, when considering a left/right gait cycle.	
Knee angle minimum	Minimum of angle at the left/right knee during the swing phase, when considering a left/right gait cycle. The knee angle is defined by the corresponding hip, knee, and ankle joints.	
Knee angle maximum	Maximum of angle at the left/right knee during the stance phase, when considering a left/right gait cycle.	
Hip angle range	Difference between maximum and minimum value of the left/right hip angle, during the stance and swing phases respectively, when considering a left/right gait cycle. The hip angle is defined by the corresponding knee joint, hip joint, and point with knee y-coordinate and hip x- and z-coordinates.	
Ankle angle range	Difference between maximum and minimum value of the angle at the left/right ankle, during the swing and stance phases respectively, when considering a left/right gait cycle. The angle at the ankle is defined by the corresponding knee, ankle, and foot joints.	

[a] Kinect v2 only

Table 6.4. Computation of the 3-D position of joints from Qualisys data.

Joint(s) tracked by Kinect	Joint(s) position computed from Qualisys markers[a]
Head	$P = P_{HEAD}$
Neck	$P = P_{NECK}$
Spine shoulder	$P = P_{IJ}$
Spine middle	$P = P_{PX}$
Spine base	$P = P_{HIP\ CENTER}$
Left and right shoulder	$P_{left} = P_{LAC}$ and $P_{right} = P_{RAC}$
Left and right elbow	$P_{left} = (P_{LLELB} + P_{LMELB})/2^b$ and $P_{right} = (P_{RLELB} + P_{RMELB})/2^b$
Left and right wrist	$P_{left} = (P_{LULN} + P_{LRAD})/2^b$ and $P_{right} = (P_{RULN} + P_{RRAD})/2^b$
Left and right hand	$P_{left} = P_{LHAND}$ and $P_{right} = P_{RHAND}$
Left and right hip	$P_{left} = P_{LASIS}$ and $P_{right} = P_{RASIS}$
Left and right knee	$P_{left} = (P_{LLK} + P_{LMK})/2^b$ and $P_{right} = (P_{RLK} + P_{RMK})/2^b$
Left and right ankle	$P_{left} = (P_{LLA} + P_{LMA})/2^b$ and $P_{right} = (P_{RLA} + P_{RMA})/2^b$
Left and right foot	$P_{left} = P_{LFM2}$ and $P_{right} = P_{RFM2}$

[a] The labels associated with each marker placed on the subject's body are indicated in Figure 5.3.

[b] The joint position is the mean of the coordinate values for the 3-D position of the two indicated markers.

6.2.5 Kinect Validation

The agreement between the Kinect and Qualisys (gold standard) was evaluated for each gait parameter by obtaining the Bland-Altman's mean difference and 95% limits of agreement (LoA), as well as the Pearson's and concordance correlation coefficients and associated 95% confidence interval (CI).

The Bland-Altman's mean difference (or bias) is the mean of the differences between the measurements obtained by two different methods ($\bar{d}$) [237, 238]. The lower and upper 95% limits of agreement correspond to $\bar{d} - 1.96s$ and $\bar{d} + 1.96s$ respectively, where s is the standard deviation for the differences between paired measurements.

The presence of fixed bias, i.e., a constant difference in measurements between systems, was verified by carrying out a one-sample t-test on the differences between Kinect and Qualisys [239]. There is no fixed bias if the mean differences is indistinguishable from zero (p-value ≤ 0.05). Proportional bias is present when the difference in measurements from two methods increases or decreases in proportion to the mean values [239]. The presence of proportional bias was detected by performing a OLS (ordinary least squares) regression analysis [239, 240]. There is proportional bias if the OLS regression line fitted to the plot of the differences versus the means has a slope that differs significantly from zero (p-value ≤ 0.05).

The Pearson's correlation coefficient (r) indicates the strength of linear relationship between variables, i.e., their relative agreement [238]. The concordance correlation coefficient (r_c) indicates the absolute agreement between variables, by measuring not only how far each observation deviates from the line fit to the data (precision), but also how far this line deviates from the 45 degrees line through the origin (accuracy) [241]. The value of both r and r_c ranges between −1 and 1, where −1 means perfect disagreement, 0 corresponds to an independence situation and 1 indicates perfect agreement [242]. Based on the guidelines given by Portney and Watkins [243], correlation thresholds were set as poor (<0.5), moderate (≥0.5 and <0.75), good (≥0.75 and <0.9) and excellent (≥0.9).

For the mean difference or estimation error, a statistically significant difference between the two Kinect versions, the two walking activities and the three Kinect configurations, was verified by performing a one-way repeated-measures analysis of variance (ANOVA). For configuration comparison, if a significant difference was detected (p-value ≤ 0.05), a post-hoc Tukey test was then carried out to find which situations have significantly different errors.

All the analyses described in this section were performed in the R environment (version 3.2.3) [209], using code implemented for performing the validation studies. The *stats* package [210] was used to compute the Pearson's correlation coefficient and associated 95% CI and p-value, as

well as for performing the *t*-test and OLS regression analysis. The concordance correlation coefficient and associated 95% CI were obtained using the *cccrm* package [244]. The Tukey's test and ANOVA were performed using the *agricolae* [245] and *car* [246] packages, respectively.

6.3 Results

To verify if the two Kinect versions can be used interchangeably for gait analysis, the validation study was firstly carried out for both Kv1 and Kv2, when considering WF data and configuration KC1. In this study, we only took into account the WF activity, since the Kinect's joint tracking algorithm assumes that the subject is always facing the camera.

To investigate if data acquired during both WF and WB activities can be used for gait analysis, a similar validation study was carried out for the two different activities when using the Kinect version that led to the best overall result in the first validation study.

Furthermore, we explored if the physical configuration used for the Kinect has any effect on the computed gait parameter values, by performing the validity study for configurations KC2 and KC3 besides KC1, when taking into account the Kinect version and walking activity that achieved the best overall result in the studies described above.

The complete results of the optimization carried out for the parameters (order and cut-off frequency) of the low-pass zero-lag Butterworth filter, which was used for filtering the measures extracted from Kinect data, are included in Appendix F. The results obtained for each Kinect version and each walking activity are presented in Appendix F.1. The results obtained for the three Kinect configurations are presented in Appendix F.2. These results do not include the spatiotemporal gait parameters for which the computation only depends on time instants and/or the position of a body joint at those instants: stride, step, stance, swing, single support and double support duration, and stride length.

For each one of the remaining parameters, the order and cut-off frequency values were chosen for Kv1 and Kv2 separately, by taking into account the mean estimation error for both WF and WB. We chose not to filter the measures used to compute the step width and gait speed, as well as most of the kinematic parameters, since the mean error did not decrease or decreased only slightly when filtering the data. The selected values for the filter's parameters are indicated in Table 6.5 for each Kinect version.

Table 6.5. Butterworth filter's order and cut-off frequency values for each gait parameter, when using Kv1 and Kv2.

Gait parameter	Kv1		Kv2	
	Order	Cut-off frequency (Hz)	Order	Cut-off frequency (Hz)
Step length	6	5	6	3
Step width	Not filtered			
Gait speed				
Gait speed variability	2	1	2	2
Foot swing velocity	4	3	6	4
Arm swing velocity	2	1	4	2
Neck angle	Not filtered			
Spine shoulder angle	—		Not filtered	
Spine middle angle	No filtering			
Elbow angle maximum	6	1	Not filtered	
Elbow angle minimum	Not filtered			
Knee angle maximum				
Knee angle minimum				
Hip angle range				
Ankle angle range	6	1	6	1

The filter parameters values that led to the best results for each considered Kinect configuration were the same as the ones included in Table 6.5, except for the step length. However, the mean error values for step length were similar. Therefore, the values of Table 6.5 were used in all studies for simplicity.

For each study, the results presented below include the practical depth range, number of actual gait cycles and validation results, for each considered situation. The practical depth range is the difference between the largest and smallest distance between the subject and the Kinect for which all joints are tracked (minimum and maximum distance). The depth range value was obtained for each gait trial, by taking into account the WF/WB data selected automatically.

The number of actual gait cycles is the number of gait cycles identified by relying on Qualisys data, when considering the practical depth range of the Kinect. The results include the number of left, right and both gait cycles, and are indicated for all subject and trials, as well as for each subject and each trial (mean and standard deviation).

The validation results were obtained for each gait parameter and situation. They include the Bland Altman's mean difference (Mean diff), Pearson's correlation coefficient (r) and concordance correlation coefficient (r_c). If there is a statistically significant difference between the considered

situations (one-way repeated-measures ANOVA, p-value ≤ 0.05), when taking into account the estimation error for all subjects, the lowest mean difference is indicated in bold. The r and r_c values are indicated using the following colours: green (≥ 0.9), yellow (≥ 0.75 and < 0.9), orange (≥ 0.5 and < 0.75), and red (< 0.5). Moreover, the r values that are statistically significant (p-value ≤ 0.05) are indicated using the * symbol.

6.3.1 Kinect Version Comparison

Table 6.6 includes the mean and standard deviation values for the practical depth range of each Kinect version (WF, KC1), as well as the associated minimum and maximum distances, when considering all subjects and trials. We can see that the mean depth range for Kv2 is almost 1 m longer than for Kv1.

Table 6.6. Mean and standard deviation values for the practical depth range of both Kinect versions (Kv1 and Kv2), when considering the WF activity and configuration KC1.

	WF, KC1	
Kinect version	**Kv1**	**Kv2**
Practical depth range[a] (m)	1.84 ± 0.13	2.71 ± 0.08
Minimum distance[b] (m)	1.89 ± 0.12	1.63 ± 0.08
Maximum distance[c] (m)	3.73 ± 0.05	4.34 ± 0.03

[a] Difference between maximum and minimum distances.

[b] Shortest distance between the subject and Kinect for which all body joints are tracked.

[c] Longest distance between the subject and Kinect for which all body joints are tracked.

The number of actual gait cycles for all subjects and trials, as well as per trial and per subject (mean and standard deviation), is presented in Table 6.7 for both Kinects (WF, KC1). As expected, the Kv2 allowed the acquisition of a greater number of gait cycles per trial due to the larger depth range, which led to a number of gait cycles for all subjects and trials that is three times greater than for Kv1.

Table 6.7. Number of actual gait cycles for each Kinect version (Kv1 and Kv2), when considering the WF activity and configuration KC1.
The values are indicated for left, right, and both gait cycles, when considering all subjects and trials, as well as each trial and each subject (mean and standard deviation).

		Number of actual gait cycles (WF, KC1, 10 trials)	
Kinect version		**Kv1**	**Kv2**
All subjects and trials	**Left**	50	265
	Right	91	209
	Both	141	474
Per subject	**Left**	2.5 ± 3.4	13.3 ± 3.4
	Right	4.5 ± 3.1	10.4 ± 2.1
	Both	7.0 ± 4.1	23.7 ± 4.1
Per trial	**Left**	0.2 ± 0.5	1.3 ± 0.6
	Right	0.5 ± 0.5	1.1 ± 0.5
	Both	0.7 ± 0.6	2.4 ± 0.9

The validation results are presented in Table 6.8 (complete results in Appendix G.1). These results were obtained using a single gait cycle for each subject, since there is a subject for which it was only possible to obtain one valid gait cycle for most parameters, when using the Kv1.

Overall, Kv2 led to lower estimation errors than Kv1 (mean difference was lower when using Kv2 for 6 out of 8 parameters with a statistically significant difference between Kinects). The Kv2 also presented a better overall agreement with Qualisys than Kv1 (relative/absolute agreement was good or excellent for 13/12 parameters versus 9/4 parameters).

There was no statistically significant difference regarding estimation error (or mean difference) between Kv1 and Kv2 for all 13 spatiotemporal parameters, except for the stride length, gait speed and arm swing velocity (lowest error for Kv2). For kinematic parameters, most presented a significant difference between Kinects (5 out of 8 parameters). The exceptions were the spine middle angle and the elbow angle minimum and maximum.

When using Kv2, relative and absolute agreement (r and r_c) was good or excellent for all spatiotemporal parameters, except the swing and single support duration (poor and moderate agreement, respectively). On the other hand, relative and absolute agreement for Kv1 was good/excellent for only 7 and 3 spatiotemporal parameters, respectively. For kinematic parameters, most presented poor or moderate agreement. The only exceptions are the neck angle (good relative agreement for Kv1), elbow angle minimum (good relative and absolute agreement for both Kinects) and knee angle minimum (good relative agreement for Kv2).

Table 6.8. Validation results for each gait parameter and Kinect version (Kv1 and Kv2), when considering the WF activity and configuration KC1.

The results include the Bland Altman's mean difference (Mean diff), Pearson's correlation coefficient (r) and concordance correlation coefficient (r_c). The r and r_c values are highlighted in green (≥0.9), yellow (≥0.75 and <0.9), orange (≥0.5 and <0.75), and red (<0.5).

Parameter[a]	Mean diff[b]		r[c]		r_c	
	Kv1	Kv2	Kv1	Kv2	Kv1	Kv2
Stride duration (s)	0.003	0.000	0.87*	0.95*	0.87	0.94
Step duration (s)	−0.003	0.000	0.82*	0.88*	0.81	0.87
Stance duration (s)	0.014	−0.003	0.69*	0.91*	0.66	0.91
Swing duration (s)	−0.010	0.003	0.42	0.49*	0.36	0.49
Single support duration (s)	−0.009	−0.002	0.42	0.67*	0.31	0.67
Double support duration (s)	0.012	0.002	0.24	0.79*	0.19	0.78
Stride length (mm)	12.9	**0.6**	0.93*	0.99*	0.56	0.99
Step length (mm)	1.7	−0.7	0.80*	0.88*	0.77	0.88
Step width (mm)	1.8	1.3	0.84*	0.95*	0.62	0.85
Gait speed (m/s)	0.128	**0.012**	0.98*	1.00*	0.59	0.99
Gait speed variability (m/s)	0.001	0.005	0.60*	0.84*	0.40	0.83
Foot swing velocity (m/s)	0.128	0.021	0.78*	0.91*	0.73	0.91
Arm swing velocity (m/s)	0.251	**0.004**	0.67*	0.98*	0.53	0.98
Neck angle (deg.)	**5.9**	17.4	0.77*	0.42	0.61	0.07
Spine middle angle (deg.)	6.1	5.2	0.09	0.50*	0.04	0.16
Elbow angle maximum (deg.)	−0.3	−0.6	0.43	0.61*	0.43	0.61
Elbow angle minimum (deg.)	1.4	0.6	0.81*	0.89*	0.81	0.88
Knee angle maximum (deg.)	**0.9**	−2.6	−0.42	−0.21	0.00	0.00
Knee angle minimum (deg.)	13.6	**4.0**	0.58*	0.75*	0.11	0.53
Hip angle range (deg.)	−4.7	**−1.3**	0.61*	0.24	0.27	0.13
Ankle angle range (deg.)	12.2	**1.3**	0.13	0.55*	0.05	0.43

[a] The units indicated for each parameter only apply to the "Mean diff" column.

[b] The lowest error (Mean diff) for each parameter is indicated in bold, when there is a statistically significant difference between the two Kinect versions (one-way repeated-measures ANOVA, p-value ≤ 0.05).

[c] The * symbol indicates a statistically significant value (p-value ≤ 0.05).

6.3.2 Walking Activity Comparison

Given the results of the previous study, the Kv2 was considered for the assessment of the validity of the Kinect when comparing the two considered walking activities (WF and WB).

The mean and standard deviation values for the practical depth range of Kv2, as well as the associated minimum and maximum distances, when considering all subjects and trials, are indicated in Table 6.9 for both walking activities. The number of actual gait cycles corresponding to WF and WB data is included in Table 6.10, for all subjects and trials, as well as per trial and per subject (mean and standard deviation). The depth range and consequently the number of gait cycles per trial is similar for the two walking activities.

Table 6.9. Mean and standard deviation values for the practical depth range of Kv2 for both walking activities (WF and WB), when using configuration KC1.

	Kv2, KC1	
Walking activity	**WF**	**WB**
Practical depth range[a] (m)	2.71 ± 0.08	2.66 ± 0.32
Minimum distance[b] (m)	1.63 ± 0.08	1.71 ± 0.23
Maximum distance[c] (m)	4.34 ± 0.03	4.37 ± 0.15

[a] Difference between maximum and minimum distances.

[b] Shortest distance between the subject and Kinect for which all body joints are tracked.

[c] Longest distance between the subject and Kinect for which all body joints are tracked.

Table 6.10. Number of actual gait cycles for Kv2 in the case of both walking activities (WF and WB), when using configuration KC1.
The values are indicated for left, right, and both gait cycles, when considering all subjects and trials, as well as each trial and each subject (mean and standard deviation values).

		Number of actual gait cycles (Kv2, KC1, 10 trials)	
Walking activity		**WF**	**WB**
All subjects and trials	**Left**	265	189
	Right	209	186
	Both	474	375
Per subject	**Left**	13.3 ± 3.4	9.4 ± 1.9
	Right	10.4 ± 2.1	9.3 ± 3.1
	Both	23.7 ± 4.1	18.8 ± 4.6
Per trial	**Left**	1.3 ± 0.6	1.0 ± 0.5
	Right	1.1 ± 0.5	0.9 ± 0.5
	Both	2.4 ± 0.9	1.9 ± 0.9

When considering WF and WB data for Kv2 only, the minimum number of gait cycles available per subject, when considering all subjects and both walking activities, was of 11 gait cycles. To verify the effect that the number of gait cycles, which is used to compute gait parameters' value for each subject, has on the validity of Kv2, we obtained the mean difference, r and r_c when varying the number of gait cycles between 1 and 11. The complete results are presented in Appendix G.4.

The mean r and r_c values considering all gait parameters and both walking activities, versus the number of used gait cycles, are shown in Figure 6.1. Both r and r_c tend to improve with the increase of the number of gait cycles. However, the difference between 1 gait cycle (r = 0.61 and r_c = 0.54) and 7 gait cycles (r = 0.67 and r_c = 0.58) is not considerable. Nevertheless, all 11 available gait cycles were used to obtain the results presented below.

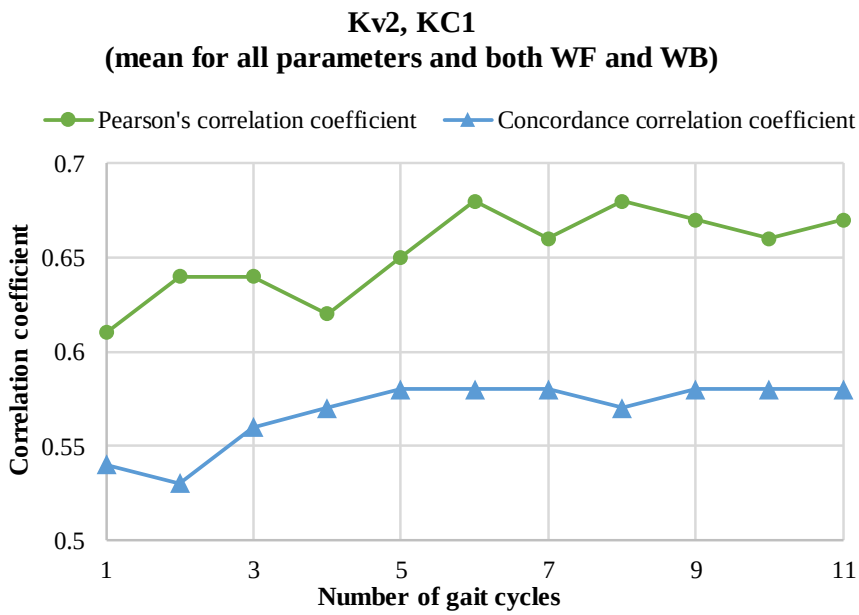

Figure 6.1. Mean value for Pearson's correlation coefficient (r) and concordance correlation coefficient (r_c) when considering all gait parameters and both walking activities, versus the number of gait cycles used to compute the parameters' value for each subject.

The validation results are presented in Table 6.11 (complete results in Appendix G.2). Overall, lower estimation errors were achieved when using WF data comparing with WB data (mean difference was lower when using WF for the 11 out of the 13 parameters with significant difference between the two walking activities). Moreover, a better overall agreement between the Kinect and Qualisys was achieved for WF when compared with WB (relative/absolute agreement was good or excellent for 16/14 parameters versus 12/8 parameters).

Table 6.11. Validation results for each gait parameter and walking activity (WF and WB), when considering Kv2 and configuration KC1.

The results include the Bland Altman's mean difference (Mean diff), Pearson's correlation coefficient (r) and concordance correlation coefficient (r_c). The r and r_c values are highlighted in green (≥0.9), yellow (≥0.75 and <0.9), orange (≥0.5 and <0.75), and red (<0.5).

Parameter[a]	Mean diff[b]		r[c]		r_c	
	WF	WB	WF	WB	WF	WB
Stride duration (s)	0.005	0.003	0.99*	0.99*	0.98	0.99
Step duration (s)	0.002	0.002	0.97*	0.95*	0.97	0.95
Stance duration (s)	**0.001**	0.013	0.97*	0.93*	0.96	0.89
Swing duration (s)	**0.003**	−0.009	0.79*	0.80*	0.79	0.72
Single support duration (s)	**0.001**	−0.027	0.81*	0.75*	0.81	0.60
Double support duration (s)	**0.003**	0.031	0.85*	0.46	0.77	0.32
Stride length (mm)	1.2	0.2	1.00*	0.98*	0.99	0.98
Step length (mm)	**0.5**	−2.1	0.97*	0.88*	0.97	0.80
Step width (mm)	1.4	0.9	0.92*	0.82*	0.73	0.72
Gait speed (m/s)	**0.013**	0.020	1.00*	1.00*	0.99	0.98
Gait speed variability (m/s)	0.006	0.000	0.90*	0.84*	0.84	0.83
Foot swing velocity (m/s)	−0.063	−0.108	0.91*	0.65*	0.89	0.62
Arm swing velocity (m/s)	**0.026**	0.050	0.99*	0.94*	0.98	0.91
Neck angle (deg.)	17.6	**9.1**	0.37	0.11	0.04	0.05
Spine shoulder angle (deg.)	18.1	**14.3**	0.63*	0.12	0.05	0.02
Spine middle angle (deg.)	5.2	5.3	0.53*	−0.07	0.15	0.00
Elbow angle maximum (deg.)	**−0.7**	7.4	0.81*	0.15	0.81	0.04
Elbow angle minimum (deg.)	**1.2**	12.9	0.95*	0.88*	0.93	0.22
Knee angle maximum (deg.)	−3.4	−2.1	−0.26	−0.21	0.00	0.00
Knee angle minimum (deg.)	4.3	5.1	0.85*	0.05	0.55	0.03
Hip angle range (deg.)	**−1.6**	−4.4	0.12	0.28	0.11	0.15
Ankle angle range (deg.)	**3.5**	18.0	0.68*	0.17	0.51	0.03

[a] The units indicated for each parameter only apply to the "Mean diff" column.

[b] The lowest error (Mean diff) for each parameter is indicated in bold, when there is a statistically significant difference between the two Kinect versions (one-way repeated-measures ANOVA, p-value ≤ 0.05).

[c] The * symbol indicates a statistically significant value (p-value ≤ 0.05).

There was a statistically significant difference regarding estimation error between WF and WB for 13 out of the 22 parameters. For these parameters, WF presented the lowest error for most of them (11 parameters).

When considering WF, the agreement between systems was good or excellent for all spatio-temporal parameters except the step width (excellent relative agreement, but moderate absolute agreement). In the case of WB, 8 out of 13 spatiotemporal parameters presented good or excellent relative and absolute agreement. All kinematic parameters presented poor or moderate agreement for both walking activities, with the exception of the elbow angle maximum (good agreement for WF only), elbow angle minimum (excellent agreement for WF and good relative agreement for WB) and the knee angle minimum (good relative agreement for WF only).

6.3.3 Kinect Configuration Comparison

Taking into account the results of the previous studies, the effect that the physical configuration of the Kinect has on its validity for gait analysis was studied only for Kv2 and WF.

Table 6.12 presents the mean and standard deviation values for the practical depth range of Kv2, as well as the associated minimum and maximum distances, when considering all subjects and trials, for each considered configuration (KC1, KC2 and KC3). The corresponding number of actual gait cycles is indicated in Table 6.13 for all subjects and trials, as well as for each subject and each trial. From these tables, we can see that the depth range, and consequently the number of gait cycles per trial, is similar for all three configurations.

Table 6.12. Mean and standard deviation values for the practical depth range of Kv2, when considering the WF activity, for configurations KC1, KC2 and KC3.

	Kv2, WF		
Kinect configuration	**KC1**	**KC2**	**KC3**
Practical depth range[a] (m)	2.72 ± 0.08	2.77 ± 0.11	2.74 ± 0.09
Minimum distance[b] (m)	1.62 ± 0.08	1.57 ± 0.11	1.57 ± 0.09
Maximum distance[c] (m)	4.34 ± 0.03	4.35 ± 0.03	4.31 ± 0.04

[a] Difference between maximum and minimum distances.

[b] Shortest distance between the subject and Kinect for which all body joints are tracked.

[c] Longest distance between the subject and Kinect for which all body joints are tracked.

Table 6.13. Number of actual gait cycles for each Kinect configuration (KC1, KC2, and KC3), when using the Kinect v2 and WF data.
The values are indicated for left, right, and both gait cycles, when considering all subjects and trials, as well as each subject and each trial (mean and standard deviation).

		Number of actual gait cycles (Kv2, WF, 5 trials)		
Kinect configuration		**KC1**	**KC2**	**KC3**
All subjects and trials	**Left**	131	158	147
	Right	105	130	123
	Both	236	288	270
Per subject	**Left**	6.5 ± 2.1	7.9 ± 2.3	7.3 ± 2.0
	Right	5.3 ± 1.3	6.5 ± 1.9	6.2 ± 2.0
	Both	11.8 ± 2.8	14.4 ± 2.8	13.5 ± 2.7
Per trial	**Left**	1.3 ± 0.7	1.6 ± 0.5	1.5 ± 0.6
	Right	1.1 ± 0.5	1.3 ± 0.5	1.2 ± 0.5
	Both	2.4 ± 1.0	2.9 ± 0.7	2.7 ± 0.8

The window sizes used for gait cycle detection over Kv2 and WF data are indicated in Table 6.14 for each Kinect configuration. These values were chosen using the same criteria described in Section 5.2. The number of gait cycles detected by our algorithm for each trial (mean and standard deviation) is also included in the table.

Table 6.14. Window sizes used for detecting gait cycles using Kinect v2 (Kv2) data acquired while the subject walked towards the camera (WF), for each considered configuration (KC1, KC2 and KC3). The mean and standard deviation of the number of detected gait cycles per gait trial are also included.

		Kv2, WF (5 trials)		
Configuration		**KC1**	**KC2**	**KC3**
Window size (number of frames)	**Ankle distance filtering (*NF1*)**	5	5	5
	Heel strike detection (*ND1*)	9	7	9
	Ankle velocity filtering (*NF2*)	7	9	5
	Heel strike side identification (*ND2*)	3	3	7
	Shank angle filtering (*NF3*)	9	7	11
Number of detected gait cycles per trial	**Left**	1.3 ± 0.5	1.5 ± 0.5	1.4 ± 0.6
	Right	1.1 ± 0.3	1.2 ± 0.4	1.1 ± 0.3
	Both	2.4 ± 0.6	2.7 ± 0.6	2.5 ± 0.7

The validation results obtained for the three configurations are presented in Table 6.15 (complete results can be found in Appendix G.3). These results were obtained considering 7 gait cycles per subject for gait parameter computation, since it was the minimum number of gait cycles available per subject when considering all configurations.

Table 6.15. Validation results for each gait parameter and Kinect configuration (KC1, KC2 and KC3), when using the Kinect v2 (Kv2) and data corresponding to walking towards the camera (WF). The results include the Bland Altman's mean difference (Mean diff), Pearson's correlation coefficient (r) and concordance correlation coefficient (r_c). The r and r_c values are highlighted in green (≥0.9), yellow (≥0.75 and <0.9), orange (≥0.5 and <0.75), and red (<0.5).

Parameter[a]	Mean diff[b]			r[c]			r_c		
	KC1	KC2	KC3	KC1	KC2	KC3	KC1	KC2	KC3
Stride duration (s)	0.003	0.007	0.005	0.99*	0.98*	0.99*	0.99	0.97	0.99
Step duration (s)	0.000	0.006	0.005	0.98*	0.92*	0.97*	0.97	0.89	0.95
Stance duration (s)	0.003[a]	−0.006[b]	0.001[a,b]	0.96*	0.92*	0.91*	0.95	0.89	0.91
Swing duration (s)	**0.000**[b]	0.013[a]	**0.004**[b]	0.78*	0.58*	0.56*	0.76	0.42	0.56
Single support duration (s)	0.000[b]	0.016[a]	0.004[a,b]	0.79*	0.69*	0.62*	0.77	0.58	0.62
Double support duration (s)	0.003[a]	−0.009[b]	0.001[a,b]	0.81*	0.49*	0.66*	0.74	0.45	0.66
Stride length (mm)	1.0	0.9	1.6	1.00*	1.00*	0.99*	1.00	0.99	0.98
Step length (mm)	0.2	−0.5	0.7	0.96*	0.97*	0.95*	0.96	0.95	0.95
Step width (mm)	1.3[a]	**0.8**[b]	1.5[a]	0.91*	0.86*	0.89*	0.69	0.80	0.61
Gait speed (m/s)	0.012	0.011	0.014	1.00*	1.00*	1.00*	0.99	0.99	0.99
Gait speed variability (m/s)	0.007	0.004	0.004	0.82*	0.91*	0.83*	0.76	0.89	0.80
Foot swing velocity (m/s)	**−0.036**[a]	**−0.057**[a]	−0.197[b]	0.91*	0.86*	0.91*	0.89	0.80	0.76
Arm swing velocity (m/s)	0.027	−0.015	0.020	0.98*	0.99*	0.97*	0.98	0.99	0.97
Neck angle (deg.)	17.7[a,b]	18.9[a]	17.2[b]	0.45	0.57*	0.45	0.06	0.08	0.06
Spine shoulder angle (deg.)	**18.3**[b]	19.4[a]	**17.8**[b]	0.67*	0.68*	0.66*	0.06	0.06	0.06
Spine middle angle (deg.)	5.3[a,b]	6.1[a]	5.0[b]	0.56*	0.55*	0.62*	0.17	0.14	0.19
Elbow angle maximum (deg.)	−0.7[a,b]	−0.3[a]	−1.3[b]	0.87*	0.83*	0.83*	0.86	0.82	0.78
Elbow angle minimum (deg.)	1.3[a]	**−0.9**[b]	1.0[a]	0.95*	0.91*	0.90*	0.93	0.90	0.87
Knee angle maximum (deg.)	−3.5[b]	**−2.1**[a]	−3.1[b]	−0.30	−0.31	−0.24	0.00	0.00	0.00
Knee angle minimum (deg.)	**4.6**[b]	6.3[a]	**4.1**[b]	0.86*	0.71*	0.81*	0.52	0.31	0.48
Hip angle range (deg.)	−1.8	−1.5	−2.7	0.10	0.14	0.31	0.09	0.13	0.26
Ankle angle range (deg.)	**3.4**[b]	−4.3[c]	9.2[a]	0.75*	0.37	0.32	0.60	0.29	0.13

[a] The units indicated for each parameter only apply to the "Mean diff" column.

[b] For each parameter, the superscript a, b and c letters indicate statistically significant differences between KC1, KC2 and/or KC3 from post-hoc Tukey test (configurations with different letters are significantly different). The lowest Mean diff value is indicated in bold, when there is a statistically significant difference between one of the configurations and the other two.

[c] The * symbol indicates a statistically significant value (p-value ≤ 0.05).

Overall, none of the configurations outperforms the other regarding estimation errors. However, KC1 led to the best overall agreement between Kinect and Qualisys (relative/absolute agreement is good or excellent for 17/13 parameters for KC1, 12/12 parameters for KC2, and 13/11 parameters for KC3).

When comparing the estimation errors for the three configurations, there is a statistically significant difference between at least two of the configurations for 14 of the 23 parameters. For these parameters, using KC1, KC2 and KC3 led to the lowest error for 5, 4 and 3 parameters, respectively.

Relative agreement was good or excellent for all 13 spatiotemporal parameters, except for the swing, single support and double support duration when using KC2 and KC3 (poor or moderate). Absolute agreement was also good or excellent for all spatiotemporal parameters, except the swing duration (poor for KC2, moderate for KC3), single support duration (moderate for KC2 and KC3), double support duration (moderate for KC1 and KC3, poor for KC2) and step width (moderate for KC1 and KC3).

All 8 kinematic parameters presented poor or moderate agreement for all configurations, with some exceptions: elbow angle maximum (good agreement); elbow angle maximum (excellent agreement, except for KC3 which had good absolute agreement); knee angle minimum (good relative agreement for KC1 and KC3); ankle angle range (good relative agreement for KC1 only).

6.4 Discussion

6.4.1 Kinect Version Comparison

For comparing the two Kinect versions, we considered not only the agreement between each version and a gold standard Qualisys system (Table 6.8), but also the practical depth range and number of actual gait cycles that can be obtained with each Kinect (Table 6.6 and Table 6.7). We verified that the depth range is larger for Kv2 than Kv1 (2.7 m vs 1.8 m). The larger range allowed obtaining data including three times the number of actual gait cycles per trial (mean of 2.4 gait cycles versus 0.8 gait cycles). In practice, this means that the duration of data acquisitions will be lower if the Kv2 is used instead of Kv1.

Besides the advantage of enabling the acquisition of more gait cycles, Kv2 is also more appropriate for supporting gait assessment than Kv1, since the obtained results show that its data can be used to estimate gait parameters with overall lower errors and better agreement with the gold

standard. Therefore, the results confirm the claims by Microsoft that the Kv2 was improved over the Kv1 regarding not only the depth range, but also the body joint position estimation [182].

Regarding the mean difference between Kinect and Qualisys (or Kinect estimation error), we found that there is a statistically significant difference between Kinects for 8 out of 21 parameters (3 out of 13 spatiotemporal and 5 out of 8 kinematic). For these parameters, the lowest mean error was achieved when using the Kv2. Therefore, both Kinects can be used for estimating the parameters' value for most of the considered parameters. However, Kv2 leads to lower estimation errors overall, when taking into account all parameters.

Regarding the relative and absolute agreement between Kinect and Qualisys (r and r_c), the Kv2 outperforms the Kv1 for 10 out of 13 spatiotemporal parameters. The biggest differences were observed for seven of those parameters: stance duration, double support duration, stride length, gait speed, gait speed variability, foot and arm swing velocity. For the kinematic parameters, although there are some difference when comparing the Kinects, the agreement is poor or moderate for most of them, with only a few exceptions: elbow angle minimum (good for both Kinects), neck angle (best for Kv1) and knee angle minimum (best for Kv2).

For both Kinect versions, the spatiotemporal parameters led to better results when compared with kinematic parameters. In the case of the Kv2, the only spatiotemporal parameters with poor or moderate agreement were the swing and single support duration. On the other hand, the relative and/or absolute agreement was poor or moderate for all kinematic parameters, except for the elbow angle minimum (good relative and absolute agreement). Nevertheless, Kv2 presented a better agreement with the gold standard system overall.

6.4.2 Walking Activity Comparison

For Kv2, we further compared the two considered walking activities (WF and WB). Since a larger number of gait cycles was available for Kv2 comparing with Kv1, we firstly investigated if the number of gait cycles used to compute the gait parameters' value, for each subject, affects the gait analysis results. We verified that the agreement between the Kv2 and the gold standard system improves when the number of gait cycles increases (until a maximum of 11 gait cycles). However, the improvement is not considerable (see Figure 6.1).

Regarding the practical depth range, it is similar for both walking activities (Table 6.9). Therefore, the number of actual gait cycles is also similar (Table 6.10). However, the obtained validation results show that the parameters are estimated with lower errors and better agreement between Kinect and Qualisys when using WF data comparing with WB data (Table 6.11). This result suggests

that the Kinect's joint tracking algorithm has more difficulties in estimating the joints' position when the subject walks away from the sensor, which was expected since the Kinect assumes that the subject is always facing the sensor.

When considering the mean difference or estimation error, there was a statistically significant difference between the two walking activities for most considered parameters (13 out of 22 parameters). For these parameters, the lowest error was achieved when considering WF in most cases (11 parameters). Therefore, using WF data for estimating gait parameters leads to lower errors overall.

The use of WF data also led to better results than WB data, when considering the agreement between Kv2 and Qualisys for all considered parameters. The biggest differences were verified for the following parameters: double support duration, foot swing velocity, elbow angle minimum and maximum and knee angle minimum. For spatiotemporal parameters, agreement was always good or excellent in the case of WF (only exception is the absolute agreement for the step width, which is moderate), while relative and/or absolute agreement is poor or moderate for 5 out of 13 spatiotemporal parameters when considering WB.

On the other hand, all kinematic parameters presented poor agreement for WB (except for the elbow angle minimum, which has a good relative agreement), while the use of WF data led to a good or excellent agreement for two parameters (elbow angle minimum and maximum) and a good relative agreement for another (knee angle minimum). Overall, using WF data leads to a better agreement with the gold standard system than WB data.

6.4.3 Kinect Configuration Comparison

To study the effect that the configuration of the Kinect has in its validity for gait analysis, we considered only the Kv2 and WF combination, taking into account the previous results. The three considered configurations (KC1, KC2 and KC3) correspond to a Kinect height of 1 m, 0.6 m, and 1.34 m, respectively.

The obtained results show that none of the three configurations has an advantage over the others regarding the amount of acquired data, since the number of actual gait cycles per trial was similar for all configurations (mean of 2.4 to 2.7 gait cycles – see Table 6.14), due to a similar practical mean depth range of 2.7–2.8 m (Table 6.13). As for the validation results (Table 6.15), the most appropriate configuration for supporting gait assessment is KC1, which corresponds to the intermediate height of 1 m and a tilt angle of −5 degrees for Kv2, since it led an overall better agreement between the Kinect and the gold standard system, when compared with the other two configurations.

The obtained results show that there is no difference between three explored configurations (similar estimation error and agreement between systems) for some gait parameters, such as the stride duration, stride and step length, gait speed, arm swing velocity and hip angle range. However, there is a statistically significant difference between at least two of the configurations for 14 out of the 23 parameters. For these parameters, there is a significant difference between one of the configurations the other two for 8 parameters, with KC1 leading to the lowest mean error for a slightly larger number of gait parameters (5 parameters) when compared with KC2 and KC3 (4 and 3 parameters, respectively).

Regarding the agreement between systems, the results are similar among the different configuration for most parameters. However, there are differences for a few parameters. The largest differences were observed for the swing, single support and double support duration, where KC1 led to a moderate or good agreement ($0.78 \leq r \leq 0.81$ and $0.74 \leq r_c \leq 0.77$), while the agreement was only moderate or poor for KC2 and KC3 ($0.49 \leq r \leq 0.69$ and $0.42 \leq r_c \leq 0.66$). Although the configuration KC1 has a better relative agreement than KC2 and/or KC3 for the knee angle minimum and ankle angle range, the absolute agreement was only moderate (poor for KC2 and KC3). Overall, the configuration KC1 leads to a better agreement between Kv2 and Qualisys when considering all gait parameters.

6.4.4 Comparison with the State of the Art

In contrast with other similar studies, we assessed the validity of both versions of the Kinect simultaneously. For the Kinect version with the best overall results, we further explored the two different activities of walking towards the sensor (WF) and walking away from it (WB). Most contributions considering a frontal view considered only WF data or did not study the two activities separately [55, 57, 60, 63-65]. We also investigated the influence of the physical configuration of the Kinect on the gait analysis results. To the best of our knowledge, no other contribution considering overground walking and a frontal view has studied different Kinect configurations (in terms of height and tilt angle).

Table 6.16 and Table 6.17 present the results obtained for spatiotemporal and kinematic gait parameters, respectively, when using our gait analysis solution, as well as other methods proposed in the literature. Our results indicated in the tables correspond to the use of a single Kv2 camera (configuration KC1) and WF data, considering overground walking at a self-selected comfortable pace, frontal view and 7 gait cycles per subject for parameter computation. For the contributions that explored different walking speeds, the presented results correspond to the speed(s) closer to the mean gait speed for our study (approximately 1.2 m/s).

Table 6.16. Comparison between our gait analysis solution (Kv2, WF, KC1) and methods proposed in the literature, regarding the validity of the Kinect for computing spatiotemporal gait parameters.

Gait parameter	Metric	Our[a]	Stone et al., 2011 [55][b]	Gabel et al., 2012 [56][c]	Clark et al., 2013 [57]	Pfister et al., 2014 [65][d]	Xu et al., 2015 [60][e]	Mentiplay et al., 2015 [64][f]	Geerse et al., 2015 [61]	Eltoukhy et al., 2017 [63][g]	Müller et al., 2017 [62][h]
Stride duration	Mean diff (s)	0.003	0.007	0.008 / 0.002	−0.20	0.157 / 0.159	0.001 / 0.000	—	0.01	0.00	—
	r	0.99	—	—	0.69	0.91 / 0.92	0.92 / 0.95		—	0.97	
	r_c	0.99			0.14	—	0.92 / 0.95			0.97	
Step duration	Mean diff (s)	0.000	—	—	−0.17	—	0.000 / 0.000	0.00 / −0.01	0.01	0.02	0.00
	r	0.98			0.82		0.77 / 0.85	0.92	—	0.96	1.00
	r_c	0.97			0.23		0.75 / 0.84	0.75		0.75	—
Stance duration	Mean diff (s)	0.003	—	−0.008 / −0.020	—	—	−0.048 / −0.036	0.03 / 0.04	—	—	—
	r	0.96		—			0.57 / 0.60	0.91			
	r_c	0.95					0.37 / 0.45	0.90			
Swing duration	Mean diff (s)	0.000	—	0.006 / 0.027	—	—	0.046 / 0.035	—	—	—	—
	r	0.78		—			0.43 / 0.30				
	r_c	0.76					0.21 / 0.16				
Double support duration	Mean diff (s)	0.003	—	—	—	—	−0.045 / −0.034	—	—	—	—
	r	0.81					0.24 / 0.20				
	r_c	0.74					0.10 / 0.09				
Stride length	Mean diff (mm)	1.0	−3.2	—	−4.2	—	—	—	1	—	2
	r	1.00	—		0.99				—		1.00
	r_c	1.00			0.99						—
Step length	Mean diff (mm)	0.2	—	—	11.5	—	—	−20 / −10	−1	−100	3.8
	r	0.96			0.99			0.90	—	0.93	1.00
	r_c	0.96			0.97			0.13		0.58	—
Step width	Mean diff (mm)	1.3	—	—	—	—	0 / 0	−60 / −70	−13	−40	3.9
	r	0.91					0.82 / 0.79	0.94	—	0.73	0.91
	r_c	0.69					0.82 / 0.79	0.00		0.38	—
Gait speed	Mean diff (m/s)	0.012	−0.004	—	−0.01	—	—	0.01 / 0.02	0.011	—	—
	r	1.00	—		0.95			0.99	—		
	r_c	0.99			0.93			0.90			
Gait speed variability	Mean diff (m/s)	0.007	—	—	—	—	—	0.04 / 0.04	—	—	—
	r	0.82						0.75			
	r_c	0.76						0.00			
Foot swing velocity	Mean diff (m/s)	−0.036	—	—	0.43	—	—	−0.49 / −0.46	—	−0.43	—
	r	0.91			0.93			0.79		0.35	
	r_c	0.89			0.54			0.11		0.05	

[a] Results for Kv2, WF and KC1.

[b] Results for the second (#2) Kinect.

[c] Results for left and right sides, in the case of experiment 1.

[d] Results for left and right sides at a controlled speed of ≈1.34 m/s (using knee angle).

[e] Results for controlled speeds of 1.07 m/s and 1.30 m/s.

[f] Mean difference results for days 1 and 2 (comfortable pace).

[g] Results for a controlled speed of 1.30 m/s.

[h] Results for the mean of the parameter value for all gait cycles per subject, considering the mean between left and rights sides. For the spatial parameters, the presented results are for the two-sided situation.

Table 6.17. Comparison between our gait analysis solution (Kv2, WF, KC1) and methods proposed in the literature, regarding the validity of the Kinect for computing kinematic gait parameters.

Gait parameter	Metric	Our[a]	Pfister et al., 2014 [65][b]	Xu et al., 2015 [60][c]	Mentiplay et al., 2015 [64][d]	Eltoukhy et al., 2017 [30][e]
Knee angle maximum	Mean diff (deg.)	−3	−1.11 / 0.452	—	1 / 2	—
	r	−0.30	0.69 / 0.77		−0.07	
	r_c	0.00	—		0.00	
Knee angle minimum	Mean diff (deg.)	5	−9.14 / −6.93	−38.1 / −38.1	−37 / −35	—
	r	0.86	0.43 / 0.71	—	−0.05	
	r_c	0.52	—		−0.02	
Ankle angle range	Mean diff (deg.)	3	—	—	7 / 2	−19.76
	r	0.75			0.11	0.03
	r_c	0.60			0.01	0.01

[a] Results for Kv2, WF and KC1.

[b] Results for left and right sides at a controlled speed of ≈1.34 m/s.

[c] Results for controlled speeds of 1.07 m/s and 1.30 m/s.

[d] Mean difference results for days 1 and 2 (comfortable pace).

[e] Results for a controlled speed of 1.30 m/s.

Our results cannot be directly compared with the results reported in the other contributions, due to differences regarding the experimental setup and/or protocol: first version of the Kinect [55-57, 60, 65]; multiple Kinects [61, 62]; Kinect placed with a given angle in relation to the walking path [56, 61, 62, 65]; treadmill walking with controlled speed(s) [60, 63, 65]. Different data processing methods (e.g., Kinect data resampling [57, 60-62, 64]) were also used in some studies. Nonetheless, it is interesting to see how our results stand in relation with those achieved in similar studies.

Our study is the most complete in terms of the number of investigated gait parameters (22 spatiotemporal and kinematic parameters). All other considered studies explored a smaller set of spatiotemporal and/or kinematic parameters, with only a few exploring both types of parameters [60, 63-65]. Furthermore, most contributions that studied kinematic parameters focused on angles associated with the lower limbs, while we also investigated angles for the trunk and upper limbs. It is interesting to note that the only kinematic parameters for which we were able to achieve a good or excellent relative and absolute agreement (elbow angle minimum and maximum) are usually not explored in studies on the Kinect validity for gait analysis.

Overall, we achieved a better agreement between the parameter values obtained relying on the Kinect and a gold standard system, when compared with the other studies. For all compared spatiotemporal parameters, we obtained results of $r \geq 0.78$ and $r_c \geq 0.69$, while the values reported

in the other studies are often lower, especially when considering r_c (absolute agreement). For the kinematic parameters, we obtained a poor agreement for the knee angle maximum. However, our results for the knee angle minimum and ankle angle range were much better than those reported in other contributions (see Table 6.17).

When considering the estimation error (Mean diff), as well as both relative and absolute agreement (r and r_c, respectively), we achieved considerably better results for some parameters. For example, we obtained a mean errors ranging from 0 to 3 ms for stance, swing and double support duration, while Xu et al. reported values varying between −48 and −36 ms (stance) 35 and 46 ms (swing) and −45 and −34 ms (double support) [60]. Our relative and absolute agreement results are also better: r between 0.78 and 0.96 and r_c between 0.74 and 0.95, versus r between 0.20 and 0.60 and r_c between 0.10 and 0.45). The difference between these results can be because the gait events used for computing the considered parameters were estimated using different methods.

For the foot swing velocity, our mean difference (−0.04 m/s) is much lower than those achieved in the studies by Clark et al. [57], Mentiplay et al. [64] and Eltoukhy et al. [63] (−0.49 to −0.43 m/s, 0.43 m/s and −0.43 m/s). The absolute agreement is also better (r_c = 0.89 instead of r_c ranging from 0.05 to 0.54). The differences between our study and the study by Eltoukhy et al. can be because they did not use the 3-D joint data provided by the Kinect, using instead their own method for tracking the joints relying on the depth data. The differences between our study and the studies by Clark et al. and Mentiplay et al. can be due to the fact that they used the same filter over the 3-D data used for computing all parameters, while we used a different optimized filter for each parameter.

The mean difference we obtained for the ankle angle range (3 degrees) is much lower than that obtained by Eltoukhy et al. (−20 degrees). Although our achieved agreement results were not very high (r = 75 and r_c = 0.60), they were higher than those reported by Mentiplay et al. and Eltoukhy et al (r and r_c ranging from 0.00 to 0.11). For the knee angle minimum, our mean difference (5 degrees) was much lower than the one obtained by Xu et al. (−38 degrees), as well as Mentiplay et al. (−37 to −35 degrees). Moreover, our agreement results (r = 0.86 and r_c = 0.52) were considerably better than those obtained by Mentiplay et al. (r = −0.05 and r_c = −0.02). The reasons for these differences in results are probably the same that were already discussed above.

From the studies that explored the use of multiple Kinects, Geerse et al. [61] reported mean difference values that are higher for stride and step duration and step length and width, and similar for stride length and gait speed, when compared with our study. The results reported by Müller et al. [62] are similar or slightly worse than our results. Therefore, there seems to be no great advantage in using multiple side-view sensors comparing with a single front-view camera.

6.5 Summary

The results of the performed validation studies show that our automated gait analysis solution using a single Kinect can be used as an alternative to the gold standard systems for obtaining several gait parameters (most of the spatiotemporal parameters and a few of the considered kinematic parameters). Overall, our solution outperformed the solutions proposed in other contributions, with a Pearson's correlation coefficient (r) ≥ 0.78 and a concordance correlation coefficient (r_c) ≥ 0.69 for all compared spatiotemporal parameters.

When comparing the two versions of the Kinect, the second version (Kv2) is more appropriate for gait assessment than the first version (Kv1). Overall, Kv2 not only led to lower estimation errors and higher agreement with a gold standard system, but also allowed obtaining three times as much gait cycles per gait task repetition as for Kv1.

Although the use of all acquired gait data would be desirable to minimize the duration of each data acquisition, our results show that it is best to discard the data corresponding to walking away from the Kinect (WB). When using the Kv2, the estimation error and/or agreement were considerably worse for WB than for walking towards the camera (WF) in the case of some parameters (e.g., double support duration, foot swing velocity, elbow angle maximum).

For the combination of Kv2 and WF, we verified that although the use of a greater number of gait cycles per subject for gait parameter computation leads to better validation results, the improvement is not considerable. Furthermore, from three explored Kinect configurations (sensor height of 0.6 m, 1 m and 1.34 m), the one corresponding to the intermediate height led to the best validation results overall.

7 Human Identification Based on Gait Using an RGB-D Camera

Biometric identification, i.e., the determination of a given subject's identity relying on biological characteristics (e.g., face, fingerprint, iris, vital signs, voice, gait) [7, 8], is being increasingly used in various situations, such as access control to restricted areas, identity confirmation at a security checks and smart surveillance at high risks areas [75]. Human identification based on gait using markerless vision-based sensors has the advantage of not being as intrusive as the other methods, since it does not require the attention or cooperation of the subject being identified [8]. Furthermore, gait is difficult to hide, steal or fake [7].

In a scenario of gait assessment, multiple assessments can be carried out for each person in a group of subjects. Therefore, automated subject identification is also useful in this scenario, since it allows saving time by avoiding the manual indication of the subject associated with each data acquisition. Given that our gait analysis solution based on an RGB-D camera already provides several gait parameters for a given data acquisition with a subject, the main aim of this chapter was to answer the following question:

- Is it possible to identify a given subject using features extracted from gait data provided by a single RGB-camera?

To answer this question, we explored if machine learning techniques can be used to obtain a predictive model for human identification, based on gait parameters and anthropometric measures extracted from the 3-D joint data provided by an RGB-D camera, namely the second version of the Kinect.

We investigated this possibility firstly for healthy subjects only, and then for patients with a disease that can affect their gait, in this case Parkinson's disease (PD). Furthermore, we studied the impact that considering both healthy subjects and PD patients together has on identification. These studies were carried out using data from the same acquisition per subject for model training and testing. An initial study with healthy subjects is presented in [77].

We also explored the identification of PD patients over time, by considering data acquired in different days or states for model training and testing. This situation corresponds to one of the most challenging ones, since PD patients can have considerable changes in gait within relatively short intervals of time (e.g., a few months or days).

7.1 Related Work

Several studies on human identification based on gait have been carried out relying on vision-based sensors [66, 67, 69-74, 247-250]. The methods used for gait recognition from image sequences can be divided in two main groups: model-free and model-based [5, 8]. The model-free approaches rely on the analysis of the subject's silhouette shape or the whole motion of the human body. Many of the studies that relied on RGB or IR cameras used the subject's binary silhouette extracted from the colour or IR images [247-250].

The model-based approaches obtain static or dynamic body features by modelling or tracking body segments or joints. These approaches typically have the advantage of being viewpoint and scale invariant [8]. The most recent studies mainly relied on the 3-D positions of body joints provided by RGB-D cameras, such as the Kinect camera [66, 67, 69-74]. Most of these studies considered both anthropometric measures (e.g., subject's height, length of body segments) and gait parameters extracted from the 3-D data for subject identification [66, 69, 70, 72, 73].

Preis et al. investigated 11 anthropometric measures and 2 spatiotemporal gait parameters (step length and gait speed) extracted from 3-D data provided by the Kinect v1 (Kv1), which were acquired from nine subjects (side-view) [70]. From the three considered machine learning algorithms (one rule, C4.5 decision tree, and Naïve Bayes), the best performance was achieved for the Naïve Bayes when using 7-fold cross-validation approach: success rate of 91% when using 4 of the 11 anthropometric features (height, leg, torso and left upper arm length).

Ball et al. studied the possibility of recognizing subjects using the k-means algorithm for unsupervised clustering, as well as 18 kinematic gait parameters (minimum, maximum, and standard deviation for lower limb angles) computed for each step (half gait cycle) [74]. For Kv1 data obtained from four subjects while they performed arbitrary walking paths, a mean accuracy of 44% was achieved (accuracy per subject ranged between 29% and 74%).

Sinha et al. also used the Kv1 to acquire joint data from ten subjects (side-view) and obtain several features for each step [73]. These features included the 12 anthropometric measures and 20 gait parameters proposed by Preis et al. [70] and Ball et al. [74]. The authors also proposed 14 new features: two related with body area and the remaining corresponding to the distance between each joint and upper body centroid. The best performance for subject identification was achieved when using the adaptive neural network algorithm with feature selection (mean F_1 score of 62%).

Andersson et al. acquired Kv1 joint data from 140 subjects, while they walked over a semicircle (camera on a spinning dish) [72]. Then, 20 anthropometric measures and 60 spatiotemporal and kinematic gait parameters were extracted from the collected data. The 10-fold cross-validation

technique was used to evaluate the performance of the models obtained using the following three algorithms: k-nearest neighbour (k-NN); multilayer perceptron (MLP); support vector machine (SVM). The best result was achieved when using all features (overall accuracy of 88% for k-NN). When varying the number of subjects between 5 and 140, the overall accuracy of the k-NN model decreased from ≈97% to ≈88%. It was also verified that performance improves when the number of examples increases: overall accuracy of 65–70% for 1 example and 85–90% for 4 examples.

In another study relying on the Kv1, Jiang et al. proposed the use of the nearest neighbour approach, together with 5 anthropometric features and 4 kinematic gait measures (lower and upper limbs angles), for subject identification [69]. For each anthropometric feature, the Euclidean distance was used as a distance measure between two examples. For each angle measure, the distance between two time series was computed using dynamic time warping (DTW). When using both types of features, a single score of similarity between two feature vectors was computed as the mean of the normalized distance score for each feature. For data acquired from ten subjects (side-view), an overall accuracy of 82% was reported (half of the examples for training and the other half for testing).

A similar approach to the one used by Jiang et al. (nearest neighbour approach, and fusion of different types of features) [69] was also used by Nambiar et al. [66]. They obtained a single score of similarity by summing the normalized Euclidean distance for each feature. The considered features included 7 anthropometric measures, as well as 35 gait parameters (stride length and duration, gait speed, as well as mean and variance of angles, distance and position measures). The proposed method was evaluated using the leave-one-out validation technique over examples obtained from twenty subjects using the Kinect v2 (Kv2). The achieved overall accuracy was of 92%, when considering the best match only and frontal direction (63 to 72% for lateral, left and right diagonal directions). The performance improved when a larger number of matches was considered (100% for the eight best matches). When the test set included a different viewpoint than the one considered in the training set, the overall accuracy ranged between 15% and 48% (best match) and between 83% and 97% (ten best matches).

Ahmed et al. also used the Kv2 to collect gait data from twenty subjects [67]. For each gait cycle, the distance and angle for all joint pairs were computed. The authors proposed the use of DTW as a measure of similarity between two examples of a given measure, and rank-level fusion based on majority voting to identify a subject taking into account all measures. A subset of the measures was selected relying on a genetic algorithm. The proposed method achieved a recognition rate of 92% (3-fold cross-validation) when considering the best match (100% for the four best matches).

Rahman et al. investigated the use of the mean and variance of the distance for each joint pair obtained for each gait cycle [71]. The performance of the models obtained for this set of 760

features, when using two different algorithms (k-NN and SVM), was evaluated relying on the 2-fold cross-validation technique. An overall accuracy of 93% (k-NN) was achieved, when considering a dataset obtained from thirty subjects using the Kv1. For a dataset obtained from twenty subjects using the Kv2, a slightly higher overall accuracy was reported: 95% for both k-NN and SVM.

Regarding identification over time, Gianaria et al. carried out a study where Kv1 gait data acquired from ten subjects were used to train a predictive model with the SVM algorithm [68]. The same subjects were then identified by relying on that model using data acquired three years later. The considered features included the mean for the distance between adjacent and non-adjacent joints, as well as the mean and mean absolute deviation for the sway of each joint in the x- and y-axis. A subset of these features was selected using principal component analysis. Taking into account the acquisitions where the subjects walked towards the camera and did not carry any object, all cases were correctly classified for 70% of the subjects, and 50% or more cases were correctly classified for 90% of the subjects. When comparing walking towards and away from the Kinect, the results are overall better for the first situation.

7.2 Materials and Methods

The datasets we used for studying subject identification were obtained from data acquired in different experiments: second and third experiments at São João hospital (HSJ), which are associated with the preliminary studies with PD patients; experiment at LABIOMEP, which is associated with the studies related with automated gait analysis.

7.2.1 Subjects

We considered the 20 healthy subjects that participated in the experiment carried out at LABIOMEP (LBMP), as well as from 5 healthy subjects and 18 PD patients treated with deep brain stimulation (DBS) that participated in the second and third experiments at the hospital (HSJ2 and HSJ3). Table 7.1 includes the demographics of the subject groups associated with each experiment, as well as for all subjects.

Table 7.1. Characterization of the subjects considered for studying subject identification. SD, Min, Max and BMI stand for standard deviation, minimum, maximum and body mass index.

		20 healthy subjects (LBMP)	5 healthy subjects (HSJ2)	25 healthy subjects (LBMP + HSJ2)	7 PD patients (HSJ2)	11 PD patients (HSJ3)	18 PD patients (HSJ2 + HSJ3)	All 43 subjects
Gender (male/female)		10/10	3/2	13/12	7/0	8/3	15/3	28/15
Age (years)	**Mean ± SD**	31 ± 8	54 ± 14	35 ± 13	63 ± 7	59 ± 5	61 ± 6	46 ± 17
	[Min, Max]	[23, 52]	[40, 74]	[23, 74]	[49, 77]	[50, 68]	[50, 77]	[23, 77]
Height (m)	**Mean ± SD**	1.71 ± 0.11	1.73 ± 0.08	1.71 ± 0.10	1.67 ± 0.08	1.68 ± 0.08	1.69 ± 0.07	1.71 ± 0.09
	[Min, Max]	[1.50, 1.94]	[1.62, 1.86]	[1.50, 1.94]	[1.50, 1.80]	[1.57, 1.85]	[1.57, 1.85]	[1.50, 1.94]
Weight (kg)	**Mean ± SD**	67.9 ± 15.3	77.6 ± 11.8	69.8 ± 14.8	80.3 ± 11.5	70.3 ± 9.7	74.9 ± 12.4	71.8 ± 14.1
	[Min, Max]	[48, 105]	[65, 99]	[48, 105]	[59, 96]	[60, 93]	[59, 96]	[48, 105]
BMI (kg/m^2)	**Mean ± SD**	23.0 ± 3.3	25.7 ± 2.6	23.6 ± 3.3	28.8 ± 4.5	24.8 ± 2.8	26.1 ± 3.5	24.5 ± 3.6
	[Min, Max]	[16.7, 31.0]	[22.5, 28.6]	[16.7, 31.0]	[22.2, 37.8]	[21.5, 30.7]	[21.5, 33.2]	[16.7, 33.2]

7.2.2 Experimental Setup and Protocol

Regarding the experimental setup, we considered only one RGB-D camera, namely the second version of the Kinect (Kv2). The physical configuration of the camera was the same for all experiments (height of 1 m and tilt angle of −5 degrees), with the exception of the second experiment at the hospital (height of 0.6 m and tilt angle of 0 degrees).

The experimental protocol included the same gait task for all experiments: walking towards and away from the Kinect, at a self-selected comfortable pace. In each data acquisition, the task was repeated 10 times by the healthy subjects at LBMP, between 6 and 15 times (11 ± 3 repetitions) by the healthy subjects at HSJ2, and between 1 and 16 times (8 ± 4 repetitions) by the PD patients.

For the second experiment at the hospital, two acquisitions were carried out with each PD patient: one with the DBS stimulator switched on (Stim-on) and another with the stimulator switched off (Stim-off). For two of the patients, it was not possible to acquire data in the Stim-off state. For the third experiment at the hospital, one or more acquisitions were carried out with each patient always in the Stim-on state.

7.2.3 Datasets

Four different datasets (DS4, DS5, DS6 and DS7) were considered for studying subject identification. In the case of healthy subjects, we used dataset DS4 corresponding to twenty healthy subjects (one acquisition per subject, all acquisitions at the same location). In the case of PD patients,

we used dataset DS5 corresponding to eleven patients (one acquisition in Stim-on state per patient, all acquisitions at the same location).

To verify if identification is also possible when considering both healthy subjects and PD patients, we used dataset DS6, which includes data acquired from thirty-seven subjects with and without the PD. This dataset corresponds to DS4 and DS5 with the addition of data from two more healthy subjects and four more PD patients (HSJ2).

For exploring the identification of PD patients at different points in time, we further considered dataset DS7, which includes data from nine PD patients acquired in two different days (same DBS state). This dataset also includes data from five PD patients in the two DBS states (same day), since it simulates changes in gait over time.

More details on the four different datasets can be found in Table 7.2, including the number of subjects, the state of the PD patients and the number of both acquisitions and gait cycles.

Table 7.2. Datasets used for studying subject identification based on gait.

Dataset	Number of subjects[a]	State[b]	Number of data acquisitions per subject	Number of acquisitions	Number of gait cycles (per subject and acquisition)
DS4	20 healthy subjects (LBMP)	—	1	20	420 (21)
DS5	11 PD patients (HSJ3)	Stim-on		11	165 (15)
DS6[c]	22 healthy subjects (LBMP + HSJ2)	—		37	370 (10)
	15 PD patients (HSJ2 + HSJ3)	Stim-on			
DS7[d]	5 PD patients (HSJ2)	Stim-on and off	2 (same days)	28	168 (6)
	9 PD patients (HSJ3)	Stim-on	2 (different days)		

[a] LBMP, HSJ2 and HSJ3 stand for LABIOMEP, second and third location in São João hospital, respectively.

[b] The state refers to the DBS state (stimulator on or off) in the case of PD patients only.

[c] For DS6, we did not consider the subjects with less than 10 detected gait cycles (see Appendix H).

[d] For DS7, we did not consider the subjects with a single acquisition or less than 5 detected gait cycles for at least one of the acquisition (see Appendix H).

More than one acquisition was carried out with some of the eleven patients at HSJ3. Therefore, a single acquisition per patient was selected for DS5, where the chosen acquisition was the one with highest number of gait cycles for that patient. In the case of DS7, two consecutive acquisitions

were chosen for the patients with more than two acquisitions. The time interval between the two selected acquisitions varied between 26 and 281 days (125 ± 93 days).

For all datasets, only the gait cycles corresponding to walking towards the Kinects were taken into account, considering the results of the validation studies presented above, as well as the fact that the number of gait cycles detected for walking away from the Kinect was much lower than for walking towards it in most cases. The number of gait cycles obtained per subject and acquisition is included in Appendix H.

Each dataset was balanced by randomly selecting the same number of gait cycles for each subject and acquisition. This resulted in a balanced dataset with $S \times A \times G$ gait cycles or instances, where S is the number of subjects or classes, A is the number of acquisitions per subject and G is the number of gait cycles selected for each subject and acquisition. For each dataset, the value of G is indicated in the last column of Table 7.2.

For all datasets, 25 features were computed for each gait cycle or instance. The features include the 22 gait parameters provided by our gait analysis solution (Table 6.2 and Table 6.3). The other three features are anthropometric measures, namely the trunk, arm and leg length. These measures were computed as the mean of the sum of the distances between adjacent joints of the trunk, arm and leg, respectively, for all gait cycle frames. The arm/leg length is the mean between the left and right arms/legs.

7.2.4 Subject Identification

The following machine learning algorithms were explored with the aim of obtaining a predictive model for subject identification: k-nearest neighbours, decision tree, random forest, support vector machines, multilayer perceptron, and multilayer perceptron ensemble. More details on the used algorithms, including the values used for the associated parameters, can be found in Section 5.2.

When considering only one acquisition per subject (DS4, DS5 and DS6), the model was built using half of the instances (or gait cycles) for each class (or subject). Then, the model's performance was evaluated using the remaining instances. For identification over time, considering two acquisitions per subject (DS7), the model was trained using the gait cycles from one acquisition and then evaluated using the same number of gait cycles from the other acquisition. In both cases, the procedure was repeated 20 times (20 evaluation runs). The instances used for training and testing were randomly selected in each run (DS4, DS5 and DS6 only).

The performance of a model was evaluated by considering the following metrics: overall accuracy (5.4), class accuracy (5.3) and class F_1 score (5.5). We also obtained the associated training and prediction time, on a computer with an i7-4600U CPU (dual-core, 2.1 GHz) and 8 GB RAM. The training time should be as low as possible, since it will be necessary to re-train the model every time there is information from a new subject. A low prediction time is also desirable for online subject identification.

When considering only healthy subjects (DS4) or PD patients (DS5), we investigated the performance of each model when relying on a single gait cycle and on all available gait cycles for identification. In the latter case, the decision on the subject's identity was performed by taking the following steps:

1. For each gait cycle, obtain the subject or class prediction;
2. Choose the class that occurs more often, considering all gait cycles;
3. If more than one class was chosen in step 2, randomly select one of the classes that occur more often.

To help decide on the minimum number of gait cycles that should be acquired in each data acquisition for enabling subject identification, we studied the model's performance when varying the number of gait cycles per subject, used for both training and prediction, between 1 and the maximum number of available gait cycles. This study was performed for the algorithm that led to the best trade-off between the considered evaluation metrics in the previous studies.

When considering both subjects with and without PD (DS6), as well as identification of PD patients over time (DS7), the performance of each model was evaluated using all available gait cycles. For the algorithm that led to the best trade-off between the considered evaluation metrics, we further explored the possibility of using only one of the following feature subsets: anthropometric measures; gait parameters; spatiotemporal gait parameters; kinematic gait parameters.

All studies presented in this chapter were carried out in the R environment [209], including dataset balancing, selection of training and test set, and subject identification from predicted probabilities. The *rminer* package [212] was used to train the models and obtain the predictions. The *caret* package [251] was used to compute the performance evaluation metrics.

7.3 Results

The results presented in Table 7.3 to Table 7.13 include the mean value for the overall accuracy considering the 20 evaluation runs. They also include the mean and standard deviation values

for the class accuracy and class F_1 score, which were computed over the mean values for all subjects when considering the 20 runs. The training time and prediction time per gait cycle (mean and standard deviation for 20 runs) are also indicated. For the prediction time, the value for a given run is the mean value for all gait cycles from all subjects.

To verify if there is a statistically significant difference between the different algorithms, number of gait cycles or feature subsets, we performed the Wilcoxon signed rank over the results for all evaluation runs, in the case of the overall accuracy, training time and prediction time. For class accuracy and class F_1 score, the same statistical test was carried out over the results for all subjects (mean of all runs per subject). The test was performed for the case(s) with the best result and each one of the remaining cases. In the tables, we indicated in bold not only the best result, but also the other results not presenting a significant difference (p-value > 0.05) in relation with the best result.

7.3.1 Identification of Healthy Subjects

The results obtained for the twenty healthy subjects (DS4), when using a single gait cycle for identification, are presented in Table 7.3. The highest performance metric values (overall accuracy, class accuracy and class F1 score) were achieved when using the random forest algorithm.

Table 7.3. Results for identification of healthy subjects (DS4) considering a single gait cycle. The results are indicated for each machine learning algorithm, when using 10 gait cycles per subject for model training/testing. The best result(s) for each evaluation metric are indicated in bold.

Algorithm	DS4, single gait cycle for identification				
	Overall accuracy (%)	Accuracy (%)	F_1 score (%)	Training time (s)	Prediction time per gait cycle (ms)
k-NN	91.5	95.6 ± 3.6	91.4 ± 5.2	**0.0 ± 0.0**	9.6 ± 0.7
Decision tree	80.3	89.6 ± 7.1	77.7 ± 12.4	**0.0 ± 0.0**	**4.3 ± 1.8**
Random forest	**98.3**	**99.1 ± 1.3**	**98.3 ± 1.3**	0.3 ± 0.0	5.6 ± 1.4
SVM	92.6	96.1 ± 2.5	92.5 ± 4.6	0.3 ± 0.1	51.8 ± 2.2
MLP	74.1	86.4 ± 5.2	73.7 ± 8.8	0.9 ± 0.3	8.0 ± 3.4
MLPE	86.9	93.1 ± 4.1	86.7 ± 6.4	0.9 ± 0.3	14.6 ± 4.8

The results achieved when deciding on the subjects' identity based on all available gait cycles are included in Table 7.4. In this case, the best performance was obtained for k-NN, random forest, SVM and MLPE. In both situations, the lowest training time was for k-NN and decision tree, and the lowest prediction time was for the decision tree.

Table 7.4. Results for identification of healthy subjects (DS4) considering all gait cycles available per subject.
The results are indicated for each machine learning algorithm, when using 10 gait cycles per subject for model training/testing. The best result(s) for each evaluation metric are indicated in bold.

Algorithm	DS4, all gait cycles per subject for identification				
	Overall accuracy (%)	Accuracy (%)	F_1 score (%)	Training time (s)	Prediction time per gait cycle (ms)
k-NN	**99.5**	**99.7 ± 0.8**	**99.3 ± 1.6**	**0.0 ± 0.0**	9.2 ± 1.5
Decision tree	91.5	95.5 ± 6.6	88.7 ± 12.8	**0.0 ± 0.0**	**3.4 ± 0.8**
Random forest	**100**	**100.0 ± 0.0**	**100.0 ± 0.0**	0.3 ± 0.1	5.1 ± 0.6
SVM	**100**	**100.0 ± 0.0**	**100.0 ± 0.0**	0.2 ± 0.1	56.7 ± 15.7
MLP	97.2	98.6 ± 2.5	96.3 ± 5.1	0.7 ± 0.2	5.8 ± 1.7
MLPE	**100**	**100.0 ± 0.0**	**100.0 ± 0.0**	0.8 ± 0.3	11.1 ± 2.0

Table 7.5 presents the results achieved by the random forest model (best trade-off between the considered metrics), when varying the number of gait cycles used for both training and testing between 1 and 10. The model's performance improved when the number of gait cycles increased. However, the results are similar from 4 gait cycles. This trend can be seen in Figure 7.1 (a) and (b), which show the mean and standard deviation respectively for the class accuracy and class F_1 score versus the number of gait cycles.

Table 7.5. Results for identification of healthy subjects (DS4) considering all gait cycles available per subject, when varying the number of gait cycles used for model training/testing.
The results correspond to the random forest algorithm. The best result(s) for each evaluation metric are indicated in bold.

Number of gait cycles per subject	DS4, all gait cycles per subject for identification, random forest				
	Overall accuracy (%)	Accuracy (%)	F1 score (%)	Training time (s)	Prediction time per gait cycle (ms)
1	54.0	75.8 ± 10.2	46.0 ± 18.4	**0.0 ± 0.0**	**3.5 ± 2.4**
2	84.8	92.0 ± 6.0	80.7 ± 11.2	0.1 ± 0.0	3.6 ± 0.8
3	98.0	98.9 ± 1.9	97.3 ± 3.5	0.1 ± 0.0	4.1 ± 1.5
4	**99.8**	**99.9 ± 0.6**	**99.7 ± 1.2**	0.1 ± 0.0	4.5 ± 1.0
5	**100**	**100.0 ± 0.0**	**100.0 ± 0.0**	0.2 ± 0.1	5.9 ± 3.0
6	**100**	**100.0 ± 0.0**	**100.0 ± 0.0**	0.2 ± 0.0	4.6 ± 1.6
7	**100**	**100.0 ± 0.0**	**100.0 ± 0.0**	0.2 ± 0.0	4.8 ± 1.2
8	**100**	**100.0 ± 0.0**	**100.0 ± 0.0**	0.3 ± 0.0	5.1 ± 1.2
9	**100**	**100.0 ± 0.0**	**100.0 ± 0.0**	0.3 ± 0.1	5.1 ± 1.2
10	**100**	**100.0 ± 0.0**	**100.0 ± 0.0**	0.3 ± 0.1	5.1 ± 0.6

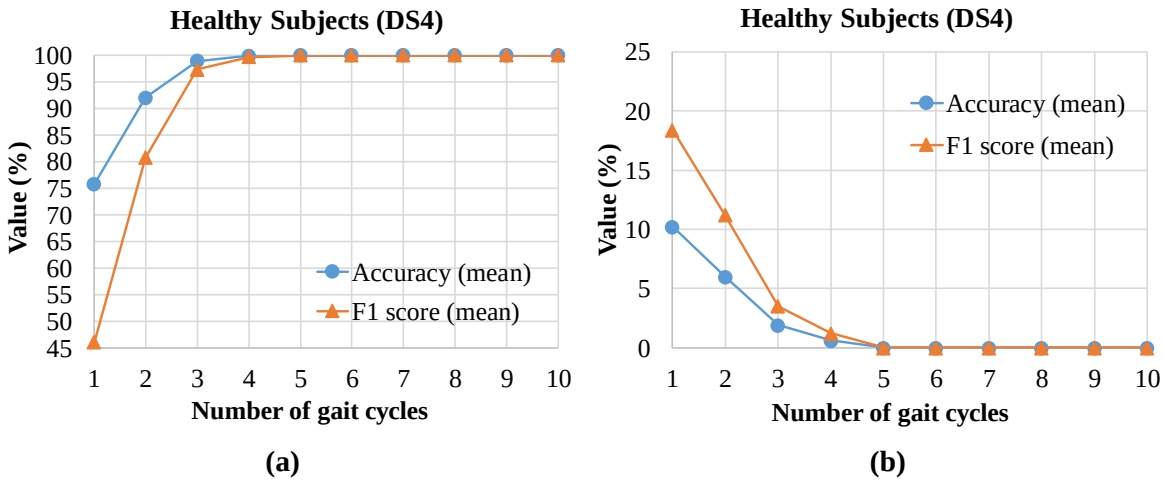

Figure 7.1. Mean (a) and standard deviation (b) values for the class accuracy and class F_1 score (DS4 and random forest) versus the number of gait cycles per subject used for training/testing, when using all gait cycles available for identification.

7.3.2 Identification of Parkinson's Disease Patients

The results obtained when considering PD patients (DS5) are presented in Table 7.6 to Table 7.8. The best performance was achieved with the random forest algorithm, when considering a single gait cycle for identification. When using all gait cycles available per subject, all algorithms except the decision tree achieved a similar performance (mean overall accuracy ≥ 99%). In both cases, the lowest training time was for k-NN, decision tree and/or SVM, and the lowest prediction time was for decision tree and random forest (mean value of 3 or 4 ms). The random forest model's performance improved when increasing the number of used gait cycles (similar results from 3 gait cycles).

Table 7.6. Results for identification of PD patients (DS5) considering a single gait cycle. The results are indicated for each machine learning algorithm, when using 7 gait cycles per subject for model training/testing. The best result(s) for each evaluation metric are indicated in bold.

Algorithm	DS5, single gait cycle for identification				
	Overall accuracy (%)	Accuracy (%)	F_1 score (%)	Training time (s)	Prediction time per gait cycle (ms)
k-NN	97.9	98.8 ± 1.8	97.8 ± 2.3	**0.0 ± 0.0**	8.3 ± 2.0
Decision tree	50.3	72.7 ± 15.9	37.9 ± 25.2	**0.0 ± 0.0**	**3.2 ± 0.2**
Random forest	**99.7**	**99.9 ± 0.3**	**99.7 ± 0.4**	0.1 ± 0.0	**3.2 ± 0.5**
SVM	98.2	99.0 ± 1.3	98.2 ± 2.2	**0.0 ± 0.0**	14.9 ± 1.0
MLP	94.5	97.0 ± 1.9	94.4 ± 2.9	0.2 ± 0.0	5.4 ± 1.3
MLPE	97.1	98.4 ± 1.4	97.0 ± 2.6	0.2 ± 0.0	11.6 ± 4.0

Table 7.7. Results for identification of PD patients (DS5) considering all gait cycles available per subject.
The results are indicated for each machine learning algorithm, when using 7 gait cycles per subject for model training/testing. The best result(s) for each evaluation metric are indicated in bold.

Algorithm	DS5, all gait cycles per subject for identification				
	Overall accuracy (%)	Accuracy (%)	F_1 score (%)	Training time (s)	Prediction time per gait cycle (ms)
k-NN	**100**	**100.0 ± 0.0**	**100.0 ± 0.0**	**0.0 ± 0.0**	12.4 ± 5.3
Decision tree	57.7	76.8 ± 16.6	43.9 ± 25.4	**0.0 ± 0.0**	**4.3 ± 1.5**
Random forest	**100**	**100.0 ± 0.0**	**100.0 ± 0.0**	0.1 ± 0.0	**3.5 ± 0.7**
SVM	**100**	**100.0 ± 0.0**	**100.0 ± 0.0**	0.1 ± 0.0	18.8 ± 6.8
MLP	**99.1**	**99.5 ± 1.0**	**98.8 ± 2.0**	0.2 ± 0.1	6.2 ± 2.2
MLPE	**100**	**100.0 ± 0.0**	**100.0 ± 0.0**	0.2 ± 0.1	13.8 ± 5.3

Table 7.8. Results for identification of PD patients (DS5) considering all gait cycles available per subject, when varying the number of gait cycles used for model training/testing.
The results correspond to the random forest algorithm. The best result(s) for each evaluation metric are indicated in bold.

Number of gait cycles per subject	DS5, all gait cycle per subjects for identification, random forest				
	Overall accuracy (%)	Accuracy (%)	F_1 score (%)	Training time (s)	Prediction time per gait cycle (ms)
1	85.9	92.2 ± 4.6	81.7 ± 8.7	**0.0 ± 0.0**	3.4 ± 1.2
2	**98.2**	99.0 ± 1.2	97.6 ± 2.2	**0.0 ± 0.0**	3.3 ± 0.8
3	**100**	**100.0 ± 0.0**	**100.0 ± 0.0**	**0.0 ± 0.0**	**2.9 ± 0.4**
4	**100**	**100.0 ± 0.0**	**100.0 ± 0.0**	0.1 ± 0.0	3.2 ± 0.8
5	**100**	**100.0 ± 0.0**	**100.0 ± 0.0**	0.1 ± 0.0	3.8 ± 1.2
6	**100**	**100.0 ± 0.0**	**100.0 ± 0.0**	0.1 ± 0.0	3.9 ± 1.0
7	**100**	**100.0 ± 0.0**	**100.0 ± 0.0**	0.1 ± 0.0	4.1 ± 1.8

Identification of Subjects with and without Parkinson's Disease

The results obtained for both PD patients and healthy subjects (DS6), when using all gait cycles available per subject for identification, are presented in Table 7.9. We can see that the random forest algorithm led to the model with the best performance. Training time was the lowest for k-NN and prediction time was the lowest for decision tree and MLP.

Table 7.9. Results for identification of both healthy subject and PD patients (DS6) considering all gait cycles available per subject.
The results are indicated for each machine learning algorithm, when using 5 gait cycles per subject for model training/testing. The best result(s) for each evaluation metric are indicated in bold.

Algorithm	DS6, all features				
	Overall accuracy (%)	Accuracy (%)	F_1 score (%)	Training time (s)	Prediction time per gait cycle (ms)
k-NN	97.6	98.8 ± 3.2	96.8 ± 6.6	**0.0 ± 0.0**	16.2 ± 6.5
Decision tree	40.9	69.7 ± 18.2	24.9 ± 22.5	0.1 ± 0.0	**6.2 ± 1.8**
Random forest	**99.7**	**99.9 ± 0.6**	**99.6 ± 1.2**	0.5 ± 0.1	8.2 ± 1.4
SVM	97.3	98.6 ± 3.5	96.4 ± 7.7	1.0 ± 0.4	213.8 ± 22.9
MLP	82.4	91.0 ± 7.2	77.9 ± 15.1	1.5 ± 0.2	**7.4 ± 2.2**
MLPE	95.8	97.8 ± 2.8	94.5 ± 6.1	1.8 ± 0.5	18.6 ± 5.5

Table 7.10 includes the results obtained with the random forest algorithm for DS6, when considering different feature sets. The best performance was achieved when using all 25 features (overall accuracy of 100%), but a good performance was also obtained when using the 22 gait parameters or the 3 anthropometric measures (overall accuracy ≥ 97%). As expected, the lowest training and prediction time corresponded to the smallest feature set (3 anthropometric measures).

Table 7.10. Results for identification of both healthy subject and PD patients (DS6) considering all gait cycles available per subject, for different feature subsets.
The results correspond to the random forest algorithm, when using 5 gait cycles per subject for model training/testing. The best result(s) for each evaluation metric are indicated in bold.

Features	DS6, random forest				
	Overall accuracy (%)	Accuracy (%)	F_1 score (%)	Training time (s)	Prediction time per gait cycle (ms)
3 anthropometric measures	96.6	98.3 ± 3.4	95.5 ± 7.8	**0.2 ± 0.0**	**4.1 ± 0.6**
13 spatiotemporal gait parameters	85.0	92.3 ± 12.1	81.6 ± 24.9	0.3 ± 0.1	6.1 ± 1.6
9 kinematic gait parameters	92.0	95.9 ± 6.1	89.6 ± 12.7	0.3 ± 0.1	5.7 ± 1.2
22 gait parameters	97.6	98.8 ± 4.7	96.8 ± 9.4	0.5 ± 0.1	7.3 ± 1.9
All 25 features	**99.7**	**99.9 ± 0.6**	**99.6 ± 1.2**	0.5 ± 0.1	8.2 ± 1.4

Identification of Parkinson's Disease Patients Over Time

Table 7.11 presents the results obtained for DS7, where the model was trained and then tested using data from two different acquisitions per patient corresponding to two different states or two different days. The k-NN, random forest and SVM algorithms led to the models with the best overall performance.

Table 7.11. Results for identification of PD patients over time (DS7) considering all gait cycles available per subject.
The results are indicated for each machine learning algorithm, when using 6 gait cycles per subject for model training and testing acquired in two different days or PD states. The best result(s) for each evaluation metric are indicated in bold.

Algorithm	DS7, all features, no outlier removal				
	Overall accuracy (%)	Accuracy (%)	F_1 score (%)	Training time (s)	Prediction time per gait cycle (ms)
k-NN	**64.3**	**80.8 ± 24.5**	**56.0 ± 46.0**	**0.0 ± 0.0**	9.3 ± 0.6
Decision tree	30.7	62.7 ± 21.0	20.1 ± 33.2	**0.0 ± 0.0**	**3.5 ± 0.4**
Random forest	**68.2**	**82.9 ± 20.8**	**61.2 ± 38.9**	0.1 ± 0.0	3.8 ± 0.4
SVM	**67.9**	**82.7 ± 22.5**	**62.3 ± 42.1**	0.1 ± 0.0	26.5 ± 1.5
MLP	48.6	72.3 ± 16.6	39.4 ± 28.0	0.2 ± 0.0	5.9 ± 0.3
MLPE	57.5	77.1 ± 18.2	**48.4 ± 31.1**	0.2 ± 0.0	11.7 ± 0.9

To investigate if the performance results could be improved, the same study was carried out, with the difference that outliers were removed prior to dataset balancing. For each patient and acquisition, we excluded the instances for which the values for at least 25% of the features corresponded to outliers. For each feature, a value was considered as an outlier if was lower than $Q_1-1.5\times IQR$ or higher than $Q_3-1.5\times IQR$, where Q_1 and Q_3 are the first and third quartiles and IQR is the interquartile range (Q_3-Q_1). The first and third quartile is the median of the values to the left and right of the median value, respectively, when all considered values are sorted in ascending order. The results achieved when removing outliers are included in Table 7.12, where we can see that the best overall performance was achieved by the SVM model.

The results obtained with the SVM algorithm when considering different feature sets (DS7, outlier removal) are included in Table 7.13. Besides the different types of features (anthropometric measures, spatiotemporal and/or kinematic gait parameters), we also explored a subset of features selected using the correlation-based feature selection (CFS) method. This feature subset included the following 12 features: 5 spatiotemporal gait parameters (stride and swing duration, stride length, step

width and gait speed), 4 kinematic gait parameters (spine middle angle, elbow angle minimum, knee angle minimum and maximum) and the 3 anthropometric measures. Overall, the best performance was achieved when using the subset of 12 features.

Table 7.12. Results for identification of PD patients over time (DS7) considering all gait cycles available per subject, with outlier removal.
The results are indicated for each machine learning algorithm, when using 6 gait cycles per subject for model training and testing acquired in two different days or PD states. The best result(s) for each evaluation metric are indicated in bold.

Algorithm	DS7, all features, outlier removal				
	Overall accuracy (%)	Accuracy (%)	F_1 score (%)	Training time (s)	Prediction time per gait cycle (ms)
k-NN	71.4	**84.6 ± 23.8**	**66.0 ± 44.8**	**0.0 ± 0.0**	8.9 ± 1.4
Decision tree	24.3	59.2 ± 20.2	16.3 ± 32.1	**0.0 ± 0.0**	**3.3 ± 0.5**
Random forest	67.9	**82.7 ± 22.1**	**62.3 ± 41.5**	0.1 ± 0.0	4.3 ± 1.3
SVM	**73.6**	**85.8 ± 23.2**	**71.1 ± 42.8**	0.1 ± 0.0	23.1 ± 1.9
MLP	51.4	73.8 ± 16.2	43.8 ± 27.0	0.3 ± 0.1	6.0 ± 1.4
MLPE	61.4	**79.2 ± 18.0**	54.8 ± 31.6	0.2 ± 0.0	10.5 ± 1.7

Table 7.13. Results for identification of PD patients over time (DS7) considering all gait cycles available per subject (outlier removal), for different feature subsets.
The results correspond to the SVM algorithm, when using 6 gait cycles per subject for model training and testing acquired in two different days or PD states. The best result(s) for each evaluation metric are indicated in bold.

Features	DS7, outlier removal, SVM				
	Overall accuracy (%)	Accuracy (%)	F_1 score (%)	Training time (s)	Prediction time per gait cycle (ms)
3 anthropometric measures	64.3	**80.8 ± 23.7**	**57.2 ± 43.7**	**0.1 ± 0.0**	**18.4 ± 1.2**
13 spatiotemporal gait parameters	50.0	**73.1 ± 20.6**	**40.9 ± 34.0**	**0.1 ± 0.0**	21.2 ± 2.7
9 kinematic gait parameters	47.1	71.5 ± 24.8	40.4 ± 44.6	**0.1 ± 0.0**	19.0 ± 2.5
22 gait parameters	65.7	**81.5 ± 24.6**	**61.5 ± 44.6**	**0.1 ± 0.0**	21.9 ± 4.0
All 25 features	73.6	**85.8 ± 23.2**	**71.1 ± 42.8**	**0.1 ± 0.0**	23.1 ± 1.9
12 selected features	**77.5**	**87.9 ± 20.7**	**70.3 ± 40.2**	**0.1 ± 0.0**	20.8 ± 2.2

The confusion matrix corresponding to the SVM model when using the 12 selected features is presented in Figure 7.2, where we can see that identification is correct in all evaluation runs for 9 patients and in most runs for 11 patients of the 14 considered patients.

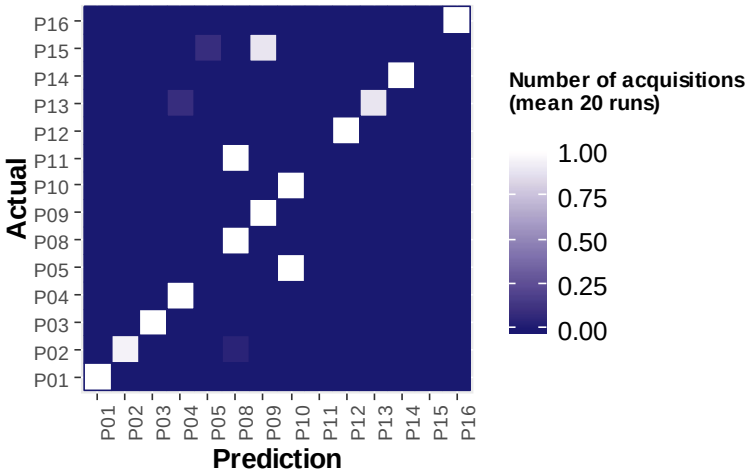

Figure 7.2. Confusion matrix for identification of PD patients over time (DS7) considering all gait cycles available per subject (outlier removal).

The results correspond to the SVM algorithm and the feature subset of 12 features, when using 6 gait cycles per subject for model training and testing acquired in two different days or PD states.

7.4 Discussion

7.4.1 Identification of Healthy Subjects

For healthy subjects (DS4), the random forest model achieved the best performance, when performing identification based on a single gait cycle: overall accuracy of 98% and F_1 score of 98 ± 1% (Table 7.3). The training time was the lowest (0 s) for k-NN and decision tree. However, it was also low for the remaining algorithms (mean value between 0.3 and 0.9 s). The decision tree had the lowest prediction time (mean of 4 ms per gait cycle), followed by the random forest (6 ms). Therefore, we considered that the random forest led to the model with the best trade-off between all considered evaluation metrics.

When relying on the class probabilities predicted for all available gait cycles to identify a subject, the performance improved for all algorithms (Table 7.4), when compared with the use of a single gait cycle, as expected. Most of the algorithms (k-NN, random forest, SVM and MLPE) achieved an overall accuracy of ≈100%. From these algorithms, the random forest had the lowest prediction time. Therefore, this algorithm was again considered as the one with best trade-off between the different metrics.

For the random forest model, we found that the performance improved when increasing the number of gait cycles used for model training and testing until 4 gait cycles (similar results for 4 or more gait cycles – see Table 7.5). The difference between using a single gait cycle or more than 3 gait cycles was considerable (overall accuracy of 65% or 100%). Therefore, it is important to use at least 4 gait cycles to perform a correct identification, but there is no advantage in using more than that number of gait cycles.

7.4.2 Identification of Parkinson's Disease Patients

The results obtained for PD patients (DS5) are similar to those obtained for healthy subjects (DS4), with a few differences. For identification based on a single gait cycle (Table 7.6), the performance metric values were higher for the patients (overall accuracy of 100% versus 98%). This may be because a lower number of subjects was considered (11 patients instead of 20 healthy subjects). It can also be because it should be easier to correctly identify PD patients, since it is expected to be greater differences in gait among PD patients than between healthy subjects.

When considering all available gait cycles, the results were the same for most algorithms (the only exception was the decision tree): overall accuracy of 100% and F_1 score of 100 ± 0% (Table 7.7). As expected, training and prediction time were overall lower for DS5, since it has less subjects and less gait cycles per subject than DS4. For both datasets, performance improved when increasing the number of used gait cycles. However, the number of gait cycles required to achieve an overall accuracy over 99% was slightly lower for PD patients than healthy subjects (3 instead of 4 gait cycles), which may be due to the same reasons referred above.

Identification of Subjects with and without Parkinson's Disease

When considering both PD patients and healthy subjects (DS6), the algorithm that led to the model with best trade-off between the evaluation metrics was the same as for the two subject groups separately (DS4 and DS5): random forest. The model's performance was similar for the three datasets, when taking into account the same number of gait cycles (5 gait cycles): overall accuracy of 100% and F_1 score of 100 ± 1%.

This result suggests that the presence of both subjects with and without PD does not have an impact on identification. It also suggests that performance is not affected when increasing the number of subjects. As expected, both training and prediction time were higher when considering a higher number of subjects/instances. Nevertheless, they were still relatively low (mean value of 0.5 s and 8 ms, respectively, for random forest – see Table 7.9).

The results obtained when comparing different feature types showed that the best performance was obtained when using all features (Table 7.10), which indicates that all types of features are important for subject identification. The 13 spatiotemporal gait parameters led to the lowest overall accuracy (85%). When using a smaller subset of 9 kinematic gait parameters, the overall accuracy was much higher (92%). The value was even higher when using the 3 anthropometric measures or the 22 gait parameters (97–98%). Although the best result was achieved when using all features (100%), it is interesting to note that a similar performance can be achieved when using only 3 anthropometric measures (half of training and prediction time).

Identification of Parkinson's Disease Patients Over Time

Regarding identification of PD patients over time, the best performance was achieved by the models built using the k-NN, random forest and SVM algorithms (overall accuracy ≥ 64% – see Table 7.11). When compared with PD patient identification using data from the same acquisition for model training and testing, there is decline in performance. This decline was expected, since the gait of PD patients can vary considerably over the course of some months or even days, due to the evolution of the disease, a new treatment and/or treatment adjustments.

However, we verified that performance improves for most models when removing outliers within each acquisition. The best overall accuracy achieved was of 74% for SVM (Table 7.12). Although the SVM model has the highest prediction time per gait cycle (mean of 23 ms), it is still corresponds to identifying a subject in less than one second (0.23 s) assuming that each acquisition has 10 gait cycles. Therefore, we considered that the SVM model is the most appropriate for PD patient identification over time.

Similar to dataset DS6, the feature subsets corresponding to the 3 anthropometric measures and the 22 gait parameters led to a similar model performance in the case of DS7. However, there is a greater difference between these two subsets and the use of both feature types together, for DS7 (overall accuracy of 64–66% versus 74%). This result shows that the two types of features are both important for identification.

Nevertheless, performance can be further improved when relying on a subset of 12 features obtained using a feature selection method, which includes features from all three considered types. With this feature subset, the model carries out identification over time with an overall accuracy of 78%, which corresponds to a correct identification in all evaluation runs for 64% of the patients and in most runs for 79% of the patients (see Figure 7.2).

When comparing the identification relying on data from the same and different acquisitions, in the context of PD, worse results were expected for identification over time when using gait parameters only, due to the reasons explained above. On the other hand, the results for anthropometric measures should be similar, since these measures (e.g., leg length) are not expected to change for a given subject (with or without PD). However, the results are also worse for anthropometric measures, which can be explained by the fact that the values of these measures estimated by the Kinect change for some of the patients. These differences may be due to differences in the patients' posture and/or different acquisitions conditions, including small variations in the Kinect configuration. Therefore, a more detailed study is required to understand if the Kinect is suitable for human identification over time.

7.4.3 Comparison with the State of the Art

The results achieved by our proposed method and methods proposed in other contributions, which also rely on gait information extracted from Kinect data for subject identification, are compared in Table 7.14. Our indicated results correspond to the dataset of twenty healthy subjects, since the other studies included in the table considered healthy subjects only.

The results cannot be directly compared due to the use of different experimental setups and protocols, as well as datasets corresponding to a different number of subjects. Despite those differences, a comparison with the state of the art allows to understand how our results compare to those reported in other studies.

When using a single gait cycle for identification, we achieved a mean class accuracy of 99%, while Ball et al. reported a much lower value of 44% using a single step [74]. However, in the latter study, the authors used the first version of the Kinect while we used the second version. Furthermore, they relied on the k-means algorithm and kinematic gait parameters only, while our best result was obtained using the random forest algorithm together with anthropometric measures and both spatio-temporal and kinematic gait parameters. Additionally, the study of Ball et al. considered arbitrary walking paths, which is a more challenging situation than walking always in the same direction.

When compared with the study by Sinha et al. [73], we obtained a much higher mean F_1 score (98% considering a single gait cycle versus 62% considering a single step). This difference may be due to different reasons, including the use of the Kv2 instead of Kv1 and a frontal instead of a side view (occlusions may occur for the latter). Moreover, Sinha et al. only investigated the k-means, adaptive neural network and Naïve Bayes algorithms (our best result was obtained with random forest).

Table 7.14. Subject identification results reported in different contributions using the Kinect camera, when considering gait and healthy subjects.

Method	Kinect	Number of subjects	Features	Overall accuracy	Mean accuracy	Mean F_1 score
Our proposed method	v2 (front-view)	20	3 anthropometric measures, and 22 spatiotemporal and kinematic gait parameters	98% (1 gait cycle) / 100% (5 gait cycles)	99% (1 gait cycle) / 100% (5 gait cycles)	98% (1 gait cycle) / 100% (5 gait cycles)
Nambiar et al. (2017) [66]	v2 (four views)	20	7 anthropometric measures, and 35 spatiotemporal and kinematic gait parameters	92% (best match) / 100% (eight best matches) for front-view only	—	—
Ahmed et al. (2015) [67]	v2	20	25 joint relative distances, and 15 joint relative angles	92% (best match) / 100% (four best matches)	—	—
Rahman et al. (2017) [71]	v1/v2	30/20	760 spatial gait parameters	93% / 95%	—	—
Andersson et al. (2014) [72]	v1 (side-view)	140	20 anthropometric measures, and 60 spatiotemporal and kinematic gait parameters	88% (≈96% for 20 subjects)	—	—
Jiang et al. (2015) [69]	v1 (side-view)	10	5 anthropometric measures, and 4 kinematic gait parameters	82% (68% for gait parameters only)	—	—
Sinha et al. (2013) [73]	v1 (side-view)	10	Selected features from 12 anthropometric measures, 20 spatiotemporal and kinematic gait parameters, and other 14 features	—	—	62%
Preis et al. (2012) [70]	v1 (side-view)	9	4 anthropometric measures / 2 spatiotemporal gait parameters	91% / 55%	—	—
Ball et al. (2012) [74]	v1 (arbitrary paths)	4	18 kinematic gait parameters	—	44%	—

Our overall accuracy when using a single gait cycle (98%) is higher than the values reported in all other studies included in Table 7.14. Preis et al. obtained a value of 91%. However, this result was achieved when using 4 anthropometric measures only [70]. Nevertheless, we were able to obtain a higher value when using only 3 anthropometric measures (97% – see Table 7.10) for a much greater

number of subjects (37 versus 9 subjects). In addition, Preis et al. used a side-view plane of the walking path in relation with the Kinect, while we considered a front-view plane.

Jiang et al. reported a much lower result (overall accuracy of 82%), but they relied only on 9 features [69], while we used 25 features. Andersson et al. reported an overall accuracy of ≈96% for 20 subjects [72], which is similar to our result. However, we used a much lower number of features (25 instead of 80 features). The result obtained by Rahman et al. when using the Kv2 (95% [71]) is also similar to ours, but they used a much larger number of features (760 features). Ahmed et al. [67] and Nambiar et al. [66] both reported an overall accuracy of 92%. We obtained a better result (98%) with a lower number of features (25 features versus 40 or 42 features/measures).

Regarding subject identification over time, Gianaria et al. carried out a study with the Kv1, where they were able to correctly classify all cases for 70% of the subjects [68]. However, their results cannot be compared with ours, since they used data acquired from healthy subjects, while our study involved PD patients, which is a more challenging situation. To the best of our knowledge, there is no other study on subject identification based on gait using the Kinect involving PD patients.

7.5 Summary

Our results show that healthy subjects can be identified using the gait parameters provided by our automated gait analysis solution, as well as three additional anthropometric measures, with an overall accuracy of 100% when relying on at least four gait cycles per subject. When compared with other contributions, our proposed method led to a predictive model with better performance while using a lower number of features (identification based on a single gait cycle).

For Parkinson's disease (PD) patients, we verified that identification is also possible with an overall accuracy of 100%, when using at least three gait cycles. Furthermore, the same overall accuracy was achieved when considering both subjects with and without PD. This last result also suggests that increasing the number of subjects does not have an impact on identification.

For identification over time in the case of PD patients, the performance results declined when compared with identification using data from the same acquisition for model training and testing. However, it was possible to build a model that achieved an overall accuracy of 78%, when performing outlier removal and feature selection. The selected feature subset included 12 features from the three considered feature types (anthropometric measures, spatiotemporal gait parameters and kinematic gait parameters), showing that they are all important for subject identification.

8 Gait Assessment Support System

One of the main results of this thesis is a system for gait assessment support. The initial motivation for developing this system was to support the clinical assessment of gait in Parkinson's disease (PD). However, the evolution of the thesis' work led to a more generic system, which can be used to analyse the gait of any subject, and not only PD patients. The results of the gait analysis provided by our system can be useful in different scenarios such as sports, healthcare and security.

The final user of the system depends on the considered scenario. For example, in the case of a clinical environment (e.g., a hospital), the user can be a clinician (e.g., physician, nurse). When considering an ambulatory scenario (i.e., at the home of a subject), the user can be the subject being assessed, a relative or a caregiver. The subject being assessed also interacts with the system, by walking in front of the RGB-D camera.

Our gait assessment support system, which is depicted in Figure 8.1, enables automated online gait analysis of a given subject. When compared with a manual and/or offline solution, it allows time savings, since it avoids any manual intervention in the whole analysis process (except for starting the acquisition of data).

The system relies on a single RGB-D camera, namely the first or second version of the Microsoft Kinect (Kinect v1 or v2). This camera provides colour and/or IR images, depth information and 3-D body joint data, which are acquired using our *KiT* application running on a portable computer.

For each data acquisition, gait analysis is performed in an automated way, i.e., without requiring any manual intervention except for starting the data acquisition in *KiT*. Firstly, the system automatically detects whether the subject is walking, by relying on several measures extracted from the 3-D joint data. For the data corresponding to the walking activity, the different gait cycles are automatically detected using only three types of measures also extracted from the 3-D data.

When the number of gait cycles to be acquired is indicated by the user, the acquisition is automatically stopped when that number of cycles has been detected. For each gait cycle, several gait parameters are computed, which can be used to support the assessment of the subject's gait. These parameters are also used to automatically identify the subject.

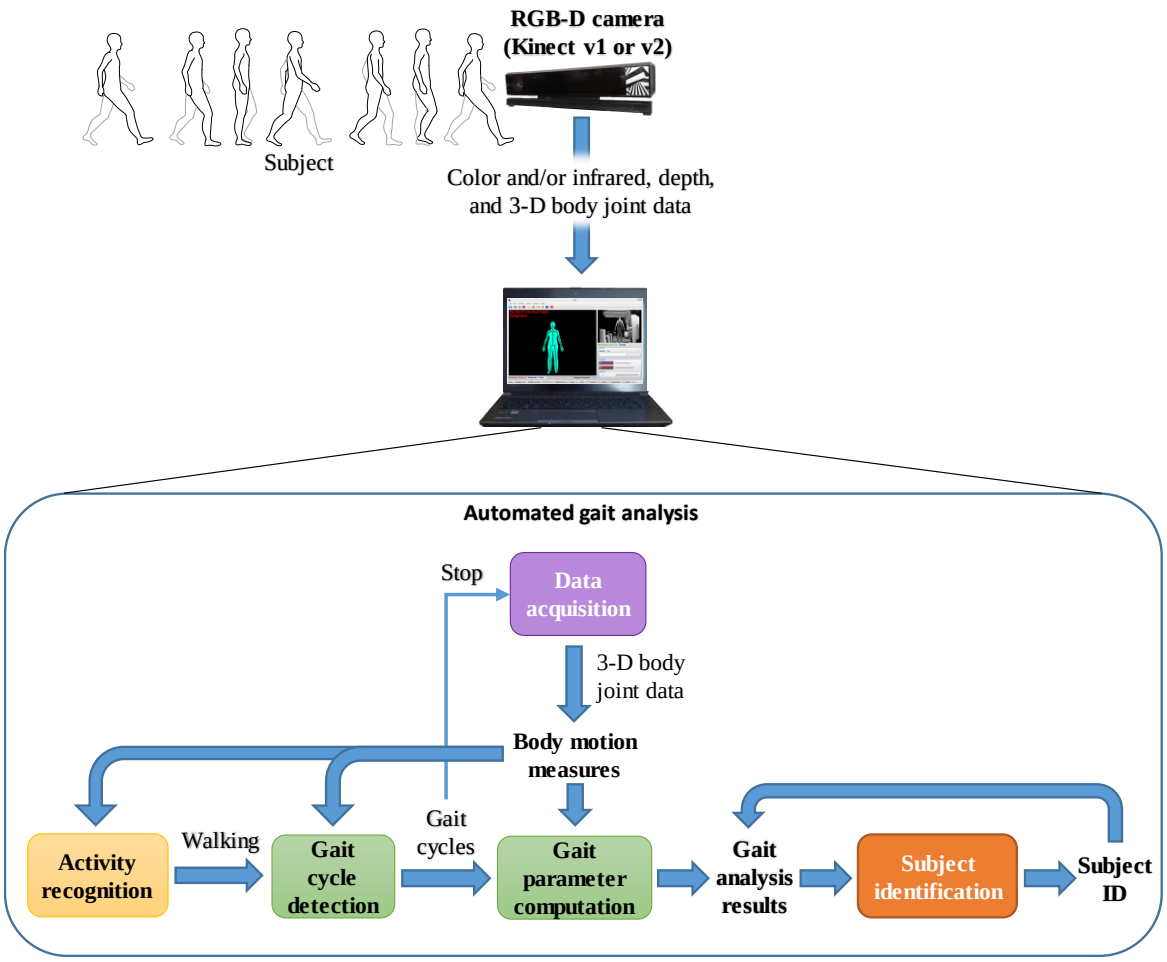

Figure 8.1. System for supporting the assessment of a given subject's gait.
The system includes an RGB-D camera (Kinect v1 or v2) that provides multimodal data, including 3-D body joint data. The camera is connected to a laptop where the automated gait analysis is performed.

8.1 System Integration

To implement the system for gait assessment support, the automatic gait cycle detection (including walking detection relying on activity recognition) and subject identification solutions were integrated into the *KiT* application, for enabling online gait analysis of a given subject. For research purposes, offline gait analysis is also enabled for a given data acquisition in the *KiMA* application, and for one or more acquisitions using a program written in Python.

8.1.1 Online Gait Analysis

To enable automated online gait analysis using a single software application, the solutions indicated above were integrated into *KiT*. In this application, the user can choose to perform gait analysis by using the checkbox that was added to the "Preferences" window, as shown in Figure 8.2.

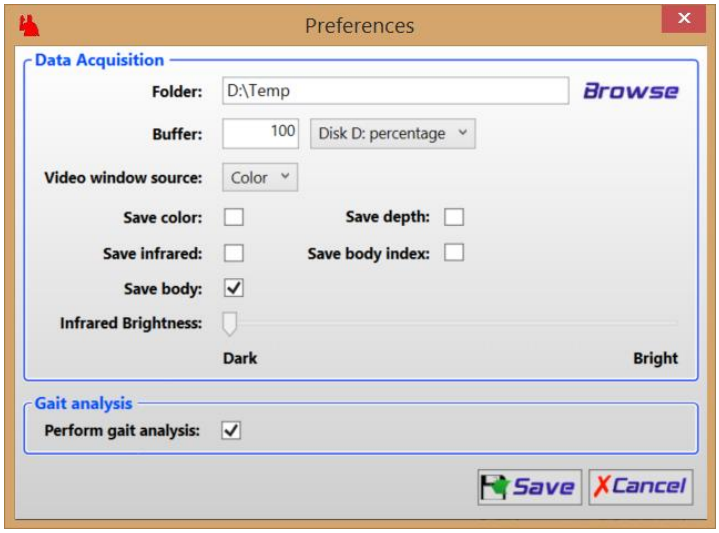

Figure 8.2. Preferences window of the *KiT* application (Kv2) after the integration of gait analysis.

When the "gait analysis" option is selected, the GUI of the main window of *KiT* is changed to include only the options and information that are relevant for gait analysis. The "Controls" group box (below the "Secondary Source" combobox) includes only the button that allow to start/stop the acquisition. There is also a "Gait Analysis" group box, which includes a text box that allows the indication of the minimum number of gait cycles that are required for gait analysis, as it can be seen in Figure 8.3.

When the user starts a data acquisition with a given subject, the activity (walking, standing or marching, while facing the Kinect or facing away from it) performed by the subject is recognized for each data frame. As explained above, when walking is detected, the carried out gait cycles are identified. The number of gait cycles that has been detected since the beginning of the acquisition is indicated in the "Gait Analysis" group box, as can be seen in Figure 8.4.

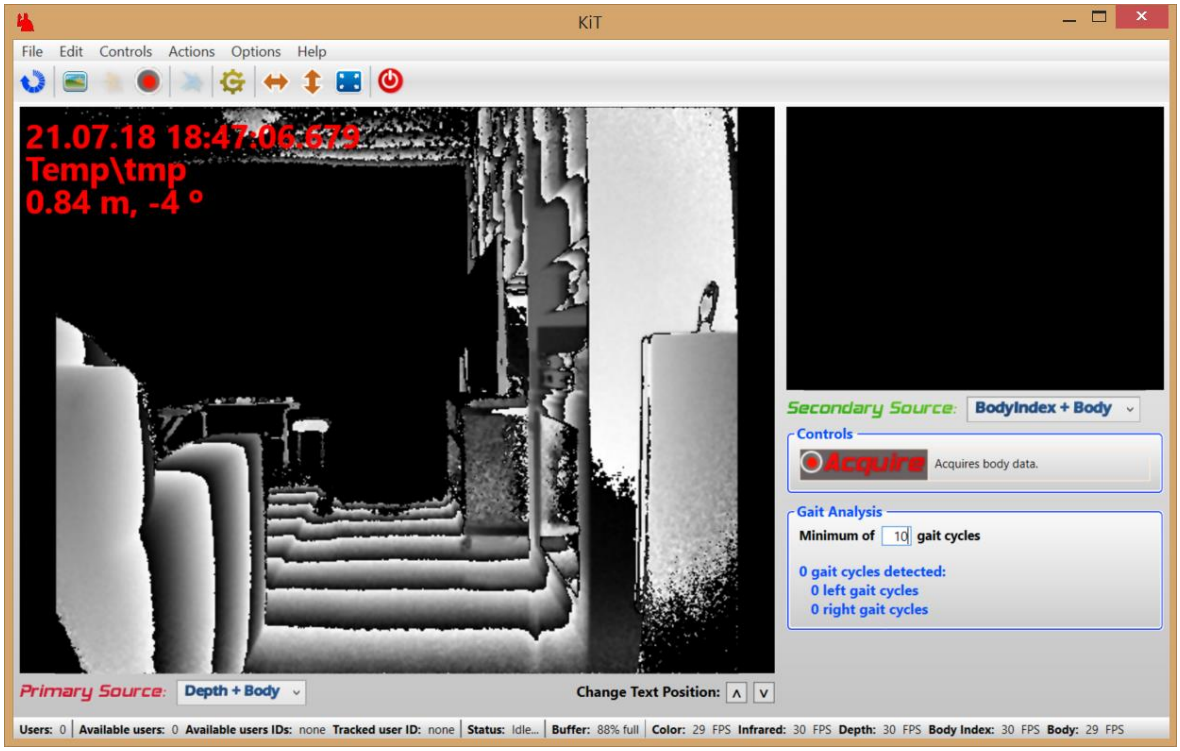

Figure 8.3. *KiT*'s main window GUI (Kv2) after the integration of automated online gait analysis, where it is possible to indicate the number of minimum gait cycles required for analysis.

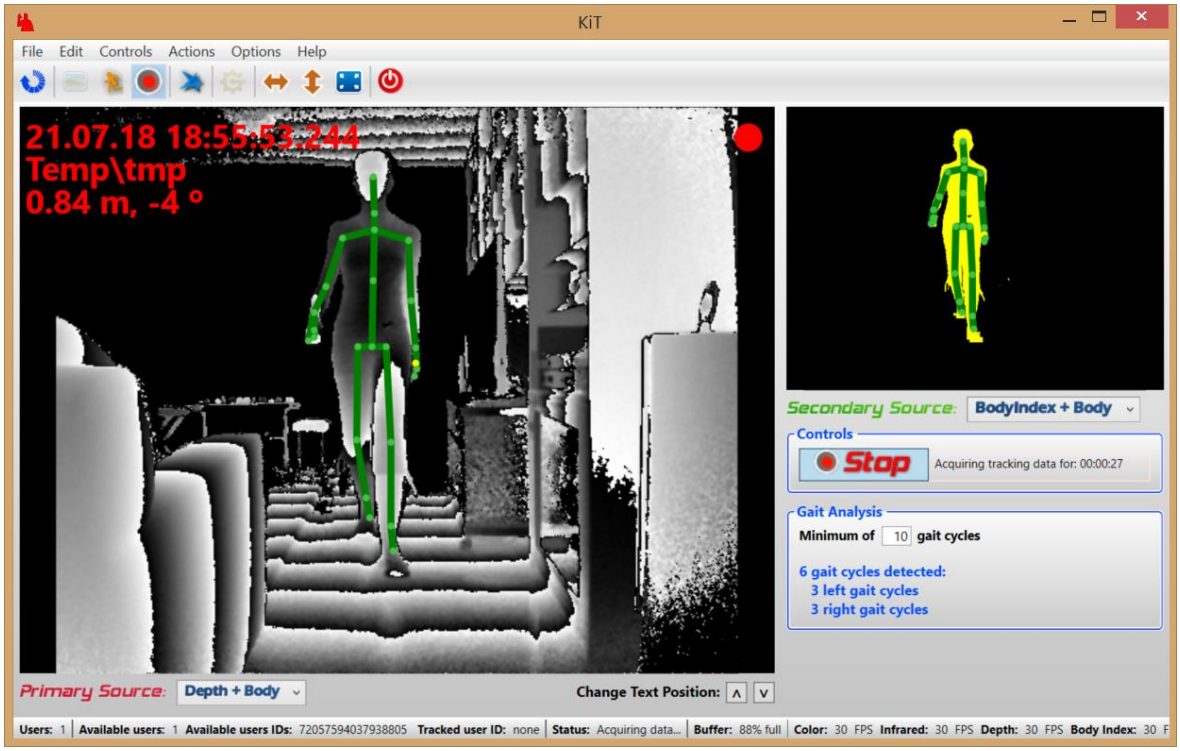

Figure 8.4. *KiT*'s main window GUI (Kv2) after the integration of automated online gait analysis, where the number of detected gait cycles since the beginning of the acquisition is displayed.

When the indicated number of gait cycles is achieved, the acquisition stops and several gait parameters are computed for each detected gait cycle. The obtained parameter values are then used to identify the corresponding subject. Since an incorrect identification can occur, especially when there are changes in the subject's gait, the user is asked to confirm if the identification is correct. If it is correct, no further action is needed. Otherwise, the user can select a subject from the list of existing subjects or indicate a new subject by inserting the corresponding information (name, ID, birth of date, weight, and height).

Finally, the mean value for each parameter is computed over all acquired gait cycles. This final results are presented to the user as shown in Figure 8.5, for both left and right gait cycles (column "Both" of the table within the "Gait Analysis Results" group box, below the subject information), as well as for left and right cycles separately to help detect asymmetries during gait.

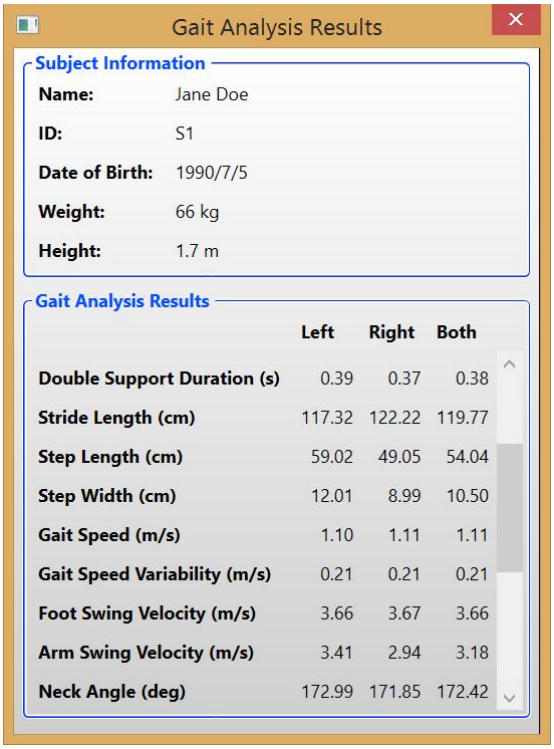

Figure 8.5. Results of gait analysis shown in the *KiT* application, including the subject's information and the mean value of the gait parameters for left, right and both gait cycles.

Regarding the system implementation, when the option of performing gait analysis is selected in *KiT*, the predictive models previously built for activity recognition and subject identification are loaded. Since the *KiT* application was written in C# and the models were built in the R environment using the *rminer* package, the *R.NET* C# library was used to load the required R package and run the R code that enables the use of the models in C#.

For online activity recognition, the 3-D joint data are filtered using a moving average filter with a window of 17 frames. For each frame, the measures used for recognition are computed over the filtered data and then used as input to the predictive model for activity recognition (relying again on the *R.NET* library). If walking is recognized, the following steps are carried out:

1. Verify if the frame corresponds to a heel strike, relying on the ankle distance measure;
2. If it is considered as a heel strike, identify the associated side (left or right), relying on the left and right ankle velocity;
3. If the time elapsed between the current and previous (if any) heel strikes of the same side is less than twice the defined maximum gait cycle duration, verify if the gait cycle defined by the those heel strike instants corresponds to walking towards or away from the camera;
4. If the gait cycle was performed while walking towards the camera, find the frames corresponding to the left and right toe offs, relying on the absolute difference between left and right shank angles;
5. If both toe off events are detected (i.e., the estimated toe off instants are different from the heel strike instants), the detected gait cycle and associated gait events are added to the gait cycle list, and the number of gait cycles is updated in *KiT*'s GUI (Figure 8.4).

All the measures used for the detection heel strike and toe off are filtered with a moving average filter, using a window with the size previously chosen for each type of measure (Table 5.9). The detection of heel strikes and associated side is also carried out using a window centred on the considered frame with the size previously selected for each case (Table 5.9).

The maximum gait cycle duration, used to decide if two consecutive heel strike of the same side constitute a gait cycle, was defined as 2 s. Since the system is to be used with any subject (with or without gait impairments), we found the maximum stride duration for all data acquisitions we performed with both healthy subjects and PD patients: 1.5 s and 1.6 s, respectively. Taking this into account, we choose the value of 2 s considering some tolerance to allow gait analysis for subject with more severe gait difficulties.

In third step above, the gait cycle is only considered if the whole body of the subject is being tracked (i.e., all body joints are tracked, without any clipped edges) for all of its frames. Otherwise, the detected gait cycle is not considered for analysis.

In the fourth step above, only the data corresponding to walking towards the Kinect are considered, since the results achieved in the first validation study were overall better when using data acquired while the subjects walked towards the sensor when compared with walking away from it.

Nevertheless, both walking activities can be taken into account for gait analysis with a small change in the code.

As explained above, when at least half of the defined minimum number of gait cycles (*M*) has been detected for each side (left and right), the acquisition is automatically stopped (it can also be manually stopped beforehand by the user). For this reason, it is required that the indicated *M* value is even integer number.

Furthermore, only an *M* value greater or equal to 4 is accepted. This value was chosen by taking into account the studies presented above. In the second validation study (WF vs WB for Kv2), it was observed that the agreement between the Kinect and the gold standard system tends to improve when varying the number of gait cycles from 1 to 11 (Figure 6.1). Moreover, in the study on subject identification, performance improved when using a larger number of gait cycles (best from 4 gait cycles for healthy subjects and from 3 gait cycles for PD patients). Therefore, we considered 4 gait cycles to be a good choice for the minimum number of gait cycles that should be used for gait analysis.

When the acquisition ends, all activity and gait information is saved to an XML file (example presented in Appendix A.2), where the intervals corresponding to a given activity are saved as events and the heel strike and toe off instants are saved as labels. This information is saved so that it can reviewed offline together with the associated acquisition in *KiMA*.

When more than $M/2$ left/right gait cycles have been detected, $M/2$ left/right gait cycles are randomly chosen, so that the number of gait cycles for each side is the same. Then, for each gait cycle, the gait parameters (Table 6.2 and Table 6.3) are computed over the 3-D joint data considering the estimated heel strike and toe off instants, and saved to a CSV file.

For some of the parameters, the measure used to compute its value is filtered using a zero-lag Butterworth filter (order and cut-off frequency values indicated in Table 6.5). The signal processing carried out in the validation studies presented above was carried out in Matlab using the "filtfilt" function for zero-phase digital filtering and the "butter" function for Butterworth filter design, from the Signal Processing Toolbox [252]. To the best knowledge, there are no similar functions implemented in C#. However, both functions are implemented in Python in the *scipy* library [253].

Therefore, the required data filtering using a Butterworth filter is performed in *KiT* by running Python code as a new process in C#. All the measures that need to be filtered are saved to a temporary text file together with the associated filter order and cut-off frequency values. The information required to start the process includes the path of the Python interpreter and the command to

be executed. The command includes the path of the file with the Python code, as well as the name of the temporary file with the data to be filtered and the filter parameter values (command arguments).

The resulting gait parameter values are used as input of the predictive model for subject identification. The *R.NET* library was again used to execute R code for: reading the contents of the CSV file with the gait analysis results; obtaining the probabilities provided by the predictive model for each gait cycle; choosing one of the subjects based on the probabilities using the method described in the study on subject identification.

Once the subject has been identified, all files including Kinect data, activity and gait information, and gait analysis results, which were saved to a temporary folder, are moved to a folder corresponding to the current date inside a folder corresponding to the subject's ID. Furthermore, the gait analysis results are added to a CSV file that includes the latest results for all subjects. If the subject already exists in this dataset, the associated data are replaced. Then, a new predictive model is built using the updated dataset (relying again on the *R.NET* library), with the aim of minimizing incorrect identifications due to gait changes over time.

8.1.2 Offline Gait Analysis

In the context of research, it may necessary to perform gait analysis offline, when there is one or more acquisitions for which online gait analysis was not performed (e.g., acquisitions acquired before the implementation of our final system). In the future, an offline solution can also be useful to validate possible changes made to our solutions for activity recognition, gait cycle detection and/or gait parameter computation.

Offline gait analysis can be carried out for a given data acquisition opened in our *KiMA* application, by choosing the "Perform Gait Analysis" option in the context menu. A video showing the analysis being carried out for the three different tasks considered in Chapter 5 can be found on the following link: https://doi.org/10.1371/journal.pone.0201728.s001. The integration of gait analysis into *KiMA* was similar to the integration described above for *KiT*, with the difference that both activity recognition and gait cycle detection are performed offline. Another difference is that subject identification is not performed, since we assume that in the context of research the identity of the subject is already know. Nonetheless, the ability of identifying the subject can be easily integrated in the same way as for *KiT*.

To enable offline analysis for more than one acquisition without the need to open them one by one in *KiMA*, we also provide the possibility of carrying out offline gait analysis using code implemented in Python. The activity recognition relies on the implemented R code, which is accessed

using the *rpy2* package. The parsing of Kinect data files and the computation and filtering of measures for gait cycle detection rely on C# methods through DLLs (dynamic link libraries), which are accessed using the *pythonnet* package. This code was used in a Python program that carried out automated gait analysis over all acquisitions in the last preliminary study with PD patients, as well as in the studies on subject identification.

8.2 Summary

The thesis' work resulted in different solutions that were integrated into a system for gait assessment support. In contrast with other systems, our system allows carrying out fully automated gait analysis (except for starting the data acquisition), by relying on activity recognition, gait cycle detection and subject identification using only measures extracted from 3-D data provided by a single RGB-D camera and machine learning techniques.

Firstly, the data corresponding to the walking activity are automatically identified by relying on activity recognition using machine learning techniques and measures extracted from the 3-D body joint data provided by a single Kinect v1 or v2 camera (acquired using our *KiT* application). For the identified gait data, the performed gait cycles are automatically detected. This detection is performed online, which allows to automatically stop the acquisition of data only when a defined number of gait cycles has been detected. Several parameters are computed for each detected gait cycle, which are then used to identify the associated subject, avoiding thus the manual indication of the subject's identity.

9 Conclusion and Future Work

This chapter presents the main conclusions of the performed work, as well as some possible future work directions.

9.1 Conclusion

The main objective of this thesis work was to provide a tool for supporting gait assessment, by studying, designing and developing solutions that enable quantitative human motion analysis during gait in an automated way. The developed solutions were integrated into a system for automated online gait analysis, which is presented in Chapter 8. The system acquires the 3-D body joint data provided by a single RGB-D camera from a given subject. Then, these data are used to automatically identify gait data, detect the performed gait cycles, stop the acquisition when a defined number of gait cycles has been detected, compute several gait parameters per gait cycle and identify the corresponding subject based on the obtained values. Therefore, our system allows saving time in the whole process of gait analysis when compared with an offline solution requiring manual selection of the relevant data and events and indication of the subject's identity.

Our system was shown to be a viable alternative to gold standard motion capture systems for obtaining several spatiotemporal parameters and a few kinematic parameters, which can be used to support gait assessment. Furthermore, the system is suitable for use in different environments, including clinical environments, since it relies on a single markerless RGB-D camera that is less expensive, more portable, less intrusive and easier to set up than the gold standard systems (multiple cameras and several markers attached to the subject's body). Although our system relies on a Kinect camera, other RGB-D cameras can be used with some adjustments to our data acquisition solution. The solutions for automated gait analysis and subject identification do not need any modification, as long as the 3-D position of the considered body joints are provided.

Although nowadays there are sensors that enable motion quantification, the clinical motor assessment in Parkinson's disease (PD) still relies mainly on ratings scales, such as the Unified PD Rating Scale (UPDRS). The UPDRS includes an item for evaluating gait relying on visual observation (subjective approach). The initial motivation of our work was thus to investigate if the quantitative data provided by an RGB-D camera can be used to support clinical gait assessment in PD. Preliminary studies carried out with data acquired in a hospital environment showed that gait information extracted from the 3-D data provided by a single Kinect could potentially be used to evaluate

the severity of gait impairments in PD patients treated with deep brain stimulation [79-84] (Chapter 3). Furthermore, the studies showed that the manual identification of gait data and events is very time consuming and prone to human errors.

Therefore, the need to automate the whole process of gait analysis was the focus of the remaining research presented in this thesis. Other contributions on quantitative gait analysis consider that the acquired data include only gait data and propose a method for automated gait event detection only [55-65]. In contrast with these studies, we enable fully automated gait analysis by carrying out the different steps involved in gait analysis (except for starting the data acquisition) in an automated way, relying on the 3-D data provided by a single RGB-D camera, as described above.

The data provided by the RGB-D camera, namely a Kinect (first or second version), are acquired using our *KiT* software application [78] (Chapter 4). The gait data are then automatically selected by detecting the walking activity using a predictive model for activity recognition, which was obtained using machine learning techniques [76] (Chapter 5). Based on measures extracted from 3-D body joint data, the model recognizes three different activities (walking, standing and marching), as well as two different positions of the subject in relation to the camera (facing the camera or facing away from it), with an overall accuracy $\geq$ 96%. The latter ability is important if we wish to use only the data corresponding to one of the considered walking activities (walking towards and away from the Kinect), or analyse the movements of left and right joint separately for both activities.

When walking is detected, the performed gait cycles and associated phases are automatically detected, by estimating the instants corresponding to relevant gait events, relying only on a few measures extracted from 3-D data [76] (Chapter 5). We were able to reduce the estimation error for one of the gait events, and consequently for the duration of gait phases, when compared with other methods proposed in the literature. Moreover, both activity recognition and gait cycle detection can be carried out online, enabling automated online gait analysis. Therefore, a minimum number of gait cycles required for gait analysis can be defined and the data acquisition will be stopped only when the defined number of gait cycles has been detected.

For each detected gait cycle, several gait parameters are computed. The validity of the gait analysis results obtained by our system was evaluated against a gold standard system (multi-camera marker-based Qualisys system), for a group of healthy subjects. The results of this study (Chapter 6) show that the best overall agreement between systems was achieved when using the second version of the Kinect, data corresponding to walking towards the camera, and a Kinect configuration corresponding to a height of 1 m. For this combination, most spatiotemporal parameters obtained with our system can be used for gait assessment support, while only a few kinematic parameters (elbow angle minimum and maximum) can be used for that purpose. When compared with the state of the art, we

considered a more complete set of parameters, including some kinematic parameters (elbow angles) that are usually not explored. Moreover, our solution had a better overall performance than other proposed methods in terms of agreement with a gold standard.

The gait analysis results provided by our system contain information regarding the gait of the subject being assessed, which can be useful not only for supporting gait assessment, but also for identifying the subject according to previous work [66, 69, 70, 72]. Therefore, to avoid the manual indication of the subject's identity, we explored the use of the obtained gait parameters and three anthropometric measures, together with machine learning techniques, for automatically identifying the corresponding subject (Chapter 7). This identification relies on a predictive model, which is re-trained after each new session with the latest information to avoid incorrect identifications due to change in gait, for example.

Our proposed method compares favourably with the state of the art, achieving a higher overall accuracy while using a lower number of features, when identifying healthy subjects using a single gait cycle and the second version of the Kinect [77]. For identification based on all available gait cycles, the overall accuracy was ≈100% when considering healthy subjects and PD patients separately and together (model training/testing using gait cycles from the same data acquisition for each subject). When considering the more challenging situation of identifying PD patients over time, the overall accuracy decreased. This decrease was expected for gait parameters, but not for anthropometric measures, since PD patients can have considerable changes in gait over short intervals of time, but their anthropometric measures should not change. Therefore, it would be interesting to further explore in the future the identification of subjects over time based on gait using the Kinect.

9.2 Future Work

The conducted research work can be further improved by enhancing the solutions proposed in this thesis and exploring other possible research directions. Some improvements over the developed solutions include the following:

- **Recognition of more activities**: the solution for activity recognition can be enhanced by considering a greater number of activities that are relevant in the context of clinical motor assessment (e.g., sitting down and standing up from a chair, lateral trunk flexion, shoulder/elbow flexion). The inclusion of more activities/tasks would allow not only performing regular or sporadic gait assessments, but also monitoring the gait of a subject more continuously at home, for example. Furthermore, it would enable automated analysis of other motor tasks besides gait.

- **Enhancement of subject identification**: explore if the identification of PD patients over time can be improved, by investigating new features (e.g., new gait parameters and/or anthropometric measures). Another possibility is to investigate the computation of a similarity measure between two gait cycles using, for example, dynamic time warping (DTW) over measures extracted from 3-D body joint data, which is an approach that has been used in studies on subject identification [67, 69]. Our subject identification solution could be further improved by avoiding incorrect identifications when the subject does not yet exist in our system. A possibility would be to detect these cases relying on probabilities provided by the predictive model and a threshold.
- **Enhancement of gait assessment support**: to enable the use of all considered gait parameters for gait assessment support, it would be important to investigate if the agreement between our system and a gold standard system can be improved for kinematic gait parameters (agreement was found to be moderate or poor for most of these parameters – Chapter 6). This improvement could be achieved by exploring, for example, the removal of outliers over the time series corresponding to measures extracted from 3-D data and/or the use of other data filtering techniques.

Previous research work can also be extended by acquiring new or larger datasets corresponding to healthy subjects and/or patients with gait impairments, to allow the validation of the solutions proposed in this thesis for the following different situations:

- **Identification of healthy subjects over time**: investigate if our method proposed for human identification can be used for identifying healthy subjects over time. The results of this study can help to better understand the reasons of the decrease in overall accuracy observed for PD patients, when comparing the use of data from a new acquisition session and the same session for identification (Chapter 7).
- **Gait assessment support in PD:** extend the preliminary studies on the use of an RGB-D camera supporting the clinical gait assessment of PD patients treated with DBS (Chapter 3). It would be interesting to explore the use of machine learning techniques together with gait information to obtain a model that provides the probability of a patient belonging to each one of three different groups (healthy subjects, PD patients in Stim-on state, and PD patients in Stim-off state). It would also be interesting to confirm the obtained results regarding the estimation of UPDRS scores and further investigate if those results can be improved, by considering other gait parameters or the use of DTW to obtain a similarity measure between gait patterns.

- **Automated gait analysis for subjects with gait impairments**: evaluate the validity of the activity recognition solution and the gait parameters provided by our automated gait analysis solution, when considering patients with diseases that can affect the gait, such as PD and TTR-FAP.

There are also new research directions that can be explored in the context of motor function assessment, including the following:

- **Integration of multimodal data:** develop solutions for representing, integrating, persisting and querying the available multimodal data (e.g., personal, clinical and quantitative data). A possibility is to rely on ontologies and/or graph databases, which also enable the addition of new data (e.g., new sensors for motion quantification, motor tasks, quantitative and clinical information) if necessary.
- **Extraction of new knowledge from the multimodal data:** explore the use of machine learning techniques to obtain new information from the multimodal data described above for a group of patients, such as the best treatment or the most adequate rehabilitation exercises for a given patient, considering the previous treatment or rehabilitation outcomes. This new knowledge can further help the physicians in their decisions during patient follow-up.
- **Support the assessment of other motor functions besides gait:** provide support to the assessment of other motor tasks (e.g., exercises involving the arms and/or legs), posture and/or balance, facial expression and speech, relying on the same Kinect sensor used for gait analysis. New sensors could also be used to enable the analysis of more fine-grained movements involving the hands/fingers (e.g., opening and closing the hands, pronation-supination movements of the hands, tremor of the hands, and finger tapping). Some sensors that could be appropriate for analysing these movements are other vision-based sensors that specifically tracks hands/fingers (e.g., Leap Motion sensor [254]), wearables sensors (e.g., accelerometer, gyroscope) and/or the touchscreen of smart devices (e.g., smartphone, smartwatch).

The solutions and sensors described above could be integrated into the system presented in this thesis, to enhance the support to clinical assessment of motor function and patient follow-up.

An aspect that may need to be taken into account in the future is the extension of our system so it can be used with other RGB-D cameras besides the Kinect, due to the discontinuation of this camera. The alternative suggested by Microsoft [255] for developers that have worked with the Kinect are the Intel's RealSense depth cameras [157]. Other alternatives include the VicoVR [158], Orbbec cameras [159], and Stereolabs' ZED camera [160]. There is also the possibility of using a

new generation of the Kinect, which has been announced as part of the Project Kinect for Azure [256]. The major necessary changes or additions to our system would be related to the connection between the new camera and the computer, as well as the processing of the data provided by the new camera for data acquisition/visualization. As long as the position of the body joints that we use for gait analysis can be obtained, no modifications are required to our automated gait analysis solution.

With the current technological advances, we envision the use of only a smartphone to support the assessment of various motor tasks, including gait. There are already a number of smartphones that include a depth camera [257-259], but its use is usually limited to facial recognition or blurring the background of a photograph. Recently, Vivo announced they are developing 3-D sensing technology for smartphones based on the time-of-flight technique (same approach used in the second version of the Kinect) [260], which enables the 3-D mapping of objects located up to a distance of 3 m. A smartphone with this capability can potentially be used to visualize and acquire full-body 3-D motion data, carry out motion analysis, and access the current and previous assessment results, using a single device that we carry with us on a daily basis. Another advantage of using a smartphone is that it also includes other sensors (e.g., microphone, accelerometer, and gyroscope) that can be used to complement the motor function assessment of a subject.

References

[1] J. K. Aggarwal and L. Xia, "Human activity recognition from 3D data: A review," *Pattern Recognition Letters,* vol. 48, pp. 70-80, Oct. 2014.

[2] O. D. Lara and M. A. Labrador, "A survey on human activity recognition using wearable sensors," *IEEE Communications Surveys & Tutorials,* vol. 15, pp. 1192-1209, Nov. 2013.

[3] L. Chen, J. Hoey, C. D. Nugent, D. J. Cook, and Z. Yu, "Sensor-based activity recognition," *IEEE Transactions on Systems, Man, and Cybernetics, Part C (Applications and Reviews),* vol. 42, pp. 790-808, Nov. 2012.

[4] L. Lo Presti and M. La Cascia, "3D skeleton-based human action classification: A survey," *Pattern Recognition,* vol. 53, pp. 130-147, May 2016.

[5] M. S. Nixon, T. Tan, and R. Chellappa, *Human Identification Based on Gait* vol. 4. Springer, Boston, MA: Springer, 2006.

[6] D. Gafurov, "A survey of biometric gait recognition: Approaches, security and challenges," in *Annual Norwegian Computer Science Conference,* 2007, pp. 19-21.

[7] N. V. Boulgouris, D. Hatzinakos, and K. N. Plataniotis, "Gait recognition: A challenging signal processing technology for biometric identification," *IEEE Signal Processing Magazine,* vol. 22, pp. 78-90, Nov. 2005.

[8] J. Wang, M. She, S. Nahavandi, and A. Kouzani, "A review of vision-based gait recognition methods for human identification," in *International Conference on Digital Image Computing: Techniques and Applications (DICTA),* Sydney, NSW, Australia, 2010, pp. 320-327.

[9] P. Connor and A. Ross, "Biometric recognition by gait: A survey of modalities and features," *Computer Vision and Image Understanding,* vol. 167, pp. 1-27, Feb. 2018.

[10] A. Parnandi, E. Wade, and M. Matarić, "Motor function assessment using wearable inertial sensors," in *International Conference of the IEEE Engineering in Medicine and Biology Society (EMBC),* Buenos Aires, Argentina, 2010, pp. 86-89.

[11] R. P. Hubble, G. A. Naughton, P. A. Silburn, and M. H. Cole, "Wearable sensor use for assessing standing balance and walking stability in people with Parkinson's disease: A systematic review," *PLoS One,* vol. 10, p. e0123705, Apr. 2015.

[12] K. Otte, B. Kayser, S. Mansow-Model, J. Verrel, F. Paul, A. U. Brandt, *et al.,* "Accuracy and reliability of the Kinect version 2 for clinical measurement of motor function," *PLoS One,* vol. 11, p. e0166532, Nov. 2016.

[13] W. Tao, T. Liu, R. Zheng, and H. Feng, "Gait analysis using wearable sensors," *Sensors,* vol. 12, pp. 2255-2283, Feb. 2012.

[14] S. Springer and G. Yogev Seligmann, "Validity of the Kinect for gait assessment: A focused review," *Sensors,* vol. 16, p. 194, Feb. 2016.

[15] R. A. Clark, Y.-H. Pua, C. C. Oliveira, K. J. Bower, S. Thilarajah, R. McGaw, *et al.,* "Reliability and concurrent validity of the Microsoft Xbox One Kinect for assessment of standing balance and postural control," *Gait & Posture,* vol. 42, pp. 210-213, Jul. 2015.

[16] B. Bonnechere, B. Jansen, P. Salvia, H. Bouzahouene, L. Omelina, F. Moiseev, *et al.,* "Validity and reliability of the Kinect within functional assessment activities: comparison with standard stereophotogrammetry," *Gait & Posture,* vol. 39, pp. 593-598, Jan. 2014.

[17] X. Xu and R. W. McGorry, "The validity of the first and second generation Microsoft Kinect™ for identifying joint center locations during static postures," *Applied Ergonomics,* vol. 49, pp. 47-54, Jul. 2015.

[18] L. Wang, W. Hu, and T. Tan, "Recent developments in human motion analysis," *Pattern Recognition,* vol. 36, pp. 585-601, Mar. 2003.

[19] T. B. Moeslund, A. Hilton, and V. Krüger, "A survey of advances in vision-based human motion capture and analysis," *Computer Vision and Image Understanding,* vol. 104, pp. 90-126, Nov.-Dec. 2006.

[20] D. M. Gavrila, "The visual analysis of human movement: A survey," *Computer Vision and Image Understanding,* vol. 73, pp. 82-98, Jan. 1999.

[21] R. Poppe, "Vision-based human motion analysis: An overview," *Computer Vision and Image Understanding,* vol. 108, pp. 4-18, Oct.-Nov. 2007.

[22] M. W. Whittle, *Gait Analysis: An Introduction*: Butterworth Heinemann Elsevier, 2007.

[23] A. Muro-De-La-Herran, B. Garcia-Zapirain, and A. Mendez-Zorrilla, "Gait analysis methods: An overview of wearable and non-wearable systems, highlighting clinical applications," *Sensors,* vol. 14, pp. 3362-3394, Feb. 2014.

[24] J. Han, L. Shao, D. Xu, and J. Shotton, "Enhanced computer vision with Microsoft Kinect sensor: A review," *IEEE Transactions on Cybernetics,* vol. 43, pp. 1318-1334, Oct. 2013.

[25] S. L. Colyer, M. Evans, D. P. Cosker, and A. I. Salo, "A review of the evolution of vision-based motion analysis and the integration of advanced computer vision methods towards developing a markerless system," *Sports Medicine - Open,* vol. 4, p. 24, Jun. 2018.

[26] J. P. S. Cunha, L. M. Paula, V. F. Bento, C. Bilgin, E. Dias, and S. Noachtar, "Movement quantification in epileptic seizures: A feasibility study for a new 3D approach," *Medical Engineering & Physics,* vol. 34, pp. 938-945, Sep. 2012.

[27] J. P. S. Cunha, C. Vollmar, J. M. Fernandes, and S. Noachtar, "Automated epileptic seizure type classification through quantitative movement analysis," in *World Congress on Medical Physics and Biomedical Engineering,* Munich, Germany, 2009, pp. 1435-1438.

[28] J. S. Cunha, C. Vollmar, Z. Li, J. Fernandes, B. Feddersen, and S. Noachtar, "Movement quantification during epileptic seizures: A new technical contribution to the evaluation of seizure semiology," in *International Conference of the IEEE Engineering in Medicine and Biology Society (EMBC),* Cancun, Mexico, 2003, pp. 671-673.

[29] Z. Li, A. M. da Silva, and J. P. S. Cunha, "Movement quantification in epileptic seizures: A new approach to video-EEG analysis," *IEEE Transactions on Biomedical Engineering,* vol. 49, pp. 565-573, Jun. 2002.

[30] J. Rémi, J. P. S. Cunha, C. Vollmar, Ö. B. Topçuoğlu, A. Meier, S. Ulowetz, *et al.*, "Quantitative movement analysis differentiates focal seizures characterized by automatisms," *Epilepsy & Behavior,* vol. 20, pp. 642-647, Apr. 2011.

[31] J. M. Fernandes, S. Tafula, and J. P. S. Cunha, "3D-Video-fMRI: 3D motion tracking in a 3T MRI environment," in *Image Analysis and Recognition*. vol. 6754, M. Kamel and A. Campilho, Eds., ed: Springer-Verlag Berlin Heidelberg, 2011, pp. 59-67.

[32] V. F. Bento, V. T. Cruz, D. D. Ribeiro, and J. P. S. Cunha, "Towards a movement quantification system capable of automatic evaluation of upper limb motor function after neurological injury," in *International Conference of the IEEE Engineering in Medicine and Biology Society (EMBC),* 2011, pp. 5456-5460.

[33] M. F. M. Colunas, J. M. A. Fernandes, I. C. Oliveira, and J. P. S. Cunha, "Droid Jacket: Using an Android based smartphone for team monitoring," in *7th International Wireless Communications and Mobile Computing Conference (IWCMC),* 2011, pp. 2157-2161.

[34] D. M. D. Ribeiro, M. F. M. Colunas, F. A. F. Marques, J. M. Fernandes, and J. P. S. Cunha, "A real time, wearable ECG and continous blood pressure monitoring system for first responders," in *International Conference of the IEEE Engineering in Medicine and Biology Society (EMBC),* 2011, pp. 6894-6898.

[35] D. C. Teles, M. F. M. Colunas, J. M. Fernandes, I. C. Oliveira, and J. P. S. Cunha, "iVital: A Real Time Monitoring System for First Response Teams," in *Mobile Networks and Management*, K. Pentikousis, R. Aguiar, S. Sargento, and R. Agüero, Eds., ed: Springer, 2012, pp. 396-404.

[36] A. P. Rocha, O. Pereira, D. Ribeiro, J. M. Fernandes, and J. P. Silva Cunha, "MonitorMe: Online video monitoring for first responders using a smartphone," in *IEEE International Conference on e-Health Networking, Applications & Services (Healthcom)*, Lisbon, Portugal, 2013, pp. 731-733.

[37] J. P. S. Cunha, B. Cunha, A. S. Pereira, W. Xavier, N. Ferreira, and L. Meireles, "Vital-Jacket®: A wearable wireless vital signs monitor for patients' mobility in cardiology and sports," in *International Conference on Pervasive Computing Technologies for Healthcare*, Munich, Germany, 2010, pp. 1-2.

[38] J. Sung, C. Ponce, B. Selman, and A. Saxena, "Unstructured human activity detection from RGBD images," presented at the IEEE International Conference on Robotics and Automation, Saint Paul, MN, USA, 2012.

[39] D. R. Faria, C. Premebida, and U. Nunes, "A probabilistic approach for human everyday activities recognition using body motion from RGB-D images," in *IEEE International Symposium on Robot and Human Interactive Communication*, Edinburgh, UK, 2014, pp. 732-737.

[40] A. A. Chaaraoui, J. R. Padilla-López, P. Climent-Pérez, and F. Flórez-Revuelta, "Evolutionary joint selection to improve human action recognition with RGB-D devices," *Expert Systems with Applications*, vol. 41, pp. 786-794, Feb. 2014.

[41] S. Gaglio, G. L. Re, and M. Morana, "Human activity recognition process using 3-D posture data," *IEEE Transactions on Human-Machine Systems*, vol. 45, pp. 586-597, Oct. 2015.

[42] C. Zhang and Y. Tian, "RGB-D camera-based daily living activity recognition," *Journal of Computer Vision and Image Processing*, vol. 2, p. 12, 2012.

[43] J. Lei, X. Ren, and D. Fox, "Fine-grained kitchen activity recognition using RGB-D," in *ACM Conference on Ubiquitous Computing*, Pittsburgh, PA, USA, 2012, pp. 208-211.

[44] X. Yang and Y. Tian, "Effective 3D action recognition using EigenJoints," *Journal of Visual Communication and Image Representation*, vol. 25, pp. 2-11, Jan. 2014.

[45] V. Bloom, D. Makris, and V. Argyriou, "G3D: A gaming action dataset and real time action recognition evaluation framework," in *IEEE Computer Society Conference on Computer Vision and Pattern Recognition Workshops*, Providence, RI, USA, 2012, pp. 7-12.

[46] W. Li, Z. Zhang, and Z. Liu, "Action recognition based on a bag of 3D points," in *IEEE Computer Society Conference on Computer Vision and Pattern Recognition - Workshops*, San Francisco, CA, USA, 2010, pp. 9-14.

[47] J. Zhang, W. Li, P. O. Ogunbona, P. Wang, and C. Tang, "RGB-D-based action recognition datasets: A survey," *Pattern Recognition*, vol. 60, pp. 86-105, Dec. 2016.

[48] H. S. Koppula, R. Gupta, and A. Saxena, "Learning human activities and object affordances from RGB-D videos," *The International Journal of Robotics Research*, vol. 32, pp. 951-970, Jul. 2013.

[49] M. Munaro, G. Ballin, S. Michieletto, and E. Menegatti, "3D flow estimation for human action recognition from colored point clouds," *Biologically Inspired Cognitive Architectures*, vol. 5, pp. 42-51, Jul. 2013.

[50] B. Ni, W. Gang, and P. Moulin, "RGBD-HuDaAct: A color-depth video database for human daily activity recognition," in *IEEE International Conference on Computer Vision Workshops (ICCV Workshops)*, Barcelona, Spain, 2011, pp. 1147-1153.

[51] I. Theodorakopoulos, D. Kastaniotis, G. Economou, and S. Fotopoulos, "Pose-based human action recognition via sparse representation in dissimilarity space," *Journal of Visual Communication and Image Representation*, vol. 25, pp. 12-23, Jan. 2014.

[52] J. Wang, Z. Liu, Y. Wu, and J. Yuan, "Mining actionlet ensemble for action recognition with depth cameras," in *IEEE Conference on Computer Vision and Pattern Recognition*, Providence, RI, USA, 2012, pp. 1290-1297.

[53] L. Xia, C. Chen, and J. K. Aggarwal, "View invariant human action recognition using histograms of 3D joints," in *IEEE Computer Society Conference on Computer Vision and Pattern Recognition Workshops*, Providence, RI, USA, 2012, pp. 20-27.

[54] T.-L. Le and M.-Q. Nguyen, "Human posture recognition using human skeleton provided by Kinect," in *International Conference on Computing, Management and Telecommunications*, Ho Chi Minh City, Vietnam, 2013, pp. 340-345.

[55] E. E. Stone and M. Skubic, "Passive in-home measurement of stride-to-stride gait variability comparing vision and Kinect sensing," in *International Conference of the IEEE Engineering in Medicine and Biology Society (EMBC)*, Boston, MA, USA, 2011, pp. 6491-6494.

[56] M. Gabel, R. Gilad-Bachrach, E. Renshaw, and A. Schuster, "Full body gait analysis with Kinect," in *International Conference of the IEEE Engineering in Medicine and Biology Society (EMBC)*, San Diego, CA, USA, 2012, pp. 1964-1967.

[57] R. A. Clark, K. J. Bower, B. F. Mentiplay, K. Paterson, and Y.-H. Pua, "Concurrent validity of the Microsoft Kinect for assessment of spatiotemporal gait variables," *Journal of Biomechanics*, vol. 46, pp. 2722-2725, Aug. 2013.

[58] J. Cancela, M. T. Arredondo, and O. Hurtado, "Proposal of a Kinect™-based system for gait assessment and rehabilitation in Parkinson's disease," in *International Conference of the IEEE Engineering in Medicine and Biology Society (EMBC)*, Chicago, IL, USA, 2014, pp. 4519-4522.

[59] E. Auvinet, F. Multon, C.-E. Aubin, J. Meunier, and M. Raison, "Detection of gait cycles in treadmill walking using a Kinect," *Gait & Posture*, vol. 41, pp. 722-725, Feb. 2015.

[60] X. Xu, R. W. McGorry, L.-S. Chou, J.-h. Lin, and C.-c. Chang, "Accuracy of the Microsoft Kinect™ for measuring gait parameters during treadmill walking," *Gait & Posture*, vol. 42, pp. 145-151, Jul. 2015.

[61] D. J. Geerse, B. H. Coolen, and M. Roerdink, "Kinematic validation of a multi-Kinect v2 instrumented 10-meter walkway for quantitative gait assessments," *PLoS One*, vol. 10, p. e0139913, Oct. 2015.

[62] B. Müller, W. Ilg, M. A. Giese, and N. Ludolph, "Validation of enhanced Kinect sensor based motion capturing for gait assessment," *PLoS One*, vol. 12, p. e0175813, Apr. 2017.

[63] M. Eltoukhy, J. Oh, C. Kuenze, and J. Signorile, "Improved kinect-based spatiotemporal and kinematic treadmill gait assessment," *Gait & Posture*, vol. 51, pp. 77-83, Jan. 2017.

[64] B. F. Mentiplay, L. G. Perraton, K. J. Bower, Y.-H. Pua, R. McGaw, S. Heywood, *et al.*, "Gait assessment using the Microsoft Xbox One Kinect: Concurrent validity and inter-day reliability of spatiotemporal and kinematic variables," *Journal of Biomechanics*, vol. 48, pp. 2166-2170, Jul. 2015.

[65] A. Pfister, A. M. West, S. Bronner, and J. A. Noah, "Comparative abilities of Microsoft Kinect and Vicon 3D motion capture for gait analysis," *Journal of Medical Engineering & Technology*, vol. 38, pp. 274-280, May 2014.

[66] A. Nambiar, A. Bernardino, J. C. Nascimento, and A. Fred, "Towards view-point invariant person re-identification via fusion of anthropometric and gait features from Kinect measurements," in *International Joint Conference on Computer Vision, Imaging and Computer Graphics Theory and Applications (VISIGRAPP)*, Porto, Portugal, 2017, pp. 108-119.

[67] F. Ahmed, P. P. Paul, and M. L. Gavrilova, "DTW-based kernel and rank-level fusion for 3D gait recognition using Kinect," *The Visual Computer*, vol. 31, pp. 915-924, Jun. 2015.

[68] E. Gianaria, M. Grangetto, and N. Balossino, "Kinect-based gait analysis for people recognition over time," in *Image Analysis and Processing - ICIAP 2017*, S. Battiato, G. Gallo, R. Schettini, and F. Stanco, Eds., ed: Springer, 2017, pp. 648-658.

[69] S. Jiang, Y. Wang, Y. Zhang, and J. Sun, "Real time gait recognition system based on Kinect skeleton feature," in *Computer Vision - ACCV 2014 Workshops*, C. V. Jawahar and S. Shan, Eds., ed: Springer, 2015, pp. 46-57.

[70] J. Preis, M. Kessel, M. Werner, and C. Linnhoff-Popien, "Gait recognition with Kinect," in *International Workshop on Kinect in Pervasive Computing*, New Castle, UK, 2012, pp. P1-P4.

[71] M. W. Rahman and M. L. Gavrilova, "Kinect gait skeletal joint feature-based person identification," in *IEEE International Conference on Cognitive Informatics & Cognitive Computing (ICCI*CC)*, Oxford, UK, 2017, pp. 423-430.

[72] V. O. Andersson and R. M. Araujo, "Full body person identification using the Kinect sensor," in *IEEE International Conference on Tools with Artificial Intelligence (ICTAI)*, Limassol, Cyprus, 2014, pp. 627-633.

[73] A. Sinha, K. Chakravarty, and B. Bhowmick, "Person identification using skeleton information from Kinect," in *International Conference on Advances in Computer-Human Interactions*, Nice, France, 2013, pp. 101-108.

[74] A. Ball, D. Rye, F. Ramos, and M. Velonaki, "Unsupervised clustering of people from 'skeleton' data," in *Annual ACM/IEEE International Conference on Human-Robot Interaction*, Boston, Massachusetts, USA, 2012, pp. 225-226.

[75] M. Milovanovic, M. Minovic, and D. Starcevic, "Walking in colors: Human gait recognition using Kinect and CBIR," *IEEE MultiMedia*, vol. 20, pp. 28-36, Oct.-Dec. 2013.

[76] A. P. Rocha, H. M. P. Choupina, M. d. C. Vilas-Boas, J. M. Fernandes, and J. P. S. Cunha, "System for automatic gait analysis based on a single RGB-D camera," *PLoS One*, vol. 13, p. e0201728, Aug. 2018.

[77] A. P. Rocha, J. M. Fernandes, H. M. P. Choupina, M. d. C. Vilas-Boas, and J. P. S. Cunha, "Subject Identification Based on Gait Using a RGB-D Camera," in *Conference on Soft Computing and Pattern Recognition*, Porto, Portugal, 2018 (forthcoming).

[78] J. P. S. Cunha, A. P. Rocha, H. M. P. Choupina, J. M. Fernandes, M. J. Rosas, R. Vaz, *et al.*, "A novel portable, low-cost Kinect-based system for motion analysis in neurological diseases," in *International Conference of the IEEE Engineering in Medicine and Biology Society (EMBC)*, Orlando, Florida, USA, 2016, pp. 2339-2342.

[79] J. P. S. Cunha, A. P. Rocha, H. Choupina, J. M. Fernandes, M. J. Rosas, and R. Vaz, "Sistema de quantificação 3D de movimento portátil e de baixo custo para estimativa do sub-score de marcha em doentes parkisónicos," *Sinapse*, vol. 14, p. 67, May 2014.

[80] A. P. Rocha, H. Choupina, J. M. Fernandes, M. J. Rosas, R. Vaz, and J. P. S. Cunha, "Estimativa do sub-score UPDRS de marcha em doentes parkinsónicos usando um sistema de quantificação 3D de movimento portátil e de baixo custo," in *Congresso Nacional da Sociedade Portuguesa de Neurocirurgia*, Lisbon, Portugal, 2014, p. 20.

[81] A. P. Rocha, H. Choupina, J. M. Fernandes, M. J. Rosas, R. Vaz, and J. P. S. Cunha, "Parkinson's disease assessment based on gait analysis using an innovative RGB-D camera system," in *International Conference of the IEEE Engineering in Medicine and Biology Society (EMBC)*, Chicago, IL, USA, 2014, pp. 3126 - 3129.

[82] A. P. Rocha, H. Choupina, J. M. Fernandes, M. J. Rosas, R. Vaz, and J. P. S. Cunha, "Quantificação de movimento para apoio ao diagnóstico da doença de Parkinson utilizando um sistema de baixo custo baseado em RGB-D," *Sinapse*, vol. 15, p. 64, May 2015.

[83] A. P. Rocha, H. Choupina, J. M. Fernandes, M. J. Rosas, R. Vaz, and J. P. S. Cunha, "Kinect v2 based system for Parkinson's disease assessment," in *International Conference of the IEEE Engineering in Medicine and Biology Society (EMBC)*, Milan, Italy, 2015, pp. 1279-1282.

[84] M. J. Rosas, J. P. S. Cunha, A. Rocha, H. Choupina, J. M. Fernandes, and R. Vaz, "Movement quantification for evaluation of gait in Parkinson's disease using a RGB-D camera system," *Movement Disorders*, vol. 30, pp. S470-471, Jun. 2015.

[85] M. d. C. Vilas-Boas, A. P. Rocha, H. M. P. Choupina, J. M. Fernandes, T. Coelho, and J. P. S. Cunha, "The first Transthyretin Familial Amyloid Polyneuropathy gait quantification study - Preliminary results," in *International Conference of the IEEE Engineering in Medicine and Biology Society (EMBC)*, Seogwipo, Jeju Island, South Korea, 2017, pp. 1368-1371.

[86] J. P. S. Cunha, H. M. P. Choupina, A. P. Rocha, J. M. Fernandes, F. Achilles, A. M. Loesch, *et al.*, "NeuroKinect: A novel low-cost 3Dvideo-EEG system for epileptic seizure motion quantification," *PLoS One*, vol. 11, p. e0145669, Jan. 2016.

[87] H. M. P. Choupina, A. P. Rocha, J. M. Fernandes, C. Vollmar, S. Noachtar, and J. P. S. Cunha, "NeuroKinect 3.0: Multi-Bed 3Dvideo-EEG System for Epilepsy Clinical Motion Monitoring," in *Building Continents of Knowledge in Oceans of Data: The Future of Co-Created eHealth*, D. K. Adrien Ugon, Gunnar O. Klein, Anne Moen, Ed., ed: IOS Press, 2018, pp. 46-50.

[88] R. Klette and G. Tee, "Understanding human motion: A historic review," in *Human Motion: Understanding, Modelling, Capture, and Animation*, B. Rosenhahn, R. Klette, and D. Metaxas, Eds., ed: Springer, 2008, pp. 1-22.

[89] B. Deng, "Motion studies: See how they run," *Nature*, vol. 525, pp. 145-146, Sep. 2015.

[90] M. Ye, Q. Zhang, L. Wang, J. Zhu, R. Yang, and J. Gall, "A survey on human motion analysis from depth data," in *Time-of-Flight and Depth Imaging. Sensors, Algorithms, and Applications: Dagstuhl 2012 Seminar on Time-of-Flight Imaging and GCPR 2013 Workshop on Imaging New Modalities*, M. Grzegorzek, C. Theobalt, R. Koch, and A. Kolb, Eds., ed: Springer, 2013, pp. 149-187.

[91] L. Chen, H. Wei, and J. Ferryman, "A survey of human motion analysis using depth imagery," *Pattern Recognition Letters*, vol. 34, pp. 1995-2006, Nov. 2013.

[92] L. Mündermann, S. Corazza, A. M. Chaudhari, T. P. Andriacchi, A. Sundaresan, and R. Chellappa, "Measuring human movement for biomechanical applications using markerless motion capture," *Proceedings SPIE 6056, Three-Dimensional Image Capture and Applications VII*, vol. 6056, p. 60560R, 2006.

[93] Y. C. Fung, *Biomechanics: Mechanical Properties of Living Tissues*: Springer, 1993.

[94] J. D. Humphrey and S. L. O'Rourke, *An Introduction to Biomechanics: Solids and Fluids, Analysis and Design*: Springer, 2016.

[95] T.-W. Lu and C.-F. Chang, "Biomechanics of human movement and its clinical applications," *The Kaohsiung Journal of Medical Sciences*, vol. 28, pp. S13-S25, Feb. 2012.

[96] D. F. L. Southgate, J. A. I. Prinold, and R. A. Weinert-Aplin, "Motion analysis in sport," in *Sports Innovation, Technology and Research*, D. F. L. S. P. R. N. Childs and A. M. J. Bull, Eds., ed: World Scientific, 2016, pp. 3-30.

[97] S. Albiol-Pérez, J. Lozano-Quilis, H. Gil-Gómez, J. Gil-Gómez, and R. Llorens, "Virtual rehabilitation system for people with Parkinson's disease," in *International Conference on Disability, Virtual Reality and Associated Technologies*, Laval, France, 2012, pp. 423-427.

[98] M. Capecci, M. G. Ceravolo, F. Ferracuti, S. Iarlori, S. Longhi, L. Romeo, *et al.*, "Accuracy evaluation of the Kinect v2 sensor during dynamic movements in a rehabilitation scenario," in *International Conference of the IEEE Engineering in Medicine and Biology Society (EMBC)*, Orlando, FL, USA, 2016, pp. 5409-5412.

[99] Y.-J. Chang, S.-F. Chen, and J.-D. Huang, "A Kinect-based system for physical rehabilitation: A pilot study for young adults with motor disabilities," *Research in Developmental Disabilities*, vol. 32, pp. 2566-2570, Nov.-Dec. 2011.

[100] M. E. Nixon, A. M. Howard, and Y.-P. Chen, "Quantitative evaluation of the Microsoft Kinect™ for use in an upper extremity virtual rehabilitation environment," in *International Conference on Virtual Rehabilitation (ICVR)*, Philadelphia, PA, USA, 2013, pp. 222-228.

[101] S. Patel, R. Hughes, T. Hester, J. Stein, M. Akay, J. G. Dy, *et al.*, "A novel approach to monitor rehabilitation outcomes in stroke survivors using wearable technology," *Proceedings of the IEEE*, vol. 98, pp. 450-461, Mar. 2010.

[102] M. d. C. Vilas-Boas and J. P. S. Cunha, "Movement quantification in neurological diseases: Methods and applications," *IEEE Reviews in Biomedical Engineering*, vol. 9, pp. 15-31, Mar. 2016.

[103] V. M. Manghisi, A. E. Uva, M. Fiorentino, V. Bevilacqua, G. F. Trotta, and G. Monno, "Real time RULA assessment using Kinect v2 sensor," *Applied Ergonomics*, vol. 65, pp. 481-491, Nov. 2017.

[104] M. Mubashir, L. Shao, and L. Seed, "A survey on fall detection: Principles and approaches," *Neurocomputing,* vol. 100, pp. 144-152, Jan. 2013.

[105] Y. Xinguo, "Approaches and principles of fall detection for elderly and patient," in *International Conference on e-health Networking, Applications and Services (HealthCom),* Singapore, 2008, pp. 42-47.

[106] Z. Bian, J. Hou, L. Chau, and N. Magnenat-Thalmann, "Fall detection based on body part tracking using a depth camera," *IEEE Journal of Biomedical and Health Informatics,* vol. 19, pp. 430-439, Mar. 2015.

[107] P. Colagiorgio, F. Romano, F. Sardi, M. Moraschini, A. Sozzi, M. Bejor, *et al.*, "Affordable, automatic quantitative fall risk assessment based on clinical balance scales and Kinect data," in *International Conference of the IEEE Engineering in Medicine and Biology Society (EMBC)*, Chicago, IL, USA, 2014, pp. 3500-3503.

[108] A. Bourke, J. O'Brien, and G. Lyons, "Evaluation of a threshold-based tri-axial accelerometer fall detection algorithm," *Gait & Posture,* vol. 26, pp. 194-199, Jul. 2007.

[109] E. E. Stone and M. Skubic, "Evaluation of an inexpensive depth camera for passive in-home fall risk assessment," in *International Conference on Pervasive Computing Technologies for Healthcare (PervasiveHealth) and Workshops*, Dublin, Ireland, 2011, pp. 71-77.

[110] C.-C. Yang and Y.-L. Hsu, "A review of accelerometry-based wearable motion detectors for physical activity monitoring," *Sensors,* vol. 10, pp. 7772-7788, Aug. 2010.

[111] S. Chaudhuri, H. Thompson, and G. Demiris, "Fall detection devices and their use with older adults: A systematic review," *Journal of Geriatric Physical Therapy,* vol. 37, pp. 178-196, Oct.-Dec. 2014.

[112] C. Bregler, "Motion capture technology for entertainment," *IEEE Signal Processing Magazine,* vol. 24, pp. 160-158, Nov. 2007.

[113] A. Menache, *Understanding Motion Capture for Computer Animation and Video Games*: Morgan Kaufmann, 2000.

[114] A. J. Davison, J. Deutscher, and I. D. Reid, "Markerless motion capture of complex full-body movement for character animation," in *Computer Animation and Simulation 2001*, N. Magnenat-Thalmann and D. Thalmann, Eds., ed: Springer, 2001, pp. 3-14.

[115] M. Magdin, "Simple MoCap system for home usage," *International Journal of Interactive Multimedia and Artificial Intelligence,* vol. 4, pp. 80-87, Jun. 2017.

[116] A. Erol, G. Bebis, M. Nicolescu, R. D. Boyle, and X. Twombly, "Vision-based hand pose estimation: A review," *Computer Vision and Image Understanding,* vol. 108, pp. 52-73, Oct. 2007.

[117] S. S. Rautaray and A. Agrawal, "Vision based hand gesture recognition for human computer interaction: A survey," *Artificial Intelligence Review,* vol. 43, pp. 1-54, Jan. 2015.

[118] A. I. Cuesta-Vargas, A. Galán-Mercant, and J. M. Williams, "The use of inertial sensors system for human motion analysis," *Physical Therapy Reviews,* vol. 15, pp. 462-473, Dec. 2010.

[119] J. Shotton, T. Sharp, A. Kipman, A. Fitzgibbon, M. Finocchio, A. Blake, *et al.*, "Real-time human pose recognition in parts from single depth images," *Communications of the ACM,* vol. 56, pp. 116-124, Jan. 2013.

[120] P. J. Figueroa, N. J. Leite, and R. M. L. Barros, "A flexible software for tracking of markers used in human motion analysis," *Computer Methods and Programs in Biomedicine,* vol. 72, pp. 155-165, Oct. 2003.

[121] R. Best and R. Begg, "Overview of movement analysis and gait features," in *Computational Intelligence for Movement Sciences: Neural Networks and Other Emerging Techniques*, ed: IGI Global, 2006, pp. 1-69.

[122] T. B. Moeslund and E. Granum, "A survey of computer vision-based human motion capture," *Computer Vision and Image Understanding,* vol. 81, pp. 231-268, Mar. 2001.

[123] F. Bugané, M. Benedetti, G. Casadio, S. Attala, F. Biagi, M. Manca, *et al.*, "Estimation of spatial-temporal gait parameters in level walking based on a single accelerometer: Validation on normal subjects by standard gait analysis," *Computer Methods and Programs in Biomedicine*, vol. 108, pp. 129-137, Oct. 2012.

[124] B. R. Greene, D. McGrath, R. O'Neill, K. J. O'Donovan, A. Burns, and B. Caulfield, "An adaptive gyroscope-based algorithm for temporal gait analysis," *Medical & Biological Engineering & Computing*, vol. 48, pp. 1251-1260, Dec. 2010.

[125] S. J. M. Bamberg, A. Y. Benbasat, D. M. Scarborough, D. E. Krebs, and J. A. Paradiso, "Gait analysis using a shoe-integrated wireless sensor system," *IEEE Transactions on Information Technology in Biomedicine*, vol. 12, pp. 413-423, Jul. 2008.

[126] A. Leu, D. Ristic-Durrant, and A. Graser, "A robust markerless vision-based human gait analysis system," in *IEEE International Symposium on Computational Intelligence and Informatics*, Timisoara, Romania, 2011, pp. 415-420.

[127] A. Ferrari, M. G. Benedetti, E. Pavan, C. Frigo, D. Bettinelli, M. Rabuffetti, *et al.*, "Quantitative comparison of five current protocols in gait analysis," *Gait & Posture*, vol. 28, pp. 207-216, Feb. 2008.

[128] C. M. O'Connor, S. K. Thorpe, M. J. O'Malley, and C. L. Vaughan, "Automatic detection of gait events using kinematic data," *Gait & Posture*, vol. 25, pp. 469-474, Mar. 2007.

[129] J. Zeni, J. Richards, and J. Higginson, "Two simple methods for determining gait events during treadmill and overground walking using kinematic data," *Gait & Posture*, vol. 27, pp. 710-714, May 2008.

[130] B. D. Hendershot, C. E. Mahon, and A. L. Pruziner, "A comparison of kinematic-based gait event detection methods in a self-paced treadmill application," *Journal of Biomechanics*, vol. 49, pp. 4146-4149, Dec. 2016.

[131] K. E. Webster, J. E. Wittwer, and J. A. Feller, "Validity of the GAITRite® walkway system for the measurement of averaged and individual step parameters of gait," *Gait & Posture*, vol. 22, pp. 317-321, Dec. 2005.

[132] H. B. Menz, M. D. Latt, A. Tiedemann, M. Mun San Kwan, and S. R. Lord, "Reliability of the GAITRite® walkway system for the quantification of temporo-spatial parameters of gait in young and older people," *Gait & Posture*, vol. 20, pp. 20-25, Aug. 2004.

[133] A. L. McDonough, M. Batavia, F. C. Chen, S. Kwon, and J. Ziai, "The validity and reliability of the GAITRite system's measurements: A preliminary evaluation," *Archives of Physical Medicine and Rehabilitation*, vol. 82, pp. 419-425, Mar. 2001.

[134] G. G. Simoneau, "Kinesiology of walking," in *Kinesiology of the Musculoskeletal System: Foundations for Physical Rehabilitation*, D. A. Neumann, Ed., ed, 2010, pp. 627-681.

[135] Kistler. (26 Jan. 2019). *Gait Analysis with Kistler – When Force Measurement Makes All the Difference*. Available: https://www.kistler.com/en/applications/sensor-technology/biomechanics-and-force-plate/gait-analysis/

[136] Bertec. (26 Jan. 2019). *Force Plates*. Available: https://bertec.com/products/force-plates/

[137] AMTI. (26 Jan. 2019). *Force Plate Selection Guide*. Available: https://www.amti.biz/fps-guide.aspx

[138] GAITRite. (26 Jan. 2019). *GAITRite®*. Available: https://www.gaitrite.com/

[139] Tekscan. (26 Jan. 2019). *Versatile Pressure Sensing Mats*. Available: https://www.tekscan.com/pressure-sensing-mats

[140] M. G. Silva, P. V. S. Moreira, and H. M. Rocha, "Development of a low cost force platform for biomechanical parameters analysis," *Research on Biomedical Engineering*, vol. 33, pp. 259-268, Sep. 2017.

[141] J. Nakamura, "Basics of image sensors," in *Image Sensors and Signal Processing for Digital Still Cameras*, J. Nakamura, Ed., ed: CRC Press, 2006, pp. 53-93.

[142] Northern Digital Inc. (26 Jan. 2019). *Optical Measurement Systems*. Available: https://www.ndigital.com/msci/products/

[143] Codamotion. (26 Jan. 2019). *3D Measurement*. Available: https://codamotion.com/3d-measurement/

[144] Vicon. (26 Jan. 2019). *Vicon*. Available: http://www.vicon.com/

[145] OptiTrack. (26 Jan. 2019). *OptiTrack*. Available: https://optitrack.com/

[146] Qualisys. (26 Jan. 2019). *Qualisys*. Available: https://www.qualisys.com/

[147] M. Windolf, N. Götzen, and M. Morlock, "Systematic accuracy and precision analysis of video motion capturing systems—exemplified on the Vicon-460 system," *Journal of Biomechanics*, vol. 41, pp. 2776-2780, Aug. 2008.

[148] A. Castelli, G. Paolini, A. Cereatti, and U. Della Croce, "A 2D markerless gait analysis methodology: Validation on healthy subjects," *Computational and Mathematical Methods in Medicine*, vol. 2015, pp. 1-11, 2015.

[149] A. Napoli, S. Glass, C. Ward, C. Tucker, and I. Obeid, "Performance analysis of a generalized motion capture system using microsoft kinect 2.0," *Biomedical Signal Processing and Control*, vol. 38, pp. 265-280, Sep. 2017.

[150] R. P. Kuster, B. Heinlein, C. M. Bauer, and E. S. Graf, "Accuracy of KinectOne to quantify kinematics of the upper body," *Gait & Posture*, vol. 47, pp. 80-85, Jun. 2016.

[151] B. Galna, G. Barry, D. Jackson, D. Mhiripiri, P. Olivier, and L. Rochester, "Accuracy of the Microsoft Kinect sensor for measuring movement in people with Parkinson's disease," *Gait & Posture*, vol. 39, pp. 1062-1068, Apr. 2014.

[152] Q. Wang, G. Kurillo, F. Ofli, and R. Bajcsy, "Evaluation of pose tracking accuracy in the first and second generations of Microsoft Kinect," in *International Conference on Healthcare Informatics*, Dallas, TX, USA, 2015, pp. 380-389.

[153] J. Beyea, C. A. McGibbon, A. Sexton, J. Noble, and C. O'Connell, "Convergent validity of a wearable sensor system for measuring sub-task performance during the timed up-and-go test," *Sensors*, vol. 17, p. 934, Apr. 2017.

[154] E. Papi, D. Osei-Kuffour, Y.-M. A. Chen, and A. H. McGregor, "Use of wearable technology for performance assessment: A validation study," *Medical Engineering & Physics*, vol. 37, pp. 698-704, Jul. 2015.

[155] H. Lee, S. Cho, J. H. You, and K. Lee, "The concurrent validity of the body center of mass in accelerometric measurement," in *International Conference of the IEEE Engineering in Medicine and Biology Society (EMBC)*, Lyon, France, 2007, pp. 659-661.

[156] M. H. Cole, W. Van Den Hoorn, J. K. Kavanagh, S. Morrison, P. W. Hodges, J. E. Smeathers, *et al.*, "Concurrent validity of accelerations measured using a tri-axial inertial measurement unit while walking on firm, compliant and uneven surfaces," *PLoS One*, vol. 9, p. e98395, May 2014.

[157] Intel. (26 Jan. 2019). *Intel® RealSense™ Technology*. Available: https://click.intel.com/realsense.html

[158] VicoVR. (26 Jan. 2019). *VicoVR*. Available: https://vicovr.com/

[159] Orbbec. (26 Jan. 2019). *Orbbec*. Available: https://orbbec3d.com/

[160] Sterolabs. (26 Jan. 2019). *ZED*. Available: https://www.stereolabs.com/zed/

[161] BBC News. (26 Jan. 2019). *Microsoft Kinect 'fastest-selling device on record'*. Available: https://www.bbc.com/news/business-12697975

[162] J.-F. Hu, W.-S. Zheng, J. Lai, and J. Zhang, "Jointly learning heterogeneous features for RGB-D activity recognition," *IEEE transactions on Pattern Analysis and Machine Intelligence*, vol. 39, pp. 2186-2200, Nov. 2017.

[163] Y. Yang, F. Pu, Y. Li, S. Li, Y. Fan, and D. Li, "Reliability and validity of Kinect RGB-D sensor for assessing standing balance," *IEEE Sensors Journal*, vol. 14, pp. 1633-1638, May 2014.

[164] R. A. Clark, Y.-H. Pua, K. Fortin, C. Ritchie, K. E. Webster, L. Denehy, *et al.*, "Validity of the Microsoft Kinect for assessment of postural control," *Gait & Posture*, vol. 36, pp. 372-377, Jul. 2012.

[165] A. Amini, K. Banitsas, and S. Hosseinzadeh, "A new technique for foot-off and foot contact detection in a gait cycle based on the knee joint angle using microsoft kinect v2," in *IEEE EMBS International Conference on Biomedical & Health Informatics (BHI)*, Orlando, FL, USA, 2017, pp. 153-156.

[166] M. Eltoukhy, C. Kuenze, J. Oh, S. Wooten, and J. Signorile, "Kinect-based assessment of lower limb kinematics and dynamic postural control during the star excursion balance test," *Gait & Posture*, vol. 58, pp. 421-427, Oct. 2017.

[167] L. F. Yeung, K. C. Cheng, C. H. Fong, W. C. C. Lee, and K.-Y. Tong, "Evaluation of the Microsoft Kinect as a clinical assessment tool of body sway," *Gait & Posture*, vol. 40, pp. 532-538, Sep. 2014.

[168] Wired. (26 Jan. 2019). *Microsoft prices Kinect at $150, or $300 with new 4-GB Xbox 360*. Available: https://www.wired.com/2010/07/kinect-price-2/

[169] Microsoft. (26 Jan. 2019). *The future of entertainment starts today as Kinect for Xbox 360 leaps and lands at retailers nationwide*. Available: https://news.microsoft.com/2010/11/04/the-future-of-entertainment-starts-today-as-kinect-for-xbox-360-leaps-and-lands-at-retailers-nationwide/

[170] Microsoft. (26 Jan. 2019). *Kinect for Windows SDK Beta*. Available: https://www.microsoft.com/en-us/research/project/kinect-for-windows-sdk-beta/

[171] Microsoft. (26 Jan. 2019). *Starting February 1, 2012: Use the power of Kinect for Windows to change the world*. Available: http://blogs.msdn.com/b/kinectforwindows/archive/2012/01/09/kinect-for-windows-commercial-program-announced.aspx

[172] Microsoft. (26 Jan. 2019). *Kinect for Windows SDK 1.8 Available With Expanded Capabilities*. Available: https://blogs.windows.com/windowsexperience/2013/09/17/kinect-for-windows-sdk-1-8-available-with-expanded-capabilities/

[173] Engadget. (26 Jan. 2019). *Microsoft's new Kinect is official: larger field of view, HD camera, wake with voice*. Available: https://www.engadget.com/2013/05/21/microsofts-new-kinect-is-official/

[174] PCWorld. (26 Jan. 2019). *Kinect v2 gets a Windows launch date, $200 price tag*. Available: https://www.pcworld.com/article/2450755/kinect-v2-gets-a-windows-launch-date-200-price-tag.html

[175] Lifewire. (26 Jan. 2019). *Kinect Buyer's Guide*. Available: https://www.lifewire.com/kinect-buyers-guide-3562808

[176] Microsoft. (26 Jan. 2019). *Coordinate mapping*. Available: https://msdn.microsoft.com/en-us/library/dn785530.aspx

[177] K. Okada. (26 Jan. 2019). *Kinect for Windows SDK - Programming Guide*. Available: https://www.slideshare.net/katsudream/kinect-for-windows-sdk-programming-guide

[178] Microsoft. (26 Jan. 2019). *Human Interface Guidelines v2.0*. Available: http://download.microsoft.com/download/6/7/6/676611b4-1982-47a4-a42e-4cf84e1095a8/kinecthig.2.0.pdf

[179] Microsoft. (26 Jan. 2019). *Human Interface Guidelines v1.7*. Available: https://download.microsoft.com/download/B/0/7/B070724E-52B4-4B1A-BD1B-05CC28D07899/Human_Interface_Guidelines_v1.7.0.pdf

[180] H. Sarbolandi, D. Lefloch, and A. Kolb, "Kinect range sensing: Structured-light versus time-of-flight Kinect," *Computer Vision and Image Understanding*, vol. 139, pp. 1-20, Oct. 2015.

[181] D. Pagliari and L. Pinto, "Calibration of Kinect for Xbox One and comparison between the two generations of Microsoft sensors," *Sensors*, vol. 15, pp. 27569-27589, Oct. 2015.

[182] Microsoft. (26 Jan. 2019). *The Kinect for Windows v2 sensor and free SDK 2.0 public preview are here*. Available: https://blogs.msdn.microsoft.com/kinectforwindows/2014/07/15/the-kinect-for-windows-v2-sensor-and-free-sdk-2-0-public-preview-are-here/

[183] H. Gonzalez-Jorge, P. Rodríguez-Gonzálvez, J. Martínez-Sánchez, D. González-Aguilera, P. Arias, M. Gesto, *et al.*, "Metrological comparison between Kinect I and Kinect II sensors," *Measurement*, vol. 70, pp. 21-26, Jun. 2015.

[184] A. J. Lees, J. Hardy, and T. Revesz, "Parkinson's disease," *Lancet*, vol. 373, pp. 2055-2066, Jun. 2009.

[185] J. Jankovic, "Parkinson's disease: Clinical features and diagnosis," *Journal of Neurology, Neurosurgery and Psychiatry*, vol. 79, pp. 368-376, Apr. 2008.

[186] C. Ramaker, J. Marinus, A. M. Stiggelbout, and B. J. van Hilten, "Systematic evaluation of rating scales for impairment and disability in Parkinson's disease," *Movement Disorders*, vol. 17, pp. 867-876, Sep. 2002.

[187] J. Parkinson, *An Essay on the Shaking Palsy*. London: Sherwoord, Nelly and Jones, 1817.

[188] L. M. L. de Lau and M. M. B. Breteler, "Epidemiology of Parkinson's disease," *The Lancet Neurology*, vol. 5, pp. 525-535, Jun. 2006.

[189] National Parkinson Foundation. (26 Jan. 2019). *Parkinson's Toolkit*. Available: http://www.toolkit.parkinson.org/

[190] M. C. de Rijk, L. J. Launer, K. Berger, M. M. Breteler, J. F. Dartigues, M. Baldereschi, *et al.*, "Prevalence of Parkinson's disease in Europe: A collaborative study of population-based cohorts," *Neurology*, vol. 54, pp. S21-23, Jun. 2000.

[191] E. R. Dorsey, R. Constantinescu, J. P. Thompson, K. M. Biglan, R. G. Holloway, K. Kieburtz, *et al.*, "Projected number of people with Parkinson disease in the most populous nations, 2005 through 2030," *Neurology*, vol. 68, pp. 384-386, Jan. 2007.

[192] R. Bhidayasiri and D. Tarsy, "Young-onset Parkinson's disease," in *Movement Disorders: A Video Atlas*, ed: Humana Press, 2012, pp. 6-7.

[193] Parkinson's Foundation. (26 Jan. 2019). *Symptoms*. Available: http://www.toolkit.parkinson.org/content/symptoms

[194] Parkinson's Foundation. (26 Jan. 2019). *Gait Disorder*. Available: http://www.toolkit.parkinson.org/node/150

[195] Parkinson's Foundation. (26 Jan. 2019). *Physical Examination*. Available: http://www.toolkit.parkinson.org/node/81

[196] A. J. Hughes, S. E. Daniel, L. Kilford, and A. J. Lees, "Accuracy of clinical diagnosis of idiopathic Parkinson's disease: a clinico-pathological study of 100 cases," *Journal of Neurology, Neurosurgery and Psychiatry*, vol. 55, pp. 181-184, Mar. 1992.

[197] H. Teräväinen, J. Tsui, and D. B. Calne, "Evaluation of Parkinson's Disease," in *Drugs for the Treatment of Parkinson's Disease*. vol. 88, D. B. Calne, Ed., ed: Springer, 1989.

[198] We Move. (26 Jan. 2019). *Unified Parkinson's Disease Rating Scale*. Available: https://img.medscape.com/fullsize/701/816/58977_UPDRS.pdf

[199] Parkinson's Foundation. (26 Jan. 2019). *First Line Meds and Dosing*. Available: http://www.toolkit.parkinson.org/node/85

[200] Parkinson's Foundation. (26 Jan. 2019). *Dyskinesias*. Available: http://www.toolkit.parkinson.org/content/dyskinesias

[201] R. Bhidayasiri and D. Tarsy, "Parkinson's Disease: "On-Off" Phenomenon," in *Movement Disorders: A Video Atlas*, ed: Humana Press, 2012, pp. 14-15.

[202] J. S. Perlmutter and J. W. Mink, "Deep brain stimulation," *Annual Review of Neuroscience*, vol. 29, pp. 229-257, Jul. 2006.

[203] G. Deuschl, C. Schade-Brittinger, P. Krack, J. Volkmann, H. Schäfer, K. Bötzel, *et al.*, "A randomized trial of deep-brain stimulation for Parkinson's disease," *The New England Journal of Medicine*, vol. 355, pp. 896-908, Aug. 2006.

[204] Parkinson's Foundation. (26 Jan. 2019). *Deep Brain Stimulation (DBS)*. Available: http://www.toolkit.parkinson.org/content/deep-brain-stimulation-dbs

[205] S. T. Gancher, "Clinical rating scales," in *Parkinson's disease: Diagnosis and clinical management*, S. A. Factor and W. J. Weiner, Eds., ed New York: Demos Medical Publishing, 2008.

[206] W. H. Kruskal and W. A. Wallis, "Use of ranks in one-criterion variance analysis," *Journal of the American Statistical Association*, vol. 47, pp. 583-621, Apr. 1952.

[207] M. Hollander, D. A. Wolfe, and E. Chicken, *Nonparametric statistical methods*: John Wiley & Sons, 2014.

[208] P. Sprent and N. C. Smeeton, *Applied Nonparametric Statistical Methods*: Chapman and Hall/CRC, 2001.

[209] R Core Team. (26 Jan. 2019). *R: A language and environment for statistical computing*. Available: https://www.r-project.org/

[210] R Core Team. (26 Jan. 2019). *The R Stats Package*. Available: https://stat.ethz.ch/R-manual/R-devel/library/stats/html/stats-package.html

[211] A. Schmitz, M. Ye, R. Shapiro, R. Yang, and B. Noehren, "Accuracy and repeatability of joint angles measured using a single camera markerless motion capture system," *Journal of Biomechanics*, vol. 47, pp. 587-591, Jan. 2014.

[212] P. Cortez, "Data mining with neural networks and support vector machines using the R/rminer tool," in *Advances in Data Mining: Applications and Theoretical Aspects*, P. Perner, Ed., ed: Springer, 2010, pp. 572-583.

[213] Microsoft. (26 Jan. 2019). *Kinect for Windows SDK v1.8*. Available: https://www.microsoft.com/en-us/download/details.aspx?id=40278

[214] Microsoft. (26 Jan. 2019). *Kinect for Windows SDK v2.0*. Available: https://www.microsoft.com/en-us/download/details.aspx?id=44561

[215] Microsoft. (26 Jan. 2019). *FloorClipPlane Property*. Available: https://docs.microsoft.com/en-us/previous-versions/windows/kinect/dn791050%28v%3dieb.10%29

[216] G. Ballin, M. Munaro, and E. Menegatti, "Human action recognition from RGB-D frames based on real-time 3D optical flow estimation," in *Biologically Inspired Cognitive Architectures 2012*, A. Chella, R. Pirrone, R. Sorbello, and K. R. Jóhannsdóttir, Eds., ed: Springer, 2013, pp. 65-74.

[217] M. Firman, "RGBD datasets: Past, present and future," in *IEEE Conference on Computer Vision and Pattern Recognition Workshops*, Las Vegas, NV, USA, 2016, pp. 19-31.

[218] Qualisys. (26 Jan. 2019). *Our motion capture cameras*. Available: https://www.qualisys.com/hardware/

[219] S. B. Kotsiantis, "Supervised machine learning: A review of classification techniques," in *Emerging Artificial Intelligence Applications in Computer Engineering*, I. Maglogiannis, K. Karpouzis, B. A. Wallace, and J. Soldatos, Eds., ed: IOS Press, 2007, pp. 3-24.

[220] K. Hechenbichler and K. Schliep, "Weighted k-nearest-neighbor techniques and ordinal classification," ed, 2004.

[221] K. Hechenbichler and K. Schliep. (26 Jan. 2019). *kknn: Weighted k-nearest neighbors (R package version 1.3.1)*. Available: https://CRAN.R-project.org/package=kknn

[222] R. J. Samworth, "Optimal weighted nearest neighbour classifiers," *The Annals of Statistics*, vol. 40, pp. 2733-2763, 2012.

[223] T. M. Therneau and E. J. Atkinson, "An introduction to recursive partitioning using the RPART routines," Mayo Foundation29 Jun. 2015.

[224] T. Therneau and B. Atkinson. (26 Jan. 2019). *rpart: Recursive partitioning and regression trees (R package version 4.1-13)*. Available: https://CRAN.R-project.org/package=rpart

[225] L. Breiman, J. Friedman, R. A. Olshen, and C. J. Stone, *Classification and Regression Trees*: Chapman & Hall, 1984.

[226] A. Liaw and M. Wiener, "Classification and regression by randomForest," *R news*, vol. 2, pp. 18-22, Dec. 2002.

[227] L. Breiman, "Random forests," *Machine Learning*, vol. 45, pp. 5-32, Oct. 2001.

[228] A. Karatzoglou, D. Meyer, and K. Hornik, "Support vector machines in R," *Journal of Statistical Software*, vol. 15, pp. 1-28, Apr. 2006.

[229] A. Karatzoglou, A. Smola, K. Hornik, and A. Zeileis, "kernlab - An S4 package for kernel methods in R," *Journal of Statistical Software*, vol. 11, pp. 1-20, Nov. 2004.

[230] A. Karatzoglou, A. Smola, and K. Hornik. (26 Jan. 2019). *kernlab: Kernel-based machine learning lab (R package version 0.9-27)*. Available: https://cran.r-project.org/web/packages/kernlab/

[231] J. C. Platt, "Fast training of support vector machines using sequential minimal optimization," in *Advances in Kernel Methods: Support Vector Learning*, B. Schölkopf, C. J. C. Burges, and A. J. Smola, Eds., ed: MIT Press, 1999, pp. 185-208.

[232] W. N. Venables and B. D. Ripley, *Modern Applied Statistics with S*: Springer, 2002.

[233] J. Han, M. Kamber, and J. Pei, *Data Mining: Concepts and Techniques*: Morgan Kaufmann, 2012.

[234] The MathWorks Inc., "MATLAB 2015a," ed. Natick, Massachusetts, United States.

[235] Microsoft. (26 Jan. 2019). *Xbox One Kinect placement*. Available: https://support.xbox.com/en-GB/xbox-one/accessories/positioning-kinect-sensor

[236] Microsoft. (26 Jan. 2019). *More about Kinect sensor placement*. Available: https://support.xbox.com/en-US/xbox-360/accessories/sensor-placement

[237] J. M. Bland and D. Altman, "Statistical methods for assessing agreement between two methods of clinical measurement," *The Lancet*, vol. 327, pp. 307-310, Feb. 1986.

[238] D. Giavarina, "Understanding Bland Altman analysis," *Biochemia Medica*, vol. 25, pp. 141-151, 2015.

[239] J. Ludbrook, "Confidence in Altman–Bland plots: a critical review of the method of differences," *Clinical and Experimental Pharmacology and Physiology*, vol. 37, pp. 143-149, Feb. 2010.

[240] J. M. Bland and D. G. Altman, "Measuring agreement in method comparison studies," *Statistical Methods in Medical Research*, vol. 8, pp. 135-160, Apr. 1999.

[241] T. S. King, V. M. Chinchilli, and J. L. Carrasco, "A repeated measures concordance correlation coefficient," *Statistics in Medicine*, vol. 26, pp. 3095-3113, Jul. 2007.

[242] J. L. Carrasco, B. R. Phillips, J. Puig-Martinez, T. S. King, and V. M. Chinchilli, "Estimation of the concordance correlation coefficient for repeated measures using SAS and R," *Computer Methods and Programs in Biomedicine*, vol. 109, pp. 293-304, Mar. 2013.

[243] L. G. Portney and M. P. Watkins, *Foundations of Clinical Research: Applications to Practice*: F.A. Davis Company, 2015.

[244] J. L. Carrasco and J. P. Martinez. (26 Jan. 2019). *cccrm: Concordance correlation coefficient for repeated (and non-repeated) measures (R package version 1.2.1)*. Available: https://CRAN.R-project.org/package=cccrm

[245] F. d. Mendiburu. (26 Jan. 2019). *agricolae: Statistical procedures for agricultural research (R package version 1.3-0)*. Available: https://CRAN.R-project.org/package=agricolae

[246] J. Fox and S. Weisberg, *An R Companion to Applied Regression*: SAGE, 2011.

[247] R. T. Collins, R. Gross, and S. Jianbo, "Silhouette-based human identification from body shape and gait," in *IEEE International Conference on Automatic Face Gesture Recognition*, Washington, DC, USA, 2002, pp. 366-371.

[248] T. H. W. Lam, K. H. Cheung, and J. N. K. Liu, "Gait flow image: A silhouette-based gait representation for human identification," *Pattern Recognition*, vol. 44, pp. 973-987, Apr. 2011.

[249] L. Wang, T. Tan, H. Ning, and W. Hu, "Silhouette analysis-based gait recognition for human identification," *IEEE Transactions on Pattern Analysis and Machine Intelligence*, vol. 25, pp. 1505-1518, Dec. 2003.

[250] M.-H. Cheng, M.-F. Ho, and C.-L. Huang, "Gait analysis for human identification through manifold learning and HMM," *Pattern Recognition*, vol. 41, pp. 2541-2553, Aug. 2008.

[251] M. Kuhn. (26 Jan. 2019). *caret: Classification and regression training (R package version 6.0-81)*. Available: https://CRAN.R-project.org/package=caret

[252] The MathWorks Inc., "MATLAB and Signal Processing Toolbox 2015a," ed. Natick, Massachusetts, United States.

[253] E. Jones, T. Oliphant, P. Peterson, and others. (26 Jan. 2019). *SciPy: Open source scientific tools for Python*. Available: http://www.scipy.org/

[254] Leap Motion. (26 Jan. 2019). *Leap Motion*. Available: https://www.leapmotion.com/

[255] Microsoft. (26 Jan. 2019). *Kinect for Windows*. Available: https://developer.microsoft.com/en-us/windows/kinect

[256] Microsoft. (26 Jan. 2019). *Project Kinect for Azure*. Available: https://azure.microsoft.com/en-us/campaigns/kinect/

[257] Samsung. (26 Jan. 2019). *Galaxy A9 Specifications*. Available: https://www.samsung.com/global/galaxy/galaxy-a9/specs/

[258] Huawei. (26 Jan. 2019). *Huawei unveils the most powerful AI Quad-Camera smartphone to date: HUAWEI nova 3*. Available: https://consumer.huawei.com/en/press/news/2018/quad-camera-smartphone-nova-3-global-launch/

[259] Apple. (26 Jan. 2019). *iPhone Xs Specifications*. Available: https://www.apple.com/lae/iphone-xs/specs/

[260] The Verge. (26 Jan. 2019). *Vivo Showcases Pioneering TOF 3D Sensing Technology at MWC Shanghai 2018*. Available: https://www.theverge.com/circuitbreaker/2018/6/27/17509036/vivo-faceid-3d-tof-biometrics-mwc-shanghai-2018

Appendix A *KiT* and *KiMA* File Format

This appendix includes the format of the files created by the *KiT* and *KiMA* software applications to store Kinect data, as well as label and event information associated to the data acquisitions.

A.1 File Format for Kinect Data

The file format used to save the Kinect data is presented below, for each Kinect version (v1 and v2) and each data type (colour, infrared, depth and/or 3-D body joint data). The file extension used for each data type is also indicated. Each file includes a header with relevant information, such as the sensor name, resolution, height and tilt angle of the Kinect, depending on the data type. Following the header, there is a line for each data frame, including the corresponding timestamp and the data itself.

Kinect v1 (*KiT* version 2.6.1)

Colour (.kvid extension)

Sensor=*sensorName*;SensorID=*uniqueKinectID*;Version=2.3;KinectSDK=*KinectSDKVersion*
Resolution=*W*x*H*;Tilt=*A*;Height=*KH*
timestamp1>frame1
...
timestampN>frameN

sensorName = Kinect_v1
W = frame width in pixels
H = frame height in pixels
A = Kinect tilt angle
KH = Kinect height (if available)
frame = bytes corresponding to pixel data

Depth (.kdpt extension)

Sensor=*sensorName*;SensorID=*uniqueKinectID*;Version=2.3;KinectSDK=*KinectSDKVersion*
Resolution=*W*x*H*;Tilt=*A*;Height=*KH*
timestamp1>frame1

…
timestampN>frameN

sensor_name = Kinect_v1
W = frame width in pixels
H = frame height in pixels
A = Kinect tilt angle
KH = Kinect height (if available)
frame = bytes corresponding to pixel data (it is necessary to convert them to shorts)

3-D body joint (.kpos extension)

Sensor=*sensorName*;SensorID=*uniqueKinectID*;Version=2.3;KinectSDK=*KinectSDKVersion*
ColorResolution=*W*x*H*;DepthResolution=*W*x*H*;Tilt=*A*;Height=*KH*
timestamp1>frame1
…
timestampN>frameN

sensor_name = Kinect_v1
W = frame width in pixels
H = frame height in pixels
A = Kinect tilt angle
KH = Kinect height (if available)
frame =
skeletonTrackingState;skeletonCenter;skeletonCenterColor;skeletonCenterDepth;clippedEdges;joint1;joint1Color;joint1Depth;joint1TrackingState;…;joint20;joint20Color;joint20Depth;bone1QuaternionAboslute;bone1MatrixAbsolute;bone1QuatenionHierarchical;bone1MatrixHierarchical;…;bone20QuaternionAbsolute;bone20MatrixAbsolute;bone20QuatenionHierarchical;bone20MatrixHierarchical
skeletonTrackingState = “PositionOnly” or “Tracked”
skeletonCenter = [x;y;z]
skeletonCenterColor = [x;y]
skeletonCenterDepth = [x;y]
clippedEdges = “None” or “Top, Bottom, Right, Left” (can be a combination of any of the four)
*joint*N = [x;y;z]
*joint*N*Color* = [x;y]

*joint*N*Depth* = [x;y]

*joint*N*TrackingState* = “Tracked”, “Inferred” or “NotTracked”

*bone*N*QuaternionAbsolute* = [x;y;z;w]

*bone*N*MatrixAbsolute* = [M11;…;M14;M21;…;M24;M31;…;M34;M41;…;M44]

*bone*N*QuatenionHierarchical* = [x;y;z;w]

*bone*N*MatrixHierarchical* = [M11;…;M14;M21;…;M24;M31;…;M34;M41;…;M44]

Kinect v2 (*KiT* version 1.6.0)

Color, Infrared, Depth, and Body Index (.kvid, .kir, .kdpt, .kbi extensions)

Sensor=*sensorName*;SensorID=*uniqueKinectID*;Version=*version*;KinectSDK=*KinectSDKVersion*
Resolution=*W*x*H*;Tilt=*A*;Height=*KH*
timestamp1>frame1
…
timestampN>frameN

sensor_name = Kinect_v2
version = 1.5
W = frame width in pixels
H = frame height in pixels
A = Kinect tilt angle (if available)
KH = Kinect height (if available)
frame = bytes corresponding to pixel data

3-D body joint (.kpos extension)

Sensor=*sensorName*;SensorID=*uniqueKinectID*;Version=*version*;KinectSDK=*KinectSDKVersion*
ColorResolution=*W*x*H*;DepthResolution=*W*x*H*;Tilt=*A*;Height=*KH*
timestamp1>frame1
…
timestampN>frameN

sensor_name = Kinect_v2
version = 1.5
W = frame width in pixels

H = frame height in pixels

A = Kinect tilt angle (if available)

KH = Kinect height (if available)

frame =

isRestricted;*clippedEdges*;*joint1*;*joint1Color*;*joint1Depth*;*joint1TrackingState*;…;*joint25*;*joint25Color*;*joint25Depth*;*bone1Orientation*;…;*bone25Orientation*;*engaged*;*handLeftState*;*handLeftConfidence*;*handRightState*;*handRightConfidence*;*lean*;*leanTrackingState*

isRestricted = 0 (false) or 1 (true)

clippedEdges = "None" or "Top, Bottom, Right, Left" (can be a combination of any of the four)

*joint*N = [x;y;z]

*joint*N*Color* = [x;y]

*joint*N*Depth* = [x;y]

*joint*N*TrackingState* = "Tracked", "Inferred" or "NotTracked"

*bone*N*Orientation* = [x;y;z;w]

engaged = "Unknown", "No", "Maybe", "Yes"

handLeft/RightState = "Unknown", "NotTracked", "Open", "Closed", "Lasso"

handLeft/RightConfidence = 0 (high) or 1 (low)

lean = [x;y] → number between −1 (leaning left or back) and 1 (leaning right or front); leaning left and right corresponds to X movement and leaning forward and back corresponds to Y movement.

leanTrackingState = "Tracked", "Inferred" or "NotTracked"

A.2 File Format for Label and Event Information

KiT and *KiMA* allow the indication/selection of given instants and time intervals for a data acquisition, which are saved as labels and events. The associated information is saved to an XML file, which is generated using the format shown in the following example:


```
<?xml version="1.0" encoding="UTF-8"?>
<Tags>
  <Event>
    <Start>
      <FrameNumber>266</FrameNumber>
      <Timestamp>20160617151131940</Timestamp>
    </Start>
    <End>
      <FrameNumber>358</FrameNumber>
      <Timestamp>20160617151135041</Timestamp>
    </End>
    <Name>Walk front</Name>
  </Event>
  <Label>
    <FrameNumber>293</FrameNumber>
    <Timestamp>20160617151132840</Timestamp>
    <Name>Right heel strike (front)</Name>
  </Label>
  <Label>
    <FrameNumber>309</FrameNumber>
    <Timestamp>20160617151133373</Timestamp>
    <Name>Left heel strike (front)</Name>
  </Label>
  <Label>
    <FrameNumber>326</FrameNumber>
    <Timestamp>20160617151133941</Timestamp>
    <Name>Right heel strike (front)</Name>
  </Label>
  <Label>
    <FrameNumber>297</FrameNumber>
    <Timestamp>20160617151132974</Timestamp>
    <Name>Left toe off (front)</Name>
  </Label>
  <Label>
    <FrameNumber>313</FrameNumber>
    <Timestamp>20160617151133507</Timestamp>
    <Name>Right toe off (front)</Name>
  </Label>
</Tags>
```

Appendix B Study on Interference between Motion Capture Systems

This appendix presents a study on the interference between the three different systems we used in our studies: first version of the Kinect (Kinect v1 – Kv1), second version of the Kinect (Kinect v2 – Kv2) and Qualisys system.

Each Kinect version relies on a different depth sensing method: Kv1 uses a structured light approach, while the Kv2 is based on the time-of-flight principle [180]. Therefore, there should be no interference between them. However, to the best of our knowledge, this has not been verified before. For this reason, we performed a study to ensure that the use of the considered systems simultaneously does not introduce additional noise to the acquired data.

The study was performed using data acquired from five healthy subjects while they stood as still as possible during 5 seconds (three trials per subject), for the following different situations:

1. Only Kv1 switched on;
2. Only Kv2 switched on;
3. Both Kinects switched on (Kv1+Kv2);
4. Both Kinects and Qualisys switched on (Kv1+Kv2+Q).

The subjects corresponded to five of the twenty subjects that participated in the experiment performed for the studies on the validity of the Kinect for gait analysis. The setup was also the same as the one used in that experiment, with the Kinects at a height of 1 m, with a tilt angle of −10 degrees for Kv1 and −5 degrees for Kv2 (KC1). Each subject performed the standing still activity while facing the Kinect, at a distance of approximately 3 m. The time intervals corresponding to the activity of interest were manually selected for each subject and trial, using *KiMA* [78].

For each situation, subject, trial, body joint and axis (x-, y-, and z-axis), we obtained the standard deviation of the joint position provided by Kv1 and/or Kv2. This measure was considered as a measure of noise. The mean and standard deviation of the noise measure, when considering all subjects and trials, are presented in Table B.1 for each body joint (all axes) and all body joints (each axis and all axes).

The obtained results show that the noise of Kv1/Kv2 data does not vary considerably between the different situations: mean value of 4.0–4.4 mm for Kv1 and 4.1–4.6 mm for Kv2 (all joints and all axes). Furthermore, a statistical test (repeated-measures ANOVA) performed over the mean

noise measure values (all joints and all axes) for all subjects showed that there is no statistically significant difference between the three situations (*p*-value > 0.05), for both Kv1 and Kv2.

Table B.1. Mean and standard deviation values for the noise measure computed over Kv1 and Kv2 data acquired from subjects while standing still, with only Kv1/Kv2 switched on, both Kv1 and Kv2 switched on (Kv1+Kv2) and both Kinects and Qualisys system switched on (Kv1+Kv2+Q). The results are presented for each joint (all axes) and all joints (each axis and all axes).

Body segment	Body joint	Axis	Noise measure (mm)[a]					
			Kv1			Kv2		
			Kv1	Kv1+Kv2	Kv1+Kv2+Q	Kv2	Kv1+Kv2	Kv1+Kv2+Q
Trunk	Head		4.1 ± 3.2	3.4 ± 2.4	3.2 ± 2.1	3.7 ± 3.9	2.8 ± 2.1	2.5 ± 1.9
	Neck		2.8 ± 2.0	2.6 ± 1.8	2.7 ± 1.6	3.3 ± 3.5	2.5 ± 1.9	2.3 ± 1.6
	Spine shoulder		—	—	—	3.0 ± 3.3	2.3 ± 1.8	2.2 ± 1.5
	Spine middle		2.0 ± 1.5	2.2 ± 1.9	1.8 ± 1.5	2.4 ± 2.8	1.8 ± 1.6	1.8 ± 1.2
	Spine base		2.0 ± 1.4	2.3 ± 2.1	1.8 ± 1.5	2.0 ± 2.2	1.6 ± 1.3	1.6 ± 1.1
Upper limbs	Left shoulder		2.5 ± 1.6	2.4 ± 1.8	2.7 ± 1.7	2.9 ± 3.0	2.4 ± 1.8	2.2 ± 1.3
	Right shoulder		2.7 ± 1.8	2.9 ± 2.1	2.7 ± 1.8	2.8 ± 3.1	2.4 ± 1.7	2.2 ± 1.4
	Left elbow		3.2 ± 1.7	2.7 ± 1.6	3.2 ± 1.8	2.9 ± 2.7	2.3 ± 1.8	2.4 ± 1.5
	Right elbow		2.5 ± 1.7	2.8 ± 1.7	3.0 ± 1.7	2.9 ± 2.9	2.5 ± 1.4	2.3 ± 1.3
	Left wrist		4.8 ± 2.5	4.8 ± 3.5	5.2 ± 3.8	3.3 ± 2.0	2.8 ± 1.9	2.9 ± 1.4
	Right wrist		3.6 ± 3.3	4.1 ± 3.0	3.7 ± 2.4	4.1 ± 3.0	4.3 ± 4.9	4.2 ± 4.4
	Left hand		6.3 ± 3.6	5.0 ± 2.8	6.9 ± 4.5	5.0 ± 2.1	4.9 ± 3.4	5.0 ± 2.8
	Right hand		6.6 ± 4.7	6.3 ± 3.8	7.1 ± 4.4	5.0 ± 3.0	4.8 ± 3.1	4.9 ± 3.5
	Left hand tip		—	—	—	10.8 ± 2.7	10.6 ± 3.9	10.1 ± 3.1
	Right hand tip		—	—	—	16.9 ± 9.4	15.4 ± 7.9	14.4 ± 8.2
	Left thumb		—	—	—	11.4 ± 4.4	8.5 ± 3.5	10.0 ± 3.9
	Right thumb		—	—	—	14.5 ± 7.6	17.0 ± 8.4	17.0 ± 9.8
Lower limbs	Left hip		2.1 ± 1.4	2.2 ± 2.1	1.8 ± 1.6	2.0 ± 2.2	1.6 ± 1.3	1.7 ± 1.1
	Right hip		2.0 ± 1.3	2.4 ± 2.2	1.8 ± 1.5	2.0 ± 2.2	1.7 ± 1.4	1.7 ± 1.1
	Left knee		3.1 ± 2.4	2.2 ± 1.4	2.3 ± 1.4	1.8 ± 1.4	1.5 ± 0.9	1.4 ± 0.5
	Right knee		2.6 ± 1.8	2.2 ± 1.1	2.5 ± 1.4	1.8 ± 2.0	1.7 ± 0.9	1.7 ± 1.1
	Left ankle		3.8 ± 3.3	3.6 ± 3.2	4.1 ± 3.6	1.8 ± 2.0	1.6 ± 1.2	1.7 ± 1.8
	Right ankle		3.9 ± 2.6	4.0 ± 3.0	3.3 ± 2.2	1.1 ± 0.8	1.1 ± 0.9	1.3 ± 1.2
	Left foot		17.4 ± 8.8	10.4 ± 8.9	11.9 ± 10.1	7.2 ± 10.5	3.8 ± 6.6	1.8 ± 1.8
	Right foot		10.3 ± 7.9	11.0 ± 8.2	9.7 ± 8.1	1.3 ± 0.8	3.1 ± 6.6	3.1 ± 6.0
All		x	2.5 ± 2.2	2.2 ± 1.5	2.5 ± 2.0	3.4 ± 5.5	3.1 ± 5.2	3.4 ± 5.6
		y	5.2 ± 5.9	4.5 ± 5.1	4.6 ± 5.7	4.2 ± 5.3	4.1 ± 5.4	4.1 ± 5.2
		z	5.5 ± 5.5	5.3 ± 4.7	5.0 ± 4.8	6.3 ± 6.3	5.3 ± 5.7	4.7 ± 5.1
		All	4.4 ± 5.0	4.0 ± 4.3	4.1 ± 4.6	4.6 ± 5.8	4.2 ± 5.5	4.1 ± 5.3

[a] The noise measure corresponds to the standard deviation for the joint position. The presented values are the mean and standard deviation of the noise measure when considering all subjects and trials.

These results indicate that there is no interference between the two versions of the Kinect, which was expected due to the use of different depth sensing approaches. Furthermore, there is also no interference between the Kinects and Qualisys system, which is an important result since the data used in some studies presented in this thesis were acquired using the three systems simultaneously.

Although the main aim of this study was to verify whether there is interference between the used systems or not, it also allowed verifying if there is any difference regarding noise between the different body joints tracked by the Kinect, the two Kinect versions and the three axes.

It is interesting to note that the joints at the extremities of the body segments have the most noise: head for the trunk; hands and/or thumbs and hand tips for the upper limbs; and feet for the lower limbs. However, the mean noise values for these joints are not considerably different from the remaining ones, with the exception of the feet for Kv1 and the hand tips and thumbs for Kv2.

The difference among the three axes regarding noise is not considerable (slightly less noise for the x-axis). Furthermore, the noise measure results are similar for the two versions of the Kinect, when considering all joints and axes. However, if only the joints tracked by both versions are considered, the data provided by the Kv2 is less noisy than Kv1 (mean noise measure of 2.4–3.0 mm vs 4.0–4.4 mm). This happens because the hand tips and thumbs, which are only tracked by the Kv2, are the joints that present the highest noise measure value for this sensor (mean of 8.5–17.0 mm). In addition, the lower limb joints have less noise for Kv2 than Kv1 (mean noise measure of 1.1–7.2 mm vs 1.8–17.4 mm).

Appendix C Additional Information Regarding Gait Cycle Detection

This appendix describes the method used to automatically select the time intervals corresponding to walking towards and away from the Kinect, for each gait trial. It also includes the detailed description of the method used to automatically identify the actual gait events relying on Qualisys data.

C.1 Selection of Walking Towards and Away from the Kinect

For each gait trial, the time intervals during which the subject was walking towards and away from the Kinect (WF and WB) were automatically selected taking into account the acquired Kinect data, by carrying out the following steps:

1. Select the frames for which all joints are being tracked or inferred;
2. Considering only the frames selected in step 1, identify the instant when the subject turns around, i.e., the frame for which the distance between the spine middle joint and the Kinect (on the z-axis) is minimum;
3. Considering only the frames before/after (WF/WB) the instant detected in step 2, find the first and last frames for which the number of tracked joints is higher or equal to $N-5$ (N is the total number of joints) and none of the joints are outside the field of view (according to the clipped edges information provided by the Kinect), or all joints are tracked except the head.

C.2 Identification of the Actual Gait Events from Qualisys Data

For the selected WF and WB data, the actual heel strike and toe off events were identified using the left and right feet vertical velocity computed from Qualisys data. For a given frame, the vertical velocity of a joint is computed using the equation $v_y \approx \Delta y/\Delta t$, where Δy is the difference between the joint y-coordinate for the current and previous frames, and Δt is the time elapsed between the same frames.

To aid in the identification of the gait events, we additionally computed the feet velocity using $v \approx \sqrt{\frac{\Delta x^2 + \Delta y^2 + \Delta z^2}{\Delta t^2}}$.

The foot velocity signals were processed using a fourth order zero-lag low-pass Butterworth filter with a cut-off frequency of 8 Hz, with the aim of removing some noise that could make it more difficult to correctly detect the considered events. The cut-off frequency value of the filter was chosen by taking into account the frequency content of the signals.

Taking into account the findings of O'Connor et al. [128], left/right heel strikes were identified by performing the following steps:

1. Find the local minima of the left/right foot vertical velocity (using the "findpeaks" Matlab function over the negative signal);
2. For each local minimum, it was considered as an actual heel strike if all the following conditions are met:
    a. The vertical velocity of the considered foot is less than or equal to the vertical velocity of the opposite foot;
    b. The absolute difference between the vertical velocity of both feet is greater than or equal to 0.1 m/s;
    c. The velocity of the considered foot is greater than or equal to the velocity of the opposite foot;
    d. The velocity of the considered foot is less than or equal to 2 m/s;
    e. The acceleration of the considered foot (computed from the foot velocity considering the current frame i and frame i+15) is non-positive;
    f. The difference between the ankle distance for the current frame i and frame $i-25$ is non-negative.

The left/right toe offs were identified by performing the following steps:

1. Find the local maxima of the left/right foot vertical velocity (using the "findpeaks" Matlab function);
2. For each local maximum, it corresponds to an actual toe off if all the following conditions are met:

a. The vertical velocity of the considered foot is greater than or equal to the vertical velocity of the opposite foot;

b. The velocity of the considered foot is greater than or equal to the velocity of the opposite foot;

c. The vertical velocity of the considered foot is greater than or equal to 0.2 m/s;

d. The difference between the ankle distance for consecutive frames between frames $i-5$ and $i+5$, where i is the number of the current frame, is non-positive.

Even after filtering the feet vertical velocity signal, there was still some noise for some trials, which led to the identification of two toe off events instead of just one. Therefore, if the time interval between two consecutive identified toe offs was lower than or equal to 0.25 s (approximately half the mean step duration for healthy subjects – see Appendix G), they were both ignored.

Appendix D Window Size Selection for Gait Cycle Detection

This appendix includes the results obtained for different sizes for the windows used to detect gait cycles, including the estimation of heel strike instants, identification of the heel strike side and estimation of toe off instants. The results obtained for Kinect v1 (Kv2) and Kinect v2 (Kv2) and for WF and WB trials, using configuration KC1, are presented in Tables D.1 to D.12. The results obtained for Kv2 and WF trials, using configurations KC1, KC2 and KC3, are presented in Tables D.13 to D.21. For each table, the results corresponding to the chosen window size are indicated in bold.

D.1 Results for Both Kinect Versions and Walking Activities

Kv1 and WF (KC1, 10 trials)

Table D.1. Results for heel strike instant estimation when using Kv1 and WF data (KC1, 10 trials), considering different value pairs for the window sizes *NF1* and *ND1*. The results include the associated precision and sensitivity, as well as true and absolute errors for estimating heel strike instants, stride duration and step duration.

Window size (frames)		Precision (%)	Sensitivity (%)	Heel strike instant (ms)		Stride duration (ms)		Step duration (ms)	
NF1	*ND1*			True error	Abs. error	True error	Abs. error	True error	Abs. error
1	**3**	63.1	97.6	−3.4 ± 40.1	29.0 ± 27.8	−4.6 ± 67.4	48.4 ± 46.9	0.5 ± 54.8	39.6 ± 37.8
1	**5**	94.9	70.0	11.2 ± 33.6	26.9 ± 22.9	1.6 ± 55.2	36.2 ± 41.3	2.5 ± 43.7	33.8 ± 27.7
1	**7**	96.9	58.4	9.9 ± 27.7	23.6 ± 17.6	0.5 ± 33.7	25.1 ± 21.7	4.4 ± 36.4	29.8 ± 21.1
1	**9**	97.0	54.1	10.9 ± 27.0	23.4 ± 17.2	2.4 ± 39.2	29.3 ± 24.8	5.2 ± 36.0	28.9 ± 22.0
3	**3**	95.1	95.1	6.4 ± 25.0	19.2 ± 17.3	0.4 ± 35.1	23.5 ± 26.0	0.0 ± 31.9	23.3 ± 21.8
3	**5**	98.8	92.5	8.0 ± 21.6	18.4 ± 13.9	2.7 ± 25.2	20.7 ± 14.6	1.3 ± 27.7	21.7 ± 17.1
3	**7**	99.6	91.4	8.1 ± 21.3	18.2 ± 13.8	3.1 ± 24.3	20.0 ± 14.0	1.7 ± 27.0	21.2 ± 16.7
3	**9**	99.6	88.1	8.3 ± 21.3	18.2 ± 13.7	3.5 ± 24.6	20.4 ± 14.1	2.1 ± 26.5	21.0 ± 16.3
5	**3**	97.7	96.6	8.7 ± 22.2	17.9 ± 15.8	0.3 ± 35.6	22.7 ± 27.3	−0.1 ± 27.4	19.4 ± 19.3
5	**5**	99.6	92.9	8.6 ± 19.3	17.3 ± 12.1	3.0 ± 25.4	20.0 ± 15.8	0.9 ± 23.4	18.1 ± 14.7
5	**7**	**99.6**	**92.4**	**8.7 ± 19.2**	**17.3 ± 12.0**	**2.5 ± 25.4**	**19.8 ± 15.9**	**0.7 ± 23.3**	**18.0 ± 14.7**
5	**9**	99.6	89.7	9.0 ± 19.1	17.3 ± 12.1	3.2 ± 25.7	20.2 ± 16.1	1.1 ± 23.4	18.1 ± 14.9
7	**3**	95.0	95.1	5.3 ± 29.8	21.7 ± 21.2	15.8 ± 34.9	29.8 ± 23.9	5.5 ± 39.6	26.0 ± 30.4
7	**5**	99.0	91.4	8.1 ± 23.1	19.7 ± 14.5	12.9 ± 31.9	27.2 ± 20.9	5.2 ± 28.0	21.2 ± 19.0
7	**7**	99.8	87.9	8.9 ± 22.5	19.4 ± 14.3	12.3 ± 32.0	27.0 ± 20.8	5.0 ± 26.4	20.2 ± 17.6
7	**9**	99.8	87.9	8.9 ± 22.5	19.4 ± 14.3	12.3 ± 32.0	27.0 ± 20.8	5.0 ± 26.4	20.2 ± 17.6
9	**3**	95.0	92.4	9.9 ± 33.7	27.8 ± 21.4	32.1 ± 58.4	53.3 ± 39.8	13.4 ± 42.3	30.6 ± 32.1
9	**5**	99.4	88.6	11.5 ± 31.9	26.8 ± 20.7	35.9 ± 55.8	52.7 ± 40.2	13.2 ± 41.0	29.0 ± 31.9
9	**7**	99.6	86.9	12.1 ± 30.9	26.4 ± 20.1	33.7 ± 54.4	50.0 ± 39.8	11.4 ± 37.7	26.7 ± 29.0
9	**9**	99.8	81.7	12.9 ± 29.9	26.3 ± 19.2	35.9 ± 48.2	47.3 ± 37.0	12.3 ± 36.1	25.3 ± 28.5

Table D.2. Results for heel strike side identification when using Kv1 and WF data (KC1, 10 trials), considering different value pairs for the window sizes *NF2* and *ND2*. The results include the associated precision and sensitivity for left and right heel strikes.

Window size (frames)		Precision (%)		Sensitivity (%)	
NF2	**ND2**	**Left**	**Right**	**Left**	**Right**
1	**3**	84.2	84.2	81.6	86.7
1	**5**	96.1	96.6	96.5	96.6
1	**7**	99.6	97.8	97.8	99.6
1	**9**	99.6	98.9	99.1	99.6
3	**3**	99.1	96.7	96.5	99.3
3	**5**	100.0	98.9	99.1	100.0
3	**7**	99.6	99.3	99.6	99.6
3	**9**	100.0	99.3	99.6	100.0
5	**3**	99.6	98.5	98.7	99.6
5	**5**	99.1	99.3	99.6	99.3
5	**7**	100.0	99.3	99.6	100.0
5	**9**	100.0	99.3	99.6	100.0
7	**3**	**100.0**	**99.3**	**99.6**	**100.0**
7	**5**	100.0	99.3	99.6	100.0
7	**7**	100.0	99.3	99.6	100.0
7	**9**	100.0	99.3	99.6	100.0
9	**3**	100.0	99.3	99.6	100.0
9	**5**	100.0	99.3	99.6	100.0
9	**7**	100.0	99.3	99.6	100.0
9	**9**	99.6	99.3	99.6	99.6

Table D.3. Results for toe off instant estimation when using Kv1 and WF data (KC1, 10 trials), considering different values for the window size *NF3*.

The results include the associated sensitivity, as well as true and absolute errors for estimating toe off instants, and the stance, swing single support and double support duration.

Window size (frames)	Sensitivity (%)	Toe off instant (ms)		Stance duration (ms)		Swing duration (ms)		Single support duration (ms)		Double support duration (ms)	
NF3		True error	Abs. error	True error	Abs. error	True error	Abs. error	True error	Abs. error	True error	Abs. error
1	98.3	28.4 ± 37.7	37.0 ± 29.4	17.2 ± 38.4	31.2 ± 28.0	−14.4 ± 35.2	28.4 ± 25.2	−27.6 ± 56.4	49.6 ± 38.6	30.8 ± 65.4	56.8 ± 44.5
3	95.6	31.1 ± 36.0	35.7 ± 31.5	16.7 ± 38.4	29.3 ± 29.8	−13.7 ± 36.1	27.8 ± 26.7	−36.8 ± 52.8	50.2 ± 40.2	39.5 ± 66.5	57.9 ± 51.0
5	93.9	27.7 ± 33.8	32.4 ± 29.3	14.9 ± 30.8	25.8 ± 22.3	−12.5 ± 27.6	23.3 ± 19.2	−30.7 ± 50.2	44.2 ± 38.8	32.0 ± 67.1	54.3 ± 50.6
7	94.9	22.5 ± 28.6	28.5 ± 22.7	11.8 ± 32.6	26.1 ± 22.7	−9.1 ± 29.1	22.9 ± 20.1	−20.0 ± 40.8	36.6 ± 26.9	21.0 ± 52.8	45.0 ± 34.5
9	**94.6**	**20.4 ± 29.3**	**27.7 ± 22.5**	**11.4 ± 34.7**	**26.8 ± 24.8**	**−8.9 ± 31.9**	**24.8 ± 21.8**	**−12.8 ± 41.9**	**34.4 ± 27.2**	**13.8 ± 54.8**	**44.5 ± 34.5**
11	94.6	12.5 ± 33.3	26.7 ± 23.4	6.7 ± 33.7	25.7 ± 22.6	−4.3 ± 32.3	24.0 ± 21.9	4.6 ± 49.6	38.4 ± 31.7	−4.0 ± 63.9	47.3 ± 42.8

Kv1 and WB (KC1, 10 trials)

Table D.4. Results for heel strike instant estimation when using Kv1 and WB data (KC1, 10 trials), considering different value pairs for the window sizes *NF1* and *ND1*. The results include the associated precision and sensitivity, as well as true and absolute errors for estimating heel strike instants, stride duration and step duration.

Window size (frames)		Precision (%)	Sensitivity (%)	Heel strike instant (ms)		Stride duration (ms)		Step duration (ms)	
NF1	*ND1*			True error	Abs. error	True error	Abs. error	True error	Abs. error
1	**3**	57.9	96.1	−9.8 ± 50.6	39.2 ± 33.4	−16.5 ± 70.4	55.3 ± 46.3	−5.9 ± 66.2	50.8 ± 42.8
1	**5**	94.6	67.8	22.0 ± 39.4	36.3 ± 26.7	0.2 ± 48.0	36.0 ± 31.3	1.7 ± 53.1	40.8 ± 33.9
1	**7**	95.5	48.6	23.2 ± 34.1	33.0 ± 24.7	1.2 ± 38.6	30.6 ± 22.6	0.2 ± 44.7	33.9 ± 28.9
1	**9**	95.9	45.4	23.0 ± 32.0	31.7 ± 23.4	−2.2 ± 39.6	29.8 ± 25.1	−0.3 ± 39.3	29.0 ± 26.4
3	**3**	90.0	94.2	20.7 ± 30.3	29.7 ± 21.5	−6.9 ± 41.3	31.8 ± 27.2	−1.7 ± 37.6	29.9 ± 22.8
3	**5**	96.6	89.0	22.7 ± 29.5	30.1 ± 21.9	−3.7 ± 38.0	28.1 ± 25.8	−1.4 ± 35.7	28.4 ± 21.7
3	**7**	97.1	87.8	22.7 ± 28.5	29.5 ± 21.3	−2.0 ± 35.0	27.0 ± 22.2	−1.0 ± 34.7	27.8 ± 20.7
3	**9**	97.2	86.9	22.8 ± 28.0	29.3 ± 21.1	−2.0 ± 34.8	26.7 ± 22.3	−1.5 ± 33.5	27.1 ± 19.6
5	**3**	95.0	94.0	19.4 ± 26.2	25.5 ± 20.3	−2.5 ± 32.3	23.9 ± 21.7	−1.2 ± 30.9	21.7 ± 22.0
5	**5**	97.9	92.0	19.7 ± 25.8	25.5 ± 20.0	−1.4 ± 33.5	24.2 ± 23.1	−0.9 ± 28.3	20.9 ± 19.1
5	**7**	97.9	91.9	19.9 ± 25.4	25.4 ± 19.8	−0.6 ± 32.1	23.5 ± 21.8	−0.6 ± 27.7	20.6 ± 18.5
5	**9**	98.5	91.0	19.7 ± 24.3	25.0 ± 18.8	−1.6 ± 30.6	22.8 ± 20.3	−1.7 ± 25.7	19.8 ± 16.4
7	**3**	96.4	93.5	19.0 ± 27.1	25.3 ± 21.3	−7.2 ± 26.7	20.9 ± 18.0	−3.4 ± 34.1	21.4 ± 26.7
7	**5**	97.8	92.8	20.3 ± 21.9	24.4 ± 17.3	−6.6 ± 26.2	20.6 ± 17.4	−2.3 ± 24.2	19.2 ± 14.9
7	**7**	**97.7**	**91.7**	**20.6 ± 21.7**	**24.5 ± 17.2**	**−5.7 ± 25.7**	**20.3 ± 16.6**	**−1.8 ± 23.9**	**19.0 ± 14.7**
7	**9**	97.9	91.0	20.8 ± 21.6	24.6 ± 17.2	−6.0 ± 25.8	20.4 ± 16.8	−2.1 ± 23.7	18.9 ± 14.5
9	**3**	96.7	92.8	21.0 ± 21.5	24.8 ± 17.0	−6.3 ± 28.1	21.8 ± 18.6	−3.3 ± 24.3	18.8 ± 15.8
9	**5**	97.6	92.4	21.0 ± 21.5	24.8 ± 16.9	−6.6 ± 28.1	21.9 ± 18.7	−3.5 ± 24.3	18.8 ± 15.8
9	**7**	98.1	91.3	21.5 ± 22.0	25.2 ± 17.6	−7.9 ± 32.2	23.5 ± 23.3	−4.0 ± 24.6	18.9 ± 16.3
9	**9**	98.0	88.2	22.0 ± 20.7	25.1 ± 16.9	−5.7 ± 27.5	21.2 ± 18.3	−2.9 ± 23.4	18.0 ± 15.2

Table D.5. Results for heel strike side identification when using Kv1 and WB data (KC1, 10 trials), considering different value pairs for the window sizes *NF2* and *ND2*. The results include the associated precision and sensitivity for left and right heel strikes.

Window size (frames)		Precision (%)		Sensitivity (%)	
NF2	**ND2**	**Left**	**Right**	**Left**	**Right**
1	**3**	84.7	80.7	80.2	86.2
1	**5**	91.1	92.3	92.8	91.2
1	**7**	94.9	99.2	99.2	95.3
1	**9**	97.7	96.5	96.6	98.4
3	**3**	95.8	94.2	94.3	96.4
3	**5**	97.0	96.9	97.0	97.6
3	**7**	97.7	96.9	97.0	98.4
3	**9**	98.5	99.6	99.6	99.2
5	**3**	95.9	97.6	97.7	96.5
5	**5**	98.5	98.1	98.1	99.2
5	**7**	98.9	99.2	99.2	99.6
5	**9**	98.1	99.2	99.2	98.8
7	**3**	97.4	98.8	98.9	98.0
7	**5**	98.5	98.4	98.5	99.2
7	**7**	98.5	98.8	98.9	99.2
7	**9**	**99.3**	**100.0**	**100.0**	**100.0**
9	**3**	97.8	98.4	98.5	98.4
9	**5**	97.7	97.3	97.4	98.4
9	**7**	98.9	99.2	99.2	99.6
9	**9**	98.9	100.0	100.0	99.6

Table D.6. Results for toe off instant estimation when using Kv1 and WB data (KC1, 10 trials), considering different values for the window size *NF3*. The results include the associated sensitivity, as well as true and absolute errors for estimating toe off instants, and the stance, swing single support and double support duration.

Window size (frames)	Sensitivity (%)	Toe off instant (ms)		Stance duration (ms)		Swing duration (ms)		Single support duration (ms)		Double support duration (ms)	
NF3		True error	Abs. error	True error	Abs. error	True error	Abs. error	True error	Abs. error	True error	Abs. error
1	98.4	32.0 ± 32.5	37.0 ± 26.7	5.8 ± 35.2	28.9 ± 20.7	−11.8 ± 35.2	29.5 ± 22.4	−27.3 ± 52.1	47.6 ± 34.7	23.5 ± 54.2	47.0 ± 35.6
3	98.1	30.7 ± 28.7	34.8 ± 23.6	3.5 ± 31.1	24.2 ± 19.8	−8.9 ± 29.4	24.2 ± 18.9	−20.1 ± 44.7	40.1 ± 28.2	18.2 ± 45.6	39.3 ± 29.3
5	98.4	25.3 ± 25.7	29.5 ± 20.6	−1.3 ± 30.5	24.0 ± 18.9	−4.7 ± 31.6	25.0 ± 19.8	−12.1 ± 44.5	37.1 ± 27.4	7.5 ± 46.2	35.5 ± 30.3
7	**98.1**	**19.9 ± 26.0**	**27.3 ± 18.1**	**−4.2 ± 31.9**	**24.8 ± 20.3**	**−2.1 ± 28.2**	**22.5 ± 17.0**	**−1.6 ± 40.7**	**32.7 ± 24.3**	**−3.8 ± 49.3**	**37.3 ± 32.3**
9	97.4	13.5 ± 27.4	24.6 ± 18.0	−8.5 ± 32.9	25.6 ± 22.2	2.7 ± 29.1	22.8 ± 18.2	9.6 ± 40.3	32.7 ± 25.4	−15.4 ± 53.7	41.6 ± 37.1
11	97.4	3.5 ± 30.8	24.1 ± 19.4	−16.9 ± 35.2	30.2 ± 24.8	11.5 ± 31.1	25.9 ± 20.6	31.1 ± 48.6	44.3 ± 37.0	−35.1 ± 60.2	52.1 ± 46.1

Kv2 and WF (KC1, 10 trials)

Table D.7. Results for heel strike instant estimation when using Kv2 and WF data (KC1, 10 trials), considering different value pairs for the window sizes *NF1* and *ND1*. The results include the associated precision and sensitivity, as well as true and absolute errors for estimating heel strike instants, stride duration and step duration.

Window size (frames)		Precision (%)	Sensitivity (%)	Heel strike instant (ms)		Stride duration (ms)		Step duration (ms)	
NF1	*ND1*			True error	Abs. error	True error	Abs. error	True error	Abs. error
1	**3**	71.3	98.3	5.5 ± 36.9	30.6 ± 21.4	8.5 ± 44.8	35.6 ± 28.4	5.8 ± 45.7	36.1 ± 28.7
1	**5**	97.2	75.2	21.7 ± 35.8	33.7 ± 24.8	9.1 ± 42.6	32.3 ± 29.2	6.0 ± 41.4	31.6 ± 27.4
1	**7**	98.3	64.9	21.8 ± 31.7	30.9 ± 22.9	6.6 ± 33.9	26.6 ± 21.9	3.3 ± 33.3	25.2 ± 21.9
1	**9**	98.4	63.7	21.0 ± 30.6	30.1 ± 21.7	6.5 ± 34.1	26.8 ± 22.0	3.8 ± 33.2	25.3 ± 21.8
3	**3**	97.9	97.4	14.4 ± 26.4	23.4 ± 18.9	6.4 ± 27.5	21.4 ± 18.3	3.3 ± 28.6	21.9 ± 18.8
3	**5**	99.2	96.7	14.9 ± 26.5	23.6 ± 19.1	7.3 ± 27.7	21.4 ± 19.0	3.8 ± 28.3	21.7 ± 18.5
3	**7**	99.4	96.1	15.0 ± 26.4	23.5 ± 19.1	7.5 ± 27.2	21.2 ± 18.6	3.9 ± 28.2	21.6 ± 18.5
3	**9**	99.6	95.3	15.2 ± 26.0	23.3 ± 19.0	7.8 ± 27.3	21.3 ± 18.8	4.4 ± 27.7	21.4 ± 18.2
5	**3**	98.7	97.9	13.4 ± 23.0	20.0 ± 17.5	4.0 ± 25.8	17.6 ± 19.2	3.1 ± 23.9	17.9 ± 16.2
5	**5**	99.6	96.7	13.4 ± 22.0	19.8 ± 16.5	4.8 ± 24.0	17.4 ± 17.1	3.6 ± 23.2	17.8 ± 15.4
5	**7**	99.6	96.4	13.4 ± 22.0	19.8 ± 16.5	4.8 ± 24.0	17.5 ± 17.2	3.6 ± 23.2	17.7 ± 15.3
5	**9**	**99.8**	**96.4**	**13.4 ± 22.0**	**19.8 ± 16.5**	**4.8 ± 24.0**	**17.5 ± 17.2**	**3.6 ± 23.2**	**17.7 ± 15.3**
7	**3**	98.3	97.6	16.6 ± 24.9	22.2 ± 20.0	6.9 ± 27.9	18.3 ± 22.2	4.3 ± 25.3	17.2 ± 19.1
7	**5**	99.5	97.1	17.3 ± 21.5	21.5 ± 17.3	5.6 ± 22.6	17.0 ± 15.9	3.3 ± 21.4	16.2 ± 14.3
7	**7**	99.8	96.1	17.2 ± 20.9	21.3 ± 16.6	6.1 ± 21.9	16.9 ± 15.1	3.6 ± 20.5	15.9 ± 13.4
7	**9**	99.8	96.1	17.2 ± 20.9	21.3 ± 16.6	6.1 ± 21.9	16.9 ± 15.1	3.6 ± 20.5	15.9 ± 13.4
9	**3**	97.5	97.5	20.5 ± 27.0	26.9 ± 20.5	9.7 ± 29.8	21.3 ± 22.9	6.9 ± 27.5	19.5 ± 20.6
9	**5**	99.8	96.1	21.8 ± 24.6	26.3 ± 19.6	8.1 ± 26.8	19.6 ± 20.0	5.6 ± 24.8	18.1 ± 17.8
9	**7**	99.9	95.4	22.3 ± 23.4	26.1 ± 19.2	7.4 ± 25.1	18.8 ± 18.2	5.1 ± 23.6	17.6 ± 16.5
9	**9**	99.9	94.4	22.1 ± 23.2	25.9 ± 18.9	7.8 ± 24.8	18.6 ± 18.2	5.2 ± 23.1	17.3 ± 16.1

Table D.8. Results for heel strike side identification when using Kv2 and WF data (KC1, 10 trials), considering different value pairs for the window sizes *NF2* and *ND2*. The results include the associated precision and sensitivity for left and right heel strikes.

Window size (frames)		Precision (%)		Sensitivity (%)	
NF2	**ND2**	**Left**	**Right**	**Left**	**Right**
1	**3**	91.4	86.1	87.2	91.3
1	**5**	99.1	96.1	96.4	99.0
1	**7**	99.8	99.0	99.1	99.7
1	**9**	100.0	100.0	100.0	100.0
3	**3**	99.5	97.0	97.3	99.5
3	**5**	100.0	99.2	99.3	100.0
3	**7**	100.0	99.5	99.5	100.0
3	**9**	100.0	99.7	99.8	100.0
5	**3**	100.0	99.2	99.3	100.0
5	**5**	100.0	99.5	99.5	100.0
5	**7**	100.0	99.7	99.8	100.0
5	**9**	100.0	100.0	100.0	100.0
7	**3**	100.0	99.5	99.5	100.0
7	**5**	100.0	99.7	99.8	100.0
7	**7**	100.0	100.0	100.0	100.0
7	**9**	100.0	100.0	100.0	100.0
9	**3**	**100.0**	**100.0**	**100.0**	**100.0**
9	**5**	100.0	100.0	100.0	100.0
9	**7**	100.0	100.0	100.0	100.0
9	**9**	100.0	100.0	100.0	100.0

Table D.9. Results for toe off instant estimation when using Kv2 and WF data (KC1, 10 trials), considering different values for the window size *NF3*.

The results include the associated sensitivity, as well as true and absolute errors for estimating toe off instants, and the stance, swing single support and double support duration.

Window size (frames)	Sensitivity (%)	Toe off instant (ms)		Stance duration (ms)		Swing duration (ms)		Single support duration (ms)		Double support duration (ms)	
NF3		True error	Abs. error	True error	Abs. error	True error	Abs. error	True error	Abs. error	True error	Abs. error
1	99.7	14.4 ± 29.0	24.7 ± 21.0	2.8 ± 29.2	22.6 ± 18.6	1.9 ± 33.3	25.6 ± 21.4	−0.6 ± 45.0	35.2 ± 27.9	5.4 ± 45.5	37.0 ± 27.1
3	99.7	13.8 ± 25.7	22.3 ± 18.7	2.2 ± 24.5	19.4 ± 15.1	2.5 ± 29.6	22.4 ± 19.4	0.8 ± 40.8	31.6 ± 25.8	4.0 ± 39.9	32.1 ± 24.0
5	99.7	13.8 ± 23.6	21.2 ± 17.3	2.6 ± 24.2	19.1 ± 15.0	2.1 ± 29.0	21.5 ± 19.6	0.6 ± 39.0	29.8 ± 25.1	4.8 ± 37.7	30.2 ± 23.1
7	99.7	12.5 ± 22.3	20.0 ± 16.0	2.2 ± 23.1	18.2 ± 14.3	2.5 ± 27.6	20.4 ± 18.8	3.1 ± 36.4	27.7 ± 23.7	1.9 ± 34.9	28.3 ± 20.4
9	**99.7**	**12.5 ± 22.3**	**20.0 ± 16.0**	**2.5 ± 22.0**	**17.2 ± 13.9**	**2.2 ± 27.0**	**19.8 ± 18.5**	**2.5 ± 35.7**	**27.1 ± 23.4**	**2.3 ± 33.4**	**26.5 ± 20.4**
11	99.7	8.1 ± 24.4	19.9 ± 16.3	−2.4 ± 24.2	19.1 ± 15.0	7.2 ± 28.0	21.4 ± 19.4	13.0 ± 37.3	30.0 ± 25.7	−7.7 ± 36.0	28.8 ± 22.9

Kv2 and WB (KC1, 10 trials)

Table D.10. Results for heel strike instant estimation when using Kv2 and WB data (KC1, 10 trials), considering different value pairs for the window sizes *NF1* and *ND1*. The results include the associated precision and sensitivity, as well as true and absolute errors for estimating heel strike instants, stride duration and step duration.

Window size (frames)		Precision (%)	Sensitivity (%)	Heel strike instant (ms)		Stride duration (ms)		Step duration (ms)	
NF1	*ND1*			True error	Abs. error	True error	Abs. error	True error	Abs. error
1	**3**	66.5	98.4	−13.6 ± 36.3	31.7 ± 22.4	−6.9 ± 47.3	36.6 ± 30.7	−1.5 ± 45.8	35.5 ± 28.9
1	**5**	96.2	69.0	0.1 ± 38.6	31.7 ± 22.1	−5.1 ± 49.8	40.2 ± 29.7	−2.8 ± 48.3	37.9 ± 29.9
1	**7**	96.7	57.6	−0.6 ± 35.7	29.0 ± 20.8	−6.5 ± 45.2	35.1 ± 29.0	−1.6 ± 41.8	32.9 ± 25.7
1	**9**	97.3	55.5	−0.7 ± 35.3	28.7 ± 20.6	−9.4 ± 43.3	34.2 ± 27.9	−1.7 ± 41.9	32.9 ± 26.0
3	**3**	96.2	98.3	6.7 ± 28.6	22.5 ± 18.9	−0.2 ± 31.0	24.1 ± 19.5	1.6 ± 32.1	24.6 ± 20.6
3	**5**	98.2	96.4	7.1 ± 28.6	22.5 ± 19.0	−0.5 ± 30.7	24.0 ± 19.2	1.6 ± 32.0	24.5 ± 20.6
3	**7**	98.4	94.9	7.4 ± 28.5	22.5 ± 19.0	−0.7 ± 30.3	23.6 ± 19.0	1.0 ± 31.3	24.0 ± 20.1
3	**9**	98.5	93.5	7.5 ± 28.5	22.6 ± 19.0	−1.2 ± 30.1	23.4 ± 18.9	0.9 ± 31.4	24.0 ± 20.2
5	**3**	98.2	98.8	11.9 ± 22.7	20.2 ± 15.7	−0.1 ± 24.7	18.3 ± 16.6	0.4 ± 25.4	19.4 ± 16.3
5	**5**	**98.6**	**97.7**	**12.2 ± 22.5**	**20.2 ± 15.7**	**−0.1 ± 23.6**	**17.7 ± 15.5**	**0.4 ± 24.8**	**19.1 ± 15.8**
5	**7**	98.5	96.8	12.2 ± 22.5	20.2 ± 15.7	0.3 ± 23.5	17.7 ± 15.5	0.5 ± 24.7	19.0 ± 15.8
5	**9**	98.5	95.8	12.3 ± 22.5	20.3 ± 15.7	−0.2 ± 23.6	17.7 ± 15.6	0.4 ± 24.7	18.9 ± 15.9
7	**3**	97.7	98.3	19.0 ± 22.5	23.6 ± 17.6	−2.1 ± 22.5	17.6 ± 14.3	0.0 ± 24.1	18.6 ± 15.3
7	**5**	98.6	97.3	19.7 ± 20.7	23.3 ± 16.6	−3.2 ± 21.2	16.9 ± 13.2	−0.5 ± 22.9	18.0 ± 14.2
7	**7**	98.7	95.7	19.9 ± 20.6	23.3 ± 16.6	−3.5 ± 20.4	16.5 ± 12.5	−0.5 ± 22.8	17.9 ± 14.2
7	**9**	98.7	95.7	19.9 ± 20.6	23.3 ± 16.6	−3.5 ± 20.4	16.5 ± 12.5	−0.5 ± 22.8	17.9 ± 14.2
9	**3**	96.6	98.2	23.0 ± 22.7	27.0 ± 17.8	−3.4 ± 24.1	17.8 ± 16.6	−1.1 ± 26.4	19.2 ± 18.1
9	**5**	98.3	96.5	24.1 ± 20.6	26.7 ± 17.2	−3.0 ± 21.0	16.7 ± 13.0	−0.6 ± 22.4	17.6 ± 13.9
9	**7**	98.3	95.8	24.1 ± 20.5	26.6 ± 17.2	−3.3 ± 20.5	16.6 ± 12.5	−0.6 ± 22.0	17.4 ± 13.5
9	**9**	98.4	93.5	24.5 ± 20.1	26.7 ± 17.1	−3.7 ± 19.8	16.1 ± 12.1	−1.0 ± 20.9	16.7 ± 12.6

Table D.11. Results for heel strike side identification when using Kv2 and WB data (KC1, 10 trials), considering different value pairs for the window sizes *NF2* and *ND2*. The results include the associated precision and sensitivity for left and right heel strikes.

Window size (frames)		Precision (%)		Sensitivity (%)	
NF2	***ND2***	**Left**	**Right**	**Left**	**Right**
1	**3**	87.2	85.4	85.1	88.4
1	**5**	96.8	97.1	97.1	96.8
1	**7**	97.6	99.5	99.5	97.6
1	**9**	99.5	98.9	98.9	99.5
3	**3**	97.3	97.9	97.9	97.3
3	**5**	98.7	99.5	99.5	98.7
3	**7**	99.2	99.7	99.7	99.2
3	**9**	100.0	99.7	99.7	100.0
5	**3**	99.2	100.0	100.0	99.2
5	**5**	99.2	99.7	99.7	99.2
5	**7**	100.0	99.7	99.7	100.0
5	**9**	99.7	100.0	100.0	99.7
7	**3**	99.2	98.9	98.9	99.2
7	**5**	99.5	99.7	99.7	99.5
7	**7**	99.7	100.0	100.0	99.7
7	**9**	100.0	99.7	99.7	100.0
9	**3**	100.0	99.2	99.2	100.0
9	**5**	**99.7**	**100.0**	**100.0**	**99.7**
9	**7**	99.7	100.0	100.0	99.7
9	**9**	99.5	100.0	100.0	99.5

Table D.12. Results for toe off instant estimation when using Kv2 and WB data (KC1, 10 trials), considering different values for the window size *NF3*. The results include the associated sensitivity, as well as true and absolute errors for estimating toe off instants, and the stance, swing single support and double support duration.

Window size (frames)	Sensitivity (%)	Toe off instant (ms)		Stance duration (ms)		Swing duration (ms)		Single support duration (ms)		Double support duration (ms)	
NF3		True error	Abs. error	True error	Abs. error	True error	Abs. error	True error	Abs. error	True error	Abs. error
1	100.0	31.9 ± 30.8	35.9 ± 26.0	18.5 ± 33.7	30.5 ± 23.5	−18.2 ± 34.9	31.3 ± 23.9	−43.1 ± 49.5	53.8 ± 37.5	41.5 ± 51.6	55.6 ± 35.9
3	100.0	29.3 ± 25.8	32.1 ± 22.2	16.1 ± 28.2	26.2 ± 19.2	−15.8 ± 27.9	26.2 ± 18.4	−38.3 ± 40.0	45.7 ± 31.3	37.1 ± 43.4	49.2 ± 28.9
5	100.0	26.2 ± 24.8	29.6 ± 20.6	13.5 ± 28.5	25.3 ± 18.7	−13.2 ± 27.8	24.9 ± 18.0	−32.8 ± 38.6	41.7 ± 28.7	31.8 ± 42.3	45.0 ± 27.7
7	**100.0**	**24.9 ± 24.4**	**28.7 ± 19.8**	**11.8 ± 27.3**	**23.9 ± 17.8**	**−11.5 ± 27.7**	**24.4 ± 17.4**	**−29.9 ± 37.4**	**39.5 ± 27.1**	**27.6 ± 41.1**	**41.4 ± 27.0**
9	100.0	26.8 ± 25.2	30.8 ± 20.1	13.8 ± 28.6	25.7 ± 18.6	−13.5 ± 28.2	25.3 ± 18.4	−33.2 ± 38.5	42.4 ± 28.1	31.6 ± 44.7	46.1 ± 29.5
11	100.0	21.1 ± 26.5	27.7 ± 19.4	8.8 ± 29.3	23.8 ± 19.2	−8.5 ± 28.9	24.2 ± 17.8	−22.8 ± 39.9	37.2 ± 26.9	21.5 ± 44.9	41.1 ± 27.9

D.2 Results for Different Kv2 Configurations (WF Trials)

KC1 (Kv2, WF, 5 trials)

Table D.13. Results for heel strike instant estimation when using configuration KC1 (Kv2, WF, 5 trials), considering different value pairs for the window sizes *NF1* and *ND1*. The results include the associated precision and sensitivity, as well as true and absolute errors for estimating heel strike instants, stride duration and step duration.

Window size (frames)		Precision (%)	Sensitivity (%)	Heel strike instant (ms)		Stride duration (ms)		Step duration (ms)	
NF1	*ND1*			True error	Abs. error	True error	Abs. error	True error	Abs. error
1	**3**	70.8	97.7	4.6 ± 36.7	30.5 ± 20.8	8.8 ± 43.9	34.9 ± 28.0	6.7 ± 46.1	36.0 ± 29.5
1	**5**	96.7	74.8	20.8 ± 35.3	33.6 ± 23.3	10.1 ± 44.8	34.2 ± 30.5	8.3 ± 42.9	32.4 ± 29.3
1	**7**	98.5	61.9	21.7 ± 29.7	30.3 ± 20.7	8.0 ± 32.9	26.3 ± 21.0	5.5 ± 30.8	23.3 ± 20.9
1	**9**	98.5	61.2	21.3 ± 29.1	29.9 ± 20.2	8.3 ± 33.0	26.5 ± 21.1	5.8 ± 31.0	23.4 ± 21.0
3	**3**	98.1	97.0	13.8 ± 26.2	23.3 ± 18.3	8.0 ± 27.6	22.0 ± 18.5	4.6 ± 27.2	21.7 ± 17.1
3	**5**	99.5	96.6	14.0 ± 26.3	23.4 ± 18.4	8.5 ± 27.7	22.0 ± 18.8	4.9 ± 26.9	21.5 ± 16.9
3	**7**	99.8	95.9	14.0 ± 26.1	23.3 ± 18.3	9.0 ± 26.5	21.4 ± 18.1	5.1 ± 26.5	21.2 ± 16.6
3	**9**	99.8	95.4	14.3 ± 25.8	23.2 ± 18.3	9.2 ± 26.5	21.4 ± 18.1	5.4 ± 26.3	21.1 ± 16.6
5	**3**	98.6	97.5	13.1 ± 21.5	20.0 ± 15.3	3.3 ± 22.5	17.5 ± 14.5	3.2 ± 21.8	17.1 ± 13.9
5	**5**	99.5	96.3	13.1 ± 21.5	20.0 ± 15.3	3.3 ± 22.5	17.5 ± 14.5	3.2 ± 21.8	17.1 ± 13.9
5	**7**	99.5	96.3	13.1 ± 21.5	20.0 ± 15.3	3.3 ± 22.5	17.5 ± 14.5	3.2 ± 21.8	17.1 ± 13.9
5	**9**	**99.8**	**96.3**	**13.1 ± 21.5**	**20.0 ± 15.3**	**3.3 ± 22.5**	**17.5 ± 14.5**	**3.2 ± 21.8**	**17.1 ± 13.9**
7	**3**	98.1	97.0	16.6 ± 25.3	22.5 ± 20.3	7.5 ± 28.7	18.3 ± 23.3	4.8 ± 25.3	17.0 ± 19.3
7	**5**	99.5	96.8	17.4 ± 21.7	21.9 ± 17.2	6.2 ± 22.3	17.0 ± 15.6	3.7 ± 21.2	16.1 ± 14.2
7	**7**	99.8	95.9	16.9 ± 20.5	21.5 ± 15.6	7.1 ± 20.3	16.4 ± 13.8	4.3 ± 19.6	15.7 ± 12.5
7	**9**	99.8	95.9	16.9 ± 20.5	21.5 ± 15.6	7.1 ± 20.3	16.4 ± 13.8	4.3 ± 19.6	15.7 ± 12.5
9	**3**	98.4	97.0	21.8 ± 24.0	26.3 ± 19.0	8.1 ± 25.9	18.8 ± 19.5	6.2 ± 24.9	18.1 ± 18.2
9	**5**	100.0	96.6	22.3 ± 23.0	26.0 ± 18.7	7.2 ± 25.0	18.2 ± 18.6	5.6 ± 23.6	17.5 ± 16.8
9	**7**	100.0	95.9	22.8 ± 21.8	25.8 ± 18.2	6.4 ± 22.8	17.3 ± 16.1	5.0 ± 22.4	17.0 ± 15.4
9	**9**	100.0	95.0	22.6 ± 21.4	25.6 ± 17.7	7.0 ± 22.0	16.9 ± 15.6	5.3 ± 21.3	16.5 ± 14.5

Table D.14. Results for heel strike side identification when using configuration KC1 (Kv2, WF, 5 trials), considering different value pairs for the window sizes *NF2* and *ND2*. The results include the associated precision and sensitivity for left and right heel strikes.

Window size (frames)		Precision (%)		Sensitivity (%)	
NF2	***ND2***	**Left**	**Right**	**Left**	**Right**
1	**3**	91.4	86.5	87.7	91.3
1	**5**	99.1	97.0	97.3	99.0
1	**7**	99.5	99.0	99.1	99.5
1	**9**	100.0	100.0	100.0	100.0
3	**3**	99.5	96.6	96.8	99.5
3	**5**	100.0	99.0	99.1	100.0
3	**7**	100.0	99.5	99.5	100.0
3	**9**	100.0	100	100.0	100.0
5	**3**	100.0	99.0	99.1	100.0
5	**5**	100.0	99.5	99.5	100.0
5	**7**	100.0	100.0	100.0	100.0
5	**9**	100.0	100.0	100.0	100.0
7	**3**	**100.0**	**100.0**	**100.0**	**100.0**
7	**5**	100.0	100.0	100.0	100.0
7	**7**	100.0	100.0	100.0	100.0
7	**9**	100.0	100.0	100.0	100.0
9	**3**	100.0	100.0	100.0	100.0
9	**5**	100.0	100.0	100.0	100.0
9	**7**	100.0	100.0	100.0	100.0
9	**9**	100.0	100.0	100.0	100.0

Table D.15. Results for toe off instant estimation when using configuration KC1 (Kv2, WF, 5 trials), considering different values for the window size *NF3*.

The results include the associated sensitivity, as well as true and absolute errors for estimating toe off instants, and the stance, swing single support and double support duration.

Window size (frames)	Sensitivity (%)	Toe off instant (ms)		Stance duration (ms)		Swing duration (ms)		Single support duration (ms)		Double support duration (ms)	
NF3		True error	Abs. error	True error	Abs. error	True error	Abs. error	True error	Abs. error	True error	Abs. error
1	100.0	13.3 ± 28.3	24.5 ± 19.4	2.7 ± 28.9	22.6 ± 18.2	0.5 ± 31.6	25.2 ± 19.0	−0.2 ± 43.2	34.7 ± 25.7	3.5 ± 44.2	36.6 ± 25.0
3	100.0	12.8 ± 26.7	22.9 ± 18.7	1.1 ± 24.3	19.2 ± 14.9	2.1 ± 28.0	21.9 ± 17.5	1.9 ± 38.9	30.7 ± 23.9	1.5 ± 39.2	31.1 ± 23.8
5	100.0	13.4 ± 24.3	21.6 ± 17.3	2.0 ± 24.2	19.3 ± 14.6	1.2 ± 27.5	20.7 ± 18.1	0.7 ± 36.4	28.1 ± 23.2	3.6 ± 37.2	29.5 ± 23.0
7	100.0	12.4 ± 23.2	20.9 ± 15.9	1.5 ± 23.3	18.5 ± 14.2	1.7 ± 26.6	20.3 ± 17.2	2.2 ± 34.6	26.9 ± 22.0	1.2 ± 33.6	27.5 ± 19.4
9	**100.0**	**12.5 ± 22.3**	**20.5 ± 15.2**	**1.8 ± 22.2**	**17.2 ± 14.1**	**1.4 ± 25.6**	**19.8 ± 16.3**	**1.2 ± 33.7**	**26.5 ± 20.9**	**1.5 ± 33.1**	**25.9 ± 20.5**
11	100.0	7.7 ± 24.9	20.5 ± 16.1	−3.2 ± 24.2	19.5 ± 14.6	6.4 ± 27.1	21.2 ± 18.0	13.3 ± 35.7	29.5 ± 24.1	−9.0 ± 36.9	30.0 ± 23.3

KC2 (Kv2, WF, 5 trials)

Table D.16. Results for heel strike instant estimation when using configuration KC2 (Kv2, WF, 5 trials), considering different value pairs for the window sizes *NF1* and *ND1*. The results include the associated precision and sensitivity, as well as true and absolute errors for estimating heel strike instants, stride duration and step duration.

Window size (frames)		Precision (%)	Sensitivity (%)	Heel strike instant (ms)		Stride duration (ms)		Step duration (ms)	
NF1	*ND1*			True error	Abs. error	True error	Abs. error	True error	Abs. error
1	**3**	75.0	98.2	7.5 ± 41.7	33.6 ± 25.8	12.0 ± 56.9	44.8 ± 37.0	4.3 ± 49.6	37.3 ± 32.9
1	**5**	97.2	78.5	23.3 ± 35.2	34.8 ± 23.8	14.1 ± 39.9	32.6 ± 26.8	7.6 ± 39.5	30.2 ± 26.5
1	**7**	97.2	71.3	23.5 ± 32.4	32.8 ± 23.0	13.3 ± 36.0	29.5 ± 24.4	7.6 ± 34.4	26.4 ± 23.2
1	**9**	97.7	69.5	23.2 ± 31.6	32.4 ± 22.1	11.4 ± 35.1	28.4 ± 23.3	7.3 ± 33.6	25.8 ± 22.6
3	**3**	97.0	97.7	19.1 ± 28.5	26.6 ± 21.6	11.9 ± 28.6	24.6 ± 18.9	6.5 ± 29.6	23.7 ± 18.8
3	**5**	98.1	96.7	19.7 ± 28.5	26.8 ± 22.0	13.2 ± 28.0	24.5 ± 18.8	7.6 ± 29.0	23.5 ± 18.7
3	**7**	98.1	96.5	19.7 ± 28.5	26.8 ± 22.0	13.0 ± 28.0	24.5 ± 18.8	7.6 ± 29.1	23.5 ± 18.7
3	**9**	98.3	95.9	19.8 ± 28.0	26.5 ± 21.7	12.3 ± 27.4	23.8 ± 18.2	7.4 ± 28.5	23.1 ± 18.2
5	**3**	97.7	97.1	16.8 ± 23.3	22.3 ± 18.2	10.7 ± 23.7	19.8 ± 16.9	6.5 ± 21.6	17.5 ± 14.1
5	**5**	99.2	95.9	17.0 ± 23.2	22.2 ± 18.1	10.4 ± 23.5	19.5 ± 16.7	6.2 ± 21.0	17.2 ± 13.6
5	**7**	**99.2**	**95.9**	**17.0 ± 23.2**	**22.2 ± 18.1**	**10.4 ± 23.5**	**19.5 ± 16.7**	**6.2 ± 21.0**	**17.2 ± 13.6**
5	**9**	99.2	95.7	17.0 ± 23.2	22.3 ± 18.1	10.4 ± 23.6	19.6 ± 16.7	6.2 ± 21.1	17.2 ± 13.6
7	**3**	98.1	96.3	20.7 ± 24.7	25.4 ± 19.8	13.0 ± 24.3	20.7 ± 18.1	8.3 ± 22.7	18.2 ± 15.9
7	**5**	98.9	95.7	20.8 ± 24.0	25.1 ± 19.5	12.4 ± 23.5	20.2 ± 17.2	8.2 ± 21.9	17.7 ± 15.2
7	**7**	99.1	95.1	21.0 ± 23.9	25.1 ± 19.5	12.5 ± 23.4	20.1 ± 17.2	8.2 ± 21.8	17.6 ± 15.2
7	**9**	99.1	95.1	21.0 ± 23.9	25.1 ± 19.5	12.5 ± 23.4	20.1 ± 17.2	8.2 ± 21.8	17.6 ± 15.2
9	**3**	95.5	94.9	24.1 ± 30.5	31.1 ± 23.2	18.6 ± 30.8	26.9 ± 23.9	12.2 ± 27.4	21.6 ± 20.8
9	**5**	98.7	92.4	26.1 ± 28.0	30.5 ± 23.2	16.4 ± 28.6	24.6 ± 22.0	10.2 ± 24.8	19.5 ± 18.3
9	**7**	99.1	91.8	26.5 ± 27.0	30.2 ± 22.8	15.5 ± 27.6	23.8 ± 20.8	9.4 ± 23.6	18.9 ± 16.9
9	**9**	99.1	90.8	26.4 ± 26.5	29.9 ± 22.5	14.8 ± 27.1	23.2 ± 20.4	9.2 ± 23.2	18.5 ± 16.7

Table D.17. Results for heel strike side identification when using configuration KC2 (Kv2, WF, 5 trials), considering different value pairs for the window sizes *NF2* and *ND2*. The results include the associated precision and sensitivity.

Window size (frames)		Precision (%)		Sensitivity (%)	
NF2	***ND2***	**Left**	**Right**	**Left**	**Right**
1	**3**	96.8	87.2	88.1	96.8
1	**5**	99.2	97.8	98.0	99.1
1	**7**	98.8	100.0	100.0	98.6
1	**9**	99.2	100.0	100.0	99.1
3	**3**	99.2	96.9	97.2	99.1
3	**5**	98.8	99.5	99.6	98.6
3	**7**	99.2	100.0	100.0	99.1
3	**9**	99.2	100.0	100.0	99.1
5	**3**	99.2	99.5	99.6	99.1
5	**5**	99.6	99.5	99.6	99.5
5	**7**	99.2	99.5	99.6	99.1
5	**9**	99.2	100.0	100.0	99.1
7	**3**	99.6	100.0	100.0	99.5
7	**5**	99.6	100.0	100.0	99.5
7	**7**	99.2	99.5	99.6	99.1
7	**9**	98.8	100.0	100.0	98.6
9	**3**	**100.0**	**100.0**	**100.0**	**100.0**
9	**5**	99.2	100.0	100.0	99.1
9	**7**	99.2	100.0	100.0	99.1
9	**9**	98.8	100.0	100.0	98.6

Table D.18. Results for toe off instant estimation when using configuration KC2 (Kv2, WF, 5 trials), considering different values for the window size *NF3*.

The results include the associated sensitivity, as well as true and absolute errors for estimating toe off instants, and the stance, swing single support and double support duration.

Window size (frames)	Sensitivity (%)	Toe off instant (ms)		Stance duration (ms)		Swing duration (ms)		Single support duration (ms)		Double support duration (ms)	
NF3		True error	Abs. error	True error	Abs. error	True error	Abs. error	True error	Abs. error	True error	Abs. error
1	99.5	8.0 ± 27.3	23.0 ± 16.8	−0.1 ± 31.2	24.6 ± 19.1	10.8 ± 32.5	27.5 ± 20.3	17.6 ± 45.3	38.9 ± 29.1	−6.2 ± 50.8	40.8 ± 30.8
3	99.5	7.6 ± 24.5	20.8 ± 14.9	−1.1 ± 26.8	21.7 ± 15.8	11.8 ± 29.3	25.5 ± 18.4	18.5 ± 39.9	35.3 ± 26.3	−7.7 ± 44.5	35.6 ± 27.7
5	99.5	7.1 ± 23.1	20.0 ± 13.5	−2.6 ± 25.0	20.1 ± 15.1	13.3 ± 27.4	24.6 ± 17.9	20.4 ± 37.4	34.3 ± 25.4	−9.2 ± 41.6	34.1 ± 25.6
7	**99.5**	**8.2 ± 22.1**	**19.0 ± 13.8**	**−2.4 ± 23.7**	**18.5 ± 15.0**	**13.1 ± 28.1**	**24.5 ± 19.0**	**18.6 ± 36.6**	**32.7 ± 24.8**	**−7.3 ± 38.7**	**30.4 ± 24.9**
9	99.5	10.0 ± 22.8	20.3 ± 14.3	−1.4 ± 24.0	19.3 ± 14.3	12.1 ± 28.6	24.3 ± 19.4	15.6 ± 37.4	31.8 ± 25.1	−4.0 ± 38.5	30.9 ± 23.2
11	99.2	8.6 ± 23.8	19.4 ± 16.2	−3.3 ± 25.1	19.5 ± 16.2	14.0 ± 29.1	24.7 ± 20.8	18.5 ± 38.2	32.9 ± 26.8	−7.2 ± 38.3	30.3 ± 24.4

KC3 (Kv2, WF, 5 trials)

Table D.19. Results for heel strike instant estimation when using configuration KC3 (Kv2, WF, 5 trials), considering different value pairs for the window sizes *NF1* and *ND1*. The results include the associated precision and sensitivity, as well as true and absolute errors for estimating heel strike instants, stride duration and step duration.

Window size (frames)		Precision (%)	Sensitivity (%)	Heel strike instant (ms)		Stride duration (ms)		Step duration (ms)	
NF1	*ND1*			True error	Abs. error	True error	Abs. error	True error	Abs. error
1	**3**	63.9	96.8	−5.9 ± 43.1	30.2 ± 31.3	10.1 ± 56.0	39.7 ± 40.7	8.5 ± 52.5	38.1 ± 37.0
1	**5**	94.4	71.2	4.9 ± 33.9	27.4 ± 20.4	5.9 ± 41.4	34.1 ± 24.0	5.8 ± 41.8	33.0 ± 26.3
1	**7**	97.9	60.1	7.4 ± 31.6	25.7 ± 19.9	2.2 ± 38.6	31.4 ± 22.4	4.4 ± 38.5	30.2 ± 24.2
1	**9**	98.5	55.9	7.5 ± 31.4	25.5 ± 19.6	0.4 ± 37.6	31.6 ± 19.9	1.4 ± 36.1	28.3 ± 22.3
3	**3**	92.5	95.3	7.3 ± 28.0	21.6 ± 19.3	5.1 ± 34.0	25.8 ± 22.6	4.8 ± 31.3	22.9 ± 21.9
3	**5**	97.8	92.8	8.2 ± 28.2	21.7 ± 19.7	7.1 ± 33.2	25.4 ± 22.4	6.4 ± 32.2	23.2 ± 23.1
3	**7**	98.2	91.3	8.8 ± 26.5	21.1 ± 18.2	7.7 ± 30.5	24.3 ± 19.9	6.4 ± 27.8	21.2 ± 19.0
3	**9**	98.6	89.8	8.7 ± 25.7	20.7 ± 17.5	6.7 ± 30.0	23.8 ± 19.4	6.1 ± 27.1	20.7 ± 18.5
5	**3**	95.2	97.0	12.3 ± 24.4	20.9 ± 17.6	6.6 ± 24.9	19.5 ± 16.9	5.8 ± 25.0	19.3 ± 16.9
5	**5**	98.4	93.6	12.8 ± 22.9	20.2 ± 16.7	6.2 ± 22.8	18.3 ± 14.9	5.6 ± 23.1	18.2 ± 15.4
5	**7**	98.4	93.0	12.6 ± 22.7	20.1 ± 16.5	6.0 ± 22.5	18.0 ± 14.6	5.4 ± 22.5	17.9 ± 14.7
5	**9**	**98.6**	**92.5**	**12.8 ± 22.4**	**20.0 ± 16.3**	**5.8 ± 22.3**	**17.9 ± 14.5**	**5.3 ± 22.4**	**17.8 ± 14.6**
7	**3**	95.8	96.2	16.5 ± 29.1	25.1 ± 22.0	10.7 ± 32.2	22.2 ± 25.6	8.1 ± 28.6	19.6 ± 22.4
7	**5**	98.4	94.0	18.6 ± 23.8	23.8 ± 18.5	7.7 ± 25.0	19.3 ± 17.6	6.0 ± 22.4	17.1 ± 15.6
7	**7**	98.8	91.3	18.8 ± 22.5	23.3 ± 17.8	7.5 ± 23.2	18.1 ± 16.3	5.7 ± 21.1	16.3 ± 14.6
7	**9**	98.8	91.3	18.8 ± 22.5	23.3 ± 17.8	7.5 ± 23.2	18.1 ± 16.3	5.7 ± 21.1	16.3 ± 14.6
9	**3**	96.5	95.3	22.6 ± 33.0	31.6 ± 24.5	17.5 ± 35.5	25.8 ± 30.0	12.1 ± 31.5	21.7 ± 25.9
9	**5**	98.9	94.2	23.8 ± 31.4	31.1 ± 24.0	15.4 ± 33.3	24.1 ± 27.7	10.6 ± 29.6	20.3 ± 23.9
9	**7**	99.1	92.8	24.6 ± 30.0	30.8 ± 23.6	14.4 ± 31.9	23.0 ± 26.3	9.9 ± 28.4	19.7 ± 22.8
9	**9**	99.1	90.6	24.5 ± 28.1	29.9 ± 22.3	14.0 ± 29.2	21.3 ± 24.4	9.6 ± 26.5	18.4 ± 21.3

Table D.20. Results for heel strike side identification when using configuration KC3 (Kv2, WF, 5 trials), considering different value pairs for the window sizes *NF2* and *ND2*. The results include the associated precision and sensitivity.

Window size (frames)		Precision (%)		Sensitivity (%)	
NF2	***ND2***	**Left**	**Right**	**Left**	**Right**
1	**3**	85.6	81.4	82.1	85.0
1	**5**	98.6	96.7	96.9	98.6
1	**7**	99.1	97.6	97.8	99.0
1	**9**	99.1	100.0	100.0	99.0
3	**3**	98.6	95.8	96.0	98.6
3	**5**	99.5	97.6	97.8	99.5
3	**7**	99.1	98.1	98.2	99.0
3	**9**	99.6	100.0	100.0	99.5
5	**3**	100.0	98.1	98.2	100.0
5	**5**	99.6	98.6	98.7	99.5
5	**7**	**100.0**	**100.0**	**100.0**	**100.0**
5	**9**	100.0	100.0	100.0	100.0
7	**3**	99.1	99.5	99.6	99.0
7	**5**	100.0	99.5	99.6	100.0
7	**7**	100.0	99.5	99.6	100.0
7	**9**	100.0	99.5	99.6	100.0
9	**3**	99.6	99.0	99.1	99.5
9	**5**	100.0	99.5	99.6	100.0
9	**7**	100.0	99.5	99.6	100.0
9	**9**	100.0	99.5	99.6	100.0

Table D.21. Results for toe off instant estimation when using configuration KC3 (Kv2, WF, 5 trials), considering different values for the window size *NF3*.

The results include the associated sensitivity, as well as true and absolute errors for estimating toe off instants, and the stance, swing single support and double support duration.

Window size (frames)	Sensitivity (%)	Toe off instant (ms)		Stance duration (ms)		Swing duration (ms)		Single support duration (ms)		Double support duration (ms)	
NF3		True error	Abs. error	True error	Abs. error	True error	Abs. error	True error	Abs. error	True error	Abs. error
1	99.1	13.1 ± 33.0	27.2 ± 22.8	0.9 ± 34.0	26.7 ± 21.0	5.0 ± 34.1	26.3 ± 22.3	2.7 ± 48.1	37.7 ± 30.0	4.8 ± 51.0	40.8 ± 30.8
3	99.4	12.8 ± 34.3	25.5 ± 26.2	1.1 ± 29.9	23.3 ± 18.7	4.8 ± 30.3	24.4 ± 18.6	2.3 ± 42.3	33.4 ± 26.0	5.0 ± 48.7	37.6 ± 31.1
5	98.8	14.6 ± 27.4	23.8 ± 19.9	1.4 ± 29.1	23.2 ± 17.6	4.5 ± 31.0	25.1 ± 18.6	1.3 ± 43.2	34.4 ± 26.2	6.9 ± 48.8	37.9 ± 31.4
7	98.8	15.4 ± 24.6	22.8 ± 18.1	4.1 ± 28.1	23.2 ± 16.4	1.8 ± 29.3	23.2 ± 17.9	−1.4 ± 39.4	31.4 ± 23.8	9.5 ± 43.6	35.1 ± 27.4
9	98.8	16.3 ± 22.8	22.3 ± 16.9	6.3 ± 27.9	23.0 ± 16.9	−0.4 ± 28.9	23.3 ± 17.0	−5.0 ± 37.8	30.5 ± 22.9	12.5 ± 41.6	35.9 ± 24.3
11	**98.8**	**9.3 ± 23.9**	**20.2 ± 15.8**	**0.6 ± 28.1**	**22.5 ± 16.8**	**5.3 ± 29.8**	**24.1 ± 18.3**	**10.4 ± 40.7**	**33.4 ± 25.5**	**−1.8 ± 42.1**	**32.9 ± 26.2**

Appendix E Kinect Physical Configuration Selection

We considered three different Kinect physical configurations corresponding to the following sensor heights: 0.6 m, 1 m, and 1.34 m. For each height and Kinect version (Kv1 and Kv2), we explored the tilt angle values indicated in Table E.1. For each angle, we verified the minimum and maximum distance between the Kinect and a given subject (height of 1.67 m) for which all joints are tracked by the sensor. We then chose the tilt angle that led to the largest practical depth range (indicated in bold in the table).

Table E.1. Practical depth range for different Kinect tilt angles, for each Kinect version (Kv1 and Kv2) considered height.
The largest range for each Kinect version and height is indicated in bold.

Kinect	Height	Tilt angle (degrees)	Minimum[a] (m)	Maximum[b] (m)	Depth range[c] (m)
Kv1	0.6 m	5	2.27	3.78	1.51
		0	**2.00**	**3.78**	**1.78**
		−5	2.38	3.73	1.35
	1 m	−5	2.25	3.77	1.52
		−10	**1.72**	**3.7**	**1.98**
		−15	2.27	3.55	1.28
	1.34 m	−5	3.08	3.76	0.68
		−10	2.53	3.78	1.25
		−18	**1.81**	**3.46**	**1.65**
Kv2	0.6 m	**5**	**1.4**	**4.43**	**3.03**
		0	1.61	4.36	2.75
		−5	1.86	4.33	2.47
	1 m	0	1.9	4.5	2.6
		−5	**1.51**	**4.42**	**2.91**
		−10	1.37	4.22	2.85
	1.34 m	−10	1.75	4.3	2.55
		−15	**1.5**	**4.08**	**2.58**
		−20	1.25	3.61	2.36

[a] Shortest distance between the subject and Kinect for which all body joints are tracked.

[b] Longest distance between the subject and Kinect for which all body joints are tracked.

[c] Difference between maximum and minimum distances.

Appendix F Butterworth Filter Optimization for Gait Parameter Computation

For computing the considered gait parameters from Kinect data, the associated measures were processed using a zero-lag low-pass Butterworth filter. To choose the best filter's parameters (order and cut-off frequency), we obtained the mean estimation error for the Kinect when compared with Qualisys (gold standard), when considering different values for the order and cut-off frequency. The results achieved for both Kinect versions (Kv1 and Kv2) and both walking activities (WF and WB) are presented in Tables F.1 to F.8 (configuration KC1). The results for the three considered physical configurations of the Kinect (KC1, KC2 and KC3) are presented in Tables F.9 to F.14.

F.1 Results for Both Kinect Versions and Walking Activities

Kv1 and WF (KC1, 10 trials)

Table F.1. Mean estimation error for spatiotemporal gait parameters (Kv1, WF, KC1, 10 trials), when considering different value pairs for the Butterworth filter parameters (order and cut-off frequency).

Butterworth filter parameters		Spatiotemporal parameters					
		Mean error					
Order	Cut-off frequency (Hz)	Step length (mm)	Step width (mm)	Gait speed (m/s)	Gait speed variability (m/s)	Foot swing velocity (m/s)	Arm swing velocity (m/s)
No filtering		4.2	2.0	0.124	0.206	0.943	1.347
2	1	3.8	17.8	0.129	0.024	0.673	0.230
	2	3.6	9.6	0.125	0.028	0.217	0.414
	3	3.5	6.1	0.124	0.041	0.208	0.535
	4	3.5	4.3	0.124	0.054	0.309	0.632
	5	3.6	3.2	0.124	0.067	0.403	0.724
	6	3.5	2.6	0.124	0.082	0.491	0.820
	7	3.7	2.3	0.124	0.101	0.584	0.930
	8	3.7	2.1	0.124	0.127	0.690	1.061
	9	4.0	2.0	0.124	0.168	0.824	1.216
4	1	4.8	21.0	0.127	0.026	0.783	0.227
	2	4.1	9.9	0.123	0.028	0.244	0.405
	3	3.8	5.4	0.123	0.040	0.209	0.491
	4	3.5	3.5	0.123	0.049	0.324	0.569
	5	3.4	2.8	0.123	0.059	0.400	0.645
	6	3.4	2.4	0.123	0.069	0.453	0.722
	7	3.5	2.2	0.123	0.080	0.508	0.806
	8	3.6	2.1	0.124	0.095	0.576	0.902
	9	3.8	2.1	0.124	0.114	0.658	1.005
6	1	6.8	22.4	0.127	0.026	0.764	0.235
	2	4.9	10.3	0.122	0.029	0.275	0.410
	3	4.0	5.2	0.123	0.040	0.215	0.484
	4	3.5	3.4	0.123	0.049	0.338	0.553
	5	3.3	2.7	0.123	0.058	0.405	0.624
	6	3.5	2.4	0.123	0.067	0.450	0.694
	7	3.5	2.2	0.123	0.076	0.489	0.770
	8	3.5	2.1	0.123	0.088	0.544	0.859
	9	3.6	2.1	0.124	0.104	0.617	0.955

Table F.2. Mean estimation error for kinematic gait parameters (Kv1, WF, KC1, 10 trials), when considering different value pairs for the Butterworth filter parameters (order and cut-off frequency).

Butterworth filter parameters		Kinematic parameters							
		Mean error							
Order	Cut-off frequency (Hz)	Neck angle (deg.)	Spine middle angle (deg.)	Elbow angle maximum (deg.)	Elbow angle minimum (deg.)	Knee angle maximum (deg.)	Knee angle minimum (deg.)	Hip angle range (deg.)	Ankle angle range (deg.)
No filtering		7.3	6.7	5.5	4.4	3.0	13.2	4.4	53.4
2	1	7.2	6.7	4.6	8.8	3.3	25.2	15.0	16.4
	2	7.2	6.7	4.0	6.8	3.0	18.3	10.1	30.7
	3	7.3	6.7	3.8	6.0	2.9	15.9	7.7	37.9
	4	7.3	6.7	3.9	5.6	2.9	14.8	6.5	42.5
	5	7.3	6.7	4.1	5.3	2.9	14.3	5.8	45.9
	6	7.3	6.7	4.2	5.1	2.9	13.9	5.3	49.0
	7	7.3	6.7	4.5	4.9	3.0	13.7	5.0	51.5
	8	7.3	6.7	4.8	4.7	3.0	13.5	4.8	53.5
	9	7.3	6.7	5.3	4.5	3.0	13.3	4.6	54.3
4	1	7.2	6.7	4.6	9.0	3.2	27.6	17.9	15.4
	2	7.3	6.7	4.1	6.6	3.0	17.6	10.6	31.2
	3	7.3	6.7	3.9	5.9	2.9	14.5	7.1	38.8
	4	7.3	6.7	3.8	5.5	2.9	13.8	5.8	43.7
	5	7.3	6.7	4.0	5.3	2.9	13.8	5.3	47.3
	6	7.3	6.7	4.1	5.2	2.9	13.7	5.1	49.6
	7	7.3	6.7	4.2	5.1	2.9	13.6	4.9	51.7
	8	7.3	6.7	4.4	5.0	3.0	13.6	4.8	53.7
	9	7.3	6.7	4.7	4.9	3.0	13.5	4.7	55.1
6	1	7.3	6.7	4.6	9.2	3.2	28.9	18.8	14.6
	2	7.3	6.7	4.1	6.6	3.1	17.7	10.9	31.5
	3	7.3	6.7	3.9	5.8	2.9	14.0	6.8	38.9
	4	7.3	6.7	3.8	5.5	2.9	13.4	5.6	44.0
	5	7.3	6.7	3.9	5.4	2.9	13.7	5.2	47.9
	6	7.3	6.7	4.1	5.2	2.9	13.8	5.1	50.4
	7	7.3	6.7	4.2	5.1	2.9	13.6	5.0	52.1
	8	7.3	6.7	4.3	5.0	3.0	13.5	4.9	53.8
	9	7.3	6.7	4.6	4.9	3.0	13.5	4.7	55.4

Kv1 and WB (KC1, 10 trials)

Table F.3. Mean estimation error for spatiotemporal gait parameters (Kv1, WB, KC1, 10 trials), when considering different value pairs for the Butterworth filter parameters (order and cut-off frequency).

Butterworth filter parameters		Spatiotemporal parameters					
		Mean error					
Order	Cut-off frequency (Hz)	Step length (mm)	Step width (mm)	Gait speed (m/s)	Gait speed variability (m/s)	Foot swing velocity (m/s)	Arm swing velocity (m/s)
No filtering		5.3	2.7	0.167	0.221	1.744	1.024
2	1	5.9	19.4	0.172	0.031	0.532	0.145
	2	5.4	11.0	0.168	0.035	0.363	0.196
	3	5.5	7.2	0.167	0.048	0.408	0.285
	4	5.5	5.3	0.167	0.064	0.522	0.366
	5	5.4	4.1	0.167	0.079	0.660	0.443
	6	5.5	3.4	0.167	0.096	0.819	0.525
	7	5.3	3.0	0.167	0.117	1.008	0.619
	8	5.3	2.8	0.167	0.143	1.236	0.737
	9	5.3	2.7	0.166	0.182	1.518	0.890
4	1	7.9	22.7	0.171	0.033	0.590	0.154
	2	5.8	11.6	0.166	0.034	0.334	0.175
	3	5.3	6.6	0.166	0.044	0.363	0.246
	4	5.4	4.5	0.166	0.056	0.430	0.316
	5	5.4	3.5	0.166	0.070	0.536	0.383
	6	5.4	3.1	0.166	0.083	0.663	0.445
	7	5.4	2.9	0.166	0.097	0.800	0.514
	8	5.6	2.8	0.167	0.113	0.953	0.594
	9	5.3	2.7	0.167	0.132	1.127	0.680
6	1	9.7	24.2	0.171	0.035	0.590	0.159
	2	6.1	12.2	0.165	0.034	0.330	0.175
	3	5.6	6.6	0.166	0.044	0.361	0.239
	4	5.5	4.3	0.166	0.055	0.409	0.302
	5	5.4	3.4	0.166	0.068	0.498	0.368
	6	5.4	3.0	0.166	0.080	0.612	0.428
	7	5.4	2.9	0.166	0.093	0.742	0.487
	8	5.4	2.8	0.167	0.107	0.883	0.558
	9	5.6	2.7	0.167	0.123	1.034	0.637

Table F.4. Mean estimation error for kinematic gait parameters (Kv1, WB, KC1, 10 trials), when considering different value pairs for the Butterworth filter parameters (order and cut-off frequency).

Butterworth filter parameters		Kinematic parameters							
		Mean error							
Order	Cut-off frequency (Hz)	Neck angle (deg.)	Spine middle angle (deg.)	Elbow angle maximum (deg.)	Elbow angle minimum (deg.)	Knee angle maximum (deg.)	Knee angle minimum (deg.)	Hip angle range (deg.)	Ankle angle range (deg.)
No filtering		15.9	9.3	6.8	10.1	5.5	6.0	6.9	27.5
2	1	15.8	9.3	4.5	15.3	8.6	17.4	12.8	9.8
	2	15.9	9.3	5.0	14.1	7.6	10.3	9.8	16.7
	3	15.9	9.3	5.4	13.4	7.0	8.1	8.6	19.5
	4	15.9	9.3	5.6	12.9	6.7	7.2	7.9	21.3
	5	15.9	9.3	5.8	12.5	6.4	6.8	7.5	22.6
	6	15.9	9.3	6.0	12.1	6.2	6.5	7.3	23.8
	7	15.9	9.3	6.1	11.7	6.0	6.3	7.1	24.9
	8	15.9	9.3	6.3	11.2	5.8	6.2	7.0	25.9
	9	15.9	9.3	6.5	10.7	5.7	6.1	6.9	26.8
4	1	15.9	9.3	4.4	15.5	8.4	20.1	13.6	9.7
	2	15.9	9.3	5.0	14.2	7.7	10.0	10.0	18.1
	3	15.9	9.3	5.4	13.5	7.1	7.3	8.3	20.2
	4	15.9	9.3	5.6	13.1	6.7	6.7	7.6	21.3
	5	15.9	9.3	5.8	12.7	6.4	6.5	7.3	22.3
	6	15.9	9.3	5.9	12.3	6.2	6.4	7.2	23.3
	7	15.9	9.3	6.1	12.0	6.1	6.3	7.1	24.3
	8	15.9	9.3	6.2	11.7	5.9	6.2	7.0	25.1
	9	15.9	9.3	6.3	11.4	5.8	6.1	7.0	26.0
6	1	15.9	9.3	4.4	15.5	7.9	21.4	14.1	9.1
	2	15.9	9.3	5.0	14.2	7.6	10.0	10.3	18.6
	3	15.9	9.3	5.4	13.6	7.1	7.0	8.3	20.5
	4	15.9	9.3	5.6	13.1	6.8	6.6	7.5	21.1
	5	15.9	9.3	5.8	12.8	6.5	6.5	7.2	22.1
	6	15.9	9.3	5.9	12.4	6.3	6.4	7.1	23.1
	7	15.9	9.3	6.0	12.1	6.1	6.4	7.1	24.1
	8	15.9	9.3	6.1	11.8	6.0	6.2	7.0	24.9
	9	15.9	9.3	6.2	11.5	5.9	6.2	7.0	25.7

Kv2 and WF (KC1, 10 trials)

Table F.5. Mean estimation error for spatiotemporal gait parameters (Kv2, WF, KC1, 10 trials), when considering different value pairs for the Butterworth filter parameters (order and cut-off frequency).

Butterworth filter parameters		Spatiotemporal parameters					
		Mean error					
Order	Cut-off frequency (Hz)	Step length (mm)	Step width (mm)	Gait speed (m/s)	Gait speed variability (m/s)	Foot swing velocity (m/s)	Arm swing velocity (m/s)
No filtering		3.8	1.5	0.013	0.119	0.901	0.386
2	1	3.3	16.5	0.019	0.020	0.873	0.217
	2	3.1	8.9	0.015	0.013	0.422	0.084
	3	3.1	5.6	0.014	0.019	0.236	0.106
	4	3.3	3.9	0.013	0.025	0.220	0.139
	5	3.4	2.9	0.013	0.031	0.276	0.173
	6	3.5	2.3	0.013	0.040	0.358	0.208
	7	3.6	1.9	0.013	0.053	0.459	0.245
	8	3.6	1.7	0.013	0.070	0.585	0.288
	9	3.7	1.6	0.013	0.094	0.751	0.341
4	1	5.0	19.4	0.017	0.025	0.976	0.230
	2	3.0	9.2	0.013	0.015	0.458	0.072
	3	2.9	5.0	0.013	0.021	0.218	0.101
	4	3.1	3.3	0.013	0.024	0.183	0.126
	5	3.3	2.5	0.013	0.027	0.217	0.152
	6	3.3	2.1	0.013	0.030	0.270	0.181
	7	3.4	1.8	0.013	0.036	0.338	0.211
	8	3.5	1.7	0.013	0.048	0.419	0.243
	9	3.6	1.6	0.013	0.064	0.513	0.276
6	1	6.8	20.7	0.018	0.028	0.962	0.235
	2	3.2	9.6	0.013	0.016	0.484	0.074
	3	2.9	4.8	0.013	0.023	0.209	0.102
	4	3.0	3.1	0.013	0.025	0.170	0.122
	5	3.3	2.4	0.013	0.026	0.200	0.145
	6	3.3	2.1	0.013	0.028	0.244	0.172
	7	3.4	1.8	0.013	0.032	0.304	0.200
	8	3.4	1.7	0.013	0.041	0.376	0.230
	9	3.6	1.6	0.013	0.056	0.458	0.263

Table F.6. Mean estimation error for kinematic gait parameters (Kv2, WF, KC1, 10 trials), when considering different value pairs for the Butterworth filter parameters (order and cut-off frequency).

Butterworth filter parameters		Kinematic parameters								
		Mean error								
Order	Cut-off frequency (Hz)	Neck angle (deg.)	Spine shoulder angle (deg.)	Spine middle angle (deg.)	Elbow angle maximum (deg.)	Elbow angle minimum (deg.)	Knee angle maximum (deg.)	Knee angle minimum (deg.)	Hip angle range (deg.)	Ankle angle range (deg.)
No filtering		17.9	18.5	5.8	2.9	3.5	4.0	4.6	4.7	45.3
2	1	17.9	18.6	5.8	5.7	7.2	7.4	17.6	12.3	9.8
	2	17.9	18.5	5.8	4.5	5.2	5.6	9.9	7.9	21.6
	3	17.9	18.5	5.8	4.0	4.5	5.0	7.2	6.0	28.7
	4	17.9	18.5	5.8	3.7	4.2	4.7	6.1	5.2	33.6
	5	17.9	18.5	5.8	3.5	4.0	4.5	5.6	4.9	37.3
	6	17.9	18.5	5.8	3.3	3.9	4.4	5.3	4.8	40.4
	7	17.9	18.5	5.8	3.2	3.7	4.3	5.0	4.7	43.0
	8	17.9	18.5	5.8	3.1	3.6	4.2	4.9	4.7	45.0
	9	17.9	18.5	5.8	3.0	3.5	4.1	4.7	4.6	46.0
4	1	17.9	18.6	5.8	5.7	7.4	7.3	20.6	14.8	9.0
	2	17.9	18.5	5.8	4.4	4.9	4.8	8.9	8.6	20.3
	3	17.9	18.5	5.8	4.0	4.2	4.7	5.5	5.7	27.8
	4	17.9	18.5	5.8	3.7	4.1	4.6	5.0	4.9	33.7
	5	17.9	18.5	5.8	3.6	4.0	4.5	5.0	4.7	38.0
	6	17.9	18.5	5.8	3.4	3.9	4.4	5.0	4.7	40.9
	7	17.9	18.5	5.8	3.3	3.8	4.3	5.0	4.7	43.0
	8	17.9	18.5	5.8	3.2	3.8	4.3	4.9	4.7	44.9
	9	17.9	18.5	5.8	3.1	3.7	4.2	4.9	4.6	46.3
6	1	17.9	18.6	5.8	5.7	7.6	6.8	22.3	16.0	8.7
	2	17.9	18.5	5.8	4.3	4.8	4.2	8.8	9.1	20.0
	3	17.9	18.5	5.8	4.0	4.2	4.6	4.9	5.5	26.8
	4	17.9	18.5	5.8	3.8	4.0	4.6	4.7	4.9	33.4
	5	17.9	18.5	5.8	3.6	4.0	4.5	5.0	4.7	38.4
	6	17.9	18.5	5.8	3.5	3.9	4.4	5.0	4.7	41.3
	7	17.9	18.5	5.8	3.3	3.9	4.3	5.0	4.6	43.3
	8	17.9	18.5	5.8	3.2	3.8	4.3	4.9	4.7	44.9
	9	17.9	18.5	5.8	3.1	3.7	4.2	4.9	4.6	46.4

Kv2 and WB (KC1, 10 trials)

Table F.7. Mean estimation error for spatiotemporal gait parameters (Kv2, WB, KC1, 10 trials), when considering different value pairs for the Butterworth filter parameters (order and cut-off frequency).

Butterworth filter parameters		Spatiotemporal parameters					
		Mean error					
Order	Cut-off frequency (Hz)	Step length (mm)	Step width (mm)	Gait speed (m/s)	Gait speed variability (m/s)	Foot swing velocity (m/s)	Arm swing velocity (m/s)
No filtering		5.6	1.8	0.020	0.163	1.173	0.539
2	1	4.9	17.7	0.025	0.022	0.747	0.209
	2	4.8	9.4	0.021	0.012	0.429	0.118
	3	5.0	5.8	0.020	0.014	0.331	0.159
	4	5.0	3.9	0.020	0.020	0.331	0.206
	5	5.1	2.8	0.020	0.030	0.385	0.251
	6	5.2	2.2	0.020	0.044	0.478	0.296
	7	5.3	1.9	0.020	0.066	0.597	0.346
	8	5.4	1.8	0.020	0.097	0.754	0.404
	9	5.5	1.8	0.020	0.134	0.967	0.477
4	1	5.5	21.0	0.023	0.026	0.804	0.221
	2	4.7	10.0	0.019	0.012	0.432	0.114
	3	4.8	5.2	0.019	0.015	0.332	0.150
	4	5.0	3.2	0.020	0.018	0.314	0.182
	5	5.0	2.3	0.020	0.021	0.327	0.217
	6	5.0	2.0	0.020	0.026	0.374	0.254
	7	5.2	1.8	0.020	0.035	0.457	0.293
	8	5.2	1.8	0.020	0.052	0.557	0.337
	9	5.3	1.8	0.020	0.081	0.675	0.383
6	1	6.7	22.4	0.023	0.027	0.795	0.231
	2	4.7	10.5	0.019	0.013	0.438	0.118
	3	4.7	5.1	0.019	0.016	0.320	0.149
	4	5.0	3.0	0.020	0.018	0.315	0.174
	5	5.0	2.3	0.020	0.020	0.321	0.207
	6	5.0	2.0	0.020	0.024	0.351	0.241
	7	5.0	1.9	0.020	0.030	0.418	0.278
	8	5.2	1.8	0.020	0.041	0.508	0.317
	9	5.2	1.8	0.020	0.062	0.610	0.361

Table F.8. Mean estimation error for kinematic gait parameters (Kv2, WB, KC1, 10 trials), when considering different value pairs for the Butterworth filter parameters (order and cut-off frequency).

Butterworth filter parameters		Kinematic parameters								
		Mean error								
Order	**Cut-off frequency (Hz)**	**Neck angle (deg.)**	**Spine shoulder angle (deg.)**	**Spine middle angle (deg.)**	**Elbow angle maximum (deg.)**	**Elbow angle minimum (deg.)**	**Knee angle maximum (deg.)**	**Knee angle minimum (deg.)**	**Hip angle range (deg.)**	**Ankle angle range (deg.)**
No filtering		11.7	15.4	6.3	8.3	13.6	3.7	6.7	5.0	49.3
2	**1**	11.7	15.4	6.3	6.4	18.3	6.3	19.6	15.4	18.8
	2	11.7	15.4	6.3	6.9	16.8	5.1	12.4	10.4	28.3
	3	11.7	15.4	6.3	7.2	16.1	4.6	10.0	8.0	32.9
	4	11.7	15.4	6.3	7.4	15.7	4.3	8.9	6.8	36.0
	5	11.7	15.4	6.3	7.6	15.3	4.1	8.3	6.2	38.6
	6	11.7	15.4	6.3	7.7	15.0	4.0	7.9	5.8	40.8
	7	11.7	15.4	6.3	7.9	14.7	3.9	7.5	5.5	43.0
	8	11.7	15.4	6.3	8.0	14.4	3.8	7.2	5.3	45.1
	9	11.7	15.4	6.3	8.2	14.0	3.7	6.9	5.1	47.4
4	**1**	11.7	15.4	6.3	6.4	18.6	6.1	22.3	18.1	18.8
	2	11.7	15.4	6.3	7.0	16.7	4.9	11.5	11.2	29.5
	3	11.7	15.4	6.3	7.3	16.1	4.5	8.6	7.4	33.0
	4	11.7	15.4	6.3	7.5	15.7	4.2	8.2	6.1	35.6
	5	11.7	15.4	6.3	7.6	15.5	4.1	8.1	5.7	38.1
	6	11.7	15.4	6.3	7.7	15.2	4.0	7.9	5.6	40.2
	7	11.7	15.4	6.3	7.8	15.0	3.9	7.6	5.5	41.9
	8	11.7	15.4	6.3	7.9	14.8	3.8	7.4	5.4	43.5
	9	11.7	15.4	6.3	8.0	14.5	3.8	7.2	5.3	45.1
6	**1**	11.7	15.4	6.3	6.5	18.8	5.8	23.9	19.1	18.2
	2	11.7	15.4	6.3	7.1	16.7	4.7	11.5	11.6	30.2
	3	11.7	15.4	6.3	7.3	16.0	4.4	8.0	7.1	33.2
	4	11.7	15.4	6.3	7.5	15.7	4.2	7.9	5.9	35.1
	5	11.7	15.4	6.3	7.6	15.5	4.1	8.1	5.6	37.7
	6	11.7	15.4	6.3	7.7	15.3	4.0	8.0	5.5	40.1
	7	11.7	15.4	6.3	7.8	15.1	3.9	7.7	5.5	41.8
	8	11.7	15.4	6.3	7.9	14.9	3.9	7.5	5.4	43.2
	9	11.7	15.4	6.3	8.0	14.7	3.8	7.3	5.3	44.7

F.2 Results for Different Kv2 Configurations (WF Trials)

Kv2 and KC1 (WF, 5 trials)

Table F.9. Mean estimation error for spatiotemporal gait parameters (Kv2, WF, KC1, 5 trials), when considering different value pairs for the Butterworth filter parameters (order and cut-off frequency).

Butterworth filter parameters		Spatiotemporal parameters					
		Mean error					
Order	Cut-off frequency (Hz)	Step length (mm)	Step width (mm)	Gait speed (m/s)	Gait speed variability (m/s)	Foot swing velocity (m/s)	Arm swing velocity (m/s)
No filtering		3.8	1.5	0.013	0.118	0.916	0.420
2	1	3.2	16.5	0.019	0.021	0.868	0.212
	2	3.3	8.9	0.014	0.014	0.415	0.086
	3	3.2	5.6	0.013	0.019	0.226	0.115
	4	3.4	3.9	0.013	0.024	0.211	0.153
	5	3.4	2.9	0.013	0.031	0.275	0.192
	6	3.5	2.3	0.013	0.039	0.363	0.230
	7	3.6	1.9	0.013	0.052	0.466	0.272
	8	3.7	1.6	0.013	0.069	0.594	0.318
	9	3.7	1.5	0.013	0.092	0.762	0.374
4	1	4.6	19.5	0.017	0.026	0.970	0.224
	2	3.1	9.1	0.013	0.015	0.454	0.077
	3	3.0	4.9	0.013	0.021	0.209	0.109
	4	3.2	3.2	0.013	0.024	0.173	0.138
	5	3.4	2.4	0.013	0.026	0.211	0.167
	6	3.4	2.0	0.013	0.029	0.267	0.199
	7	3.5	1.8	0.013	0.036	0.339	0.233
	8	3.5	1.6	0.013	0.047	0.424	0.268
	9	3.7	1.6	0.013	0.062	0.522	0.305
6	1	6.6	20.8	0.017	0.028	0.959	0.229
	2	3.2	9.5	0.012	0.016	0.480	0.079
	3	3.1	4.8	0.013	0.023	0.200	0.110
	4	3.1	3.1	0.013	0.024	0.162	0.133
	5	3.4	2.4	0.013	0.026	0.196	0.159
	6	3.4	2.0	0.013	0.028	0.242	0.189
	7	3.5	1.8	0.013	0.031	0.304	0.221
	8	3.4	1.7	0.013	0.040	0.378	0.254
	9	3.6	1.6	0.013	0.055	0.466	0.289

Table F.10. Mean estimation error for kinematic gait parameters (Kv2, WF, KC1, 5 trials), when considering different value pairs for the Butterworth filter parameters (order and cut-off frequency).

Butterworth filter parameters		Kinematic parameters								
		Mean error								
Order	**Cut-off frequency (Hz)**	**Neck angle (deg.)**	**Spine shoulder angle (deg.)**	**Spine middle angle (deg.)**	**Elbow angle maximum (deg.)**	**Elbow angle minimum (deg.)**	**Knee angle maximum (deg.)**	**Knee angle minimum (deg.)**	**Hip angle range (deg.)**	**Ankle angle range (deg.)**
No filtering		18.0	18.7	5.9	2.9	3.6	4.1	4.7	4.5	45.3
2	**1**	18.0	18.7	5.9	5.6	7.1	7.3	17.7	12.2	10.2
	2	18.0	18.7	5.9	4.4	5.2	5.5	10.0	7.7	21.7
	3	18.0	18.7	5.9	3.9	4.6	5.0	7.3	5.8	28.7
	4	18.0	18.7	5.9	3.6	4.3	4.7	6.2	5.0	33.5
	5	18.0	18.7	5.9	3.4	4.1	4.5	5.6	4.8	37.2
	6	18.0	18.7	5.9	3.2	3.9	4.4	5.3	4.6	40.3
	7	18.0	18.7	5.9	3.1	3.8	4.3	5.1	4.5	42.9
	8	18.0	18.7	5.9	3.0	3.7	4.2	4.9	4.5	44.9
	9	18.0	18.7	5.9	2.9	3.7	4.1	4.8	4.5	46.0
4	**1**	18.1	18.7	5.9	5.6	7.4	7.1	20.6	14.7	9.4
	2	18.0	18.7	5.9	4.3	4.9	4.8	8.9	8.5	20.7
	3	18.0	18.7	5.9	3.9	4.3	4.7	5.6	5.5	27.8
	4	18.0	18.7	5.9	3.7	4.2	4.6	5.1	4.8	33.6
	5	18.0	18.7	5.9	3.5	4.1	4.5	5.1	4.6	37.8
	6	18.0	18.7	5.9	3.3	4.0	4.4	5.1	4.6	40.6
	7	18.0	18.7	5.9	3.2	3.9	4.4	5.0	4.5	42.8
	8	18.0	18.7	5.9	3.1	3.8	4.3	5.0	4.5	44.6
	9	18.0	18.7	5.9	3.0	3.8	4.2	4.9	4.5	46.1
6	**1**	18.1	18.7	5.9	5.6	7.5	6.7	22.3	15.9	8.9
	2	18.0	18.7	5.9	4.3	4.9	4.2	8.9	8.9	20.4
	3	18.0	18.7	5.9	4.0	4.3	4.6	4.9	5.3	27.0
	4	18.0	18.7	5.9	3.7	4.1	4.6	4.7	4.7	33.3
	5	18.0	18.7	5.9	3.5	4.1	4.6	5.1	4.6	38.2
	6	18.0	18.7	5.9	3.4	4.0	4.5	5.1	4.5	41.1
	7	18.0	18.7	5.9	3.2	3.9	4.4	5.1	4.5	43.0
	8	18.0	18.7	5.9	3.1	3.9	4.3	5.0	4.5	44.6
	9	18.0	18.7	5.9	3.0	3.8	4.2	4.9	4.5	46.1

Kv2 and KC2 (WF, 5 trials)

Table F.11. Mean estimation error for spatiotemporal gait parameters (Kv2, WF, KC2, 5 trials), when considering different value pairs for the Butterworth filter parameters (order and cut-off frequency).

Butterworth filter parameters		Spatiotemporal parameters					
		Mean error					
Order	Cut-off frequency (Hz)	Step length (mm)	Step width (mm)	Gait speed (m/s)	Gait speed variability (m/s)	Foot swing velocity (m/s)	Arm swing velocity (m/s)
No filtering		3.3	1.2	0.013	0.114	0.838	0.350
2	1	3.1	16.3	0.018	0.021	0.776	0.248
	2	2.8	8.5	0.014	0.013	0.380	0.100
	3	3.0	5.2	0.013	0.016	0.219	0.100
	4	3.2	3.5	0.013	0.021	0.209	0.125
	5	3.3	2.4	0.013	0.028	0.260	0.153
	6	3.3	1.8	0.013	0.037	0.336	0.183
	7	3.3	1.5	0.013	0.049	0.428	0.217
	8	3.2	1.3	0.013	0.067	0.541	0.258
	9	3.2	1.2	0.013	0.090	0.692	0.310
4	1	4.7	19.2	0.016	0.026	0.852	0.259
	2	3.0	8.9	0.013	0.014	0.388	0.073
	3	2.8	4.6	0.013	0.018	0.201	0.093
	4	3.0	2.8	0.013	0.021	0.174	0.116
	5	3.2	2.0	0.013	0.023	0.202	0.137
	6	3.3	1.6	0.013	0.026	0.248	0.160
	7	3.3	1.4	0.013	0.033	0.313	0.184
	8	3.3	1.3	0.013	0.044	0.393	0.211
	9	3.3	1.3	0.013	0.060	0.483	0.242
6	1	6.3	20.6	0.017	0.027	0.844	0.261
	2	3.0	9.3	0.012	0.015	0.401	0.071
	3	2.8	4.5	0.013	0.019	0.187	0.091
	4	2.8	2.6	0.013	0.021	0.162	0.113
	5	3.1	1.9	0.013	0.022	0.186	0.133
	6	3.3	1.6	0.013	0.024	0.221	0.153
	7	3.3	1.4	0.013	0.028	0.275	0.176
	8	3.3	1.3	0.013	0.038	0.349	0.200
	9	3.3	1.3	0.013	0.053	0.433	0.228

Table F.12. Mean estimation error for kinematic gait parameters (Kv2, WF, KC2, 5 trials), when considering different value pairs for the Butterworth filter parameters (order and cut-off frequency).

Butterworth filter parameters		Kinematic parameters								
		Mean error								
Order	**Cut-off frequency (Hz)**	**Neck angle (deg.)**	**Spine shoulder angle (deg.)**	**Spine middle angle (deg.)**	**Elbow angle maximum (deg.)**	**Elbow angle minimum (deg.)**	**Knee angle maximum (deg.)**	**Knee angle minimum (deg.)**	**Hip angle range (deg.)**	**Ankle angle range (deg.)**
No filtering		19.0	19.4	6.6	3.3	3.3	3.4	6.4	4.2	39.3
2	**1**	19.0	19.4	6.6	5.8	5.7	6.4	19.1	11.9	8.4
	2	19.0	19.4	6.6	4.5	3.8	4.5	11.6	7.3	13.7
	3	19.0	19.4	6.6	4.1	3.4	4.0	9.1	5.5	18.8
	4	19.0	19.4	6.6	3.8	3.2	3.8	8.0	4.7	23.0
	5	19.0	19.4	6.6	3.6	3.2	3.6	7.5	4.4	26.6
	6	19.0	19.4	6.6	3.5	3.1	3.6	7.2	4.3	30.0
	7	19.0	19.4	6.6	3.4	3.1	3.5	6.9	4.3	33.0
	8	19.0	19.4	6.6	3.3	3.1	3.5	6.7	4.2	35.7
	9	19.0	19.4	6.6	3.2	3.2	3.4	6.5	4.2	38.0
4	**1**	19.0	19.4	6.6	5.7	5.8	6.5	21.9	14.4	9.2
	2	19.0	19.4	6.6	4.4	3.6	3.9	10.5	8.0	12.9
	3	19.0	19.4	6.6	4.1	3.3	3.8	7.4	5.2	17.9
	4	19.0	19.4	6.6	3.9	3.2	3.7	7.0	4.4	22.3
	5	19.0	19.4	6.6	3.7	3.2	3.6	7.0	4.3	26.1
	6	19.0	19.4	6.6	3.5	3.2	3.6	7.0	4.2	29.2
	7	19.0	19.4	6.6	3.4	3.1	3.5	6.9	4.2	31.9
	8	19.0	19.4	6.6	3.3	3.1	3.5	6.8	4.2	34.3
	9	19.0	19.4	6.6	3.3	3.1	3.4	6.7	4.2	36.3
6	**1**	19.0	19.4	6.6	5.8	6.0	6.1	23.6	15.6	9.6
	2	19.0	19.4	6.6	4.4	3.6	3.5	10.4	8.5	12.7
	3	19.0	19.4	6.6	4.1	3.3	3.8	6.8	5.0	17.5
	4	19.0	19.4	6.6	3.9	3.2	3.8	6.6	4.4	22.1
	5	19.0	19.4	6.6	3.7	3.2	3.7	7.0	4.2	26.1
	6	19.0	19.4	6.6	3.6	3.2	3.6	7.0	4.2	29.1
	7	19.0	19.4	6.6	3.5	3.1	3.5	7.0	4.2	31.7
	8	19.0	19.4	6.6	3.4	3.1	3.5	6.9	4.2	34.0
	9	19.0	19.4	6.6	3.3	3.1	3.4	6.8	4.2	35.9

Kv2 and KC3 (WF, 5 trials)

Table F.13. Mean estimation error for spatiotemporal gait parameters (Kv2, WF, KC3, 5 trials), when considering different value pairs for the Butterworth filter parameters (order and cut-off frequency).

Butterworth filter parameters		Spatiotemporal parameters					
		Mean error					
Order	Cut-off frequency (Hz)	Step length (mm)	Step width (mm)	Gait speed (m/s)	Gait speed variability (m/s)	Foot swing velocity (m/s)	Arm swing velocity (m/s)
No filtering		3.6	1.7	0.014	0.121	0.728	0.401
2	1	3.1	15.8	0.020	0.019	0.984	0.247
	2	2.9	8.5	0.015	0.014	0.558	0.098
	3	3.0	5.4	0.014	0.019	0.349	0.108
	4	3.2	3.9	0.014	0.025	0.254	0.137
	5	3.2	3.0	0.014	0.031	0.243	0.170
	6	3.4	2.4	0.014	0.041	0.281	0.206
	7	3.5	2.0	0.014	0.054	0.351	0.246
	8	3.5	1.8	0.014	0.073	0.457	0.291
	9	3.5	1.7	0.014	0.097	0.602	0.351
4	1	5.0	18.6	0.017	0.023	1.081	0.257
	2	3.0	8.6	0.014	0.015	0.584	0.085
	3	2.9	4.7	0.014	0.021	0.340	0.107
	4	3.0	3.1	0.014	0.024	0.244	0.128
	5	3.2	2.5	0.014	0.026	0.216	0.150
	6	3.3	2.1	0.014	0.030	0.224	0.176
	7	3.5	1.9	0.014	0.037	0.260	0.207
	8	3.5	1.8	0.014	0.050	0.323	0.241
	9	3.6	1.7	0.014	0.066	0.401	0.277
6	1	6.7	19.9	0.018	0.025	1.067	0.264
	2	3.2	8.9	0.013	0.016	0.607	0.086
	3	3.0	4.5	0.014	0.022	0.328	0.109
	4	2.9	3.0	0.014	0.024	0.232	0.125
	5	3.2	2.4	0.014	0.026	0.208	0.145
	6	3.3	2.1	0.014	0.028	0.213	0.168
	7	3.4	1.9	0.014	0.032	0.237	0.195
	8	3.6	1.8	0.014	0.043	0.287	0.227
	9	3.6	1.7	0.014	0.059	0.357	0.261

Table F.14. Mean estimation error for kinematic gait parameters (Kv2, WF, KC3, 5 trials), when considering different value pairs for the Butterworth filter parameters (order and cut-off frequency).

Butterworth filter parameters		Kinematic parameters								
		Mean error								
Order	**Cut-off frequency (Hz)**	**Neck angle (deg.)**	**Spine shoulder angle (deg.)**	**Spine middle angle (deg.)**	**Elbow angle maximum (deg.)**	**Elbow angle minimum (deg.)**	**Knee angle maximum (deg.)**	**Knee angle minimum (deg.)**	**Hip angle range (deg.)**	**Ankle angle range (deg.)**
No filtering		16.9	17.5	5.2	3.0	3.6	3.9	4.5	5.1	45.2
2	**1**	16.9	17.5	5.2	6.2	7.0	7.5	17.4	12.7	14.6
	2	16.9	17.5	5.2	4.9	5.2	5.7	9.7	8.4	27.5
	3	16.9	17.5	5.2	4.3	4.6	5.0	7.1	6.6	33.2
	4	16.9	17.5	5.2	3.9	4.4	4.7	6.0	5.8	36.4
	5	16.9	17.5	5.2	3.7	4.2	4.5	5.5	5.5	38.8
	6	16.9	17.5	5.2	3.5	4.1	4.4	5.2	5.3	40.9
	7	16.9	17.5	5.2	3.3	3.9	4.2	5.0	5.2	42.8
	8	16.9	17.5	5.2	3.2	3.8	4.1	4.8	5.1	44.6
	9	16.9	17.5	5.2	3.1	3.7	4.0	4.6	5.1	45.7
4	**1**	16.9	17.5	5.2	6.1	7.1	7.4	20.2	14.8	12.7
	2	16.9	17.5	5.2	4.8	4.9	5.0	8.6	9.2	28.7
	3	16.9	17.5	5.2	4.3	4.4	4.8	5.5	6.4	34.7
	4	16.9	17.5	5.2	4.0	4.2	4.7	5.0	5.6	38.1
	5	16.9	17.5	5.2	3.8	4.2	4.5	5.0	5.3	40.3
	6	16.9	17.5	5.2	3.6	4.1	4.4	5.0	5.2	41.6
	7	16.9	17.5	5.2	3.5	4.1	4.3	4.9	5.2	42.9
	8	16.9	17.5	5.2	3.3	4.0	4.2	4.9	5.1	44.2
	9	16.9	17.5	5.2	3.2	3.9	4.1	4.8	5.1	45.4
6	**1**	16.9	17.5	5.2	6.1	7.3	6.9	21.9	15.8	11.6
	2	16.9	17.5	5.2	4.8	4.9	4.5	8.5	9.7	29.1
	3	16.9	17.5	5.2	4.4	4.3	4.8	4.9	6.3	34.8
	4	16.9	17.5	5.2	4.1	4.2	4.7	4.7	5.5	38.6
	5	16.9	17.5	5.2	3.8	4.2	4.5	4.9	5.3	41.0
	6	16.9	17.5	5.2	3.7	4.1	4.4	5.0	5.2	42.3
	7	16.9	17.5	5.2	3.5	4.1	4.3	4.9	5.2	43.3
	8	16.9	17.5	5.2	3.4	4.0	4.2	4.9	5.1	44.5
	9	16.9	17.5	5.2	3.2	3.9	4.2	4.8	5.1	45.6

Appendix G Additional Kinect Validation Results

This appendix includes the complete results obtained for the studies on the Kinect's validity for gait analysis (Chapter 6): Kinect version comparison (Appendix G.1); walking activity comparison (Appendix G.2); Kinect configuration comparison (Appendix G.3). It also presents the results obtained for the Kinect v2 when varying the number of gait cycles considered for gait parameter computation (Appendix G.4).

G.1 Kinect Version Comparison

Table G.1. Mean and standard deviation values for each gait parameter obtained when using the Kinect and Qualisys, in the case of both Kinect versions (Kv1 and Kv2), considering the WF activity and configuration KC1.

Parameter	Mean ± standard deviation			
	Kv1		Kv2	
	Kinect	Qualisys	Kinect	Qualisys
Stride duration (s)	1.065 ± 0.060	1.062 ± 0.056	1.055 ± 0.066	1.056 ± 0.061
Step duration (s)	0.534 ± 0.028	0.537 ± 0.032	0.532 ± 0.042	0.532 ± 0.035
Stance duration (s)	0.681 ± 0.051	0.667 ± 0.044	0.669 ± 0.045	0.672 ± 0.048
Swing duration (s)	0.384 ± 0.037	0.395 ± 0.022	0.387 ± 0.030	0.384 ± 0.029
Single support duration (s)	0.772 ± 0.079	0.781 ± 0.035	0.770 ± 0.045	0.773 ± 0.045
Double support duration (s)	0.293 ± 0.072	0.281 ± 0.038	0.285 ± 0.037	0.283 ± 0.042
Stride length (mm)	134.6 ± 12.4	121.7 ± 10.5	122.5 ± 12.4	121.9 ± 12.7
Step length (mm)	58.0 ± 6.6	56.2 ± 6.0	54.9 ± 7.7	55.6 ± 8.1
Step width (mm)	13.7 ± 3.3	11.9 ± 2.0	13.2 ± 2.7	11.9 ± 2.5
Gait speed (m/s)	1.297 ± 0.114	1.169 ± 0.106	1.184 ± 0.13	1.172 ± 0.128
Gait speed variability (m/s)	0.097 ± 0.040	0.096 ± 0.015	0.099 ± 0.030	0.095 ± 0.027
Foot swing velocity (m/s)	3.789 ± 0.320	3.661 ± 0.312	3.721 ± 0.340	3.700 ± 0.355
Arm swing velocity (m/s)	2.549 ± 0.642	2.298 ± 0.366	2.234 ± 0.341	2.230 ± 0.355
Neck angle (deg.)	161.8 ± 7.3	155.9 ± 8.5	172.1 ± 3.5	154.7 ± 8.6
Spine middle angle (deg.)	174.8 ± 3.4	168.7 ± 5.6	176.2 ± 1.8	171.1 ± 4.1
Elbow angle maximum (deg.)	167.7 ± 4.7	168.0 ± 5.6	167.2 ± 5.1	167.8 ± 4.9
Elbow angle minimum (deg.)	137.9 ± 8.2	136.6 ± 8.4	139.3 ± 7.9	138.7 ± 9.0
Knee angle maximum (deg.)	177.9 ± 1.1	177.0 ± 2.5	174.5 ± 2.7	177.1 ± 2.2
Knee angle minimum (deg.)	138.5 ± 4.4	124.9 ± 4.7	128.7 ± 4.1	124.7 ± 4.6
Hip angle range (deg.)	15.7 ± 2.7	20.4 ± 3.4	19.3 ± 4.6	20.7 ± 3.1
Ankle angle range (deg.)	40.1 ± 14.1	28.0 ± 5.7	29.1 ± 12.8	27.7 ± 6.2

Table G.2. Bland Altman's mean difference (Mean diff) and 95% limits of agreement (LoA) for each gait parameter, in the case of both Kinect versions (Kv1 and Kv2), considering the WF activity and configuration KC1.

Parameter	Mean diff[a]		95% LoA	
	Kv1	Kv2	Kv1	Kv2
Stride duration (s)	0.003	0.000	−0.055 to 0.061	−0.042 to 0.041
Step duration (s)	−0.003	0.000	−0.040 to 0.033	−0.039 to 0.039
Stance duration (s)	0.014	−0.003	−0.061 to 0.089	−0.042 to 0.036
Swing duration (s)	−0.010^	0.003	−0.077 to 0.057	−0.055 to 0.061
Single support duration (s)	−0.009^	−0.002	−0.149 to 0.132	−0.074 to 0.069
Double support duration (s)	0.012^	0.002	−0.132 to 0.156	−0.049 to 0.053
Stride length (mm)	12.9~	**0.6**	3.5 to 22.2	−3.0 to 4.3
Step length (mm)	1.7	−0.7	−6.2 to 9.7	−8.4 to 6.9
Step width (mm)	1.8~^	1.3~	−2.0 to 5.6	−0.3 to 2.8
Gait speed (m/s)	0.128~	**0.012**~	0.085 to 0.170	−0.003 to 0.027
Gait speed variability (m/s)	0.001^	0.005	−0.065 to 0.067	−0.027 to 0.037
Foot swing velocity (m/s)	0.128~	0.021	−0.282 to 0.537	−0.262 to 0.304
Arm swing velocity (m/s)	0.251~^	**0.004**	−0.689 to 1.192	−0.121 to 0.128
Neck angle (deg.)	**5.9**~	17.4~^	−4.8 to 16.6	2.2 to 32.6
Spine middle angle (deg.)	6.1~^	5.2~^	−6.3 to 18.5	−1.7 to 12.1
Elbow angle maximum (deg.)	−0.3	−0.6~^	−11.2 to 10.6	−9.3 to 8.1
Elbow angle minimum (deg.)	1.4	0.6	−8.7 to 11.4	−7.4 to 8.6
Knee angle maximum (deg.)	**0.9**^	−2.6~	−5.3 to 7.0	−10 to 4.8
Knee angle minimum (deg.)	13.6~	**4.0**~	5.4 to 21.7	−2.1 to 10
Hip angle range (deg.)	−4.7~	**−1.3**	−10.1 to 0.6	−11.5 to 8.9
Ankle angle range (deg.)	12.2~^	**1.3**^	−16.4 to 40.7	−19.7 to 22.3

[a] The ~ and ^ symbols indicate fixed and proportional bias, respectively. The lowest error (Mean diff) for each parameter is indicated in bold, when there is a statistically significant difference between the two Kinect versions (one-way repeated-measures ANOVA, p-value ≤ 0.05).

Table G.3. Pearson's correlation coefficient (r) and concordance correlation coefficient (r_c), and associated 95% confidence interval (CI), for each gait parameter, in the case of both Kinect versions (Kv1 and Kv2), considering the WF activity and configuration KC1.

Parameter	r^a (95% CI)		r_c (95% CI)	
	Kv1	Kv2	Kv1	Kv2
Stride duration	0.87* (0.70 to 0.95)	0.95* (0.87 to 0.98)	0.87 (0.71 to 0.95)	0.94 (0.87 to 0.98)
Step duration	0.82* (0.59 to 0.93)	0.88* (0.72 to 0.95)	0.81 (0.59 to 0.92)	0.87 (0.70 to 0.94)
Stance duration	0.69* (0.36 to 0.87)	0.91* (0.78 to 0.96)	0.66 (0.35 to 0.85)	0.91 (0.79 to 0.96)
Swing duration	0.42 (−0.03 to 0.73)	0.49* (0.05 to 0.76)	0.36 (−0.06 to 0.67)	0.49 (0.08 to 0.75)
Single support duration	0.42 (−0.03 to 0.73)	0.67* (0.32 to 0.86)	0.31 (−0.13 to 0.64)	0.67 (0.35 to 0.85)
Double support duration	0.24 (−0.23 to 0.61)	0.79* (0.53 to 0.91)	0.19 (−0.25 to 0.57)	0.78 (0.54 to 0.91)
Stride length	0.93* (0.82 to 0.97)	0.99* (0.97 to 1.00)	0.56 (0.36 to 0.72)	0.99 (0.97 to 1.00)
Step length	0.80* (0.54 to 0.92)	0.88* (0.71 to 0.95)	0.77 (0.52 to 0.90)	0.88 (0.72 to 0.95)
Step width	0.84* (0.64 to 0.94)	0.95* (0.88 to 0.98)	0.62 (0.34 to 0.80)	0.85 (0.72 to 0.93)
Gait speed	0.98* (0.96 to 0.99)	1.00* (1.00 to 1.00)	0.59 (0.41 to 0.73)	0.99 (0.99 to 1.00)
Gait speed variability	0.60* (0.22 to 0.82)	0.84* (0.63 to 0.94)	0.40 (−0.03 to 0.70)	0.83 (0.63 to 0.93)
Foot swing velocity	0.78* (0.52 to 0.91)	0.91* (0.79 to 0.97)	0.73 (0.47 to 0.87)	0.91 (0.80 to 0.96)
Arm swing velocity	0.67* (0.33 to 0.86)	0.98* (0.96 to 0.99)	0.53 (0.17 to 0.76)	0.98 (0.96 to 0.99)
Neck angle	0.77* (0.49 to 0.91)	0.42 (−0.04 to 0.73)	0.61 (0.33 to 0.79)	0.07 (−0.04 to 0.17)
Spine middle angle	0.09 (−0.37 to 0.51)	0.50* (0.07 to 0.77)	0.04 (−0.22 to 0.30)	0.16 (−0.04 to 0.35)
Elbow angle maximum	0.43 (−0.01 to 0.74)	0.61* (0.23 to 0.83)	0.43 (0.01 to 0.72)	0.61 (0.26 to 0.82)
Elbow angle minimum	0.81* (0.57 to 0.92)	0.89* (0.74 to 0.96)	0.81 (0.58 to 0.92)	0.88 (0.74 to 0.95)
Knee angle maximum	−0.42 (−0.73 to 0.03)	−0.21 (−0.59 to 0.26)	0.00 (0.00 to 0.00)	0.00 (0.00 to 0.00)
Knee angle minimum	0.58* (0.17 to 0.82)	0.75* (0.46 to 0.89)	0.11 (0.01 to 0.20)	0.53 (0.26 to 0.72)
Hip angle range	0.61* (0.22 to 0.83)	0.14 (−0.32 to 0.55)	0.27 (0.06 to 0.46)	0.13 (−0.3 to 0.52)
Ankle angle range	0.13 (−0.35 to 0.55)	0.55* (0.14 to 0.80)	0.05 (−0.23 to 0.33)	0.43 (0.01 to 0.72)

[a] The * symbol indicates a statistically significant value (p-value ≤ 0.05).

G.2 Walking Activity Comparison

Table G.4. Mean and standard deviation values for each gait parameter obtained when using the Kv2 and Qualisys, in the case of both walking activities (WF and WB), considering the configuration KC1.

Parameter	Mean ± standard deviation			
	WF		WB	
	Kinect	Qualisys	Kinect	Qualisys
Stride duration (s)	1.064 ± 0.053	1.059 ± 0.054	1.065 ± 0.059	1.062 ± 0.059
Step duration (s)	0.533 ± 0.029	0.531 ± 0.028	0.527 ± 0.031	0.525 ± 0.030
Stance duration (s)	0.674 ± 0.037	0.673 ± 0.043	0.690 ± 0.041	0.677 ± 0.047
Swing duration (s)	0.389 ± 0.019	0.386 ± 0.018	0.380 ± 0.023	0.390 ± 0.019
Single support duration (s)	0.779 ± 0.036	0.777 ± 0.033	0.760 ± 0.043	0.787 ± 0.037
Double support duration (s)	0.285 ± 0.024	0.282 ± 0.038	0.305 ± 0.029	0.274 ± 0.036
Stride length (mm)	123.3 ± 11.9	122.2 ± 12.0	129.6 ± 9.6	129.4 ± 9.4
Step length (mm)	56.6 ± 6.6	56.1 ± 6.4	59.1 ± 6.1	61.2 ± 4.6
Step width (mm)	13.1 ± 2.0	11.7 ± 1.8	12.2 ± 1.8	11.3 ± 1.6
Gait speed (m/s)	1.186 ± 0.123	1.173 ± 0.123	1.241 ± 0.104	1.221 ± 0.105
Gait speed variability (m/s)	0.100 ± 0.017	0.094 ± 0.016	0.080 ± 0.011	0.079 ± 0.012
Foot swing velocity (m/s)	3.645 ± 0.295	3.709 ± 0.339	3.776 ± 0.330	3.884 ± 0.281
Arm swing velocity (m/s)	2.306 ± 0.329	2.280 ± 0.331	2.184 ± 0.294	2.134 ± 0.246
Neck angle (deg.)	172.2 ± 2.9	154.6 ± 7.6	165.3 ± 4.5	156.3 ± 8.4
Spine shoulder angle (deg.)	174.1 ± 2.3	155.9 ± 6.5	171.7 ± 2.3	157.4 ± 6.5
Spine middle angle (deg.)	176.2 ± 1.5	171.0 ± 4.0	176.9 ± 0.8	171.6 ± 4.4
Elbow angle maximum (deg.)	167.6 ± 4.1	168.3 ± 4.3	173.8 ± 2.4	166.5 ± 4.2
Elbow angle minimum (deg.)	138.9 ± 6.2	137.7 ± 7.4	153.6 ± 6.0	140.7 ± 4.7
Knee angle maximum (deg.)	173.8 ± 1.9	177.2 ± 2.3	174.9 ± 1.6	177.0 ± 2.5
Knee angle minimum (deg.)	128.8 ± 4.1	124.5 ± 4.1	129.2 ± 3.4	124.1 ± 4.4
Hip angle range (deg.)	18.6 ± 3.9	20.2 ± 3.3	18.1 ± 3.2	22.4 ± 3.4
Ankle angle range (deg.)	32.4 ± 7.5	28.9 ± 4.3	48.5 ± 6.1	30.4 ± 4.5

Table G.5. Bland Altman's mean difference (Mean diff) and 95% limits of agreement (LoA) for each gait parameter, in the case of both walking activities (WF and WB), considering the Kv2 and configuration KC1.

Parameter	Mean diff[a]		95% LoA	
	WF	WB	WF	WB
Stride duration (s)	0.005~	0.003	−0.012 to 0.021	−0.014 to 0.02
Step duration (s)	0.002	0.002	−0.011 to 0.016	−0.018 to 0.022
Stance duration (s)	**0.001**^	0.013~	−0.021 to 0.024	−0.022 to 0.047
Swing duration (s)	**0.003**	−0.009~	−0.021 to 0.027	−0.037 to 0.018
Single support duration (s)	**0.001**	−0.027~	−0.041 to 0.044	−0.084 to 0.03
Double support duration (s)	**0.003**^	0.031~	−0.039 to 0.045	−0.036 to 0.098
Stride length (mm)	1.2~	**0.2**	0.0 to 2.4	−3.2 to 3.6
Step length (mm)	**0.5**	−2.1~^	−2.5 to 3.6	−7.9 to 3.7
Step width (mm)	1.4~	**0.9**~	−0.2 to 3.0	−1.2 to 3
Gait speed (m/s)	**0.013**~	0.020~	0.005 to 0.021	0.009 to 0.032
Gait speed variability (m/s)	0.006~	**0.000**	−0.009 to 0.021	−0.013 to 0.014
Foot swing velocity (m/s)	−0.063	−0.108	−0.340 to 0.213	−0.614 to 0.398
Arm swing velocity (m/s)	0.026	0.050	−0.086 to 0.138	−0.159 to 0.259
Neck angle (deg.)	17.6~^	**9.1**~^	3.7 to 31.5	−8.6 to 26.8
Spine shoulder angle (deg.)	18.1~^	**14.3**~^	7.7 to 28.6	1.2 to 27.4
Spine middle angle (deg.)	5.2~^	5.3~^	−1.7 to 12.0	−3.5 to 14.1
Elbow angle maximum (deg.)	**−0.7**	7.4~^	−5.7 to 4.3	−1.5 to 16.3
Elbow angle minimum (deg.)	**1.2**~^	12.9~	−3.3 to 5.8	7.3 to 18.4
Knee angle maximum (deg.)	−3.4~	−2.1~	−9.8 to 3.0	−8.6 to 4.4
Knee angle minimum (deg.)	4.3~	5.1~	−0.1 to 8.6	−5.5 to 15.6
Hip angle range (deg.)	**−1.6**	−4.4~	−11.0 to 7.8	−12.2 to 3.5
Ankle angle range (deg.)	**3.5**~^	18.0~	−7.4 to 14.4	4.4 to 31.6

[a] The ~ and ^ symbols indicate fixed and proportional bias, respectively. The lowest error (Mean diff) for each parameter is indicated in bold, when there is a statistically significant difference between the two Kinect versions (one-way repeated-measures ANOVA, p-value ≤ 0.05).

Table G.6. Pearson's correlation coefficient (r) and concordance correlation coefficient (r_c), and associated 95% confidence interval (CI), for each gait parameter, in the case of both walking activities (WF and WB), considering the Kv2 and configuration KC1.

Parameter	r^a (95% CI)		r_c (95% CI)	
	WF	WB	WF	WB
Stride duration	0.99* (0.97 to 1.00)	0.99* (0.97 to 1.00)	0.98 (0.96 to 0.99)	0.99 (0.97 to 1.00)
Step duration	0.97* (0.93 to 0.99)	0.95* (0.87 to 0.98)	0.97 (0.93 to 0.99)	0.95 (0.87 to 0.98)
Stance duration	0.97* (0.93 to 0.99)	0.93* (0.81 to 0.97)	0.96 (0.90 to 0.98)	0.89 (0.75 to 0.95)
Swing duration	0.79* (0.54 to 0.92)	0.80* (0.53 to 0.92)	0.79 (0.55 to 0.91)	0.72 (0.44 to 0.88)
Single support duration	0.81* (0.57 to 0.92)	0.75* (0.40 to 0.91)	0.81 (0.58 to 0.92)	0.60 (0.28 to 0.81)
Double support duration	0.85* (0.66 to 0.94)	0.46 (−0.04 to 0.78)	0.77 (0.51 to 0.90)	0.32 (−0.03 to 0.60)
Stride length	1.00* (1.00 to 1.00)	0.98* (0.96 to 0.99)	0.99 (0.99 to 1.00)	0.98 (0.96 to 0.99)
Step length	0.97* (0.93 to 0.99)	0.88* (0.72 to 0.95)	0.97 (0.92 to 0.99)	0.80 (0.59 to 0.91)
Step width	0.92* (0.81 to 0.97)	0.82* (0.59 to 0.92)	0.73 (0.53 to 0.85)	0.72 (0.47 to 0.86)
Gait speed	1.00* (1.00 to 1.00)	1.00* (1.00 to 1.00)	0.99 (0.99 to 1.00)	0.98 (0.96 to 0.99)
Gait speed variability	0.90* (0.75 to 0.96)	0.84* (0.63 to 0.93)	0.84 (0.66 to 0.93)	0.83 (0.62 to 0.93)
Foot swing velocity	0.91* (0.78 to 0.96)	0.65* (0.27 to 0.86)	0.89 (0.75 to 0.95)	0.62 (0.26 to 0.83)
Arm swing velocity	0.99* (0.96 to 0.99)	0.94* (0.84 to 0.98)	0.98 (0.96 to 0.99)	0.91 (0.79 to 0.96)
Neck angle	0.37 (−0.1 to 0.71)	0.11 (−0.36 to 0.54)	0.04 (−0.04 to 0.13)	0.05 (−0.19 to 0.29)
Spine shoulder angle	0.63* (0.25 to 0.84)	0.12 (−0.34 to 0.54)	0.05 (−0.01 to 0.11)	0.02 (−0.06 to 0.09)
Spine middle angle	0.53* (0.12 to 0.79)	−0.07 (−0.50 to 0.40)	0.15 (−0.04 to 0.33)	0.00 (0.00 to 0.00)
Elbow angle maximum	0.81* (0.58 to 0.92)	0.15 (−0.34 to 0.58)	0.81 (0.59 to 0.92)	0.04 (−0.10 to 0.18)
Elbow angle minimum	0.95* (0.89 to 0.98)	0.88* (0.71 to 0.96)	0.93 (0.84 to 0.97)	0.22 (0.09 to 0.35)
Knee angle maximum	−0.26 (−0.63 to 0.21)	−0.21 (−0.64 to 0.31)	0.00 (0.00 to 0.00)	0.00 (0.00 to 0.00)
Knee angle minimum	0.85* (0.66 to 0.94)	0.05 (−0.46 to 0.53)	0.55 (0.32 to 0.72)	0.03 (−0.24 to 0.29)
Hip angle range	0.12 (−0.34 to 0.53)	0.28 (−0.23 to 0.67)	0.11 (−0.31 to 0.49)	0.15 (−0.12 to 0.40)
Ankle angle range	0.68* (0.32 to 0.86)	0.17 (−0.35 to 0.62)	0.51 (0.16 to 0.75)	0.03 (−0.05 to 0.10)

[a] The * symbol indicates a statistically significant value (p-value ≤ 0.05).

G.3 Kinect Configuration Comparison

Table G.7. Mean and standard deviation values for each gait parameter obtained when using the Kv2 and Qualisys, in the case of the three configurations (KC1, KC2 and KC3), considering the WF activity.

Parameter	Mean ± standard deviation					
	KC1		KC2		KC3	
	Kinect	Qualisys	Kinect	Qualisys	Kinect	Qualisys
Stride duration (s)	1.065 ± 0.055	1.062 ± 0.052	1.071 ± 0.054	1.064 ± 0.051	1.059 ± 0.059	1.054 ± 0.056
Step duration (s)	0.535 ± 0.029	0.534 ± 0.026	0.541 ± 0.027	0.535 ± 0.024	0.534 ± 0.032	0.529 ± 0.028
Stance duration (s)	0.674 ± 0.036	0.671 ± 0.042	0.671 ± 0.036	0.677 ± 0.046	0.67 ± 0.043	0.669 ± 0.046
Swing duration (s)	0.391 ± 0.022	0.391 ± 0.018	0.399 ± 0.022	0.387 ± 0.013	0.389 ± 0.022	0.385 ± 0.02
Single support duration (s)	0.783 ± 0.040	0.783 ± 0.033	0.793 ± 0.042	0.777 ± 0.028	0.776 ± 0.036	0.772 ± 0.035
Double support duration (s)	0.284 ± 0.024	0.282 ± 0.037	0.278 ± 0.025	0.287 ± 0.037	0.283 ± 0.035	0.282 ± 0.038
Stride length (mm)	124.3 ± 11.7	123.3 ± 11.6	121 ± 10	120.1 ± 9.9	121.7 ± 10.7	120.2 ± 10.2
Step length (mm)	57.1 ± 6.6	56.9 ± 6.2	54.3 ± 5.2	54.8 ± 6	55.5 ± 6	54.8 ± 6.1
Step width (mm)	12.9 ± 1.8	11.6 ± 1.5	12.4 ± 2.3	11.7 ± 1.9	13 ± 1.8	11.5 ± 1.5
Gait speed (m/s)	1.189 ± 0.125	1.176 ± 0.123	1.162 ± 0.116	1.151 ± 0.115	1.177 ± 0.118	1.164 ± 0.117
Gait speed variability (m/s)	0.1 ± 0.017	0.093 ± 0.016	0.103 ± 0.018	0.1 ± 0.018	0.101 ± 0.021	0.097 ± 0.017
Foot swing velocity (m/s)	3.681 ± 0.29	3.716 ± 0.359	3.573 ± 0.232	3.631 ± 0.327	3.463 ± 0.297	3.661 ± 0.33
Arm swing velocity (m/s)	2.323 ± 0.347	2.296 ± 0.33	2.223 ± 0.315	2.238 ± 0.314	2.312 ± 0.329	2.292 ± 0.338
Neck angle (deg.)	171.8 ± 3.4	154.2 ± 8.0	171.1 ± 3.4	152.1 ± 8.7	171.6 ± 3.1	154.4 ± 7.7
Spine shoulder angle (deg.)	173.9 ± 2.7	155.6 ± 6.8	173.3 ± 2.6	153.9 ± 6.9	173.5 ± 2.5	155.7 ± 6.5
Spine middle angle (deg.)	176.1 ± 1.7	170.7 ± 4.2	175.8 ± 1.6	169.7 ± 4.9	175.7 ± 1.6	170.7 ± 4.4
Elbow angle maximum (deg.)	167.2 ± 4.2	167.9 ± 4.3	167.5 ± 4.6	167.8 ± 4.1	167.0 ± 4.3	168.3 ± 3.7
Elbow angle minimum (deg.)	138.1 ± 6.7	136.8 ± 7.7	136.8 ± 6.6	137.8 ± 7.1	138.2 ± 5.2	137.1 ± 6.7
Knee angle maximum (deg.)	173.7 ± 2.0	177.2 ± 2.3	175.0 ± 1.7	177.1 ± 2.1	174.0 ± 1.9	177.1 ± 2.3
Knee angle minimum (deg.)	129.1 ± 3.9	124.4 ± 4.1	130.9 ± 3.6	124.6 ± 4.3	128.8 ± 3.2	124.7 ± 4.0
Hip angle range (deg.)	18.6 ± 3.6	20.4 ± 3.4	18.5 ± 3.3	20.1 ± 3.1	17.4 ± 4.3	20.1 ± 3.6
Ankle angle range (deg.)	32.7 ± 8.3	29.3 ± 5.0	24.3 ± 7.0	28.7 ± 5.0	37.9 ± 6.4	28.7 ± 4.5

Table G.8. Bland Altman's mean difference (Mean diff) and 95% limits of agreement (LoA) for each gait parameter, in the case of the three configurations (KC1, KC2 and KC3), considering the Kv2 and WF activity.

Parameter	Mean diff[a]			95% LoA		
	KC1	KC2	KC3	KC1	KC2	KC3
Stride duration (s)	0.003	0.007$^{\sim}$	0.005$^{\sim}$	−0.015 to 0.02	−0.014 to 0.028	−0.013 to 0.022
Step duration (s)	0.000$^{\wedge}$	0.006$^{\sim}$	0.005$^{\sim}$	−0.013 to 0.014	−0.015 to 0.027	−0.012 to 0.022
Stance duration (s)	0.003$^{\wedge a}$	−0.006$^{\wedge b}$	0.001^{a,b}	−0.021 to 0.026	−0.042 to 0.031	−0.036 to 0.038
Swing duration (s)	**0.000**^{b}	0.013$^{\sim\wedge a}$	**0.004**^{b}	−0.027 to 0.027	−0.022 to 0.048	−0.035 to 0.042
Single support duration (s)	0.000^{b}	0.016$^{\sim\wedge a}$	0.004^{a,b}	−0.048 to 0.048	−0.044 to 0.077	−0.056 to 0.064
Double support duration (s)	0.003$^{\wedge a}$	−0.009^{b}	0.001^{a,b}	−0.042 to 0.047	−0.074 to 0.055	−0.058 to 0.06
Stride length (mm)	1.0$^{\sim}$	0.9$^{\sim}$	1.6$^{\sim}$	−0.2 to 2.1	−0.5 to 2.3	−0.9 to 4
Step length (mm)	0.2	−0.5$^{\wedge}$	0.7	−3.4 to 3.7	−3.8 to 2.8	−3 to 4.3
Step width (mm)	1.3$^{\sim a}$	**0.8**$^{\sim b}$	1.5$^{\sim\wedge a}$	−0.3 to 2.8	−1.5 to 3	−0.2 to 3.2
Gait speed (m/s)	0.012$^{\sim}$	0.011$^{\sim}$	0.014$^{\sim}$	0.005 to 0.019	0.002 to 0.02	−0.001 to 0.028
Gait speed variability (m/s)	0.007$^{\sim}$	0.004	0.004	−0.012 to 0.026	−0.012 to 0.019	−0.019 to 0.027
Foot swing velocity (m/s)	**−0.036**$^{\wedge a}$	**−0.057**$^{\wedge a}$	−0.197$^{\sim b}$	−0.341 to 0.27	−0.399 to 0.284	−0.47 to 0.076
Arm swing velocity (m/s)	0.027	−0.015	0.020	−0.112 to 0.167	−0.087 to 0.058	−0.138 to 0.179
Neck angle (deg.)	17.7$^{\sim\wedge a,b}$	18.9$^{\sim\wedge a}$	17.2$^{\sim\wedge b}$	3.6 to 31.7	4.6 to 33.2	3.6 to 30.7
Spine shoulder angle (deg.)	**18.3**$^{\sim\wedge b}$	19.4$^{\sim\wedge a}$	**17.8**$^{\sim\wedge b}$	7.7 to 28.9	8.7 to 30.2	7.6 to 28
Spine middle angle (deg.)	5.3$^{\sim\wedge a.b}$	6.1$^{\sim\wedge a}$	5.0$^{\sim\wedge b}$	−1.5 to 12.2	−2.2 to 14.4	−2.1 to 12
Elbow angle maximum (deg.)	−0.7$^{a.b}$	−0.3^{a}	−1.3$^{\sim b}$	−5 to 3.6	−5.4 to 4.8	−6.1 to 3.4
Elbow angle minimum (deg.)	1.3$^{\sim a}$	**−0.9**^{b}	1.0$^{\wedge a}$	−3.5 to 6	−6.7 to 4.8	−4.9 to 7
Knee angle maximum (deg.)	−3.5$^{\sim b}$	**−2.1**$^{\sim a}$	−3.1$^{\sim b}$	−10.2 to 3.3	−8.2 to 4.1	−9.7 to 3.4
Knee angle minimum (deg.)	**4.6**$^{\sim b}$	6.3$^{\sim a}$	**4.1**$^{\sim b}$	0.5 to 8.7	0.2 to 12.3	−0.5 to 8.7
Hip angle range (deg.)	−1.8	−1.5	−2.7$^{\sim}$	−11 to 7.5	−9.7 to 6.6	−11.9 to 6.5
Ankle angle range (deg.)	**3.4**$^{\sim\wedge b}$	−4.3$^{\sim c}$	9.2$^{\sim a}$	−7.7 to 14.4	−17.9 to 9.2	−3.7 to 22

[a] The ~ and ^ symbols indicate fixed and proportional bias, respectively. For each parameters, the superscript a, b and c letters indicate statistically significant differences between the KC1, KC2 and/or KC3 from post-hoc Tukey test (configurations with different letters are significantly different). The lowest error (Mean diff) is indicated in bold, when there is a statistically significant difference between one of the configurations and the other two.

Table G.9. Pearson's correlation coefficient (r) and concordance correlation coefficient (r_c), and associated 95% confidence interval (CI), for each gait parameter, in the case of the three configurations (KC1, KC2 and KC3), considering the Kv2 and WF activity.

Parameter	r^a (95% CI)			r_c (95% CI)		
	KC1	KC2	KC3	KC1	KC2	KC3
Stride duration	0.99* (0.97 to 0.99)	0.98* (0.95 to 0.99)	0.99* (0.97 to 1.00)	0.99 (0.96 to 0.99)	0.97 (0.93 to 0.99)	0.99 (0.97 to 0.99)
Step duration	0.98* (0.94 to 0.99)	0.92* (0.81 to 0.97)	0.97* (0.92 to 0.99)	0.97 (0.93 to 0.99)	0.89 (0.75 to 0.95)	0.95 (0.88 to 0.98)
Stance duration	0.96* (0.91 to 0.99)	0.92* (0.81 to 0.97)	0.91* (0.79 to 0.96)	0.95 (0.89 to 0.98)	0.89 (0.75 to 0.95)	0.91 (0.79 to 0.96)
Swing duration	0.78* (0.52 to 0.91)	0.58* (0.19 to 0.82)	0.56* (0.16 to 0.80)	0.76 (0.51 to 0.90)	0.42 (0.08 to 0.68)	0.56 (0.18 to 0.79)
Single support duration	0.79* (0.51 to 0.92)	0.69* (0.35 to 0.87)	0.62* (0.25 to 0.84)	0.77 (0.50 to 0.91)	0.58 (0.25 to 0.80)	0.62 (0.27 to 0.83)
Double support duration	0.81* (0.55 to 0.93)	0.49* (0.07 to 0.77)	0.66* (0.31 to 0.85)	0.74 (0.44 to 0.89)	0.45 (0.04 to 0.73)	0.66 (0.33 to 0.85)
Stride length	1.00* (1.00 to 1.00)	1.00* (0.99 to 1.00)	0.99* (0.98 to 1.00)	1.00 (0.99 to 1.00)	0.99 (0.99 to 1.00)	0.98 (0.96 to 0.99)
Step length	0.96* (0.90 to 0.99)	0.97* (0.91 to 0.99)	0.95* (0.89 to 0.98)	0.96 (0.90 to 0.98)	0.95 (0.89 to 0.98)	0.95 (0.88 to 0.98)
Step width	0.91* (0.77 to 0.96)	0.86* (0.68 to 0.94)	0.89* (0.73 to 0.95)	0.69 (0.47 to 0.83)	0.80 (0.58 to 0.91)	0.61 (0.38 to 0.77)
Gait speed	1.00* (1.00 to 1.00)	1.00* (1.00 to 1.00)	1.00* (1.00 to 1.00)	0.99 (0.99 to 1.00)	0.99 (0.99 to 1.00)	0.99 (0.98 to 1.00)
Gait speed variability	0.82* (0.60 to 0.93)	0.91* (0.77 to 0.96)	0.83* (0.61 to 0.93)	0.76 (0.53 to 0.89)	0.89 (0.76 to 0.95)	0.80 (0.57 to 0.91)
Foot swing velocity	0.91* (0.78 to 0.96)	0.86* (0.67 to 0.94)	0.91* (0.78 to 0.96)	0.89 (0.74 to 0.95)	0.80 (0.58 to 0.91)	0.76 (0.56 to 0.87)
Arm swing velocity	0.98* (0.95 to 0.99)	0.99* (0.98 to 1.00)	0.97* (0.93 to 0.99)	0.98 (0.94 to 0.99)	0.99 (0.98 to 1.00)	0.97 (0.93 to 0.99)
Neck angle	0.45 (0.00 to 0.75)	0.57* (0.16 to 0.81)	0.45 (0.00 to 0.75)	0.06 (−0.03 to 0.16)	0.08 (−0.02 to 0.17)	0.06 (−0.03 to 0.15)
Spine middle angle	0.67* (0.32 to 0.86)	0.68* (0.34 to 0.86)	0.66* (0.31 to 0.85)	0.06 (0.00 to 0.13)	0.06 (0.00 to 0.12)	0.06 (0.00 to 0.12)
Elbow angle maximum	0.56* (0.15 to 0.80)	0.55* (0.14 to 0.80)	0.62* (0.25 to 0.84)	0.17 (−0.03 to 0.35)	0.14 (−0.06 to 0.32)	0.19 (−0.02 to 0.39)
Elbow angle minimum	0.87* (0.69 to 0.95)	0.83* (0.61 to 0.93)	0.83* (0.61 to 0.93)	0.86 (0.69 to 0.94)	0.82 (0.62 to 0.92)	0.78 (0.56 to 0.90)
Knee angle maximum	0.95* (0.88 to 0.98)	0.91* (0.78 to 0.96)	0.90* (0.77 to 0.96)	0.93 (0.84 to 0.97)	0.90 (0.78 to 0.96)	0.87 (0.70 to 0.94)
Knee angle minimum	−0.30 (−0.66 to 0.16)	−0.31 (−0.67 to 0.16)	−0.24 (−0.63 to 0.24)	0.00 (0.00 to 0.00)	0.00 (0.00 to 0.00)	0.00 (0.00 to 0.00)
Hip angle range	0.86* (0.67 to 0.95)	0.71* (0.38 to 0.88)	0.81* (0.56 to 0.92)	0.52 (0.30 to 0.69)	0.31 (0.11 to 0.50)	0.48 (0.24 to 0.67)
Ankle angle range	0.10 (−0.37 to 0.53)	0.14 (−0.33 to 0.56)	0.31 (−0.17 to 0.67)	0.09 (−0.31 to 0.46)	0.13 (−0.29 to 0.51)	0.26 (−0.13 to 0.57)

[a] The * symbol indicates a statistically significant value (p-value ≤ 0.05).

G.4 Results for Kinect v2 when varying the Number of Gait Cycles

Table G.10. Bland Altman's mean difference values obtained for Kv2 and WF (KC1), when varying the number of gait cycles used to compute the gait parameters.

Gait Parameter	Mean difference										
	1 cycle	2 cycles	3 cycles	4 cycles	5 cycles	6 cycles	7 cycles	8 cycles	9 cycles	10 cycles	11 cycles
Stride duration (s)	0.000	−0.003	0.009	0.004	0.005	0.003	0.002	0.004	0.001	0.006	0.005
Step duration (s)	0.000	−0.002	0.006	0.001	0.001	−0.001	0.003	0.002	0.002	0.004	0.002
Stance duration (s)	−0.003	−0.002	0.001	0.004	0.005	0.002	0.002	0.000	0.003	0.004	0.001
Swing duration (s)	0.003	−0.001	0.008	0.000	0.000	0.002	0.000	0.004	−0.001	0.002	0.003
Single support duration (s)	−0.002	−0.001	0.010	−0.002	−0.003	0.000	0.000	0.000	−0.002	0.001	0.001
Double support duration (s)	0.002	−0.002	−0.001	0.006	0.007	0.003	0.002	0.004	0.003	0.005	0.003
Stride length (cm)	0.6	1.0	1.6	1.0	1.1	1.0	1.0	1.0	1.0	1.1	1.2
Step length (cm)	−0.7	0.3	0.2	0.6	0.0	0.2	−0.4	0.0	0.4	0.1	0.5
Step width (cm)	1.3	1.8	1.3	1.4	1.2	1.3	1.4	1.2	1.3	1.3	1.4
Gait speed (m/s)	0.012	0.013	0.011	0.013	0.014	0.013	0.013	0.012	0.013	0.012	0.013
Gait speed variability (m/s)	0.005	0.005	0.008	0.008	0.007	0.008	0.006	0.005	0.007	0.005	0.006
Foot swing velocity (m/s)	0.021	−0.069	−0.037	−0.056	−0.079	−0.062	−0.049	−0.048	−0.069	−0.045	−0.063
Arm swing velocity (m/s)	0.004	−0.006	0.017	0.031	0.028	0.018	0.036	0.020	0.029	0.008	0.026
Neck angle (deg.)	17	17	18	17	18	18	18	18	18	18	18
Spine shoulder angle (deg.)	18	18	18	18	18	18	18	18	18	18	18
Spine middle angle (deg.)	5	5	5	5	5	5	5	5	5	5	5
Elbow angle maximum (deg.)	−1	0	−1	−1	−1	−1	−1	−1	−1	−1	−1
Elbow angle minimum (deg.)	1	2	2	1	1	1	1	1	1	1	1
Knee angle maximum (deg.)	−3	−4	−4	−3	−3	−3	−3	−4	−3	−3	−3
Knee angle minimum (deg.)	4	5	4	5	4	5	5	5	5	4	4
Hip angle range (deg.)	−1	−2	−2	−2	−2	−2	−2	−2	−2	−2	−2
Ankle angle range (deg.)	1	6	2	3	2	4	5	3	2	3	4
Temporal [a] (s)	0.000	−0.002	0.006	0.002	0.003	0.002	0.002	0.002	0.001	0.004	0.003
Spatial[a] (cm)	0.4	1.0	1.0	1.0	0.8	0.8	0.7	0.7	0.9	0.8	1.0
Velocity[a] (m/s)	0.011	−0.014	0.000	−0.001	−0.008	−0.006	0.002	−0.003	−0.005	−0.005	−0.005
Kinematic[a] (deg.)	5	5	5	5	5	5	5	5	5	5	5

[a] mean value when considering all corresponding parameters.

Table G.11. Pearson's correlation coefficient (*r*) values obtained for Kv2 and WF (KC1), when varying the number of gait cycles used to compute the gait parameters.

Gait Parameter	Mean difference										
	1 cycle	2 cycles	3 cycles	4 cycles	5 cycles	6 cycles	7 cycles	8 cycles	9 cycles	10 cycles	11 cycles
Stride duration	0.95	0.98	0.97	0.98	0.99	0.99	0.98	0.98	1.00	0.98	0.99
Step duration	0.88	0.92	0.88	0.93	0.96	0.96	0.94	0.88	0.97	0.94	0.97
Stance duration	0.91	0.95	0.91	0.93	0.94	0.95	0.96	0.98	0.97	0.97	0.97
Swing duration	0.49	0.39	0.70	0.71	0.86	0.71	0.76	0.58	0.78	0.64	0.79
Single support duration	0.67	0.63	0.74	0.72	0.82	0.78	0.81	0.68	0.82	0.71	0.81
Double support duration	0.79	0.75	0.67	0.67	0.66	0.77	0.84	0.81	0.85	0.85	0.85
Stride length	0.99	1.00	1.00	1.00	1.00	1.00	1.00	1.00	1.00	1.00	1.00
Step length	0.88	0.97	0.95	0.97	0.95	0.96	0.92	0.95	0.97	0.96	0.97
Step width	0.95	0.91	0.83	0.94	0.93	0.91	0.92	0.90	0.87	0.92	0.92
Gait speed	1.00	1.00	1.00	1.00	1.00	1.00	1.00	1.00	1.00	1.00	1.00
Gait speed variability	0.84	0.84	0.86	0.81	0.81	0.83	0.85	0.89	0.91	0.84	0.90
Foot swing velocity	0.91	0.93	0.92	0.83	0.82	0.90	0.88	0.86	0.90	0.90	0.91
Arm swing velocity	0.98	0.99	0.97	0.98	0.99	0.98	0.97	0.98	0.99	1.00	0.99
Neck angle	0.42	0.57	0.51	0.38	0.35	0.45	0.46	0.43	0.50	0.49	0.37
Spine shoulder angle	0.62	0.77	0.69	0.64	0.59	0.64	0.63	0.69	0.68	0.69	0.63
Spine middle angle	0.50	0.62	0.59	0.54	0.45	0.53	0.48	0.54	0.55	0.58	0.53
Elbow angle maximum	0.61	0.88	0.85	0.82	0.77	0.80	0.81	0.82	0.83	0.79	0.81
Elbow angle minimum	0.89	0.95	0.90	0.95	0.94	0.93	0.94	0.95	0.94	0.94	0.95
Knee angle maximum	−0.21	−0.36	0.10	−0.35	−0.26	−0.16	−0.38	−0.14	−0.40	−0.26	−0.26
Knee angle minimum	0.75	0.72	0.87	0.68	0.71	0.84	0.81	0.78	0.82	0.80	0.85
Hip angle range	0.14	0.22	0.10	0.13	0.11	0.15	0.12	0.03	0.13	0.09	0.12
Ankle angle range	0.55	0.38	0.77	0.65	0.71	0.63	0.63	0.73	0.67	0.70	0.68
Spatiotemporal[a]	0.86	0.87	0.88	0.88	0.90	0.90	0.88	0.93	0.90	0.93	0.88
Kinematic[a]	0.46	0.50	0.59	0.48	0.47	0.52	0.52	0.51	0.52	0.51	0.52

[a] mean value when considering all corresponding parameters.

Table G.12. Concordance correlation coefficient (r_c) values obtained for Kv2 and WF (KC1), when varying the number of gait cycles used to compute the gait parameters.

Gait Parameter	Mean difference										
	1 cycle	2 cycles	3 cycles	4 cycles	5 cycles	6 cycles	7 cycles	8 cycles	9 cycles	10 cycles	11 cycles
Stride duration	0.94	0.98	0.96	0.98	0.98	0.99	0.98	0.97	1.00	0.97	0.98
Step duration	0.87	0.92	0.87	0.93	0.96	0.96	0.94	0.87	0.95	0.93	0.97
Stance duration	0.91	0.95	0.89	0.93	0.92	0.94	0.95	0.97	0.96	0.96	0.96
Swing duration	0.49	0.39	0.67	0.70	0.86	0.71	0.75	0.57	0.78	0.64	0.79
Single support duration	0.67	0.61	0.72	0.71	0.82	0.78	0.79	0.67	0.82	0.69	0.81
Double support duration	0.78	0.73	0.63	0.62	0.59	0.71	0.77	0.73	0.83	0.76	0.77
Stride length	0.99	1.00	0.99	0.99	0.99	0.99	1.00	0.99	0.99	0.99	0.99
Step length	0.88	0.96	0.95	0.96	0.95	0.96	0.92	0.95	0.97	0.96	0.97
Step width	0.85	0.64	0.68	0.77	0.76	0.74	0.71	0.73	0.64	0.71	0.73
Gait speed	0.99	1.00	0.99	0.99	0.99	0.99	0.99	0.99	0.99	0.99	0.99
Gait speed variability	0.83	0.82	0.81	0.71	0.76	0.75	0.80	0.87	0.84	0.81	0.84
Foot swing velocity	0.91	0.92	0.89	0.82	0.80	0.86	0.87	0.85	0.88	0.88	0.89
Arm swing velocity	0.98	0.99	0.97	0.97	0.99	0.98	0.97	0.98	0.98	1.00	0.98
Neck angle	0.07	0.09	0.07	0.04	0.03	0.06	0.05	0.04	0.06	0.07	0.04
Spine shoulder angle	0.07	0.09	0.07	0.05	0.04	0.06	0.05	0.05	0.05	0.06	0.05
Spine middle angle	0.16	0.21	0.17	0.14	0.11	0.15	0.13	0.14	0.15	0.17	0.15
Elbow angle maximum	0.61	0.88	0.85	0.81	0.76	0.79	0.81	0.79	0.83	0.78	0.81
Elbow angle minimum	0.88	0.93	0.88	0.92	0.91	0.90	0.91	0.93	0.92	0.92	0.93
Knee angle maximum	0.00	0.00	0.04	0.00	0.00	0.00	0.00	0.00	0.00	0.00	0.00
Knee angle minimum	0.53	0.40	0.62	0.36	0.38	0.46	0.44	0.45	0.46	0.46	0.55
Hip angle range	0.13	0.21	0.10	0.12	0.10	0.14	0.11	0.03	0.12	0.09	0.11
Ankle angle range	0.43	0.22	0.50	0.50	0.61	0.46	0.43	0.56	0.56	0.53	0.51
Spatiotemporal[a]	0.85	0.84	0.85	0.87	0.87	0.87	0.88	0.86	0.89	0.87	0.90
Kinematic[a]	0.35	0.37	0.40	0.36	0.37	0.37	0.36	0.37	0.39	0.38	0.39

[a] mean value when considering all corresponding parameters.

Table G.13. Bland Altman's mean difference values obtained for Kv2 and WB (KC1), when varying the number of gait cycles used to compute the gait parameters.

Gait Parameter	Mean difference										
	1 cycle	2 cycles	3 cycles	4 cycles	5 cycles	6 cycles	7 cycles	8 cycles	9 cycles	10 cycles	11 cycles
Stride duration (s)	0.008	−0.002	0.000	0.000	−0.002	0.000	0.001	0.001	0.002	−0.002	0.000
Step duration (s)	0.000	−0.002	0.001	0.002	0.001	−0.003	0.001	0.001	0.002	−0.001	0.002
Stance duration (s)	0.017	0.011	0.012	0.015	0.010	0.014	0.011	0.011	0.011	0.014	0.013
Swing duration (s)	−0.010	−0.014	−0.011	−0.015	−0.013	−0.014	−0.010	−0.010	−0.008	−0.016	−0.012
Single support duration (s)	−0.019	−0.036	−0.032	−0.036	−0.033	−0.030	−0.026	−0.026	−0.028	−0.036	−0.031
Double support duration (s)	0.027	0.034	0.032	0.036	0.031	0.030	0.029	0.029	0.031	0.035	0.032
Stride length (cm)	−1.3	−0.3	0.0	0.1	−0.3	−0.6	0.1	0.1	0.0	−0.1	−0.5
Step length (cm)	−4.6	−2.6	−2.3	−2.4	−1.9	−2.7	−2.8	−2.8	−2.5	−2.5	−2.6
Step width (cm)	0.6	0.9	1.0	1.0	0.4	0.7	0.7	0.7	0.6	0.9	0.5
Gait speed (m/s)	0.021	0.021	0.020	0.020	0.021	0.020	0.020	0.020	0.021	0.020	0.019
Gait speed variability (m/s)	−0.001	0.001	0.002	−0.002	0.001	−0.002	0.000	0.000	0.003	0.000	−0.001
Foot swing velocity (m/s)	−0.029	−0.096	−0.087	−0.113	−0.106	−0.103	−0.139	−0.139	−0.114	−0.095	−0.121
Arm swing velocity (m/s)	0.065	0.152	0.145	0.049	0.082	0.064	0.050	0.050	0.048	0.078	0.046
Neck angle (deg.)	10	10	8	9	9	10	10	10	9	9	9
Spine shoulder angle (deg.)	15	14	13	14	14	15	14	14	14	14	14
Spine middle angle (deg.)	6	6	6	5	6	6	6	6	6	6	5
Elbow angle maximum (deg.)	6	7	8	8	8	8	8	8	8	8	8
Elbow angle minimum (deg.)	11	11	9	11	12	12	12	12	13	12	13
Knee angle maximum (deg.)	−2	−3	−2	−3	−3	−2	−3	−3	−3	−2	−2
Knee angle minimum (deg.)	5	5	5	5	5	6	5	5	6	5	6
Hip angle range (deg.)	−4	−3	−5	−4	−4	−4	−4	−4	−4	−5	−4
Ankle angle range (deg.)	12	15	16	19	16	16	15	15	15	16	16
Temporal [a] (s)	0.004	−0.002	0.000	0.000	−0.001	−0.001	0.001	0.002	−0.001	0.001	0.002
Spatial[a] (cm)	−1.8	−0.7	−0.4	−0.4	−0.6	−0.9	−0.7	−0.6	−0.6	−0.9	−0.3
Velocity[a] (m/s)	0.014	0.020	0.020	−0.012	0.000	−0.005	−0.017	−0.011	0.001	−0.014	−0.010
Kinematic[a] (deg.)	7	7	6	7	7	7	7	7	7	7	7

[a] mean value when considering all corresponding parameters.

Table G.14. Pearson's correlation coefficient (*r*) values obtained for Kv2 and WB (KC1), when varying the number of gait cycles used to compute the gait parameters.

Gait Parameter	Mean difference										
	1 cycle	2 cycles	3 cycles	4 cycles	5 cycles	6 cycles	7 cycles	8 cycles	9 cycles	10 cycles	11 cycles
Stride duration	0.87	0.94	0.99	0.98	0.98	0.99	0.99	0.99	0.99	0.99	0.99
Step duration	0.62	0.82	0.93	0.94	0.90	0.95	0.96	0.93	0.97	0.96	0.95
Stance duration	0.86	0.91	0.90	0.93	0.94	0.93	0.92	0.94	0.95	0.95	0.93
Swing duration	0.31	0.66	0.66	0.67	0.72	0.69	0.69	0.71	0.83	0.77	0.80
Single support duration	0.60	0.65	0.76	0.70	0.77	0.72	0.81	0.77	0.80	0.76	0.75
Double support duration	0.53	0.44	0.58	0.67	0.66	0.63	0.70	0.66	0.65	0.67	0.46
Stride length	0.82	0.96	0.98	0.98	0.97	0.99	0.98	0.98	0.98	0.98	0.98
Step length	0.68	0.75	0.74	0.80	0.87	0.84	0.87	0.89	0.89	0.92	0.88
Step width	0.63	0.50	0.86	0.71	0.78	0.80	0.83	0.77	0.83	0.82	0.82
Gait speed	1.00	1.00	1.00	1.00	1.00	1.00	1.00	1.00	1.00	1.00	1.00
Gait speed variability	0.72	0.60	0.79	0.77	0.78	0.87	0.87	0.68	0.79	0.84	0.84
Foot swing velocity	0.52	0.50	0.67	0.60	0.63	0.72	0.69	0.67	0.66	0.72	0.65
Arm swing velocity	0.97	0.61	0.54	0.86	0.76	0.90	0.91	0.92	0.83	0.97	0.94
Neck angle	0.50	0.56	−0.07	0.14	0.18	0.47	0.38	0.52	0.28	0.10	0.11
Spine shoulder angle	0.45	0.53	0.02	0.11	0.22	0.45	0.36	0.51	0.26	0.09	0.12
Spine middle angle	−0.03	0.26	0.04	−0.18	0.10	0.06	−0.06	0.10	−0.07	0.03	−0.07
Elbow angle maximum	0.25	0.24	0.05	−0.06	0.17	0.18	0.15	0.06	0.23	0.09	0.15
Elbow angle minimum	0.56	0.66	0.60	0.71	0.71	0.80	0.80	0.86	0.80	0.81	0.88
Knee angle maximum	−0.29	0.08	−0.49	−0.33	−0.49	−0.55	−0.34	−0.10	−0.20	−0.42	−0.21
Knee angle minimum	0.32	0.01	0.08	−0.04	0.13	0.18	−0.15	0.13	0.11	−0.03	0.05
Hip angle range	0.18	0.26	0.25	0.40	0.37	0.36	0.45	0.36	0.21	0.28	0.28
Ankle angle range	0.13	−0.13	0.42	0.01	0.28	0.15	0.02	0.18	−0.10	0.14	0.17
Spatiotemporal[a]	0.70	0.72	0.80	0.82	0.83	0.85	0.86	0.84	0.86	0.87	0.85
Kinematic[a]	0.20	0.24	0.11	0.08	0.18	0.21	0.16	0.26	0.16	0.13	0.17

[a] mean value when considering all corresponding parameters.

Table G.15. Concordance correlation coefficient (r_c) values obtained for Kv2 and WB (KC1), when varying the number of gait cycles used to compute the gait parameters.

Gait Parameter	Mean difference										
	1 cycle	2 cycles	3 cycles	4 cycles	5 cycles	6 cycles	7 cycles	8 cycles	9 cycles	10 cycles	11 cycles
Stride duration	0.87	0.94	0.99	0.98	0.98	0.99	0.99	0.99	0.99	0.99	0.99
Step duration	0.62	0.81	0.92	0.94	0.90	0.95	0.95	0.93	0.97	0.96	0.95
Stance duration	0.82	0.88	0.88	0.89	0.92	0.90	0.89	0.91	0.90	0.91	0.89
Swing duration	0.26	0.52	0.58	0.51	0.58	0.53	0.61	0.65	0.60	0.64	0.72
Single support duration	0.54	0.46	0.56	0.48	0.58	0.55	0.65	0.61	0.52	0.57	0.60
Double support duration	0.43	0.30	0.40	0.47	0.48	0.48	0.49	0.47	0.38	0.45	0.32
Stride length	0.82	0.96	0.98	0.98	0.97	0.99	0.98	0.98	0.98	0.98	0.98
Step length	0.51	0.67	0.68	0.72	0.81	0.73	0.76	0.80	0.79	0.81	0.80
Step width	0.51	0.42	0.70	0.61	0.76	0.72	0.76	0.72	0.74	0.77	0.72
Gait speed	0.98	0.98	0.98	0.99	0.98	0.98	0.98	0.98	0.98	0.98	0.98
Gait speed variability	0.71	0.57	0.79	0.77	0.77	0.85	0.87	0.67	0.78	0.82	0.83
Foot swing velocity	0.46	0.49	0.65	0.58	0.59	0.68	0.62	0.62	0.64	0.66	0.62
Arm swing velocity	0.95	0.50	0.43	0.83	0.73	0.88	0.90	0.90	0.79	0.95	0.91
Neck angle	0.20	0.20	0.00	0.07	0.08	0.17	0.13	0.19	0.10	0.04	0.05
Spine shoulder angle	0.07	0.06	0.00	0.01	0.03	0.05	0.04	0.06	0.03	0.01	0.02
Spine middle angle	0.00	0.04	0.01	0.00	0.01	0.01	0.00	0.01	0.00	0.00	0.00
Elbow angle maximum	0.11	0.07	0.01	0.00	0.04	0.04	0.04	0.01	0.06	0.02	0.04
Elbow angle minimum	0.30	0.31	0.31	0.29	0.27	0.28	0.27	0.26	0.28	0.20	0.22
Knee angle maximum	0.00	0.04	0.00	0.00	0.00	0.00	0.00	0.00	0.00	0.00	0.00
Knee angle minimum	0.20	0.01	0.05	0.00	0.06	0.08	0.00	0.06	0.05	0.00	0.03
Hip angle range	0.10	0.17	0.12	0.21	0.21	0.21	0.24	0.19	0.09	0.15	0.15
Ankle angle range	0.06	0.00	0.08	0.00	0.08	0.04	0.00	0.04	0.00	0.03	0.03
Spatiotemporal[a]	0.65	0.65	0.73	0.77	0.79	0.79	0.80	0.79	0.77	0.81	0.79
Kinematic[a]	0.12	0.11	0.07	0.09	0.10	0.10	0.09	0.10	0.07	0.06	0.07

[a] mean value when considering all corresponding parameters.

Appendix H Additional Results for Subject Identification

This appendix includes the number of gait cycles that was detected by our gait cycle detection solution for each subject, when considering our study on subject identification. This study involved both healthy subjects (Table H.1) and Parkinson's disease (PD) patients treated with deep brain stimulation (DBS) (Table H.2). The results are divided according to the location where the associated acquisitions took place.

Table H.1. Number of gait cycles detected for the healthy subjects, when using the Kv2 and considering walking towards the sensor.

Location[a]	Subject	Number of gait cycles
LBMP	S1	32
	S2	30
	S3	27
	S4	28
	S5	33
	S6	23
	S7	25
	S8	23
	S9	33
	S10	32
	S11	35
	S12	25
	S13	21
	S14	22
	S15	29
	S16	22
	S17	30
	S18	22
	S19	21
	S20	22
HSJ2	S21	0
	S22	0
	S23	6
	S24	10
	S25	14

[a] LBMP and HSJ2 stand for LABIOMEP and second location at São João hospital, respectively.

Table H.2. Number of gait cycles detected for the PD patients, when using the Kv2 and considering walking towards the sensor.

Location[a]	Patient	State[b]	Acquisition session	Number of gait cycles
HSJ2	P1	Stim-on	#1	7
		Stim-off	#2	29
	P2	Stim-on	#1	6
		Stim-off	#2	23
	P3	Stim-on	#1	18
		Stim-off	#2	21
	P4	Stim-on	#1	11
		Stim-off	#2	8
	P5	Stim-on	#1	10
		Stim-off	#2	12
	P6	Stim-on	#1	5
	P7	Stim-on	#1	11
HSJ3	P8	Stim-on	#1	15
			#2	26
			#3	19
	P9		#1	25
			#2	24
			#3	60
	P10		#1	20
			#2	23
			#3	33
			#4	34
	P11		#1	20
			#2	21
	P12		#1	21
			#2	19
			#3	15
	P13		#1	36
			#2	36
			#3	35
	P14		#1	14
			#2	18
			#3	20
	P15		#1	8
			#2	26
	P16		#1	38
			#2	25
	P17		#1	2
			#2	19
	P18		#1	15

[a] HSJ2 and HSJ3 stand for second and third location at São João hospital, respectively.

[b] The state refers to the DBS state (stimulator on or off) in the case of PD patients only.